



Uncertainty Quantification for Regional-Climate-Model Output

Noel Cressie

University of Wollongong

This research is joint with Emily Kang, U. Cincinnati. It was partially supported by NASA's Earth Science Technology Office through its AIST Program. The regional-climate-model output was obtained through the North American Regional Climate Change Assessment Program (NARCCAP).



Climate

- Distribution of temperature, rainfall, air pressure, etc., over long time scales (the mean is one possible summary of the distribution)
- One of the greatest environmental concerns of the 21st century



Climate models

- Time scales are usually on the order of years (different from weather forecasting)
- Models are driven by a series of (discretized) differential equations, representing the climate system
- Many processes are simplified; models attempt to capture flows of energy and water
- Climate-change projections are made based on specific assumptions about the evolution of greenhouse gases and aerosols

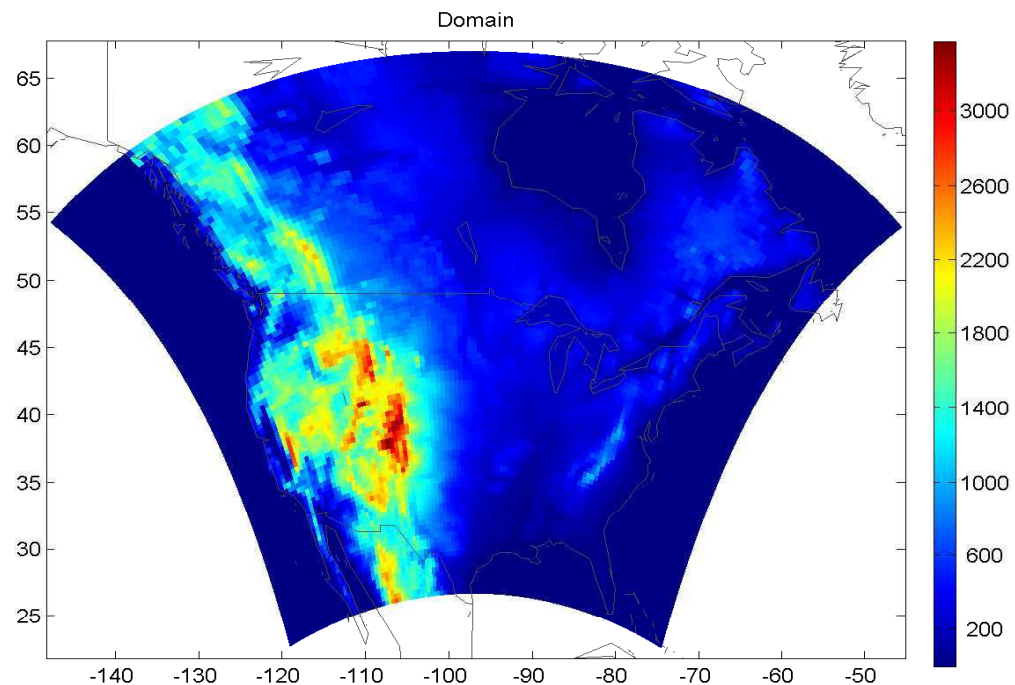
Regional Climate Models (RCMs)

Different from the coarse-scale atmosphere-ocean general circulation models (GCMs), RCMs

- Focus on **regional-scale**, or even local-scale climate in some specific regions
- Outputs: **20–50 km grid spacing**
- **Smaller-scale** processes (e.g., mountains, large lakes, complex coastlines) are explicitly incorporated into the models
- As well as initial conditions, **time-dependent boundary conditions** are required (usually provided by GCMs): “**dynamic downscaling**”

North American Regional Climate Change Assessment Program

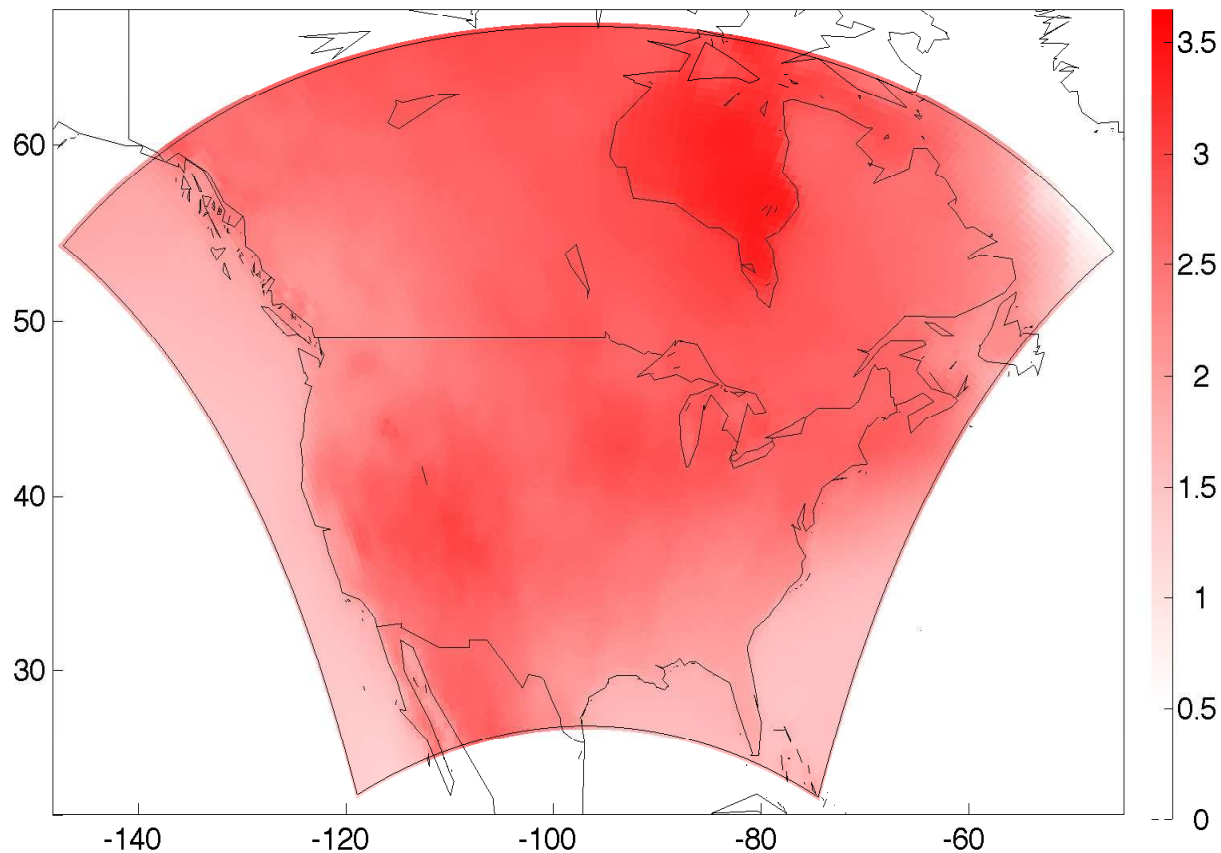
- **NARCCAP** investigates uncertainties in RCM outputs and provides high-resolution (approx. 50 km) climate output in North America (Mearns et al., 2009); the NARCCAP region \mathbb{D} is shown with height above sea level (in m.) superimposed, for context



North American map showing altitude

Map of Climate Change (in °C) by 2070

- Temperature differences for 2070 minus 2000 (in °C) at a 50km scale



All temperatures in this talk are in:

Degrees Celsius ($^{\circ}\text{C}$)

- Individual RCMs can differ in many aspects, such as parameterizations, dynamical modeling, treatment of boundary conditions, etc.
 - Different RCMs use different map projections
 - There may be some difference in spatial coverage of RCMs due to different map projections
 - In our analysis, RCM outputs have been interpolated by the NARCCAP team to the same two-dimensional grid with about 50 km spacing
- NARCCAP includes six RCMs that are used in different combinations for dynamic downscaling

NARCCAP: Phase II Study

- Time frame:
 - **Current** period: 1971–2000
 - **Future** period: 2041-2070 with the SRES A2 (i.e., status quo) emissions scenario assumed (Nakicenovic et al., 2000)
- Each RCM produces surface temperature, precipitation, wind speed, etc., every 3 hours on a 50km × 50km scale
- In the spatial statistical analysis that follows, we use **seasonally averaged, surface-temperature output (in °C)** from two RCMs, namely **CRCM** (Canadian Regional Climate Model, OURANOS/UQAM) and **RCM3** (Regional Climate Model Version 3, UCSC) with boundary conditions provided by the same GCM, namely **CGCM3**
- The SRES A2 greenhouse gases emissions scenario (i.e., status quo) for the 21st century is assumed; see Nakicenovic et al. (2000)

Seasonal Average Temperature Changes

We consider the **current and future** 30-year-averaged seasonal surface temperature fields from the i -th RCM for the j -th Boreal season:

$$Z_{ij}^{current}(\mathbf{s}_\ell) \equiv \sum_{t=1971}^{2000} Z_{ij}(\mathbf{s}_\ell; t)/30,$$

$$Z_{ij}^{future}(\mathbf{s}_\ell) \equiv \sum_{t=2041}^{2070} Z_{ij}(\mathbf{s}_\ell; t)/30,$$

for $\{\mathbf{s}_\ell : \ell = 1, \dots, n\}$ in \mathbb{D} with $n = 98 \times 120 = 11760$;

- i indicates the RCM with $i = 1$ for CRCM and $i = 2$ for RCM3
- j indicates the season with $j = 1$ for the Boreal spring (MAM), \dots , $j = 4$ for the Boreal winter (DJF)

We are interested in the **temperature change** from “current” period 1971–2000, to “future” period 2041–2070. **Temperature-change projections** are:

$$D_{ij}(\mathbf{s}_\ell) \equiv Z_{ij}^{future}(\mathbf{s}_\ell) - Z_{ij}^{current}(\mathbf{s}_\ell); i = 1, 2, j = 1, \dots, 4, \ell = 1, \dots, n$$

Target the Spatial-Only Component

- The “data” from NARCCAP Phases I and II are spatio-temporal: $Z_{ij}(\mathbf{s}; t)$ represents season j in year t at pixel \mathbf{s}
- Temperature differences 70 years apart are: $Z_{ij}(\mathbf{s}; t) - Z_{ij}(\mathbf{s}; t - 70)$, for $t = 2041, \dots, 2070$
- We target the spatial-only component without the pixel-year interaction. That is, we make inference on $Y_{ij}(\mathbf{s}_\ell)$ in the decomposition:

$$Z_{ij}(\mathbf{s}_\ell; t) - Z_{ij}(\mathbf{s}_\ell; t - 70) = Y_{ij}(\mathbf{s}_\ell) + \text{S-T interaction}_{ij}(\mathbf{s}_\ell; t)$$

- Then

$$D_{ij}(\mathbf{s}_\ell) = Y_{ij}(\mathbf{s}_\ell) + \varepsilon_{ij}(\mathbf{s})$$

- The spatial fields of temperature-change projections, $\{D_{ij}(\mathbf{s}_k) : \mathbf{s}_k \in \mathbb{D}\}$, are our “data” and are in units of $^{\circ}\text{C}$

- We define vectors of spatially indexed data:

- $\mathbf{D}_{ij} \equiv (D_{ij}(\mathbf{s}_1), \dots, D_{ij}(\mathbf{s}_n))'$.

- Average over climate models and seasons: $D_{..}(\mathbf{s}_{\ell}) \equiv \sum_{i=1}^2 \sum_{j=1}^4 D_{ij}(\mathbf{s}_{\ell})/8$,
which results in

$$\mathbf{D}_{..} \equiv (D_{..}(\mathbf{s}_1), \dots, D_{..}(\mathbf{s}_n))'$$

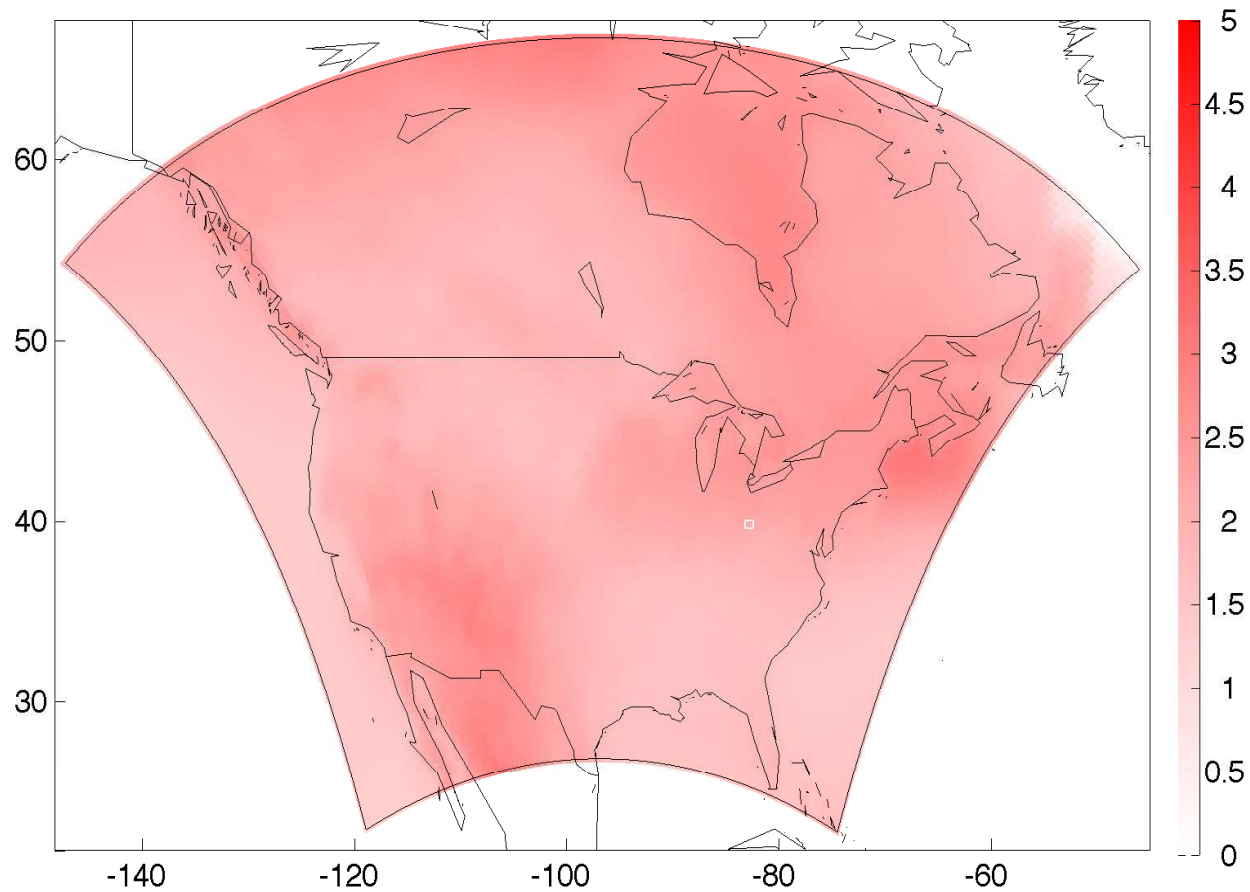
- Average over seasons for each climate model, and over climate models for each season: $D_{i.}(\mathbf{s}_{\ell}) \equiv \sum_{j=1}^4 D_{ij}(\mathbf{s}_{\ell})/4$, $D_{.j}(\mathbf{s}_{\ell}) \equiv \sum_{i=1}^2 D_{ij}(\mathbf{s}_{\ell})/2$, which results in

$$\mathbf{D}_{i.} \equiv (D_{i.}(\mathbf{s}_1), \dots, D_{i.}(\mathbf{s}_n))', \quad \mathbf{D}_{.j} \equiv (D_{.j}(\mathbf{s}_1), \dots, D_{.j}(\mathbf{s}_n))'$$

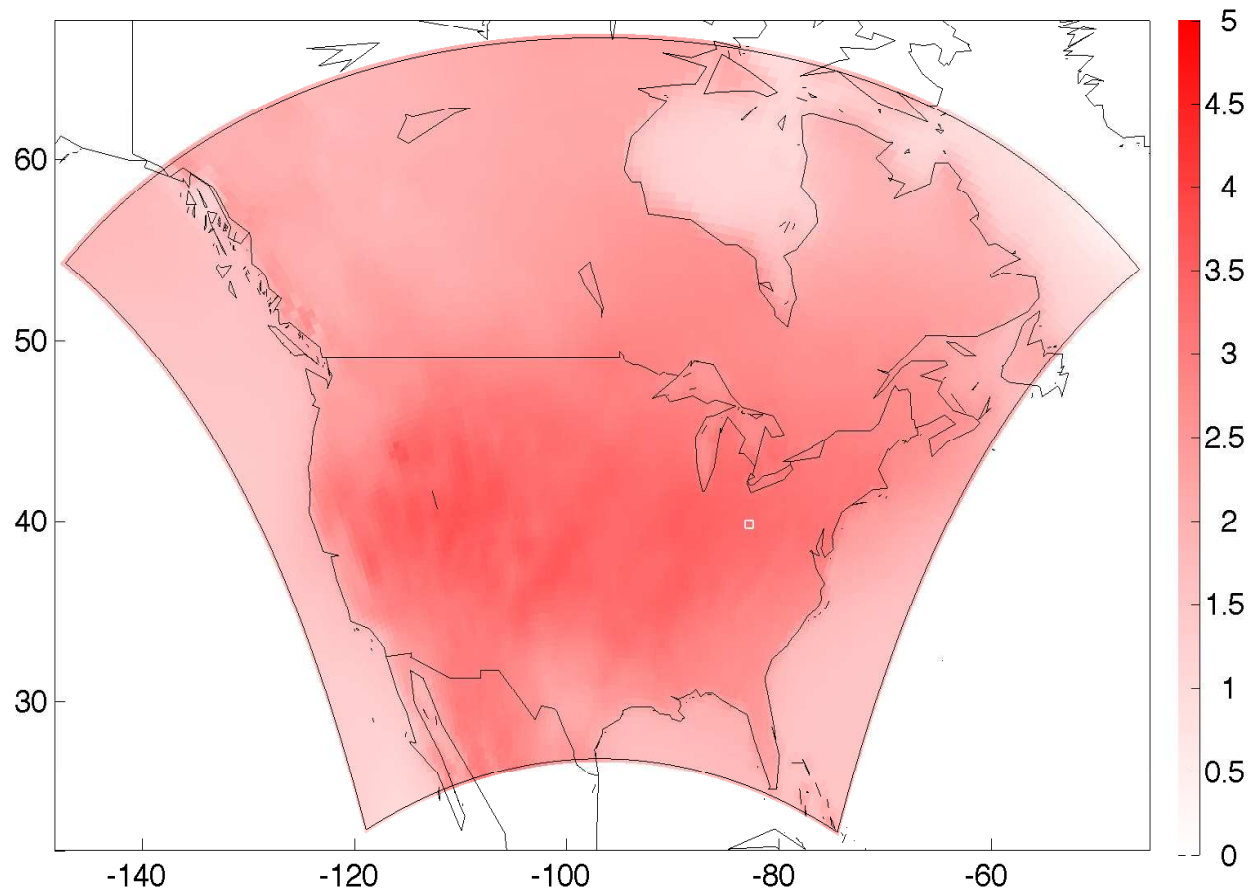
- We shall consider $\{\mathbf{D}_{.j} : j = 1(sp), \dots, 4(wi)\}$ and $\mathbf{D}_{..}$ (overall)

Exploratory Spatial Data Analysis (ESDA)

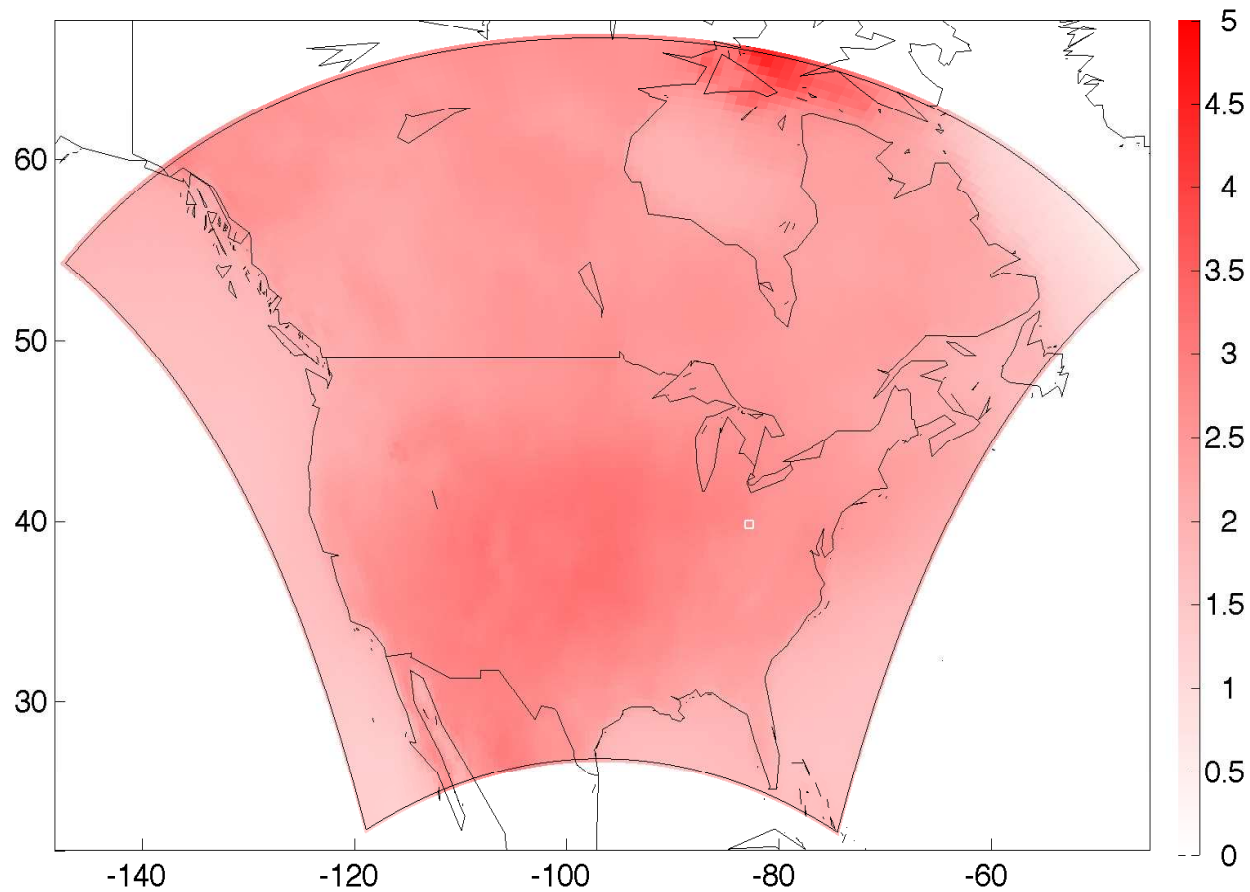
Temperature Change: D.₁ (spring)



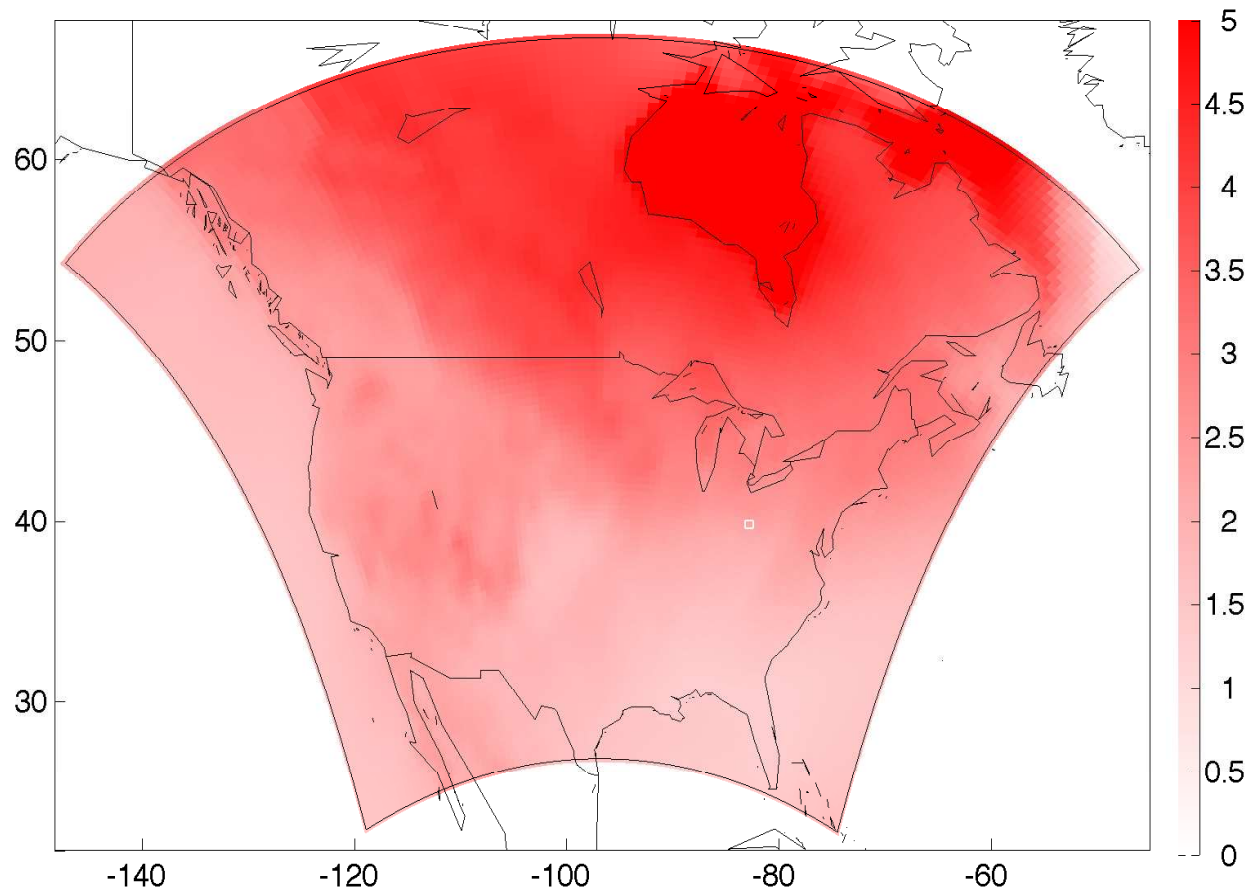
Temperature Change: D.₂ (summer)



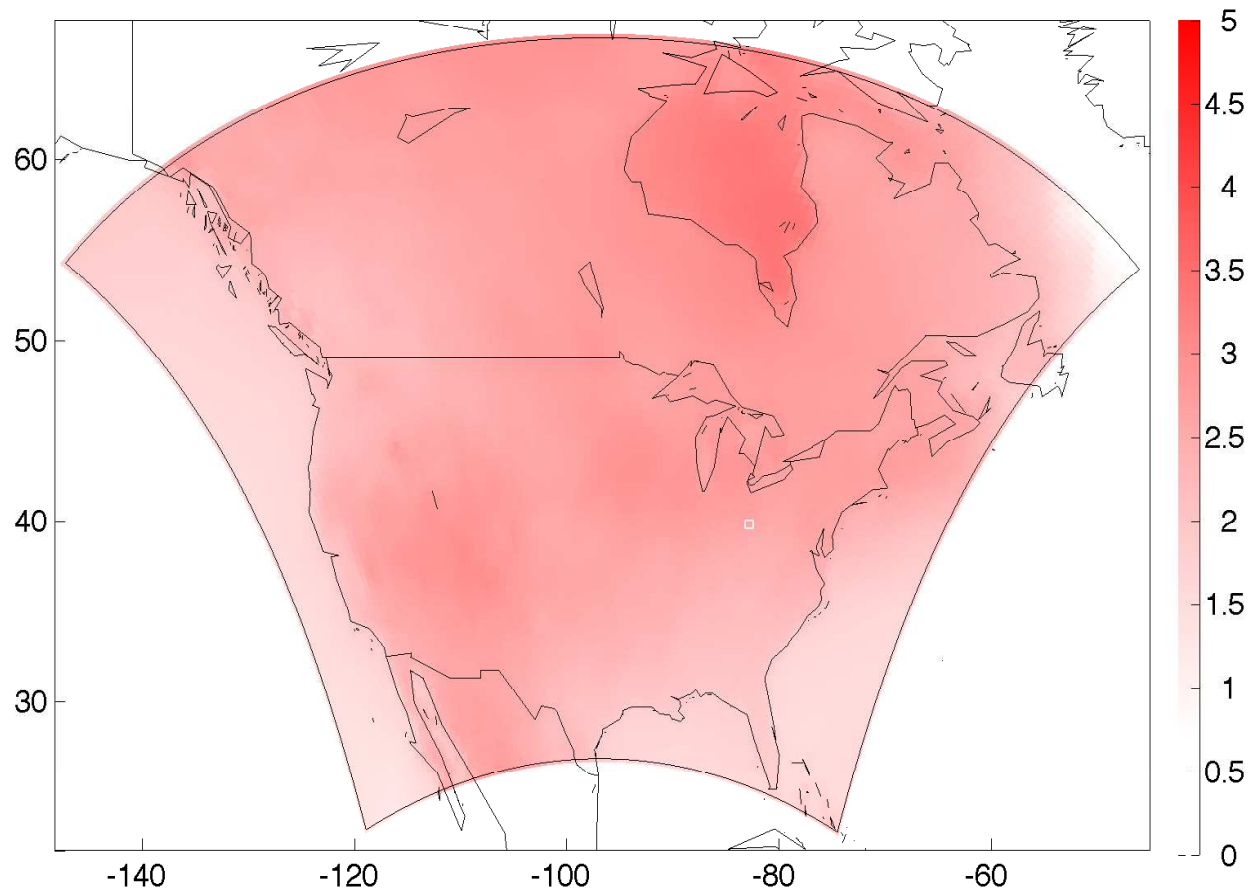
Temperature Change: D.₃ (autumn)



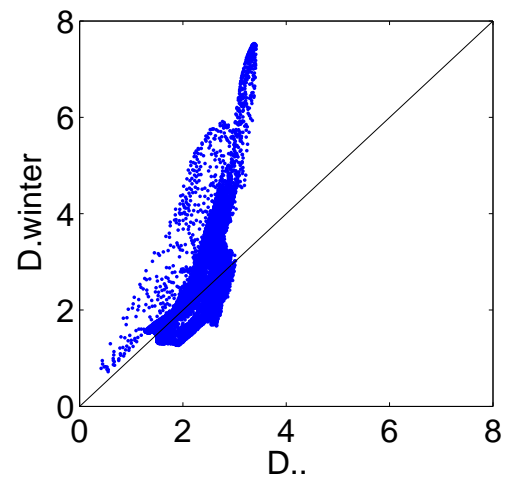
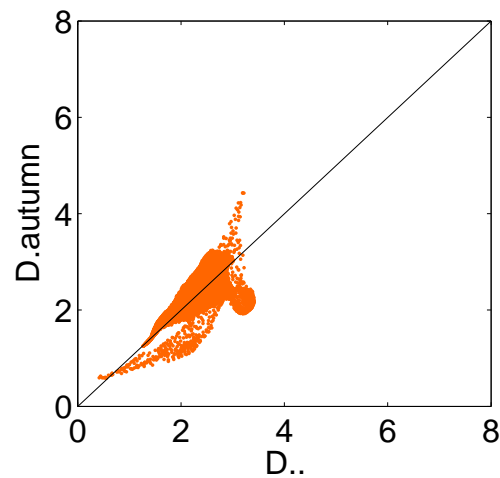
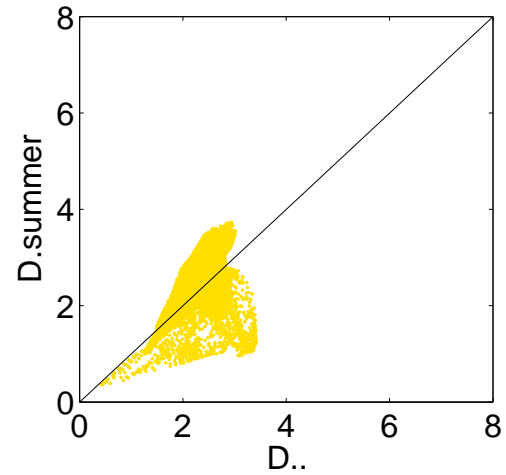
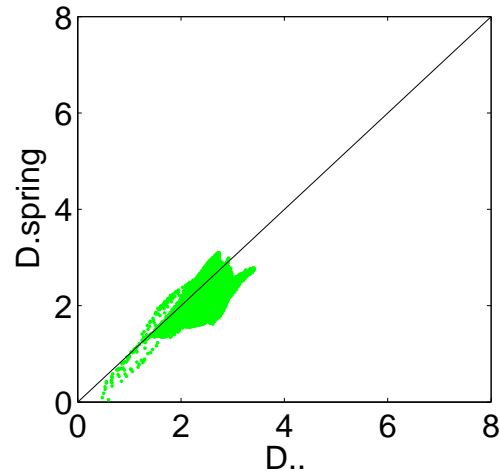
Temperature Change: $D_{.4}$ (winter)



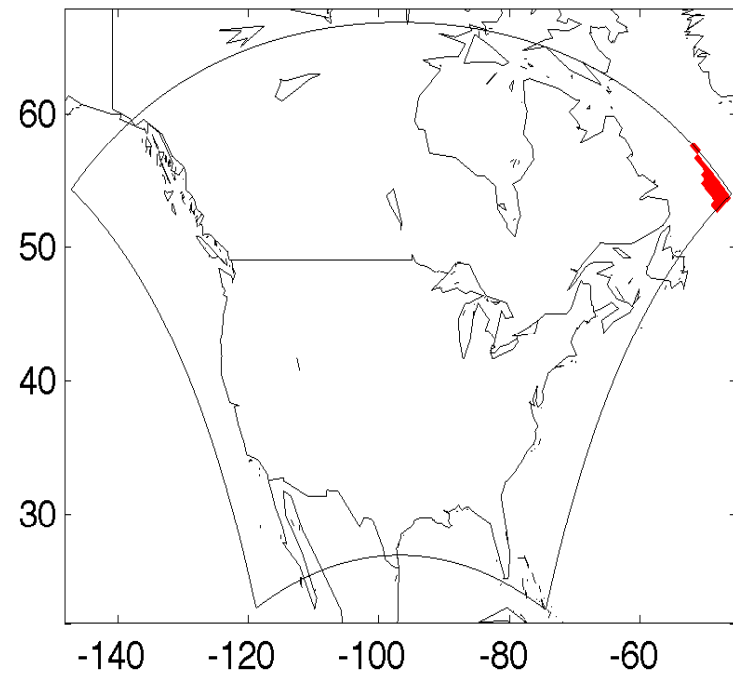
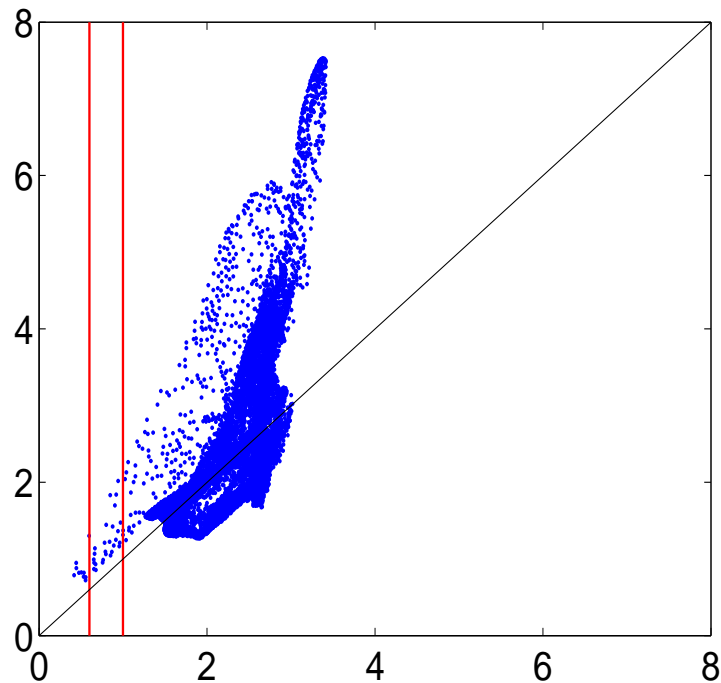
Temperature Change: D.. (overall)



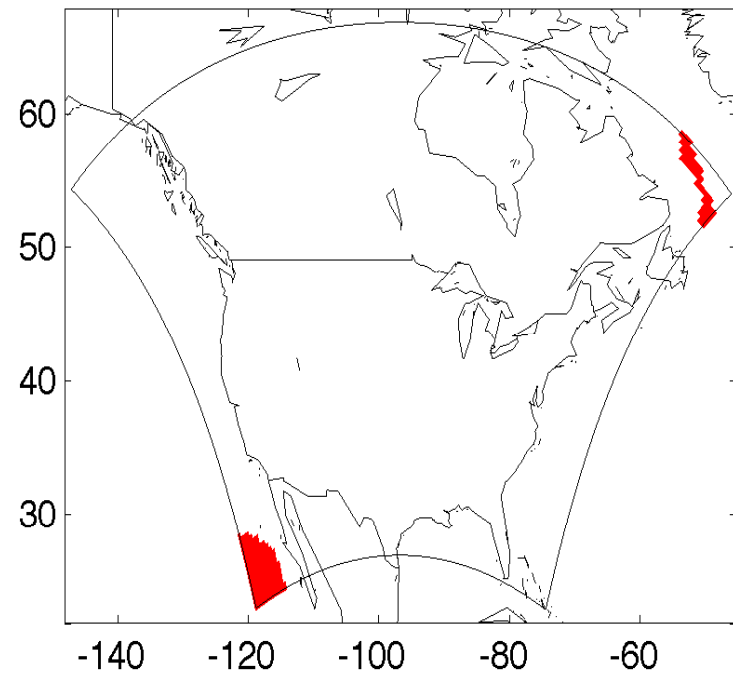
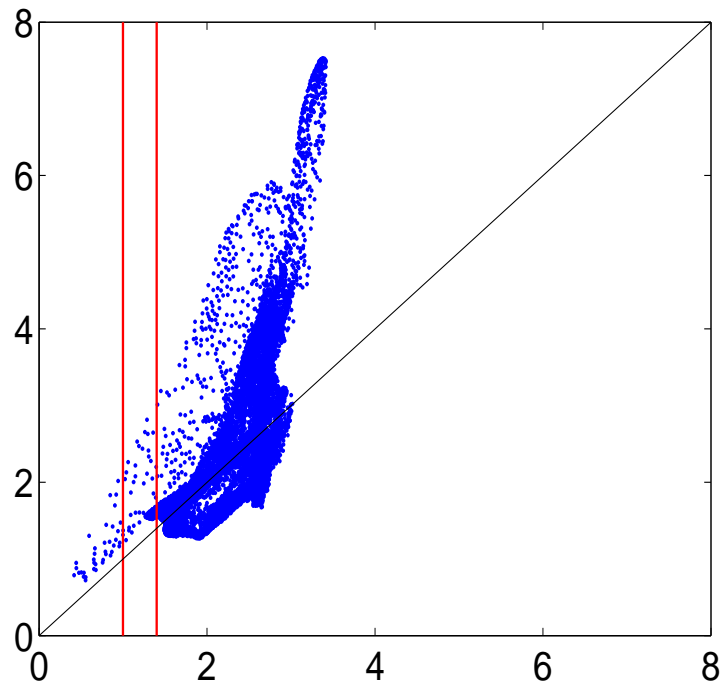
Temperature Change in Sp, Su, Au, Wi vs. Overall



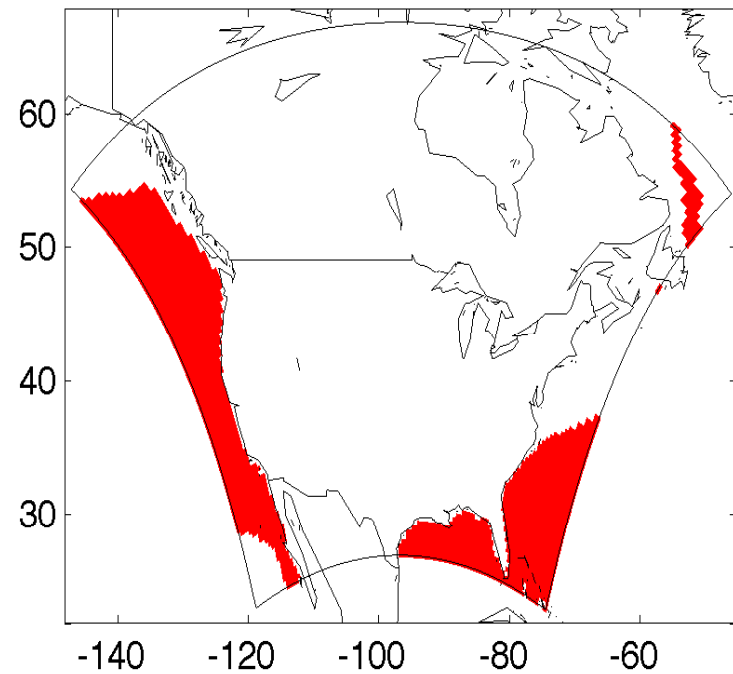
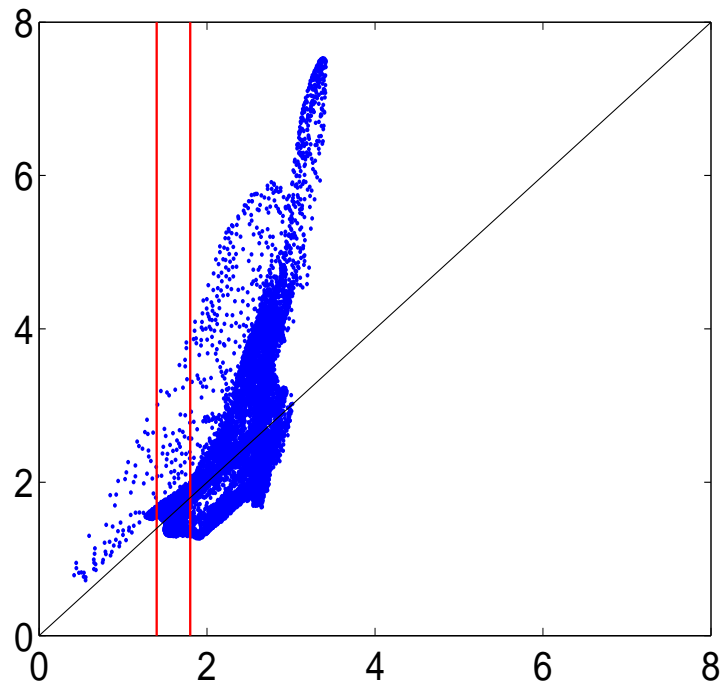
Linked Scatterplot of Winter vs. Overall



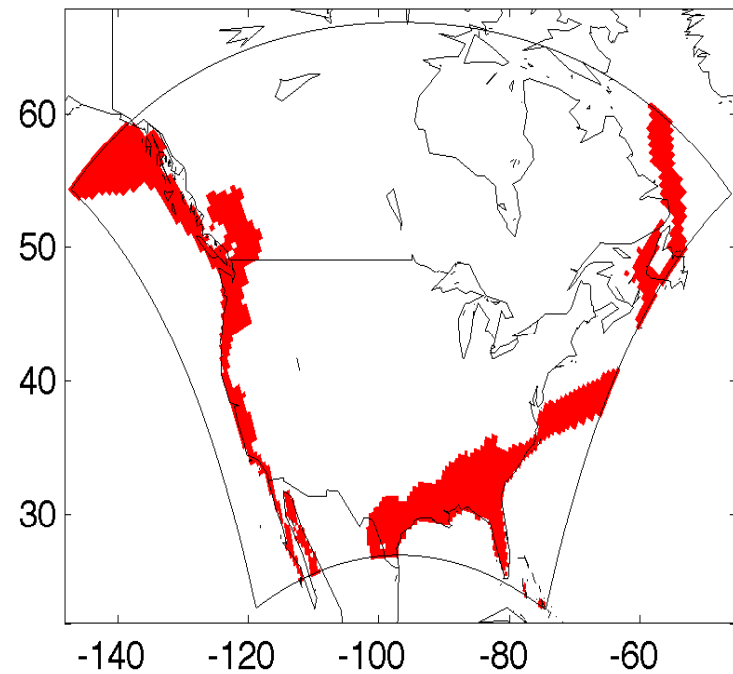
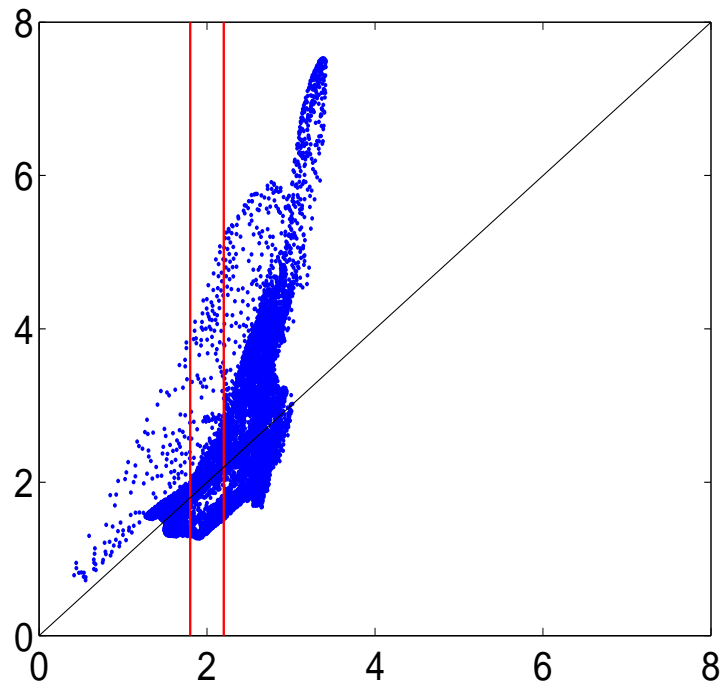
Linked Scatterplot of Winter vs. Overall



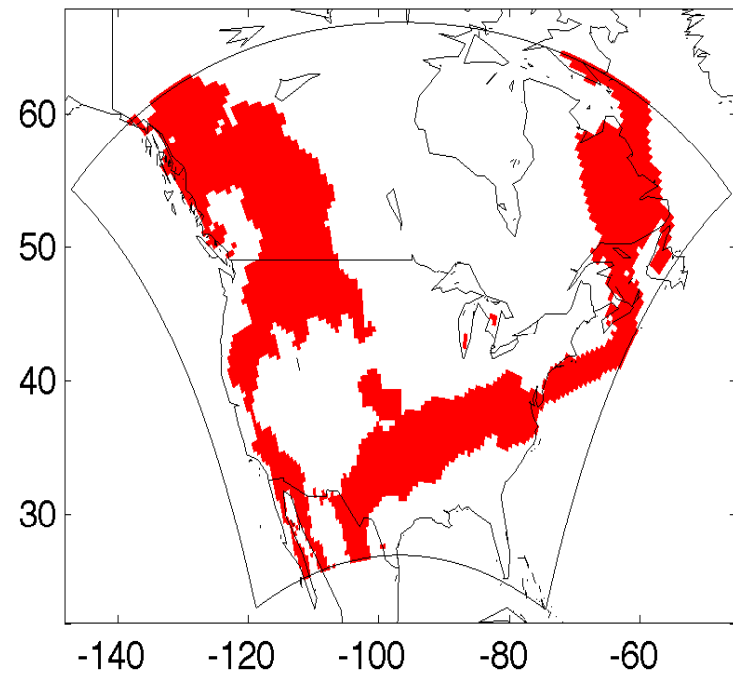
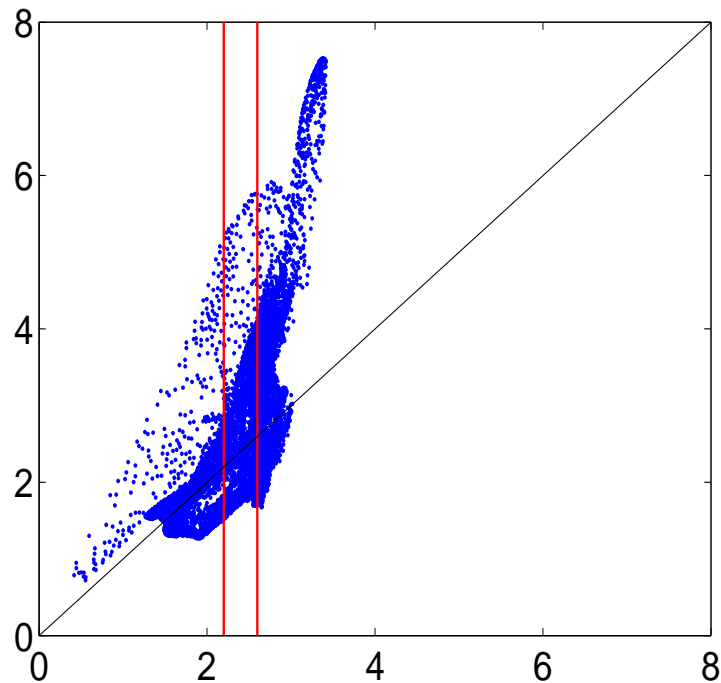
Linked Scatterplot of Winter vs. Overall



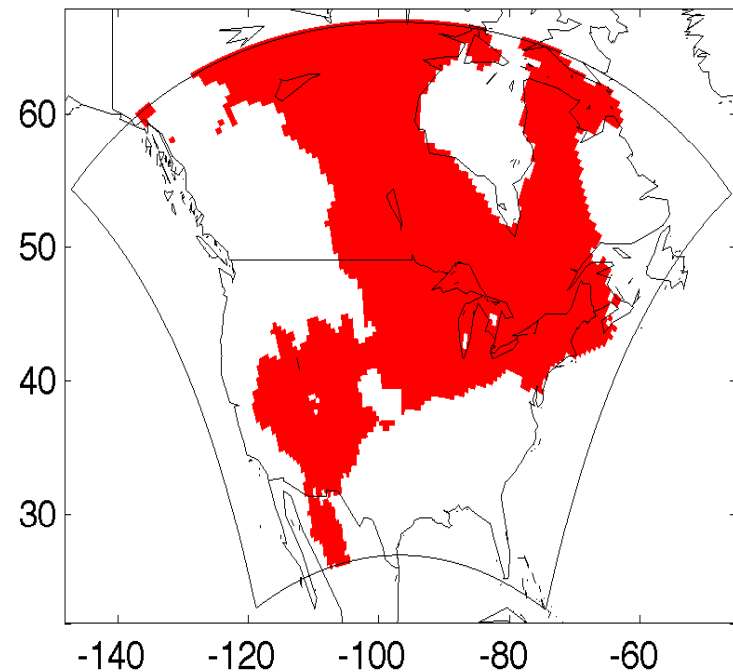
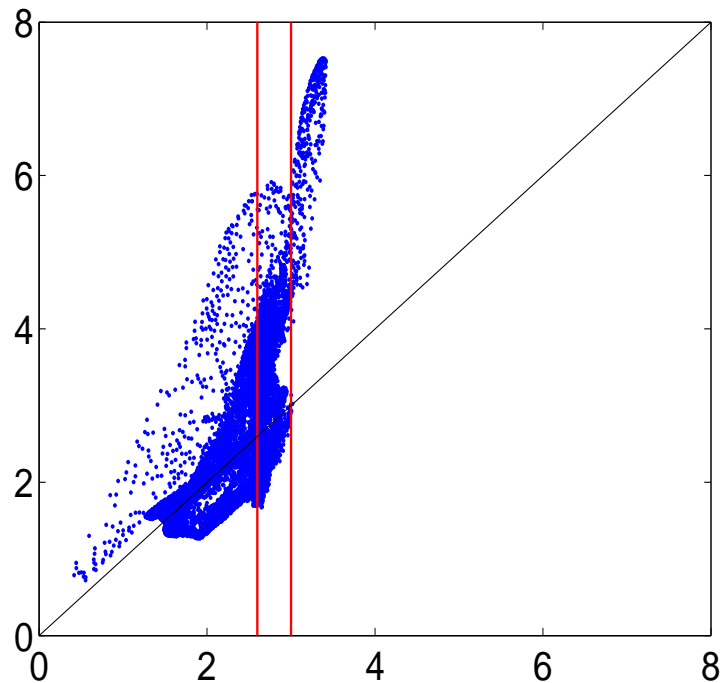
Linked Scatterplot of Winter vs. Overall



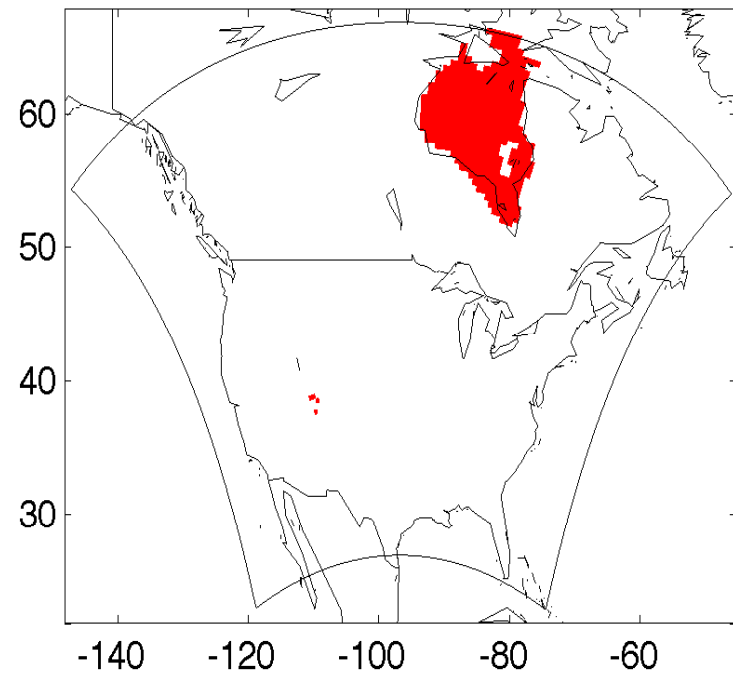
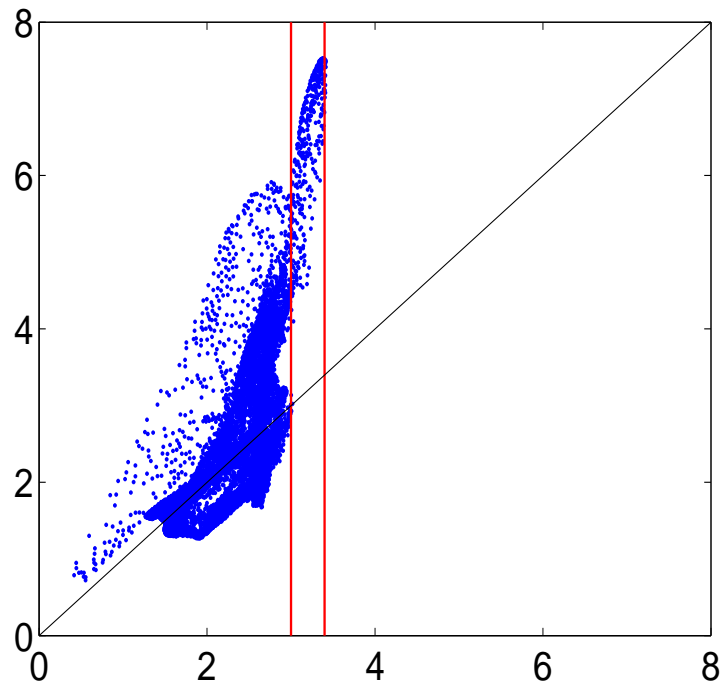
Linked Scatterplot of Winter vs. Overall



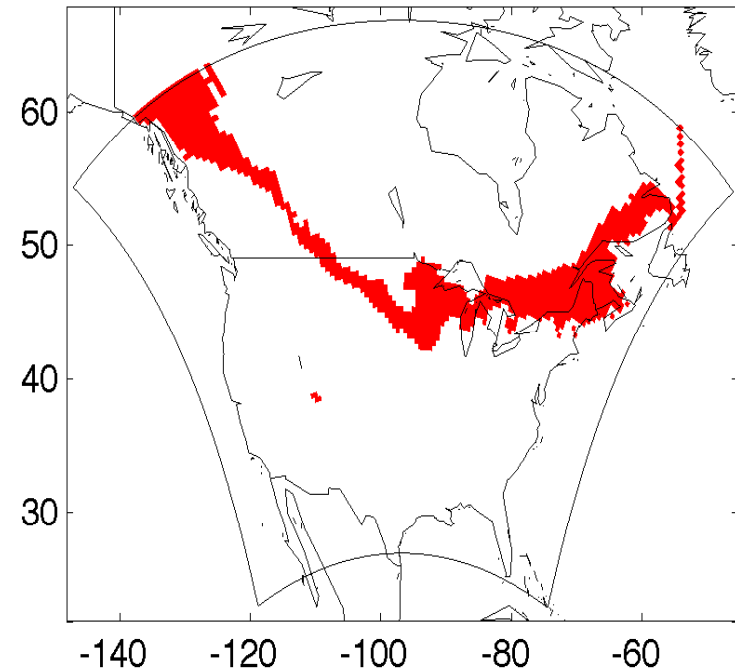
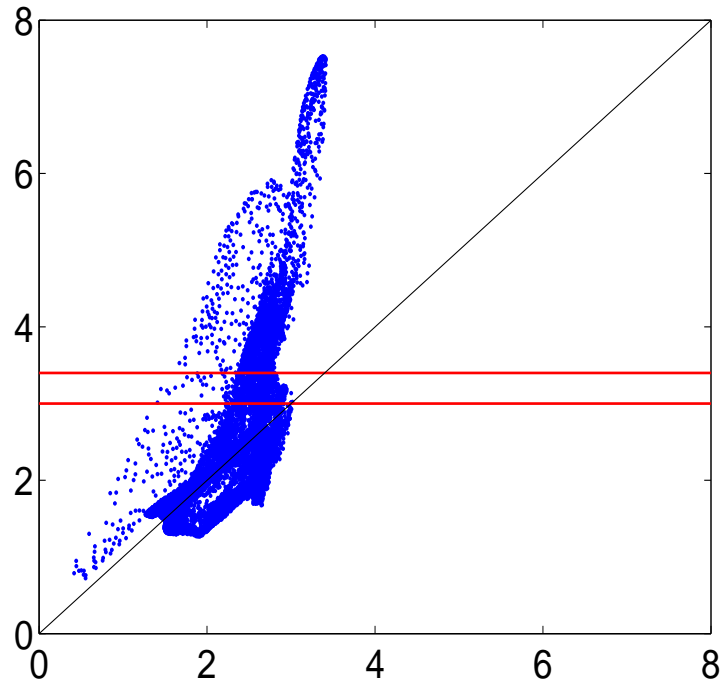
Linked Scatterplot of Winter vs. Overall



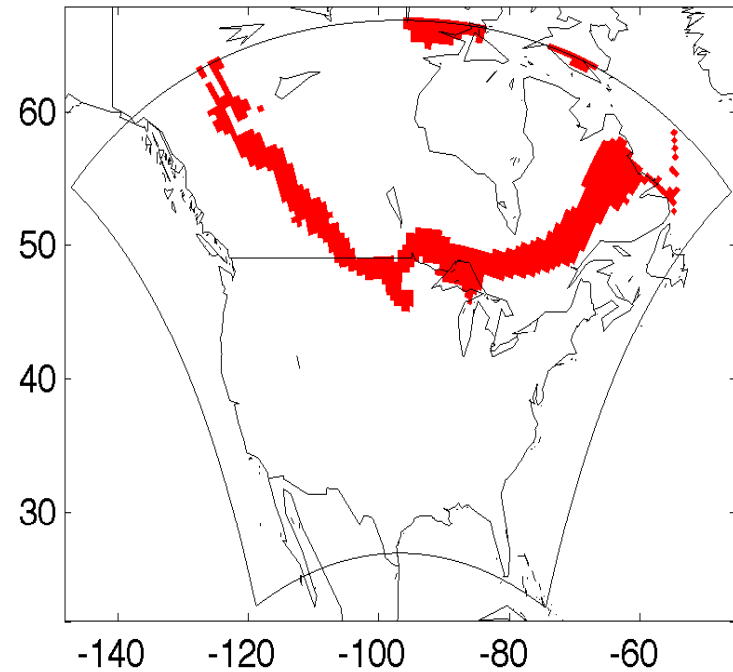
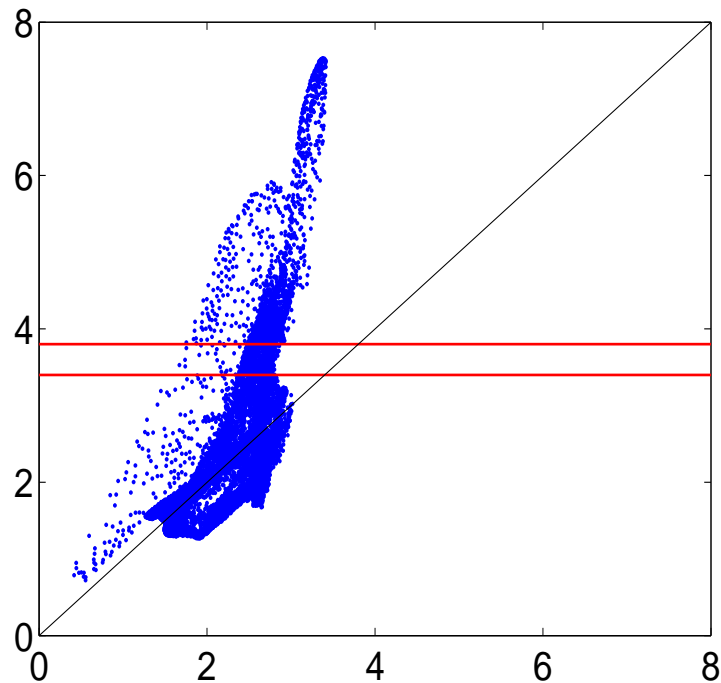
Linked Scatterplot of Winter vs. Overall



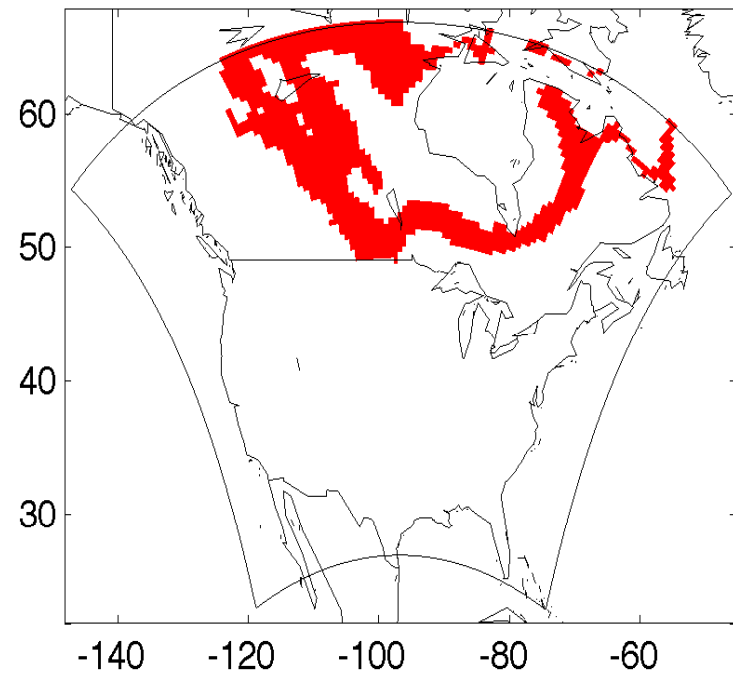
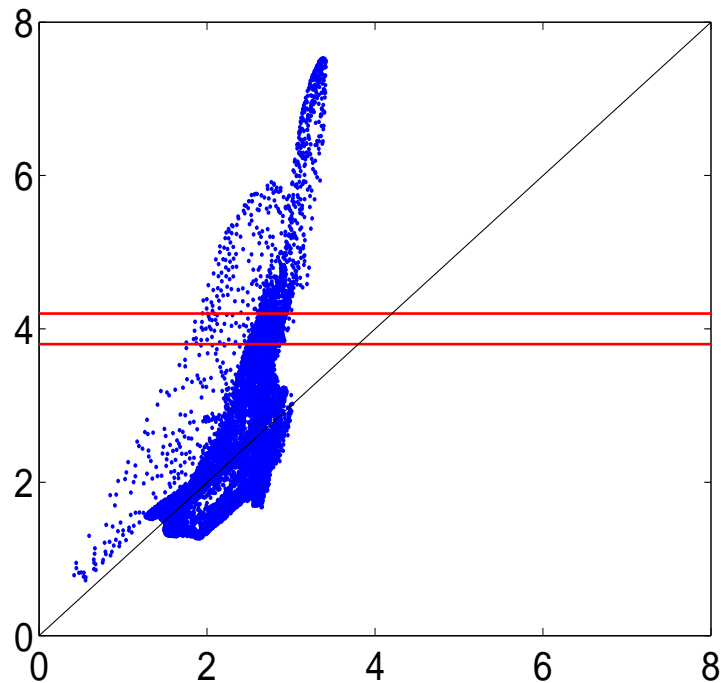
Linked Scatterplot of Winter vs. Overall



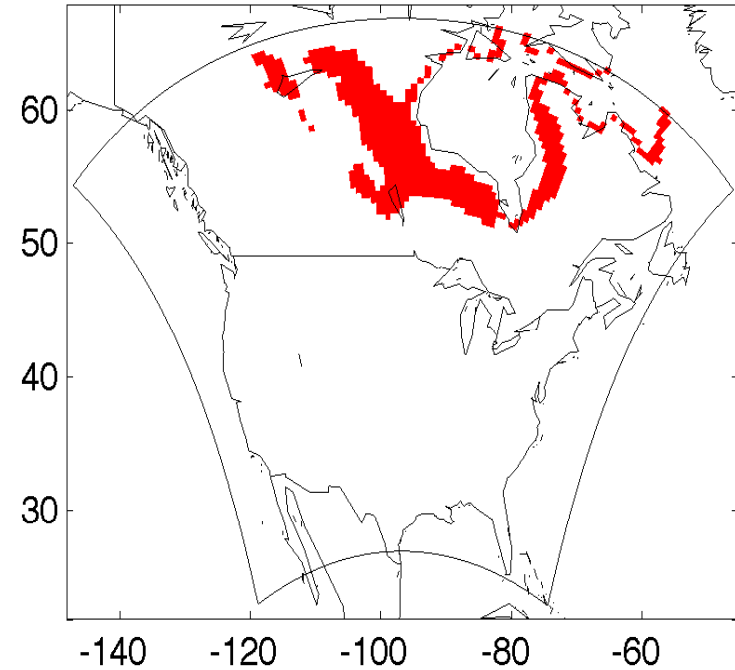
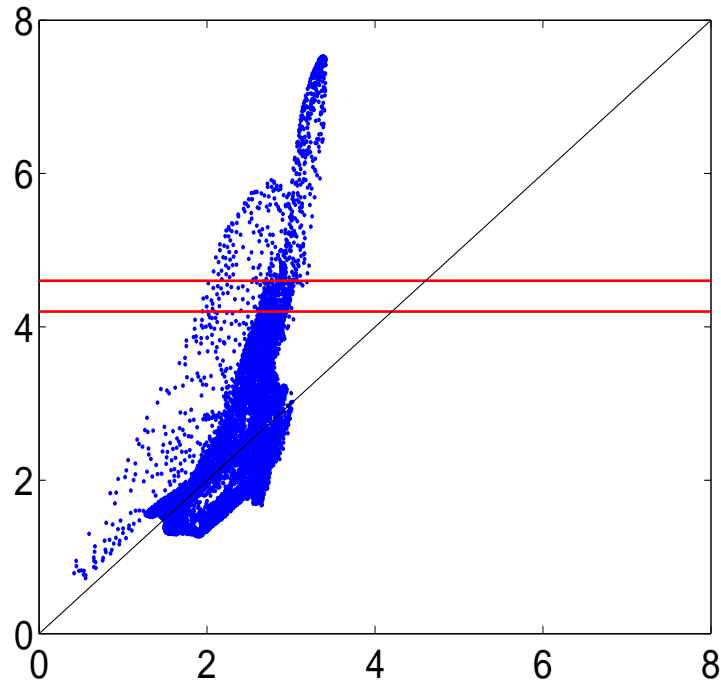
Linked Scatterplot of Winter vs. Overall



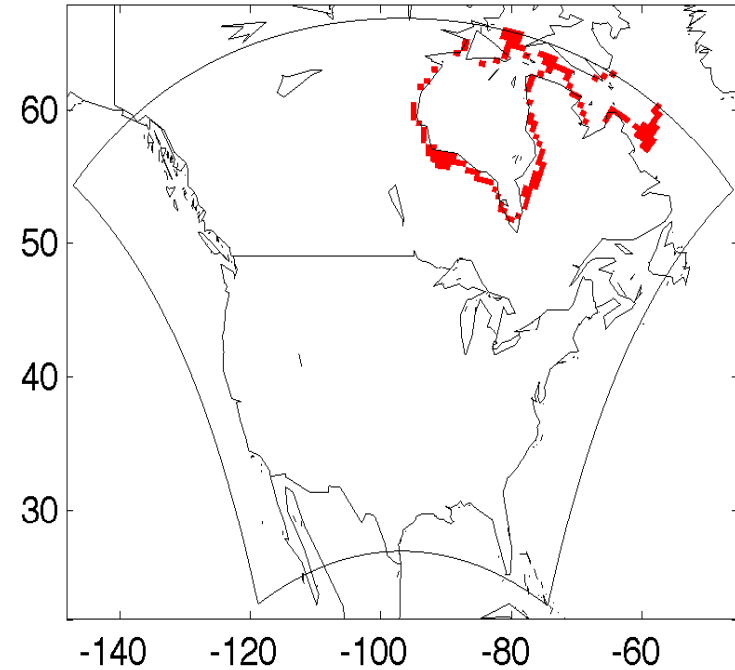
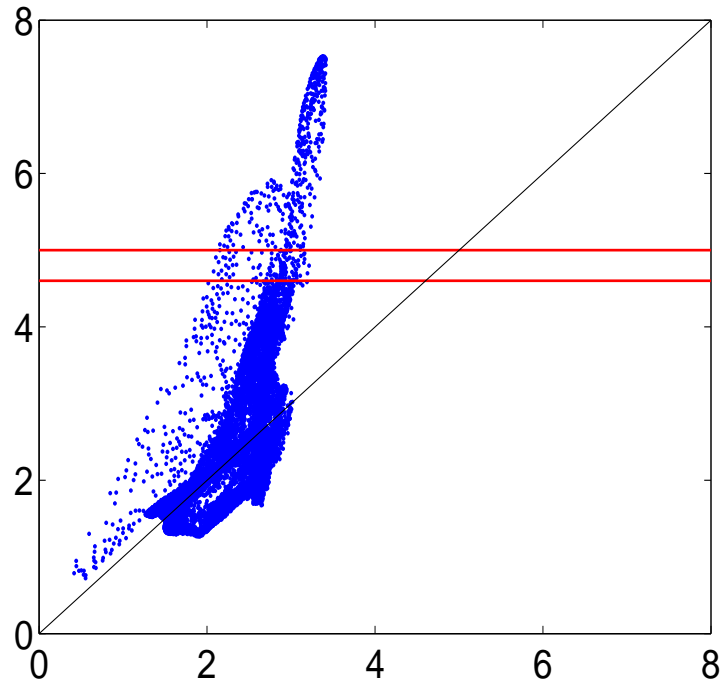
Linked Scatterplot of Winter vs. Overall



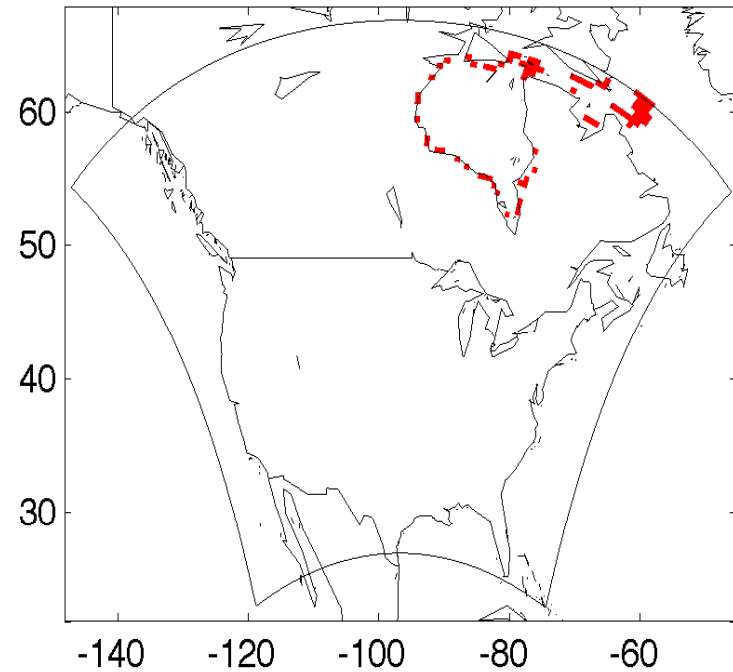
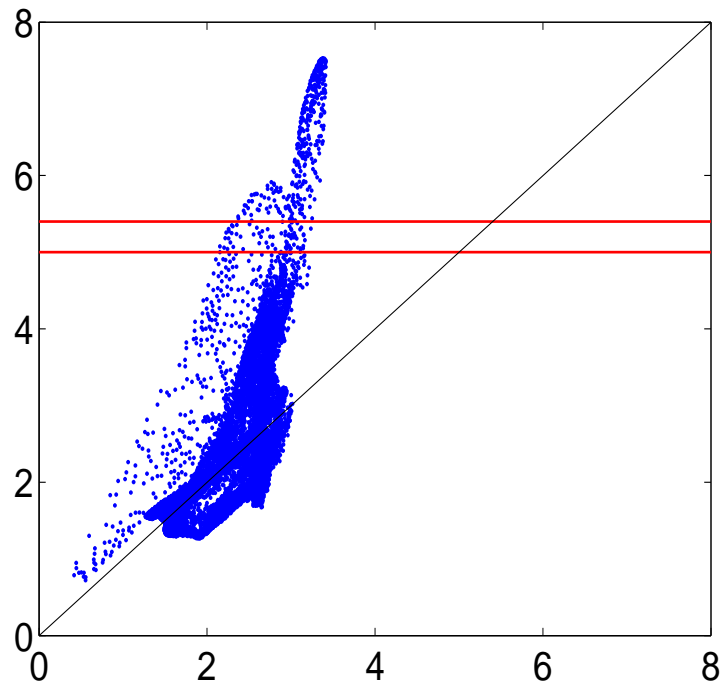
Linked Scatterplot of Winter vs. Overall



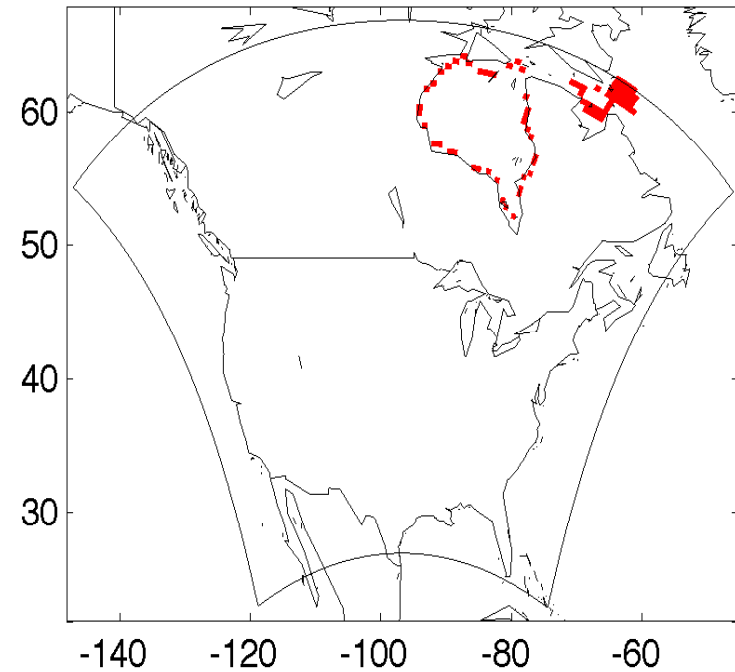
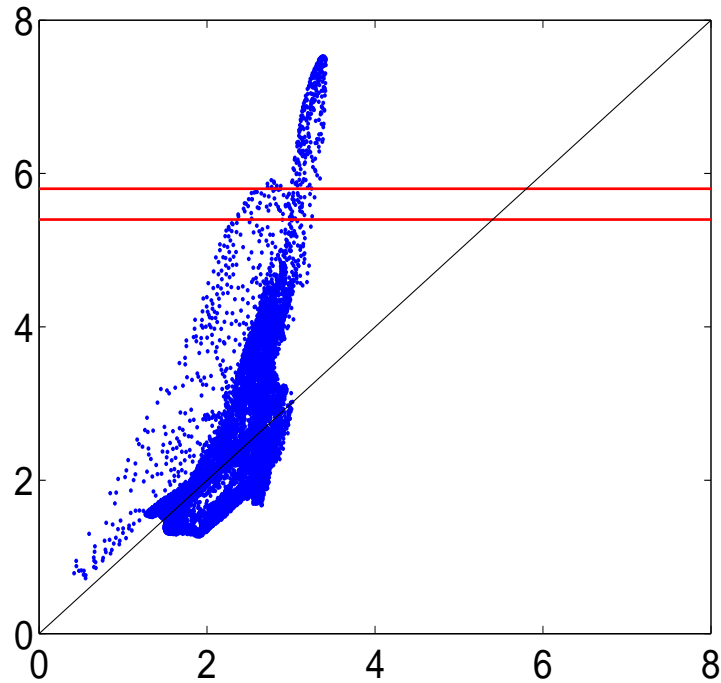
Linked Scatterplot of Winter vs. Overall



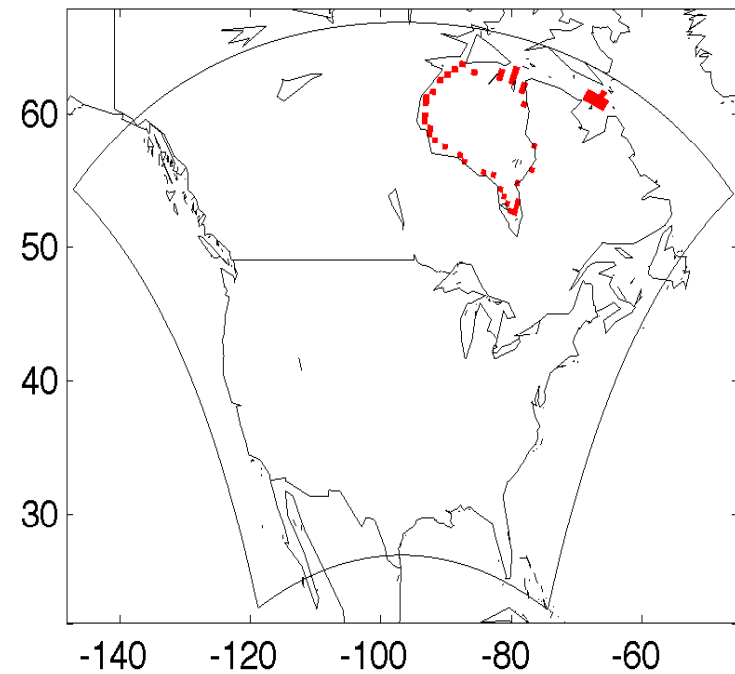
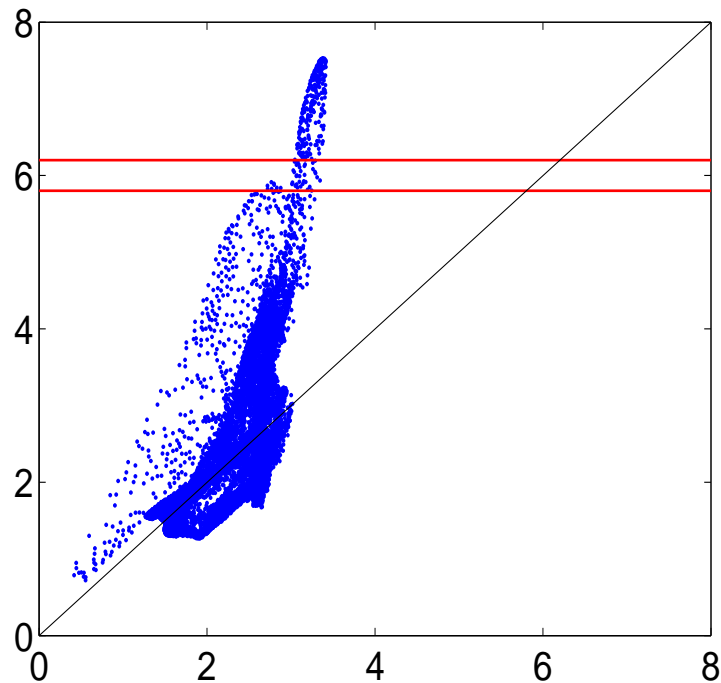
Linked Scatterplot of Winter vs. Overall



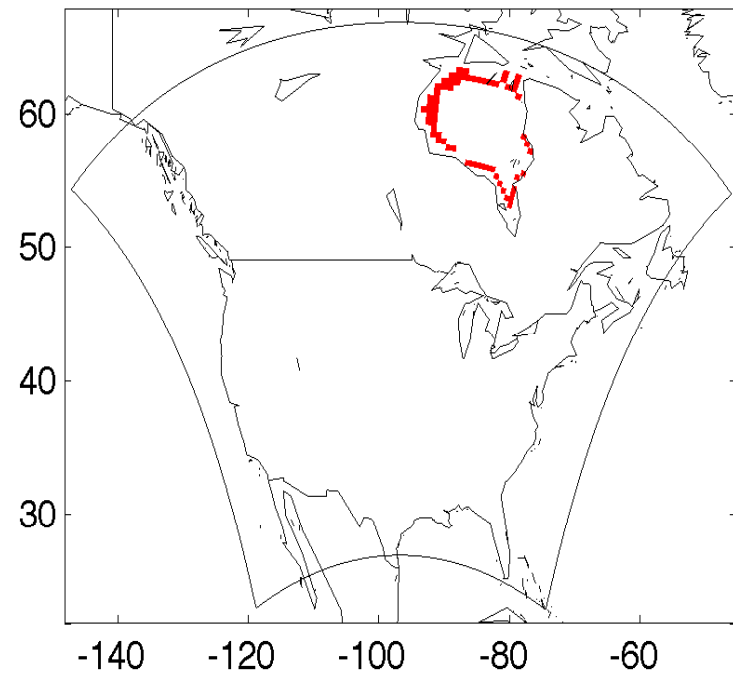
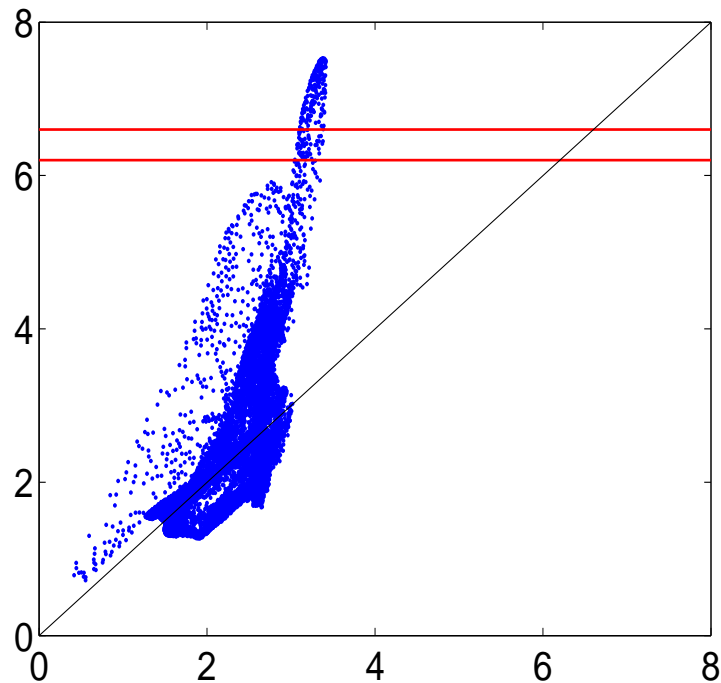
Linked Scatterplot of Winter vs. Overall



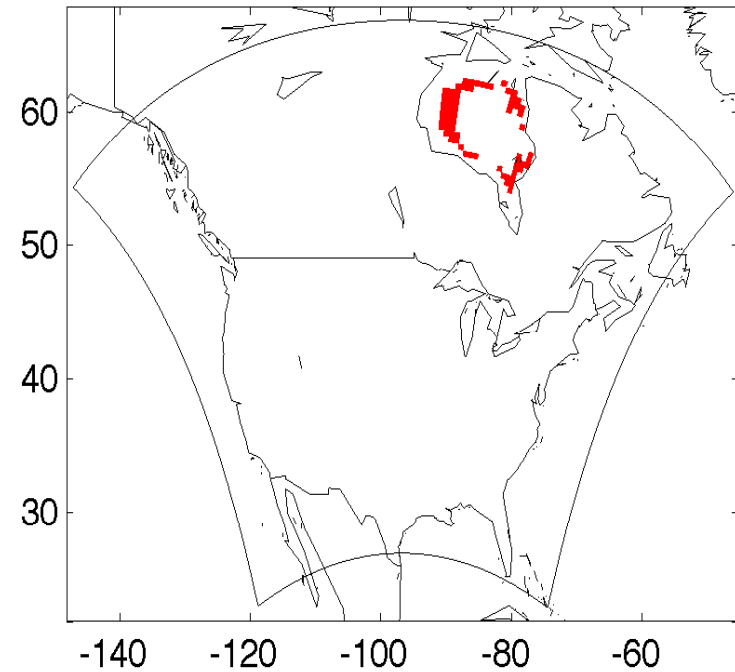
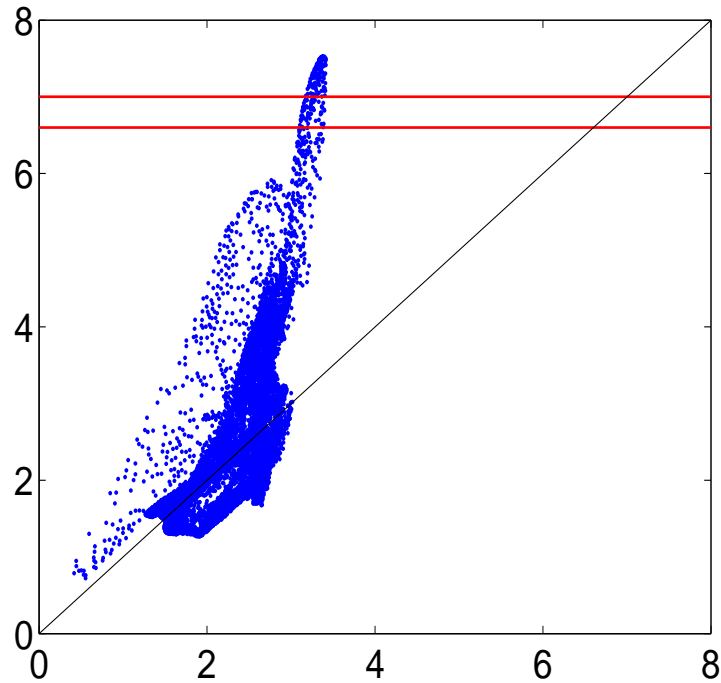
Linked Scatterplot of Winter vs. Overall



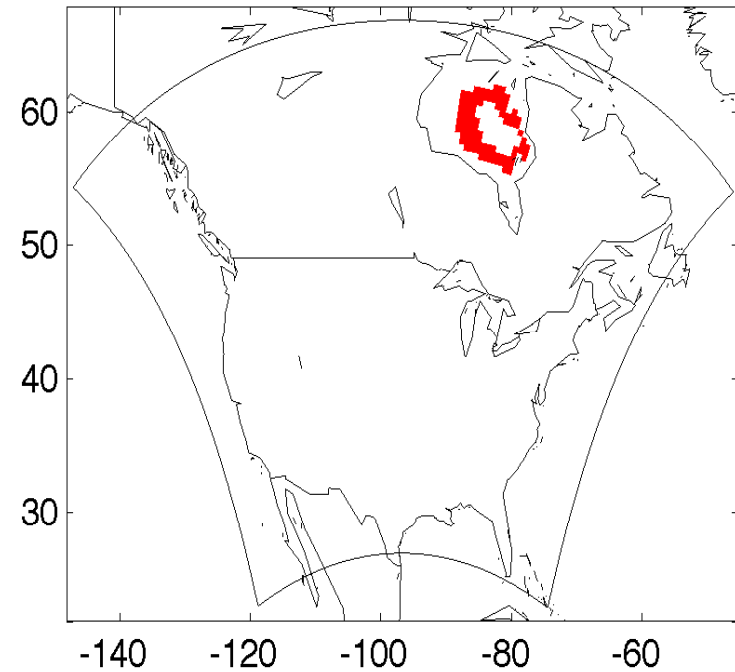
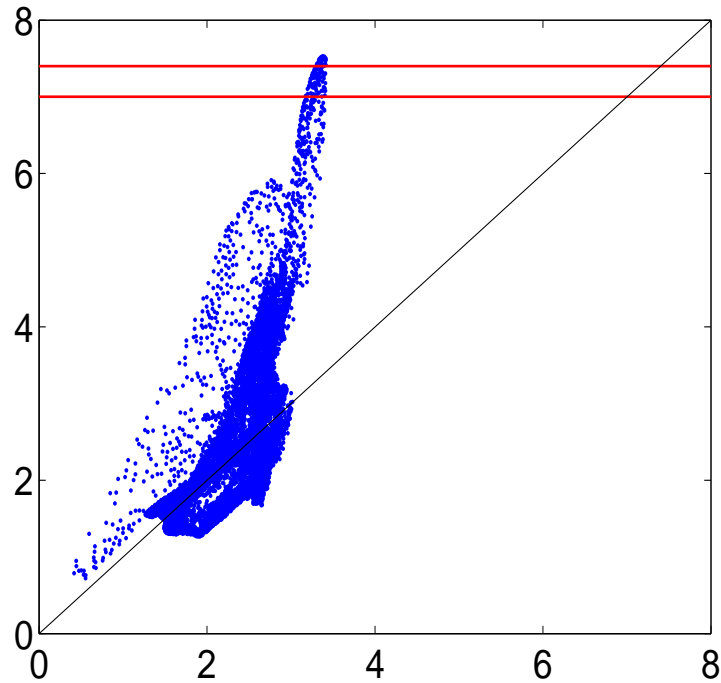
Linked Scatterplot of Winter vs. Overall



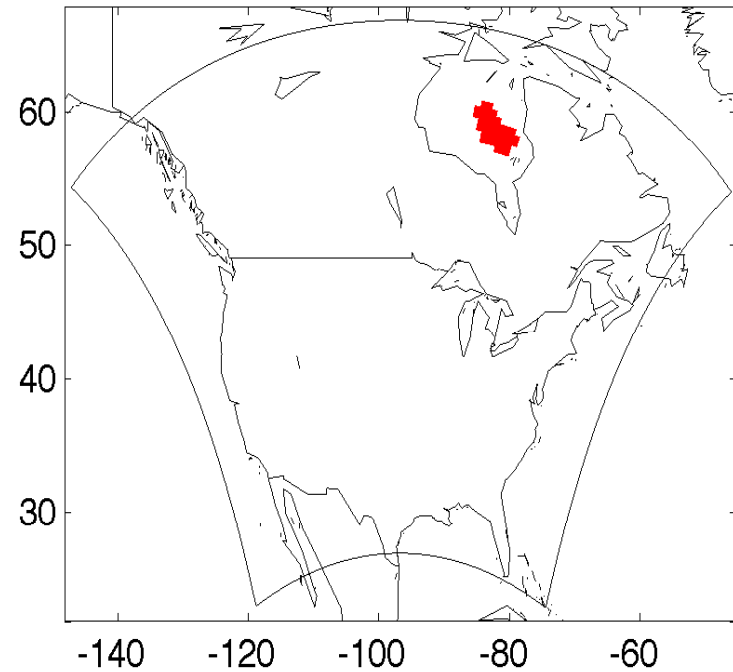
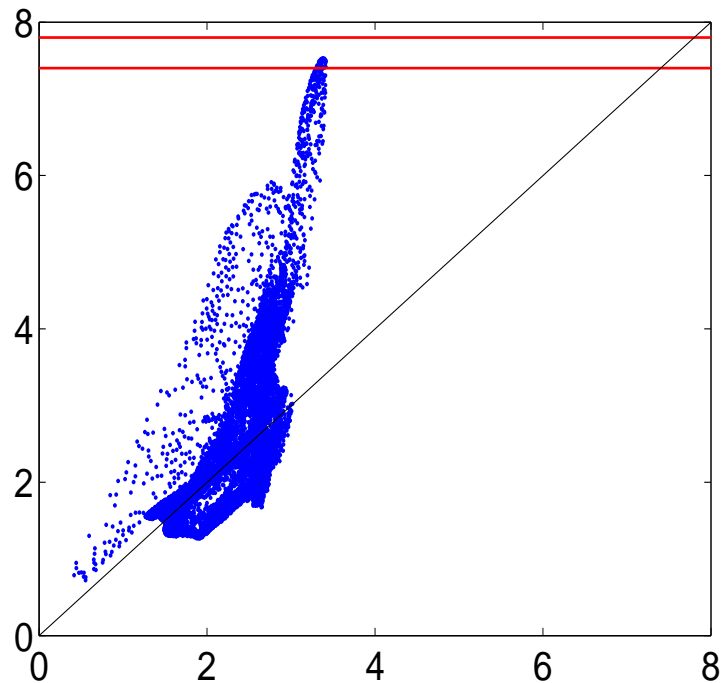
Linked Scatterplot of Winter vs. Overall



Linked Scatterplot of Winter vs. Overall



Linked Scatterplot of Winter vs. Overall



Summaries of Spatial Data, $\{X(\mathbf{s}_\ell) : \ell = 1, \dots, n\}$

- Spatial mean: $\bar{X} \equiv \sum_{\ell=1}^n X(\mathbf{s}_\ell)/n$
- Spatial variance: $S^2 \equiv \sum_{\ell=1}^n (X(\mathbf{s}_\ell) - \bar{X})^2/(n-1)$
- Spatial Cumulative Distribution Function (SCDF):

$$F(k) \equiv \sum_{\ell=1}^n I(X(\mathbf{s}_\ell) \leq k)/n; \quad -\infty < k < \infty$$

(e.g., Lahiri et al., 1999)

- Spatial Proportion Over Threshold (SPOT) function:

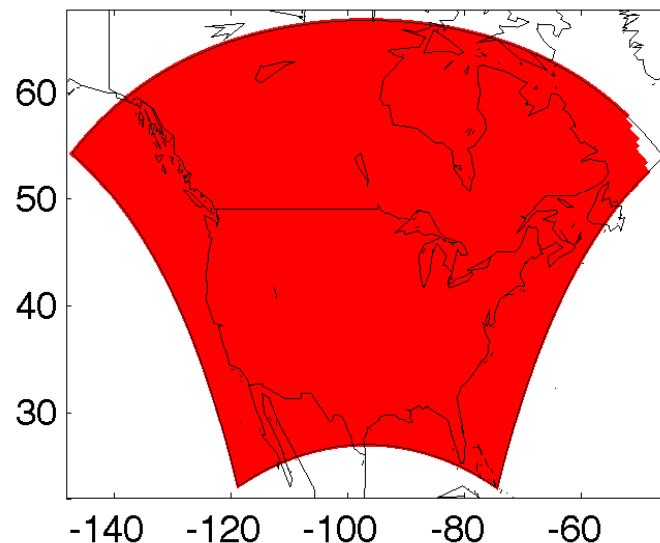
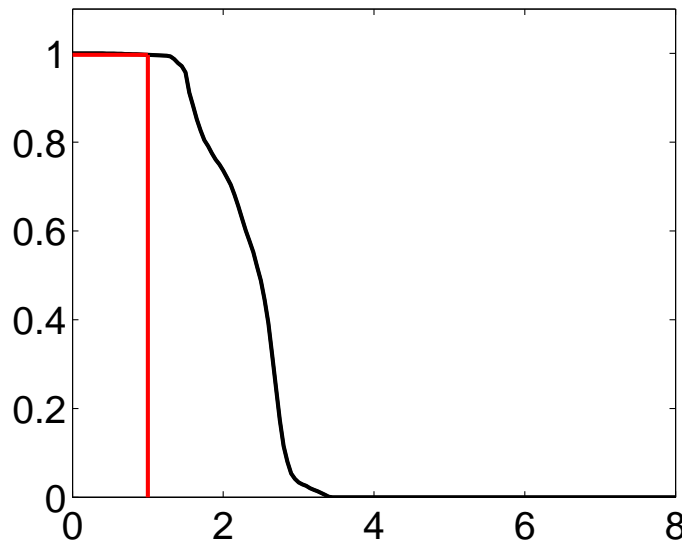
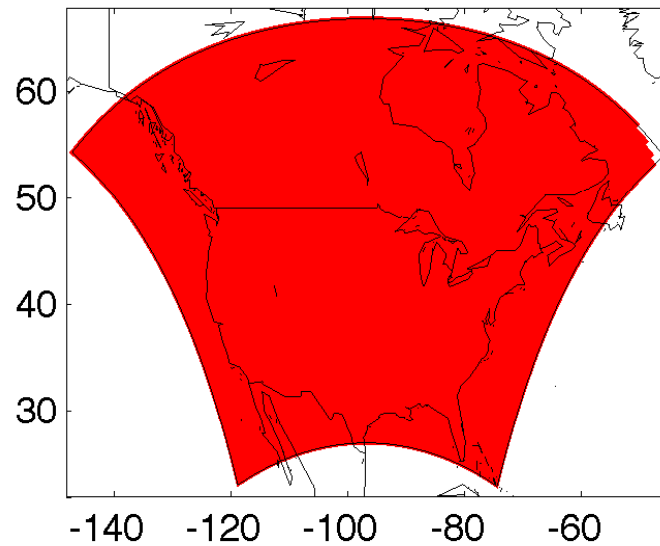
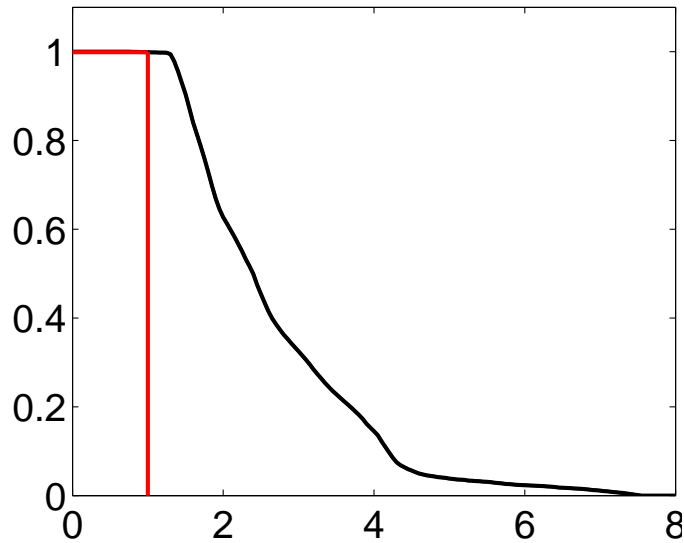
$$T(k) \equiv \sum_{\ell=1}^n I(X(\mathbf{s}_\ell) > k)/n; \quad -\infty < k < \infty$$

$T(\cdot)$ emphasises the **proportion of pixels above a threshold**. Notice that $T(k) = 1 - F(k)$.

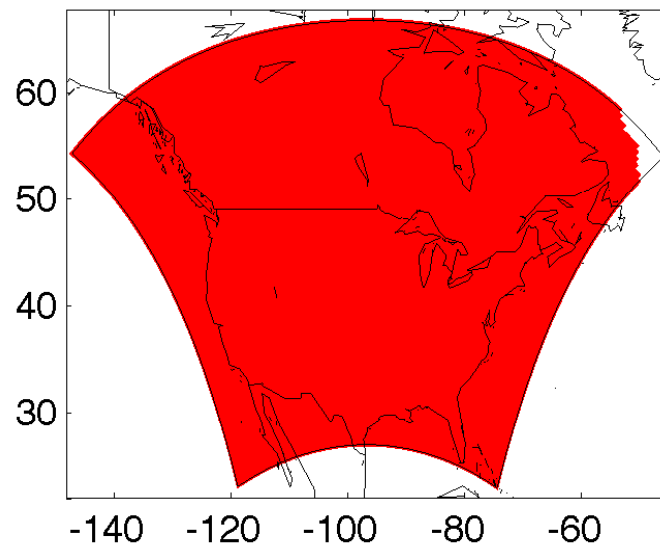
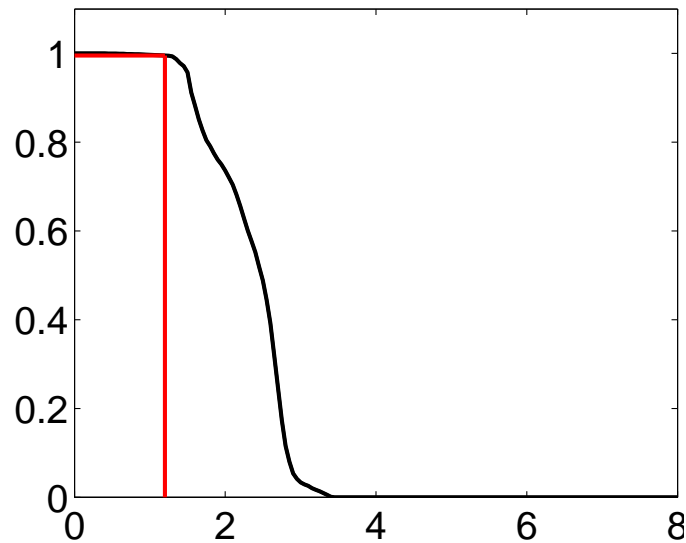
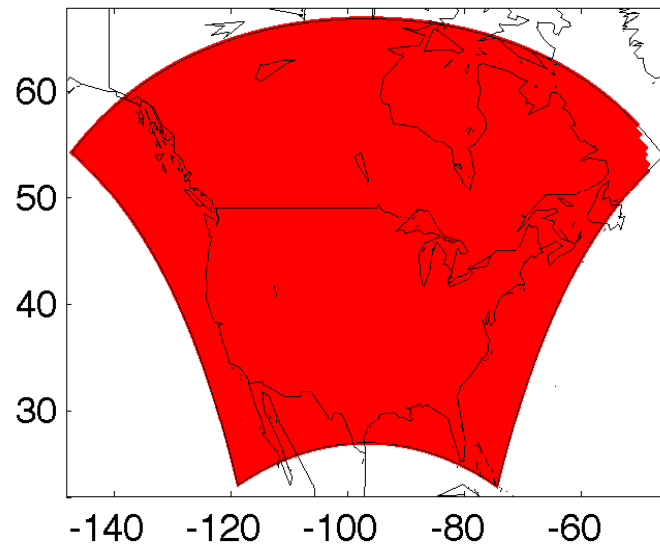
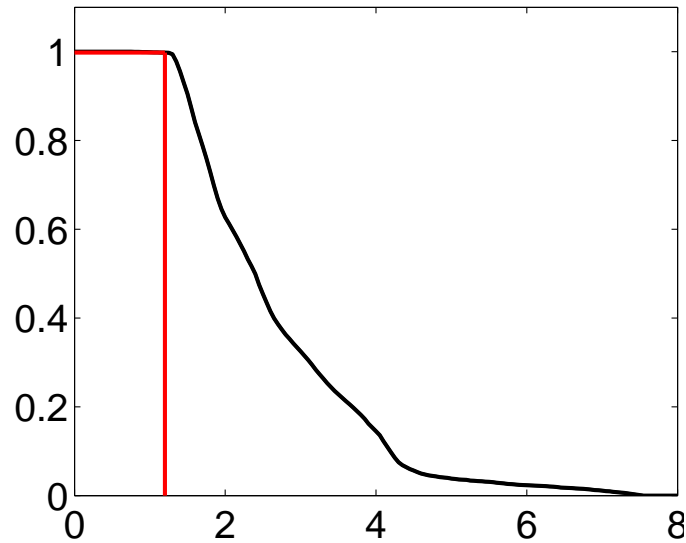
SPOT-Function Plots Linked to “Geography”

- Keep track of the pixels $\{s_\ell : X(s_\ell) > k\}$ that are above the threshold k
- For a given k , plot $T(k)$ vs. k and a map of the pixels where $I(X(s_\ell) > k) = 1$.
- Vary k from small thresholds to large thresholds and observe the evolving geographic patterns
- Apply this idea to $D_{.4}$ (winter) compared to $D_{..}$ (overall)
- On the next sequence of slides, linked SPOT-function plots are shown for temperature change in the winter (top panel) and overall (bottom panel)

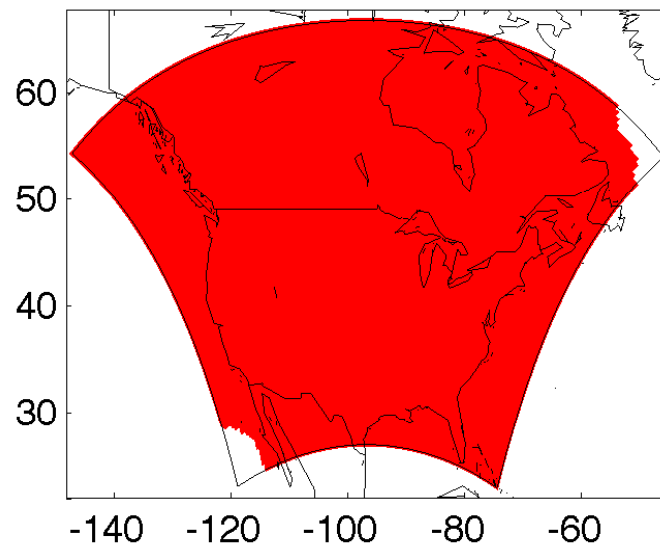
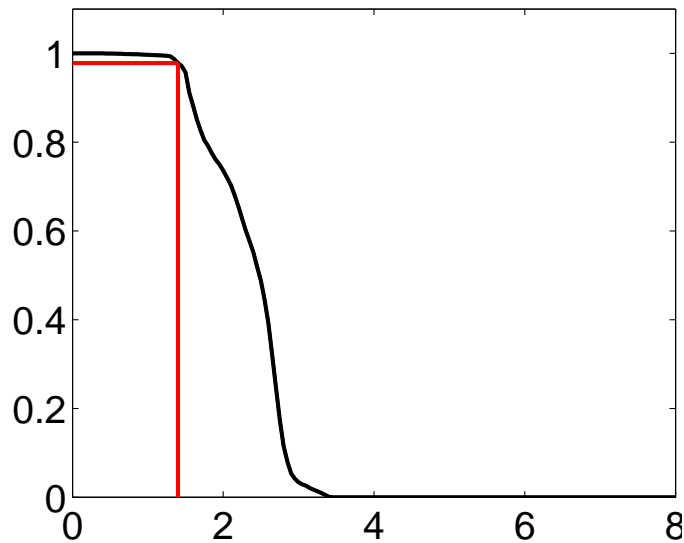
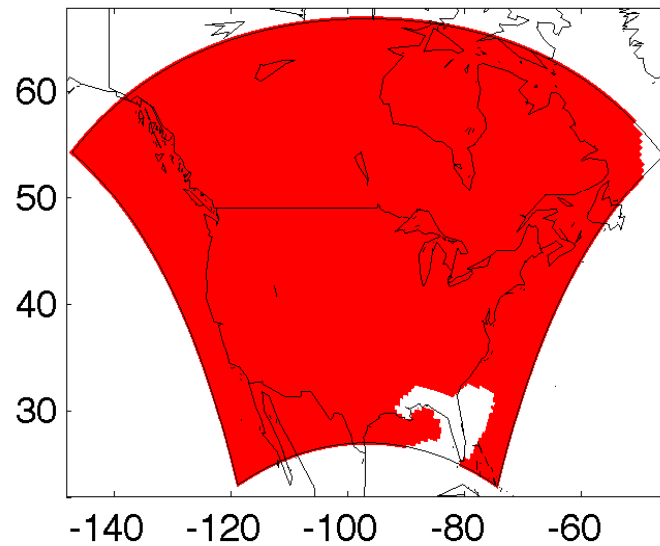
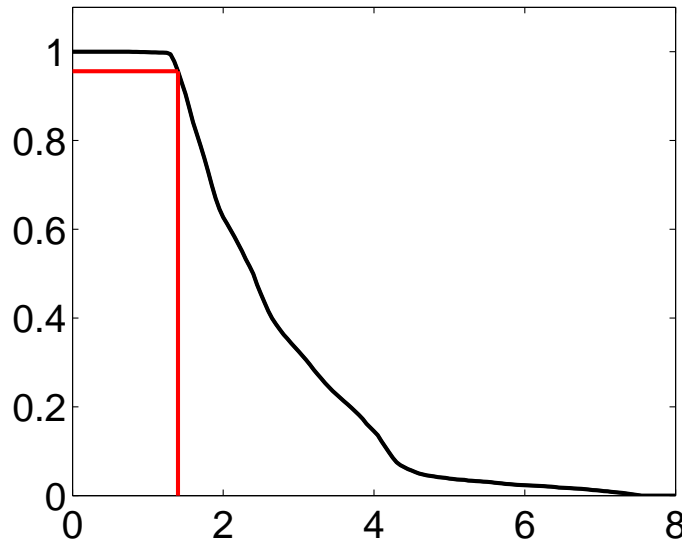
Linked SPOT-Function Plots, for $k = 1.0^\circ C$



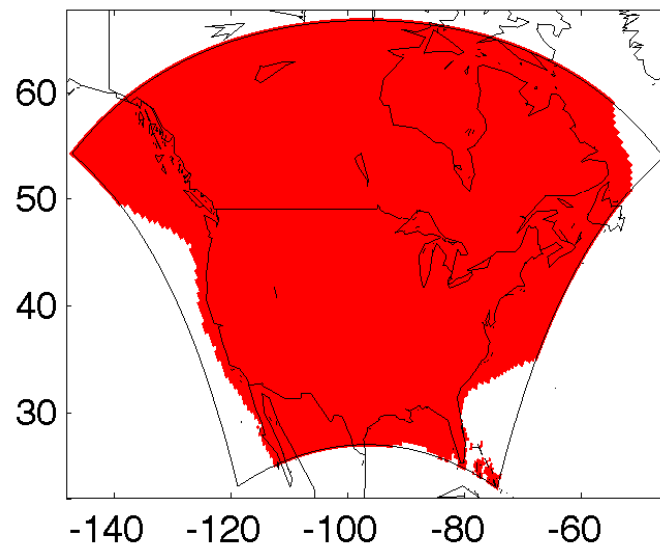
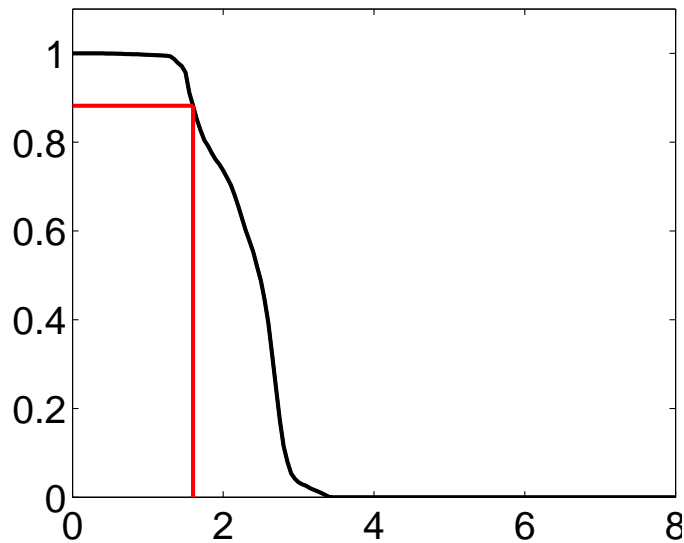
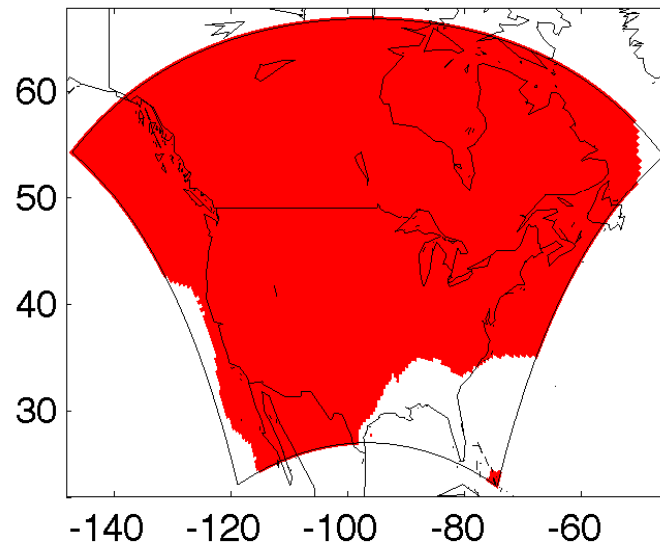
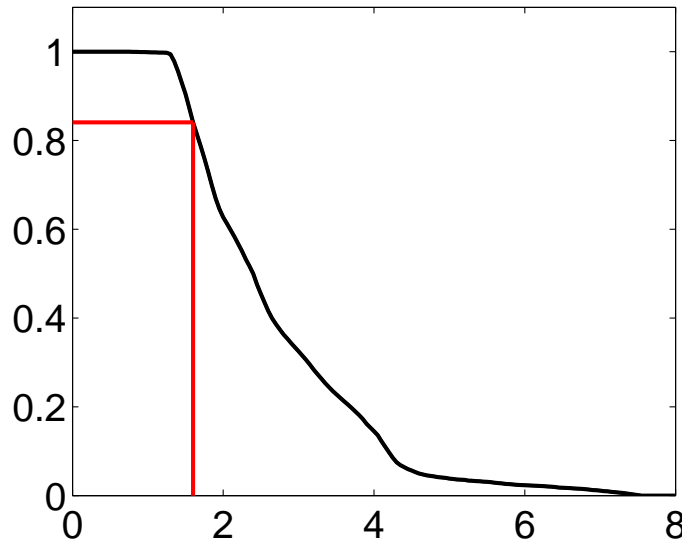
Linked SPOT-Function Plots, for $k = 1.2^\circ C$



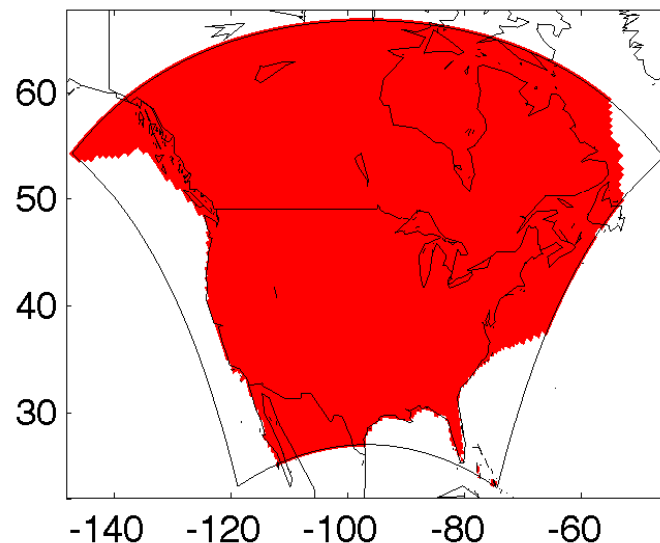
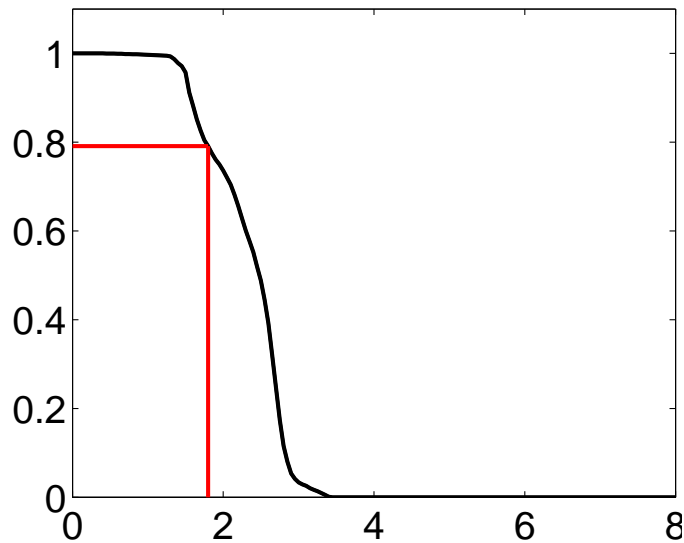
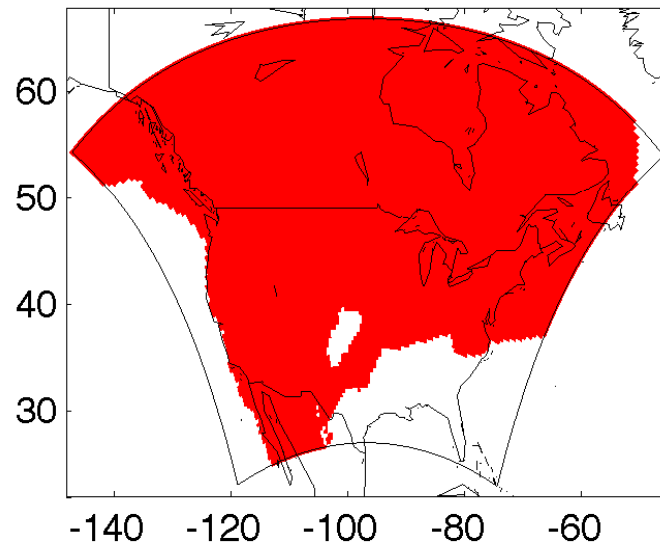
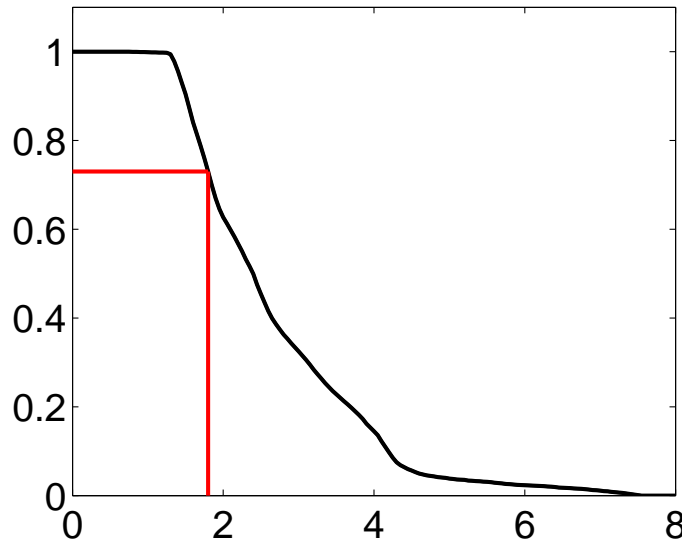
Linked SPOT-Function Plots, for $k = 1.4^\circ\text{C}$



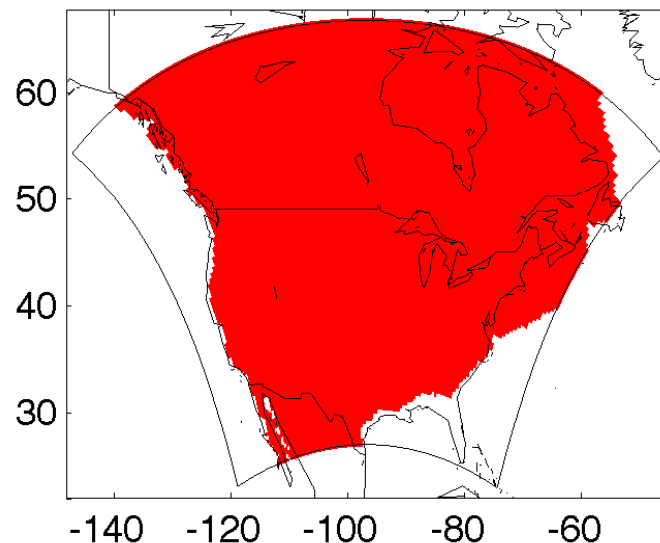
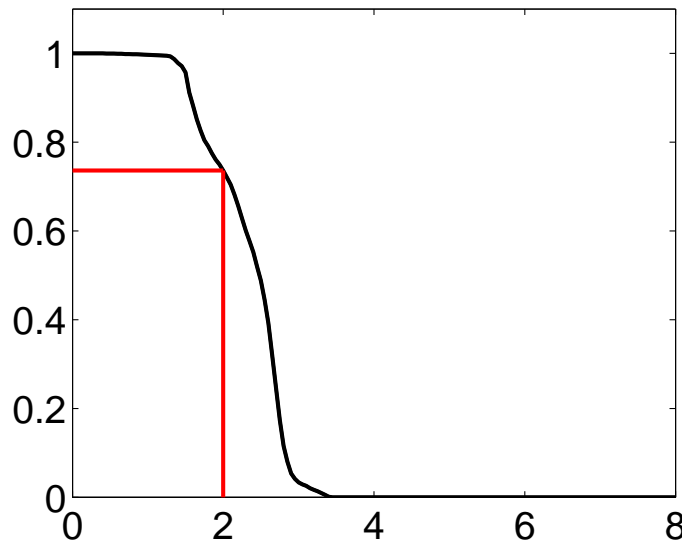
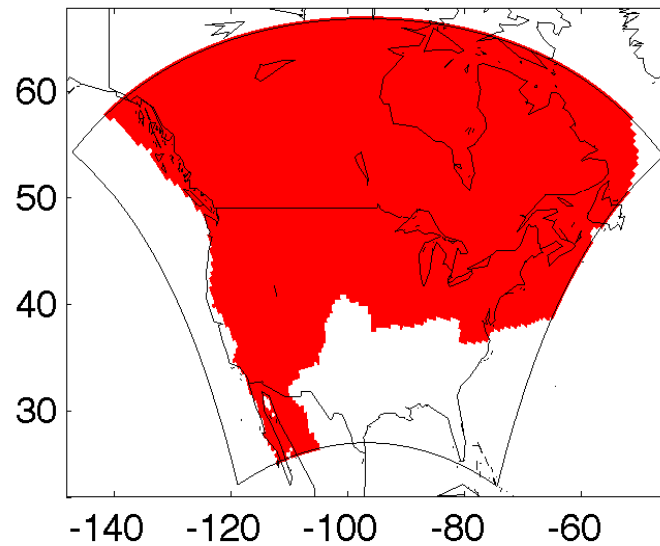
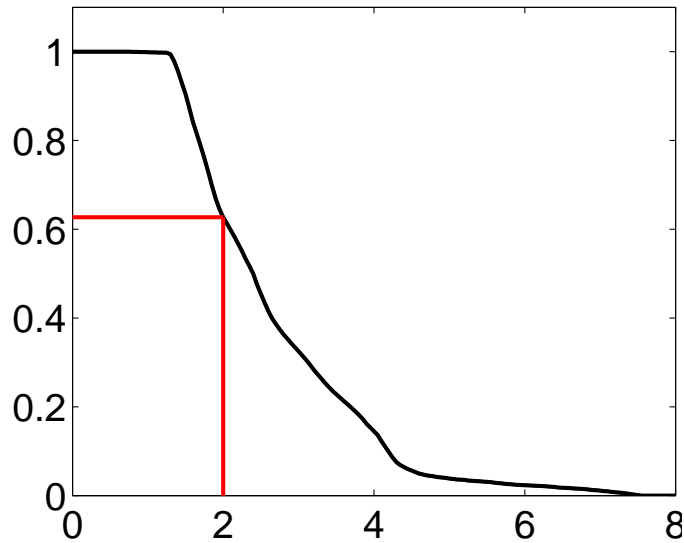
Linked SPOT-Function Plots, for $k = 1.6^\circ C$



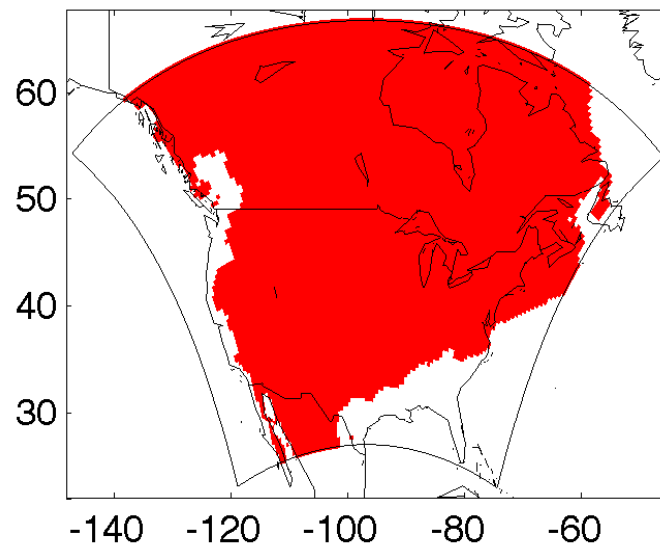
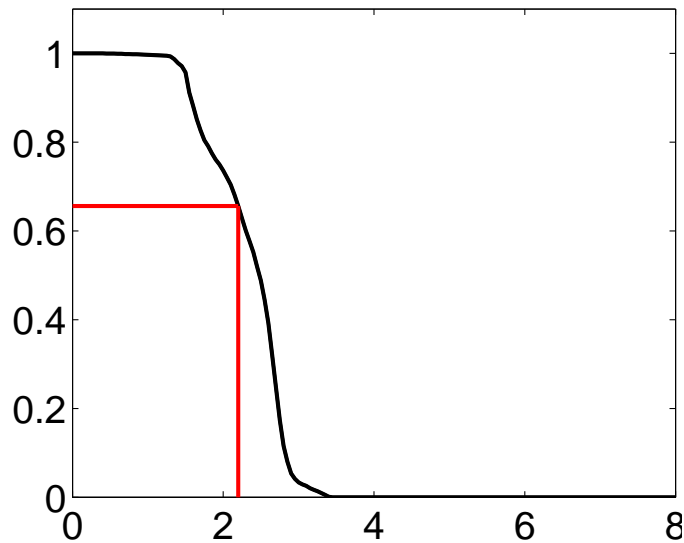
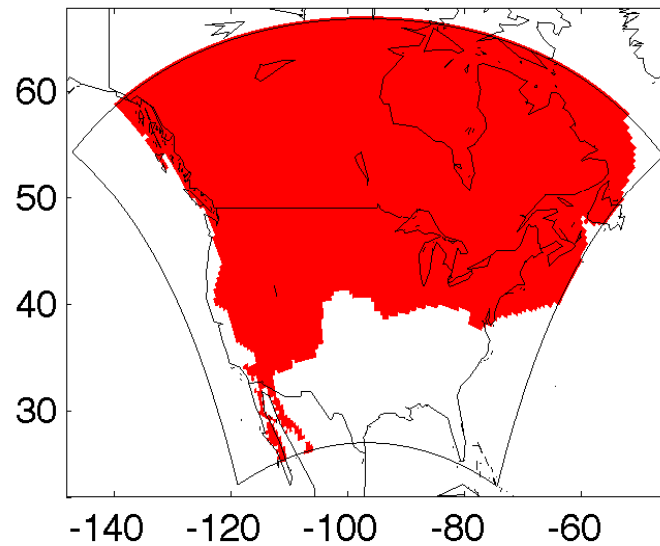
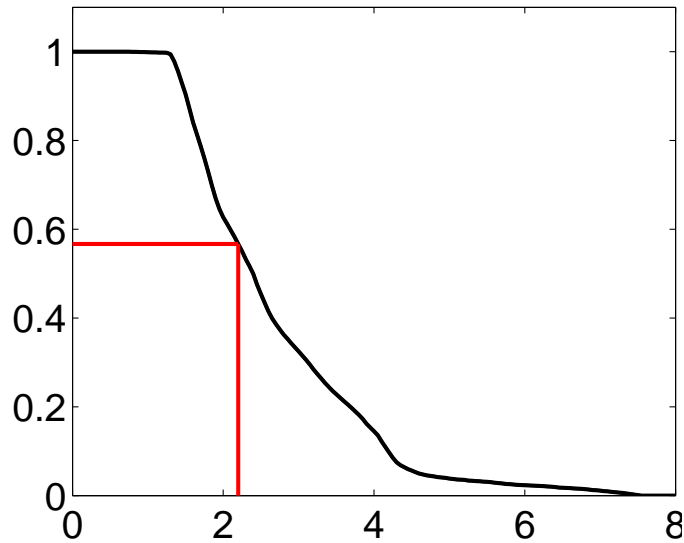
Linked SPOT-Function Plots, for $k = 1.8^\circ\text{C}$



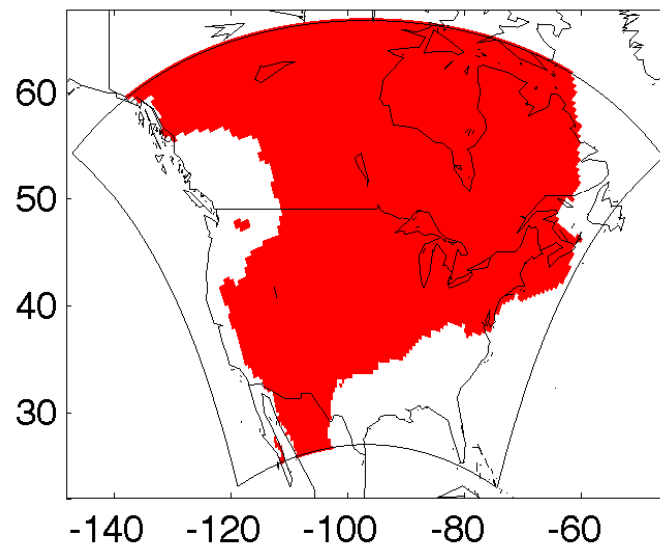
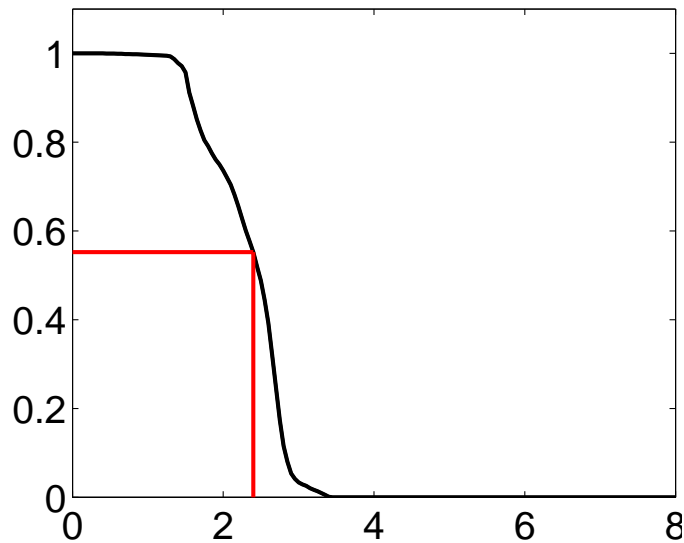
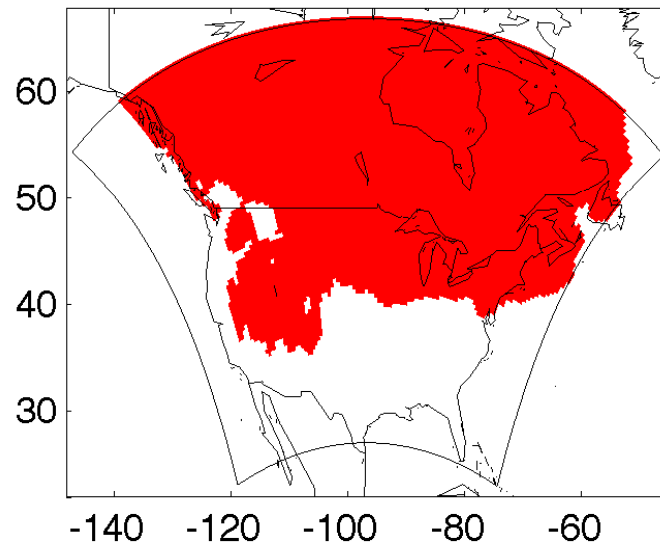
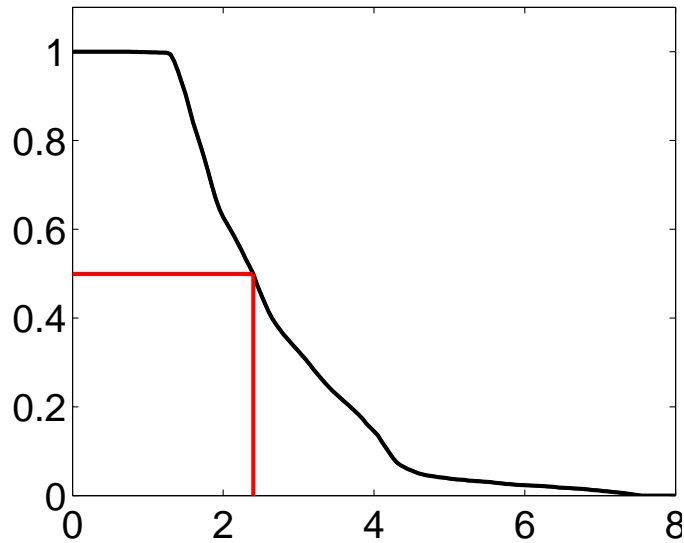
Linked SPOT-Function Plots, for $k = 2.0^\circ C$



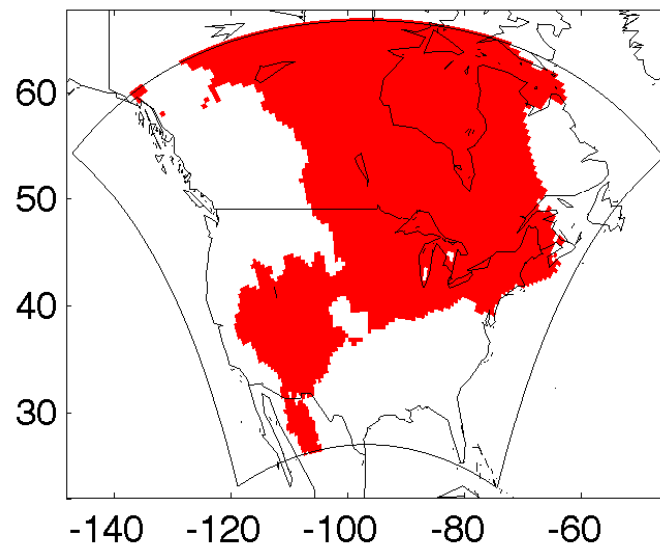
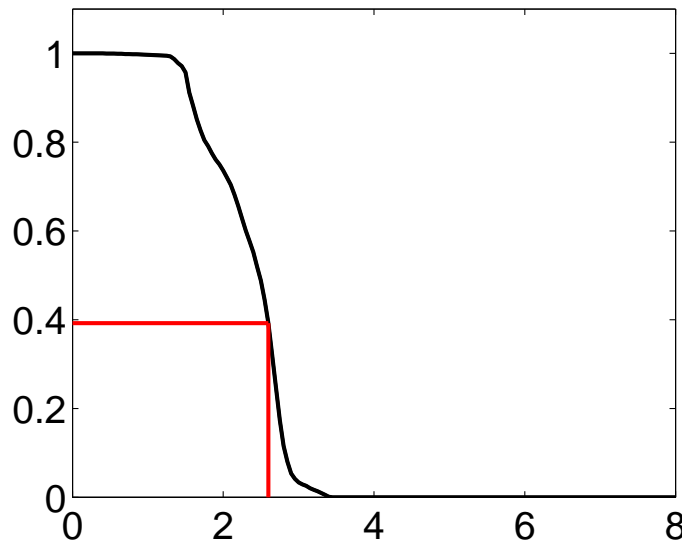
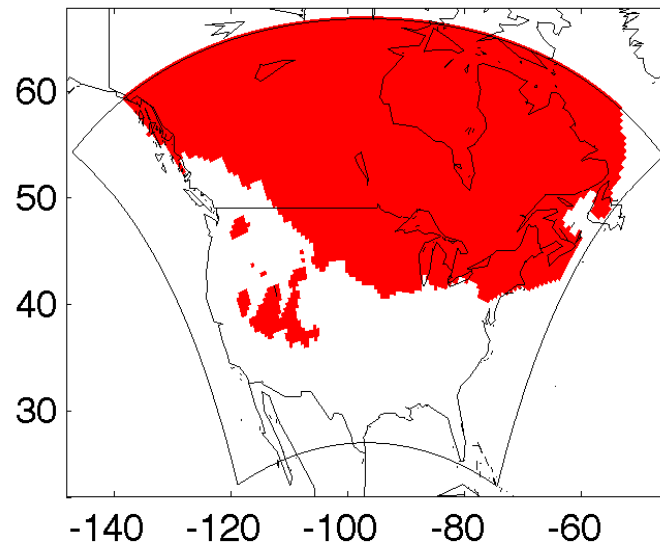
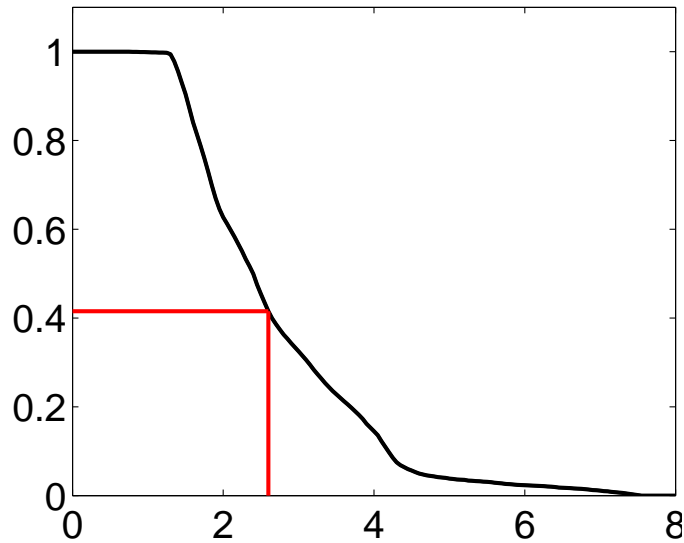
Linked SPOT-Function Plots, for $k = 2.2^\circ C$



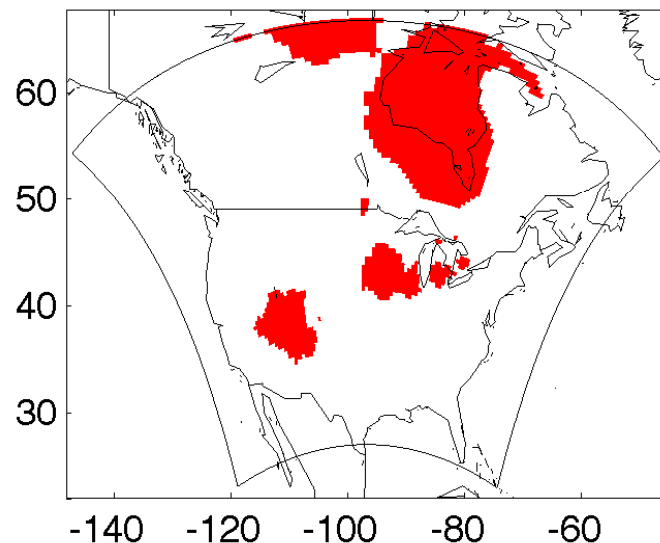
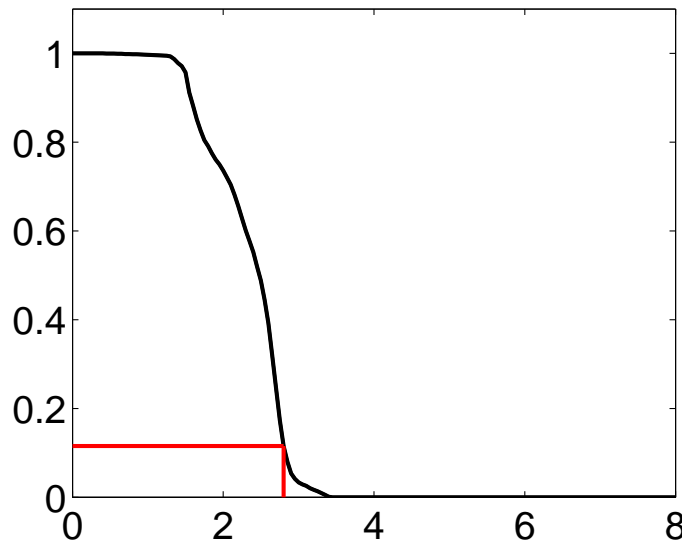
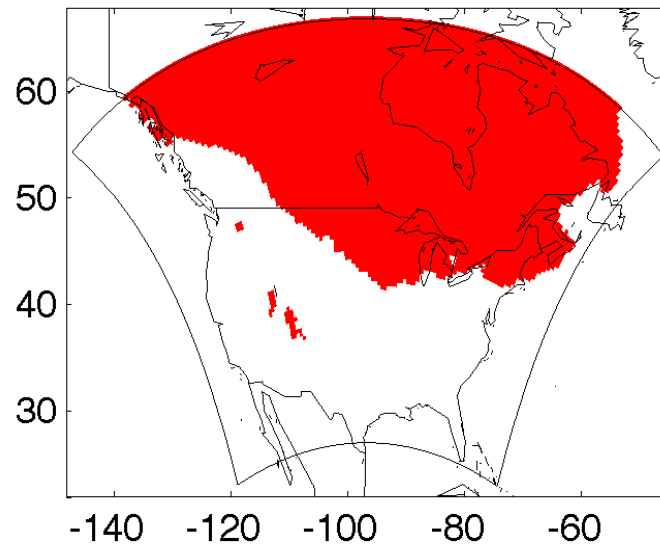
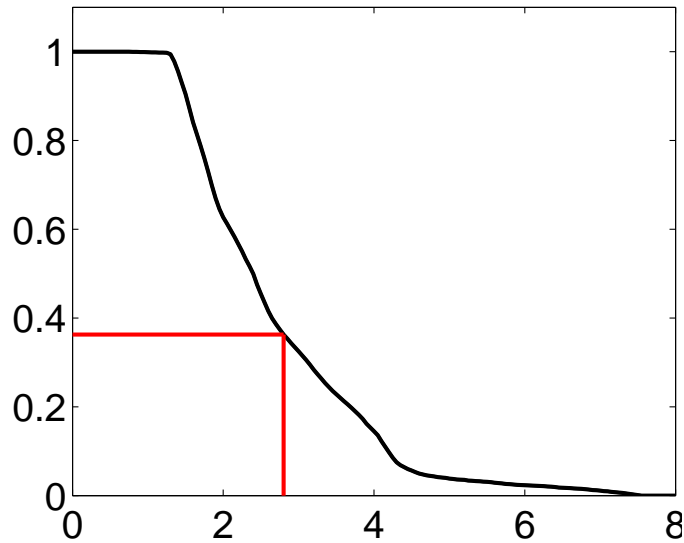
Linked SPOT-Function Plots, for $k = 2.4^\circ\text{C}$



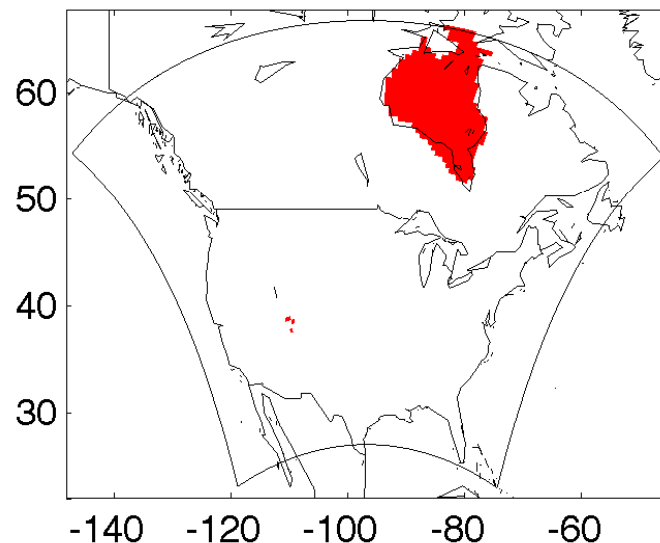
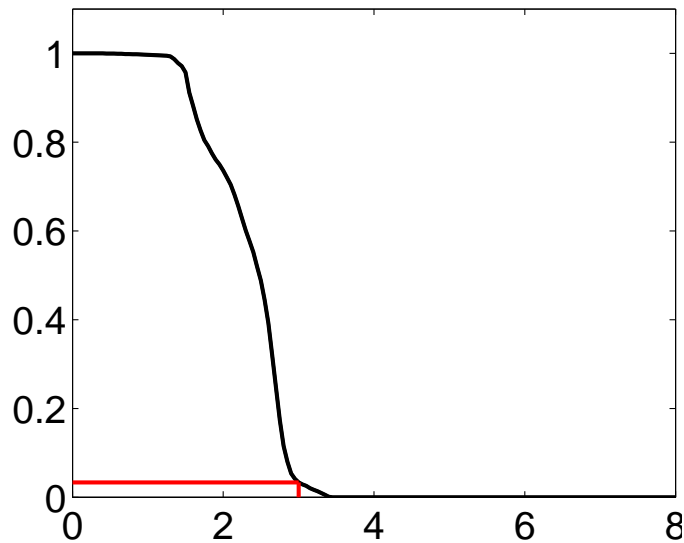
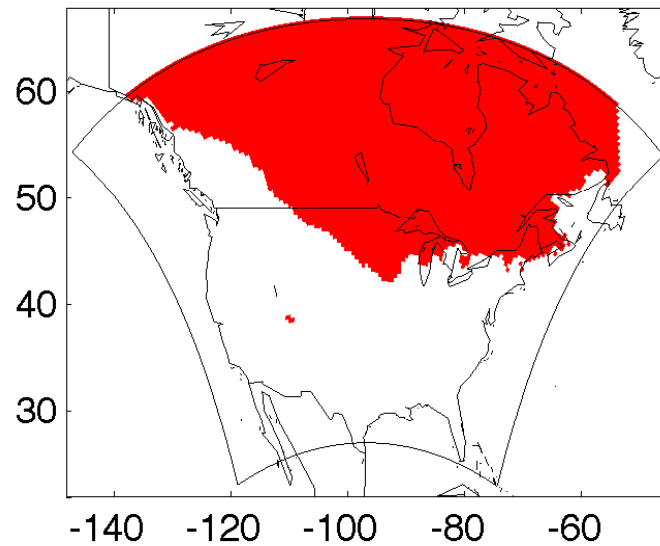
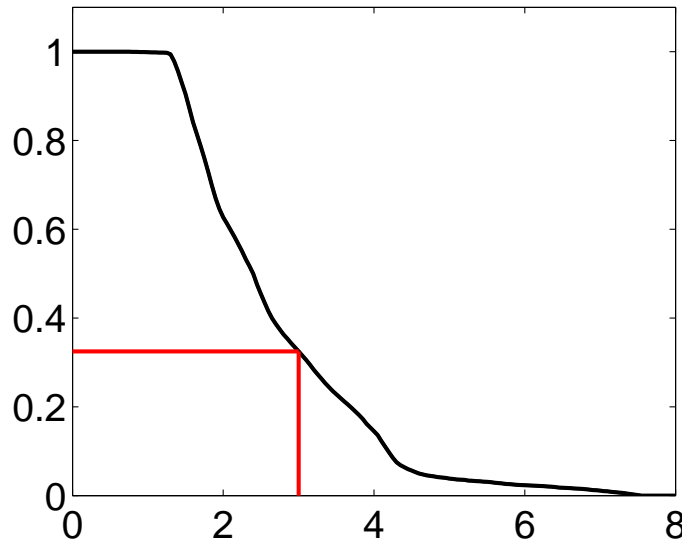
Linked SPOT-Function Plots, for $k = 2.6^\circ C$



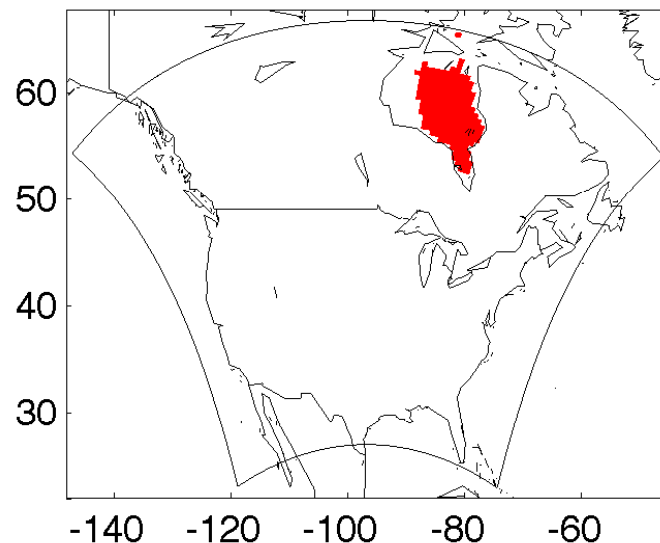
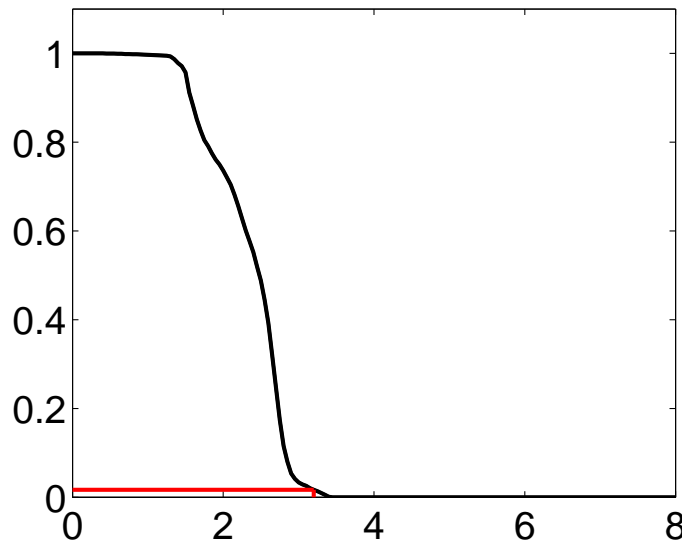
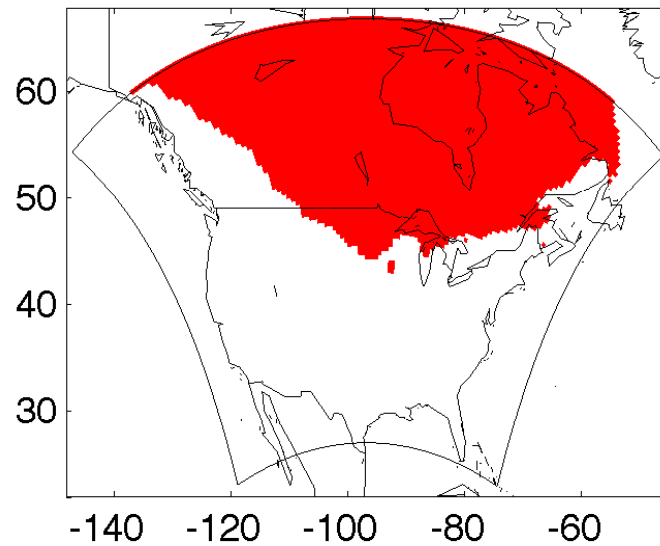
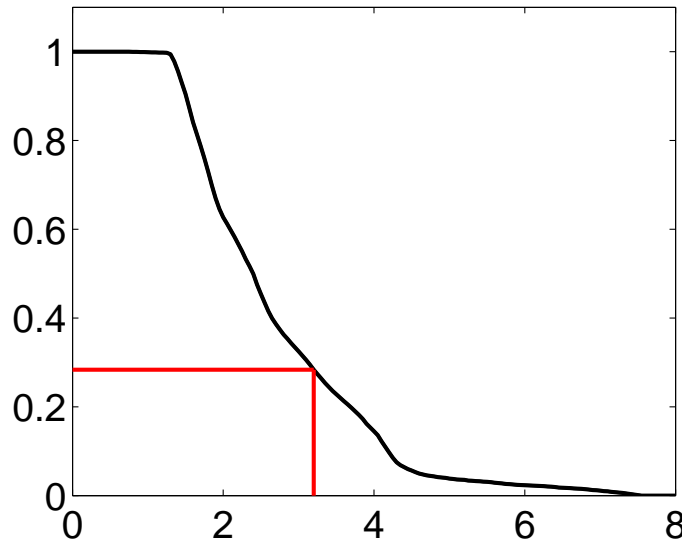
Linked SPOT-Function Plots, for $k = 2.8 \circ C$



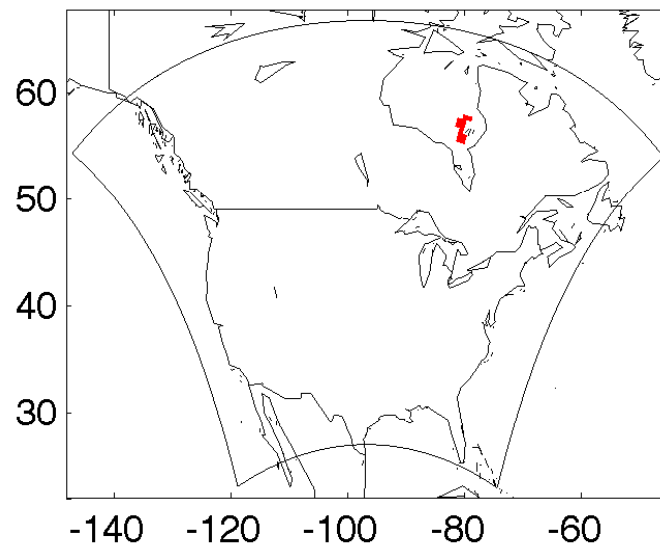
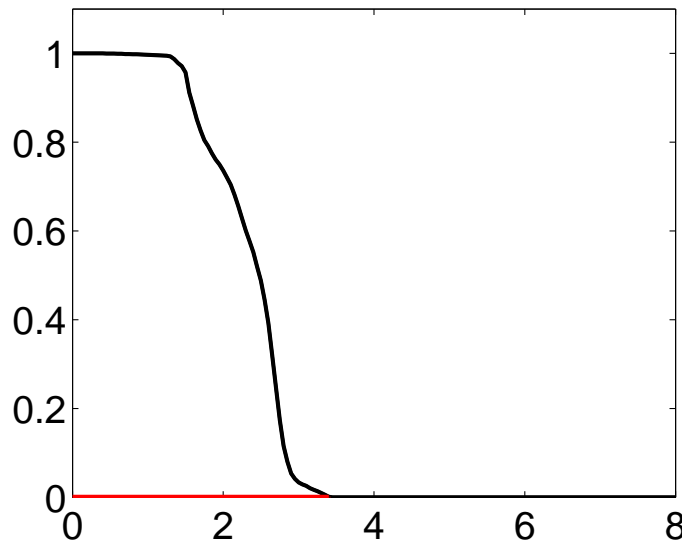
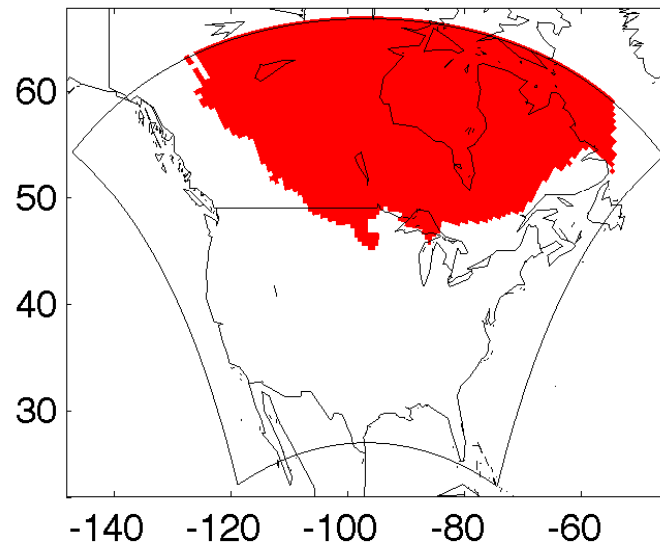
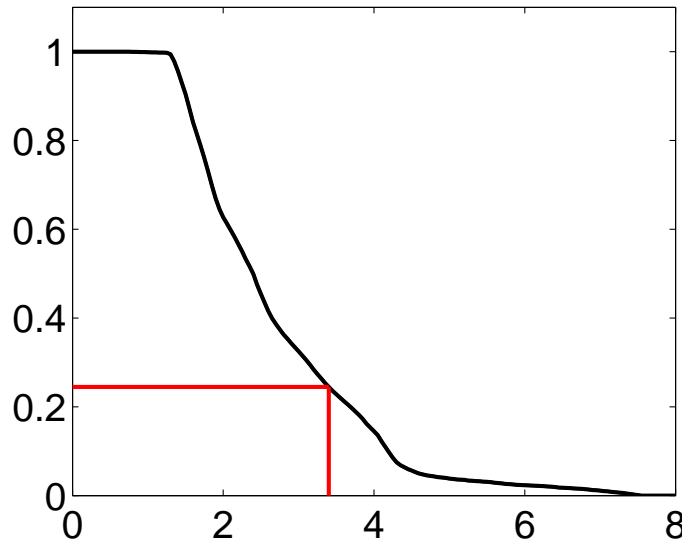
Linked SPOT-Function Plots, for $k = 3.0^\circ C$



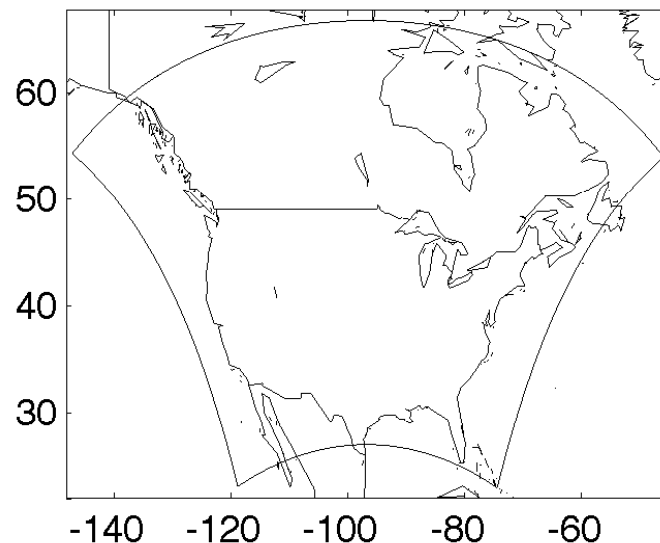
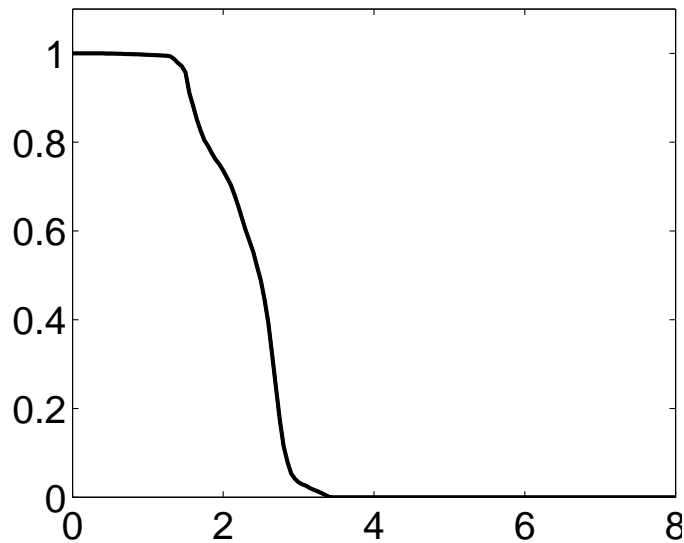
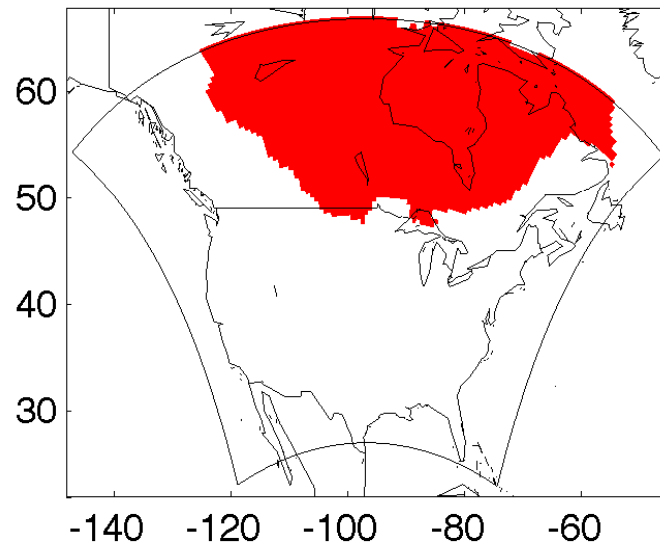
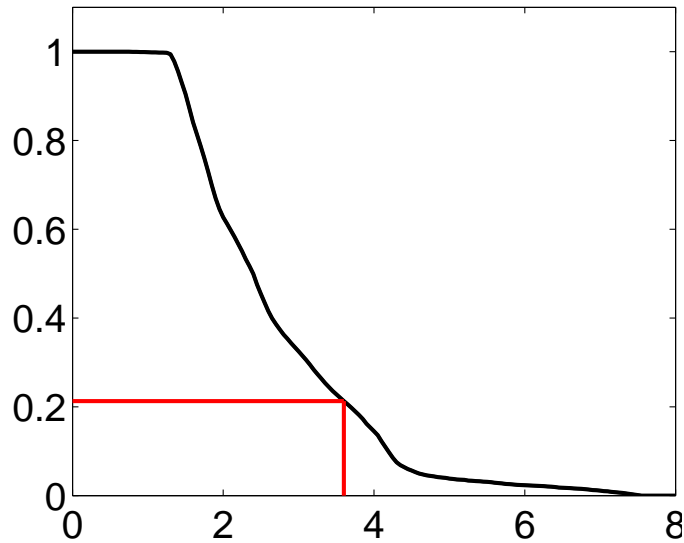
Linked SPOT-Function Plots, for $k = 3.2^\circ C$



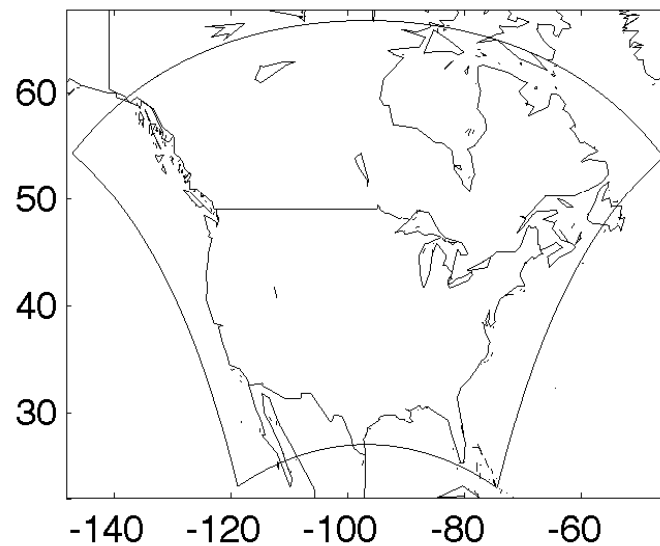
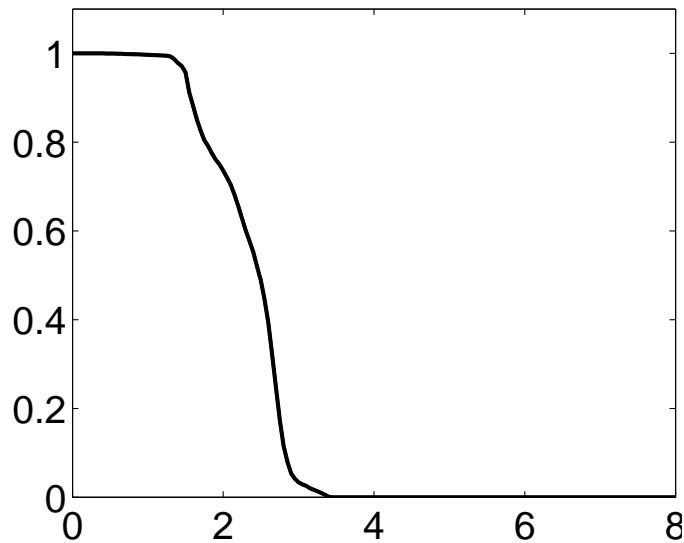
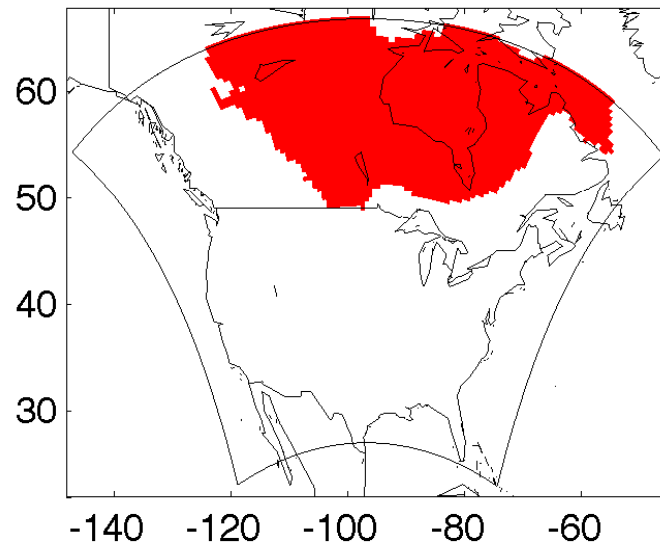
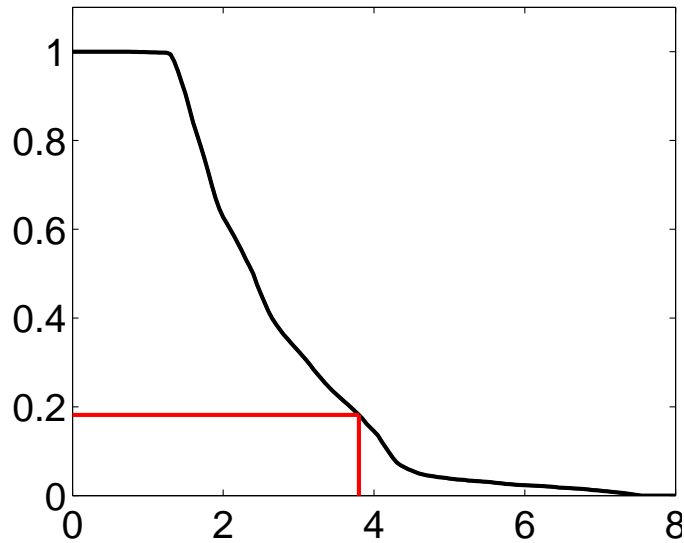
Linked SPOT-Function Plots, for $k = 3.4^\circ\text{C}$



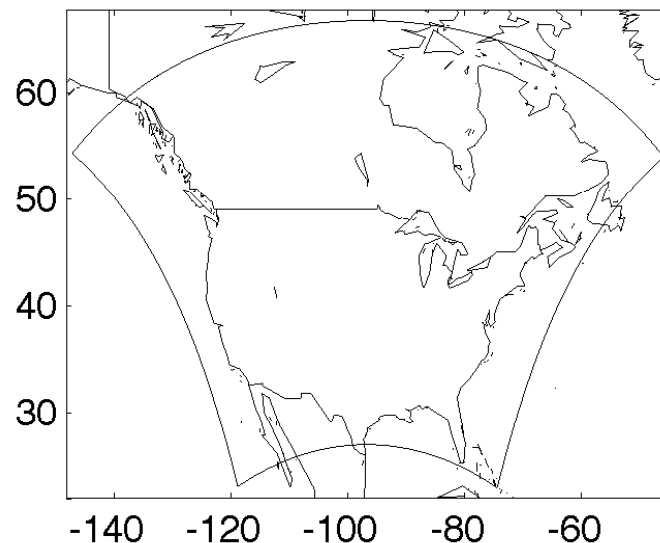
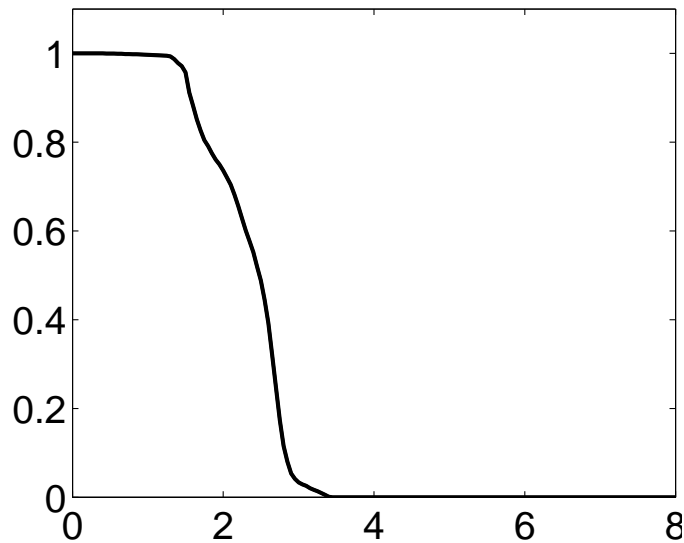
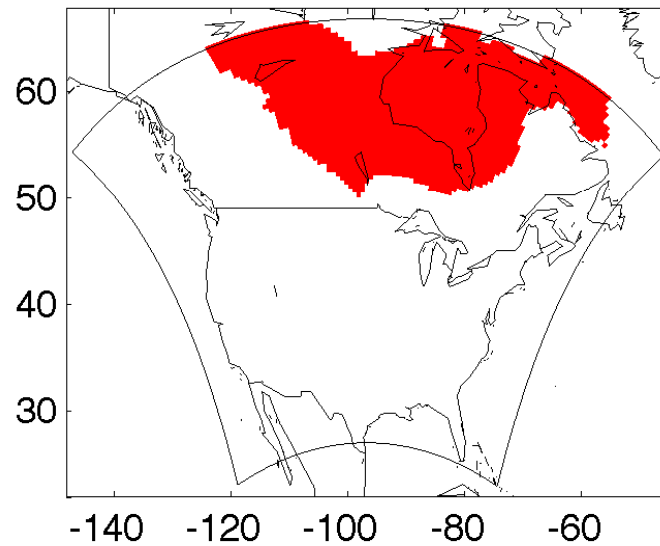
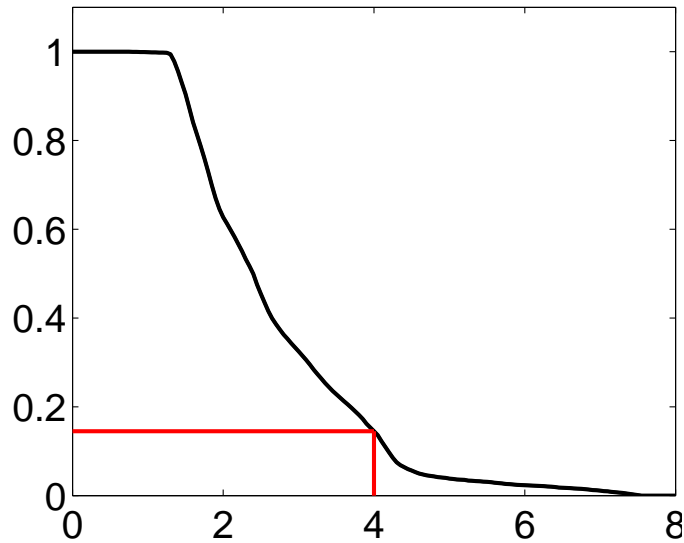
Linked SPOT-Function Plots, for $k = 3.6^\circ C$



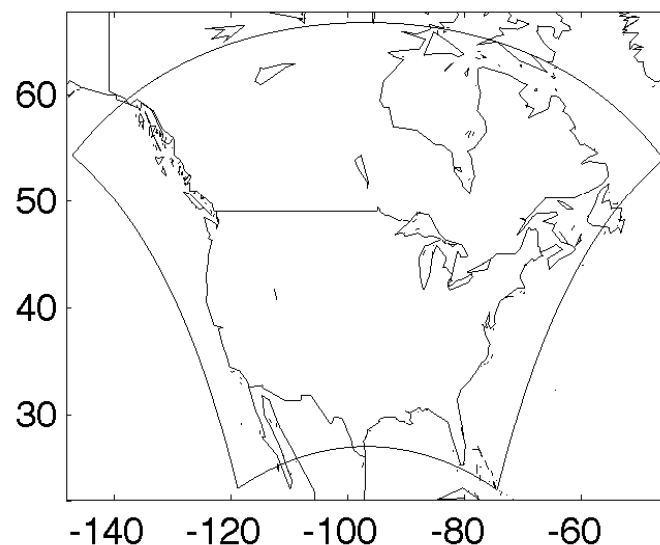
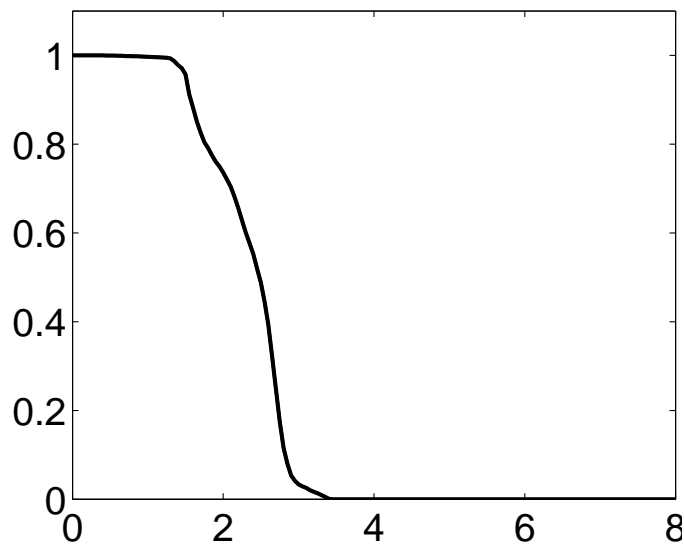
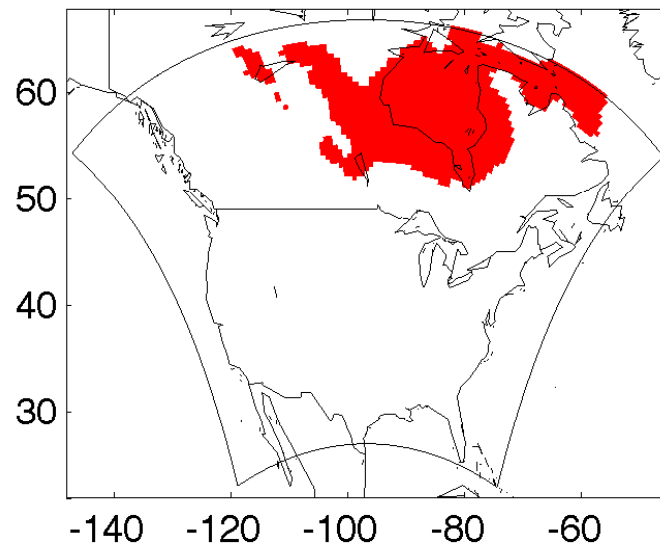
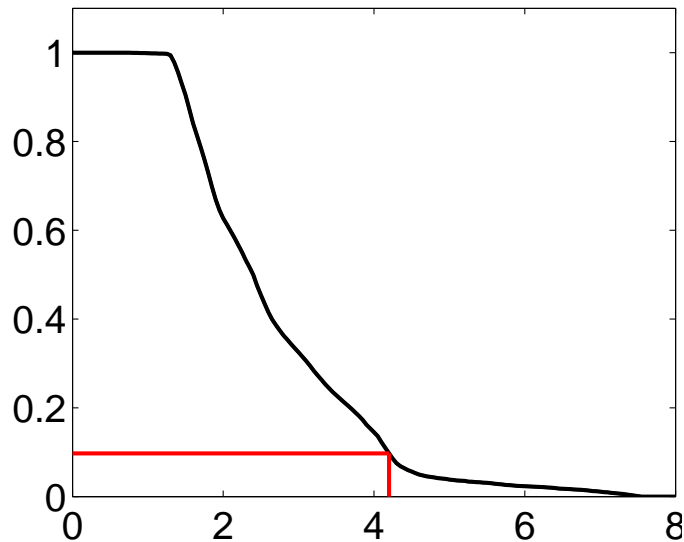
Linked SPOT-Function Plots, for $k = 3.8^\circ\text{C}$



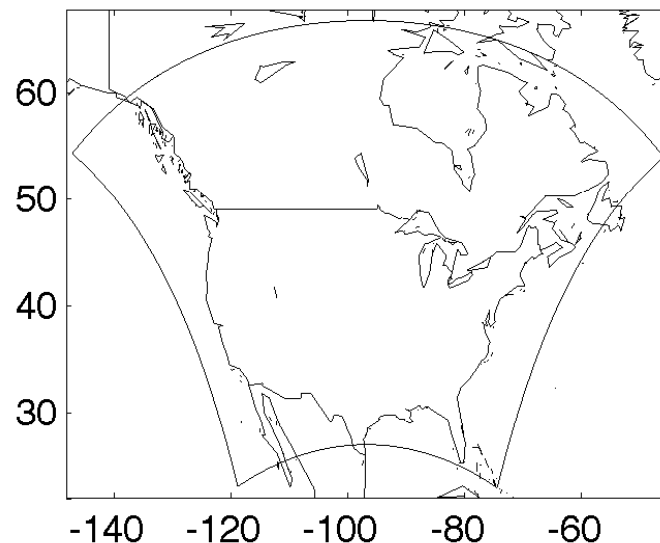
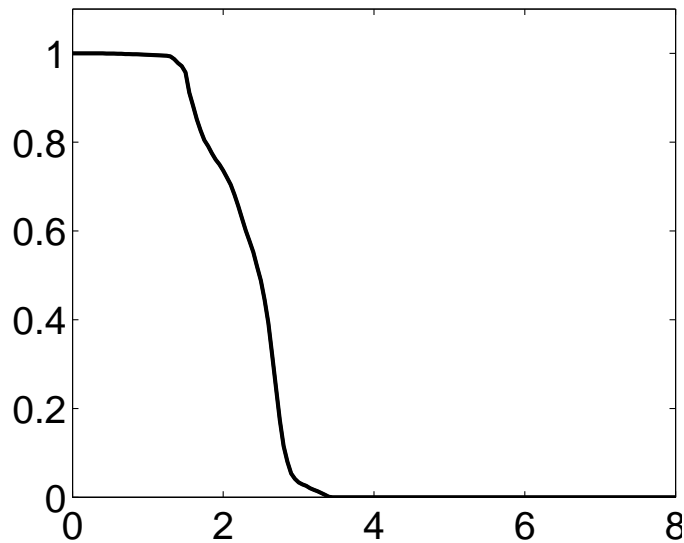
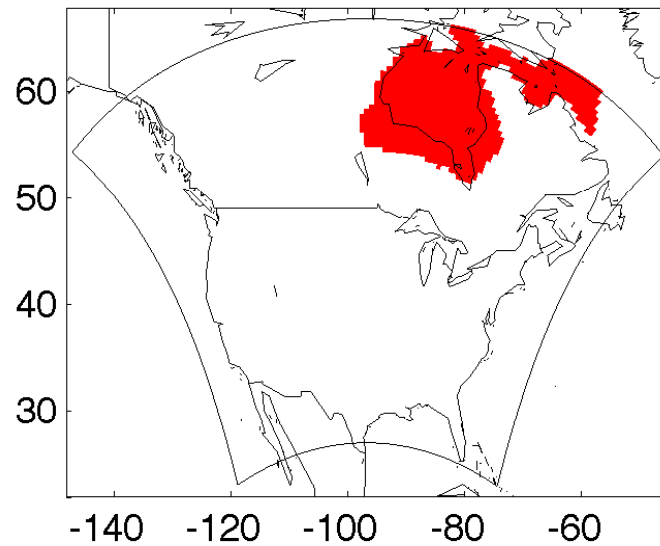
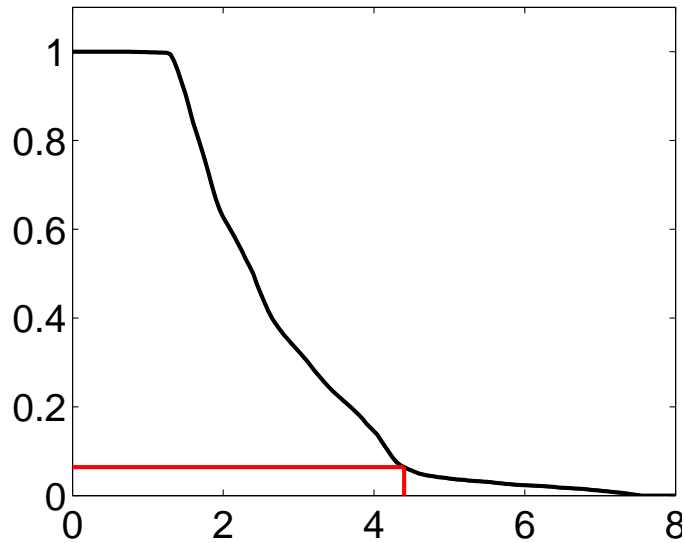
Linked SPOT-Function Plots, for $k = 4.0^\circ\text{C}$



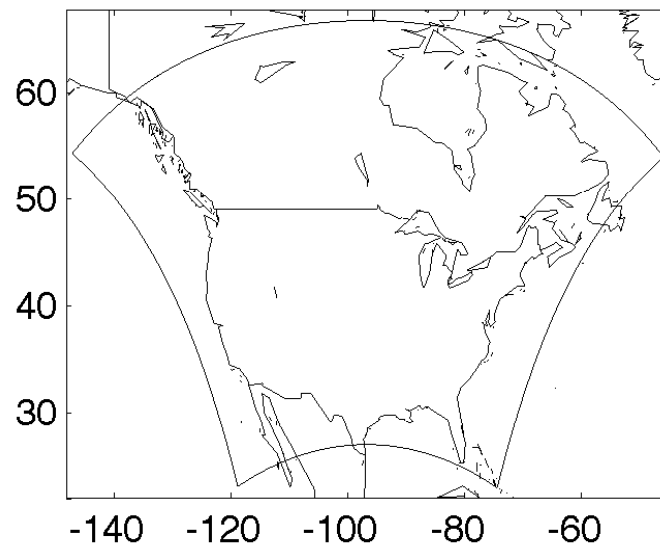
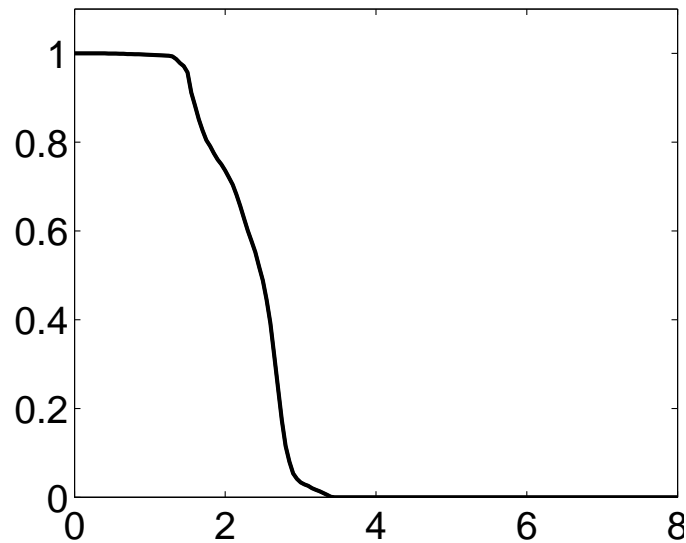
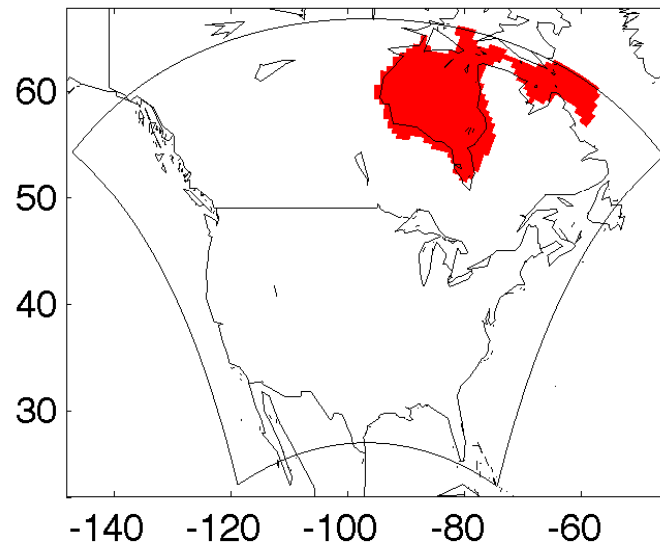
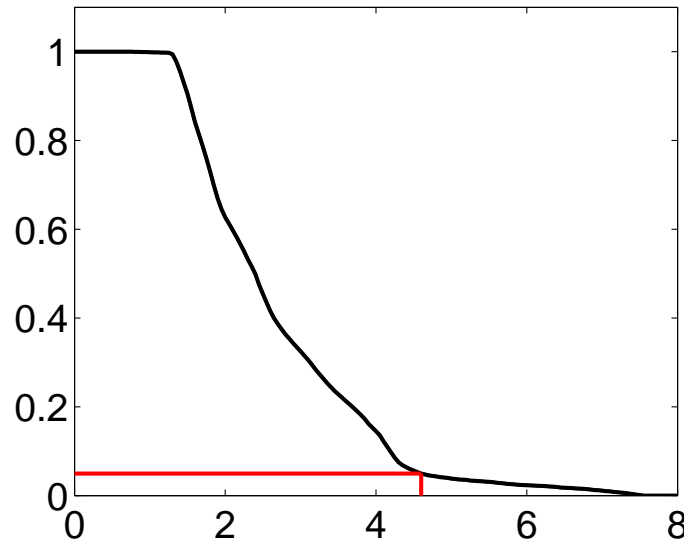
Linked SPOT-Function Plots, for $k = 4.2^\circ C$



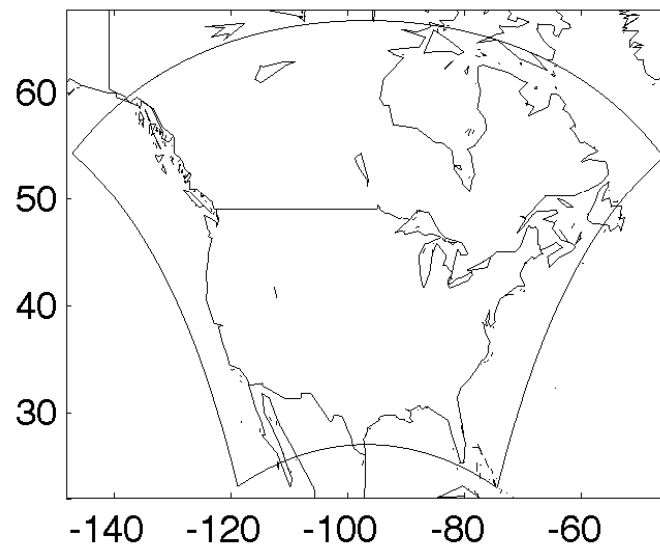
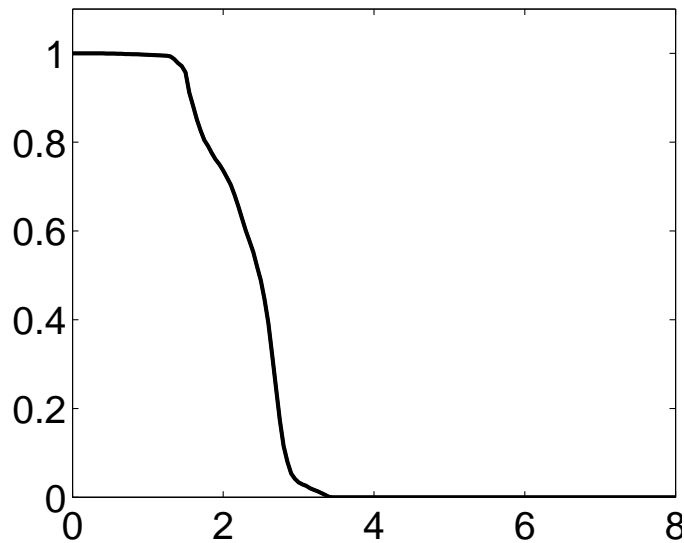
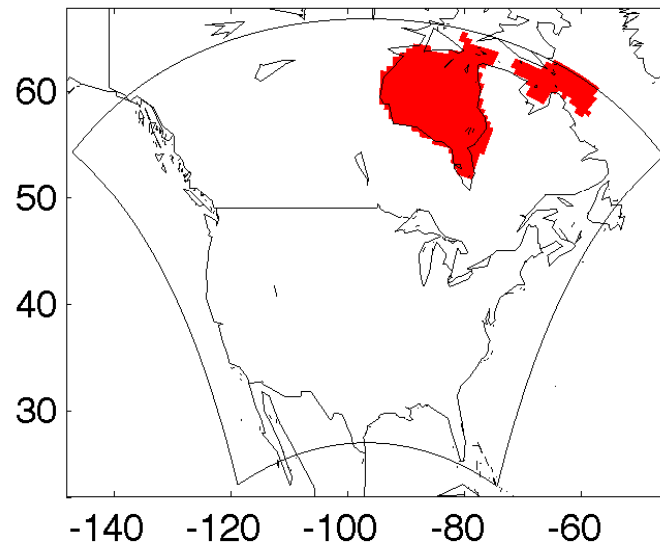
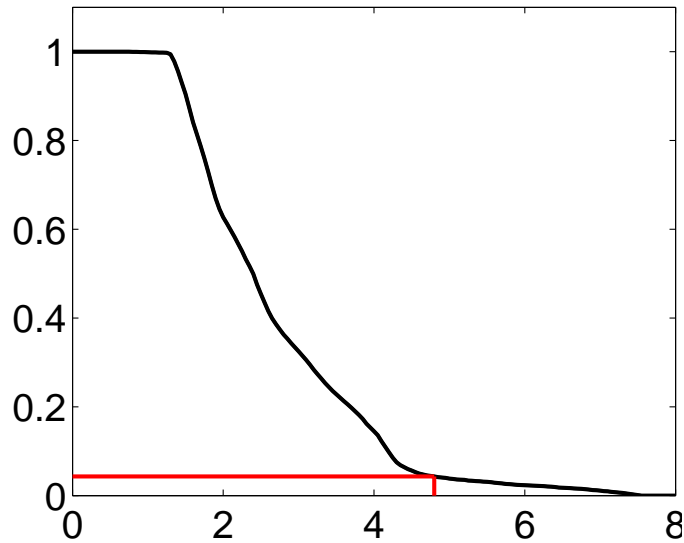
Linked SPOT-Function Plots, for $k = 4.4^\circ\text{C}$



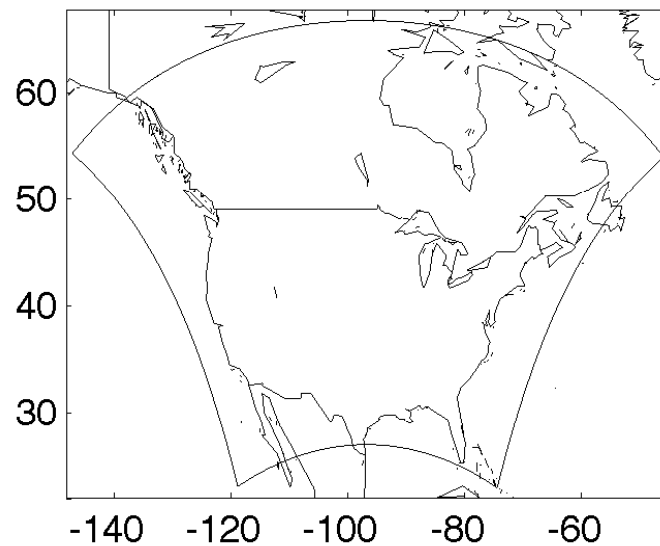
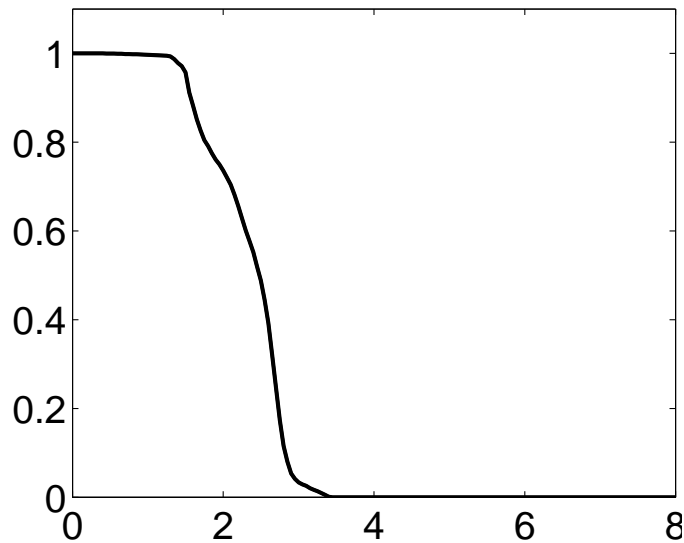
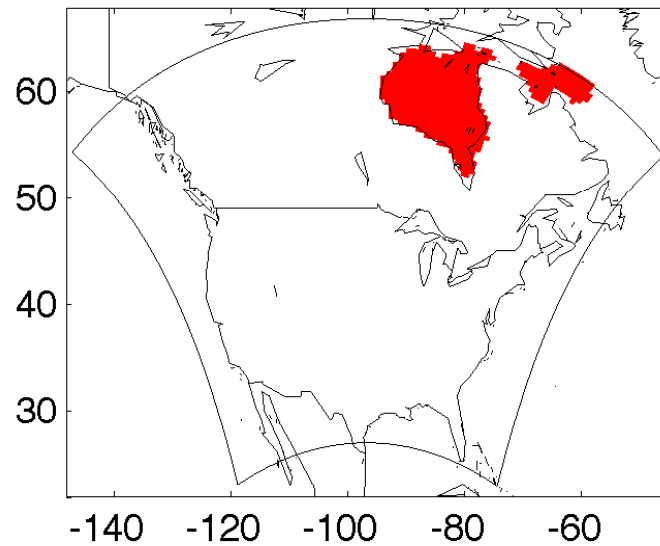
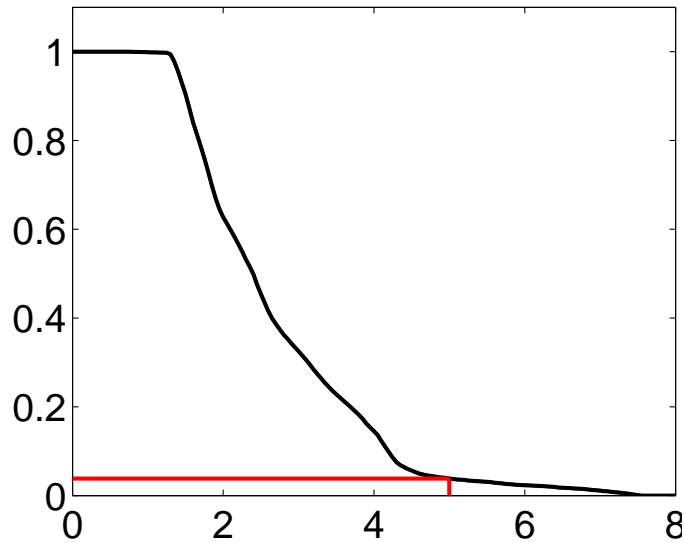
Linked SPOT-Function Plots, for $k = 4.6^\circ\text{C}$



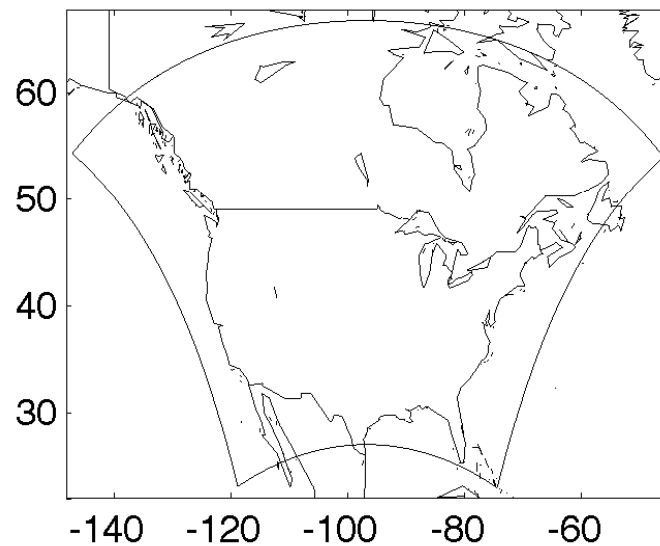
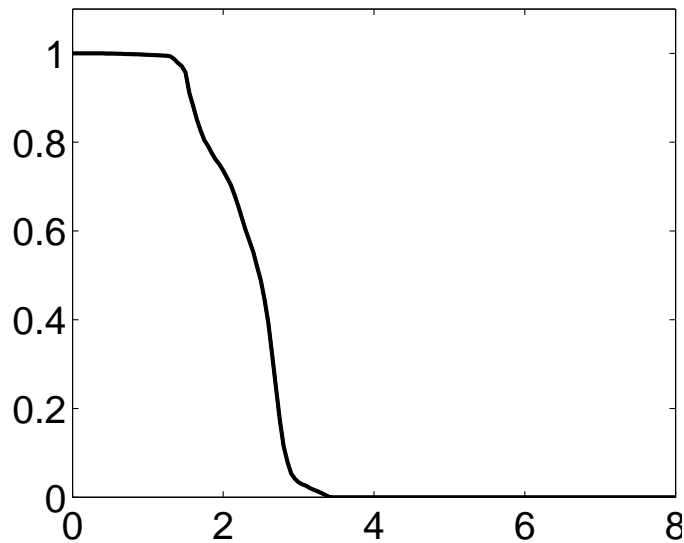
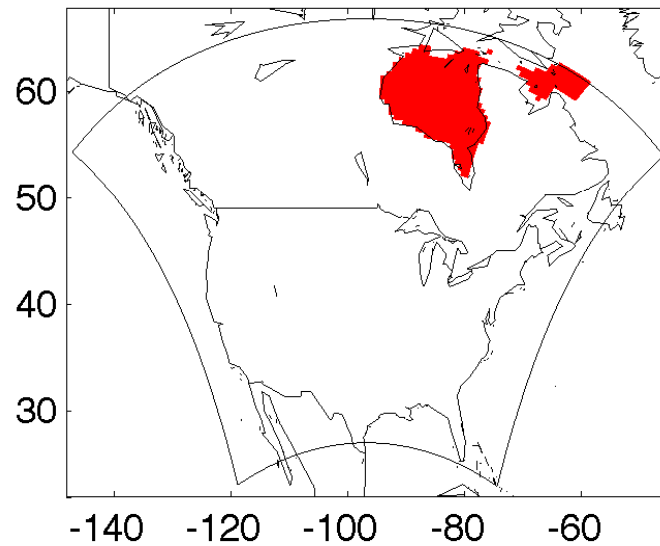
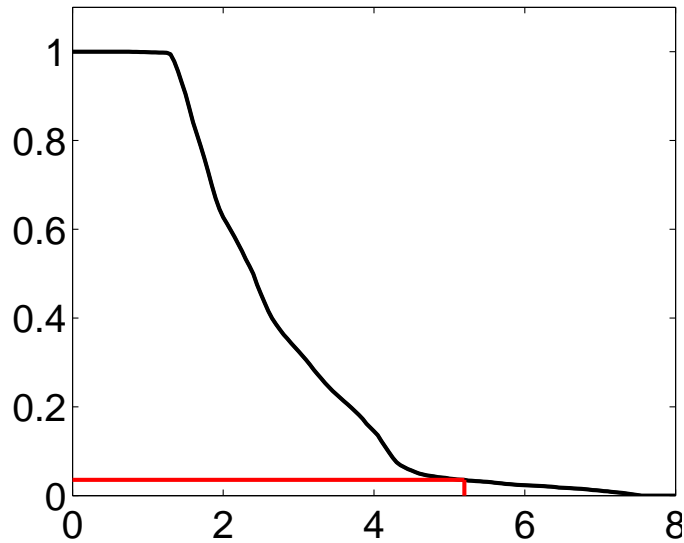
Linked SPOT-Function Plots, for $k = 4.8^\circ\text{C}$



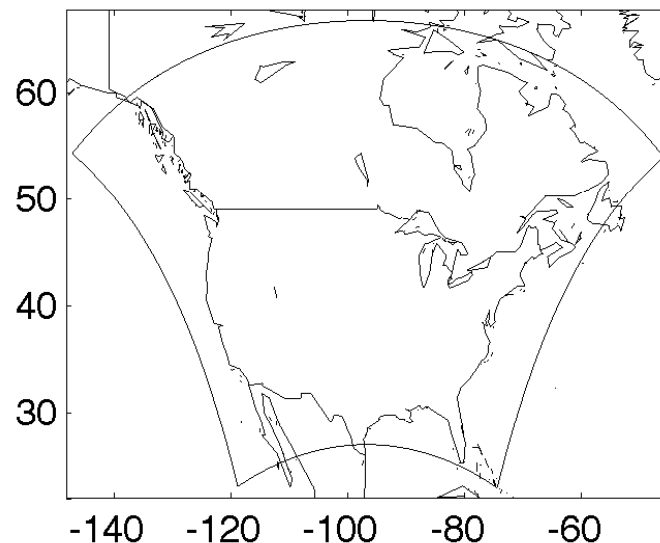
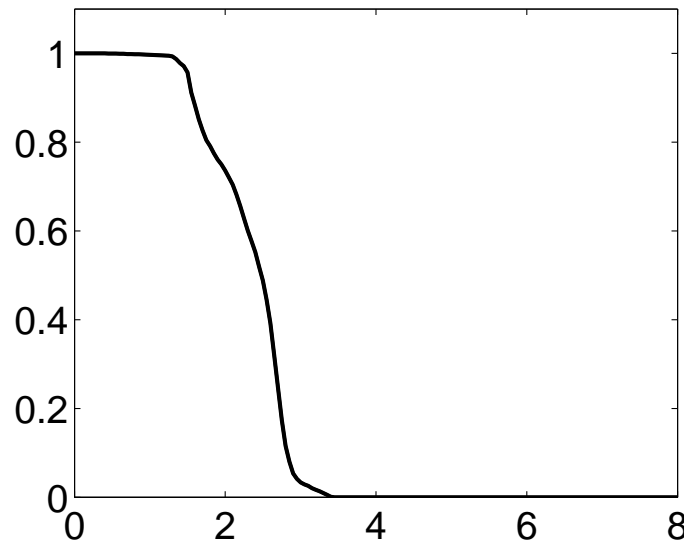
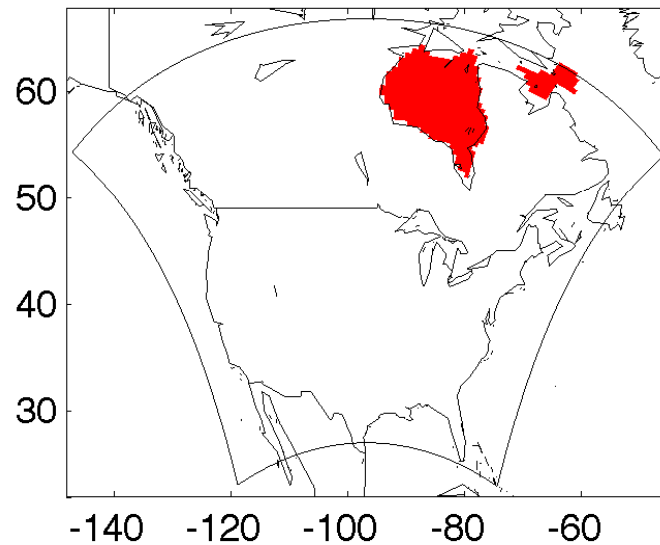
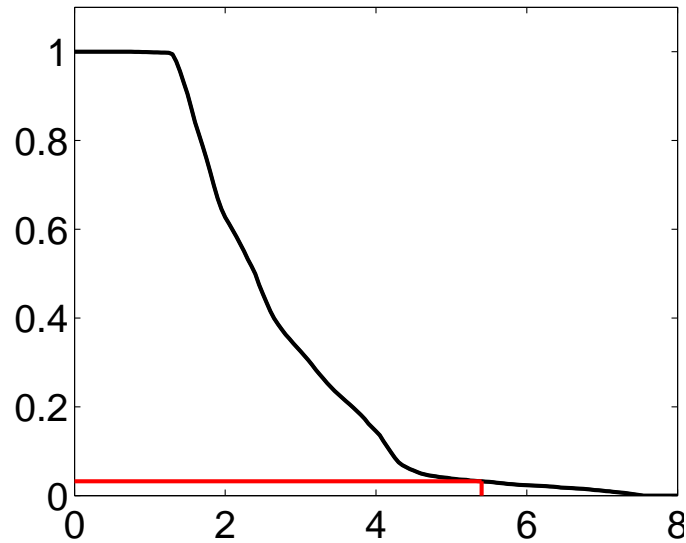
Linked SPOT-Function Plots, for $k = 5.0^\circ\text{C}$



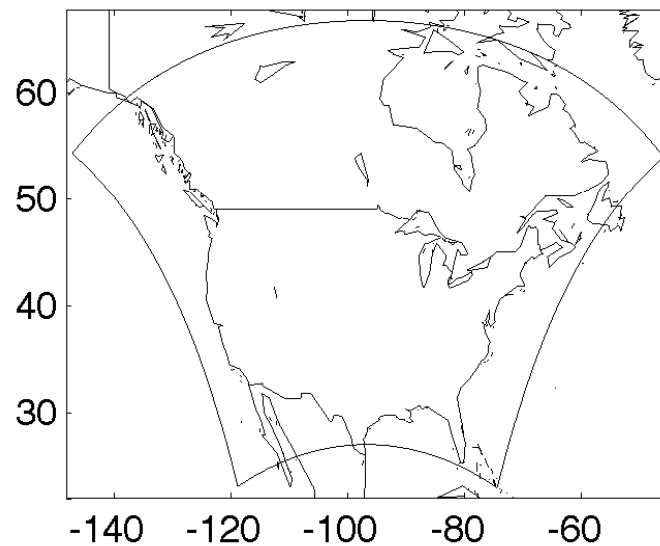
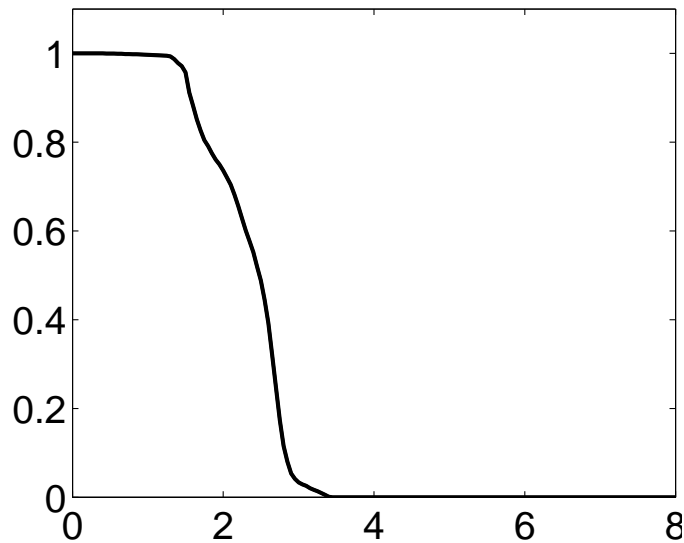
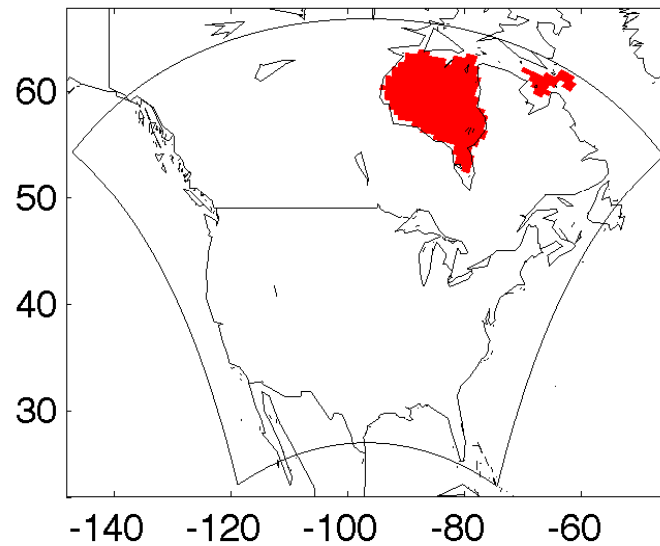
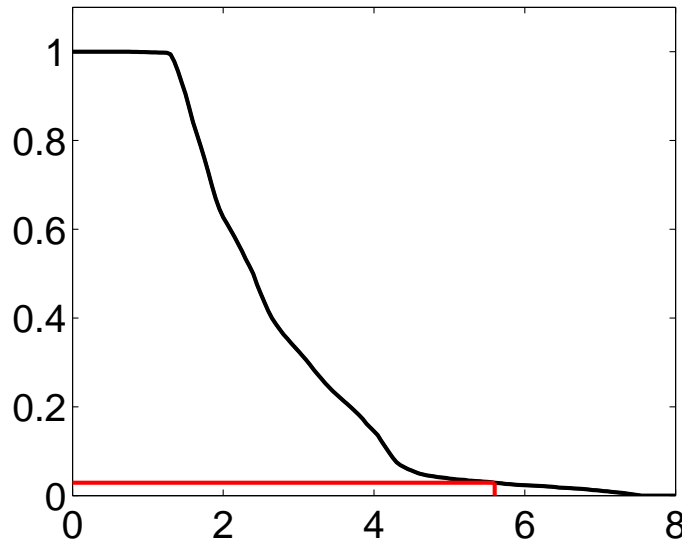
Linked SPOT-Function Plots, for with $k = 5.2^{\circ}\text{C}$



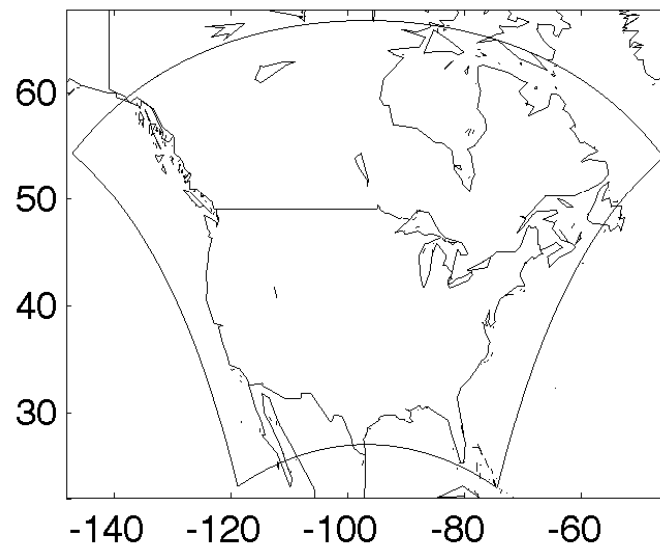
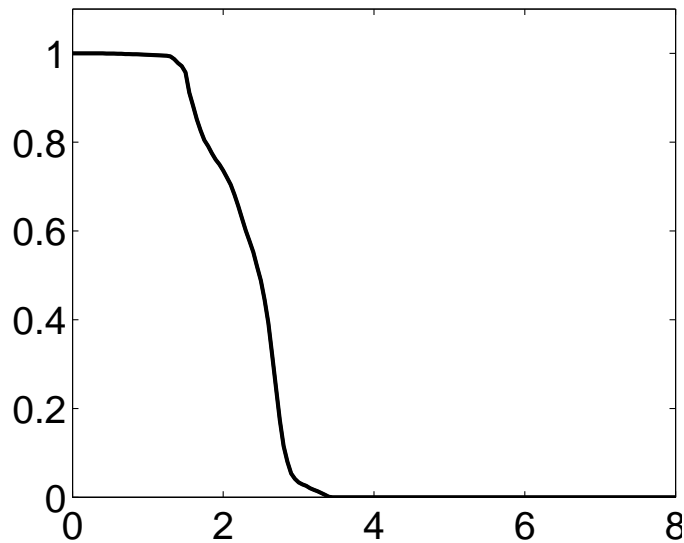
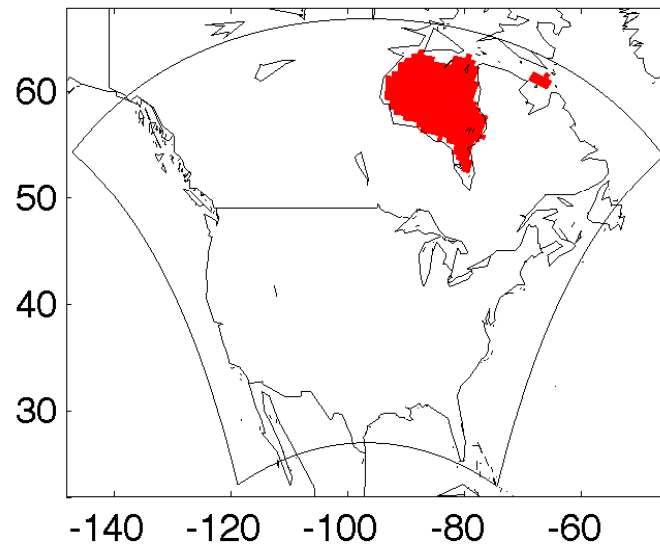
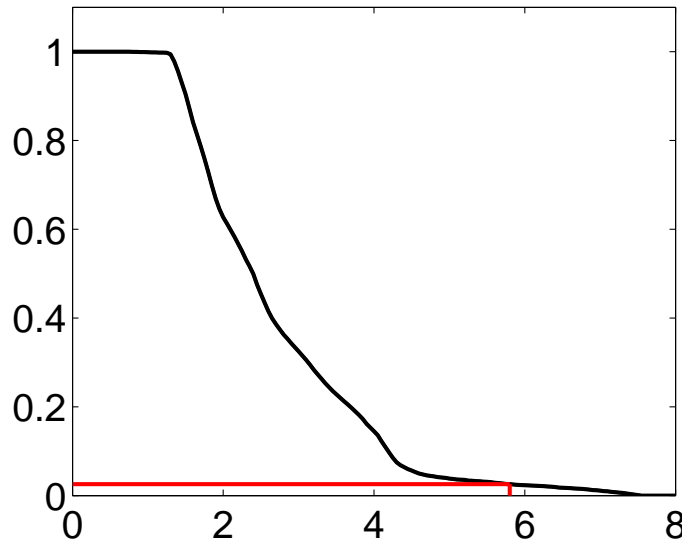
Linked SPOT-Function Plots, for $k = 5.4^\circ\text{C}$



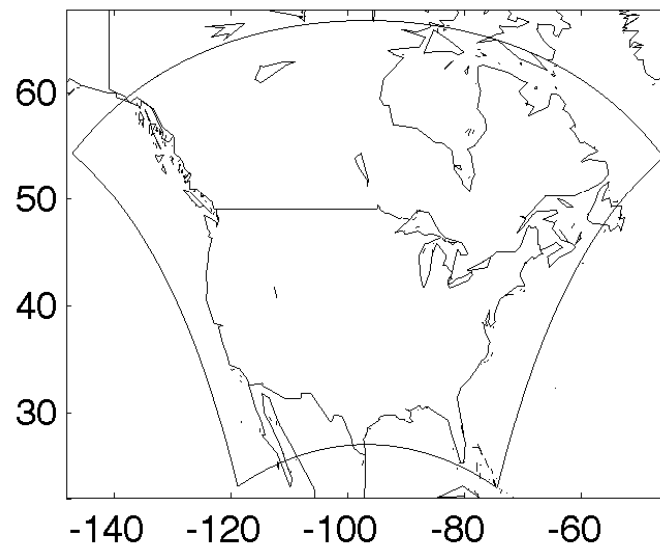
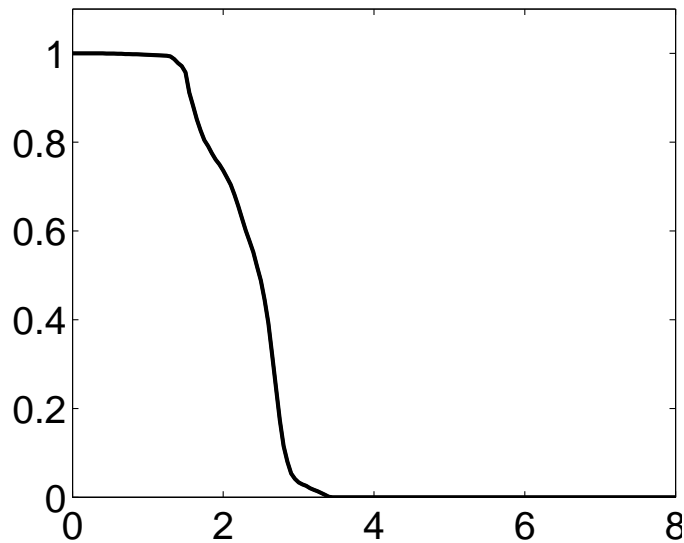
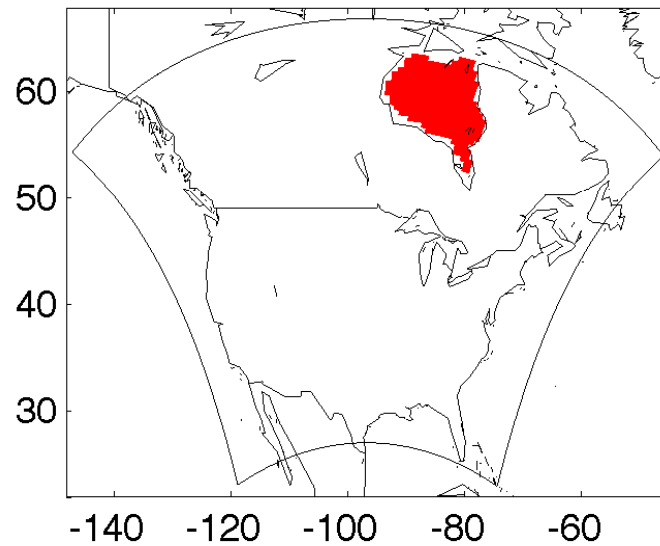
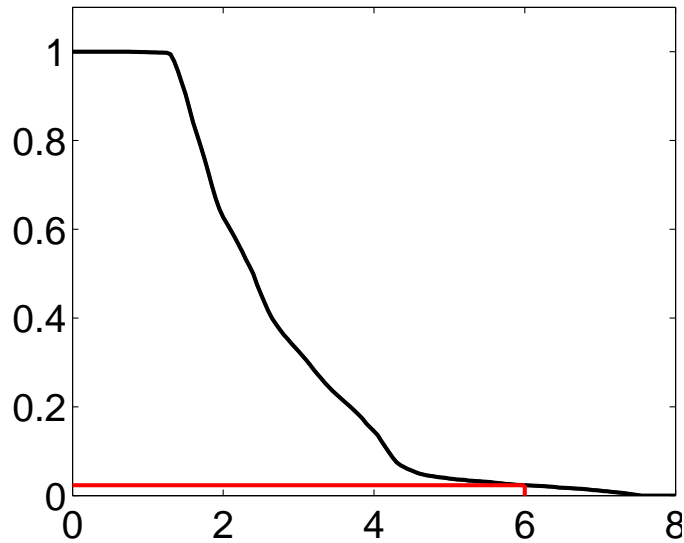
Linked SPOT-Function Plots, for $k = 5.6^\circ C$



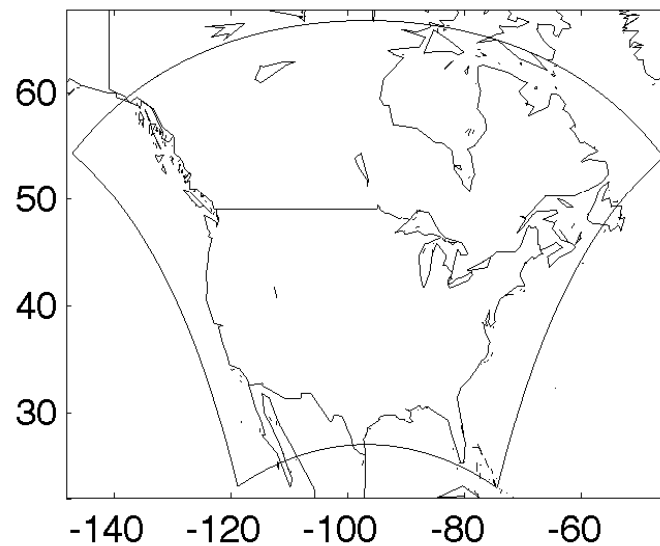
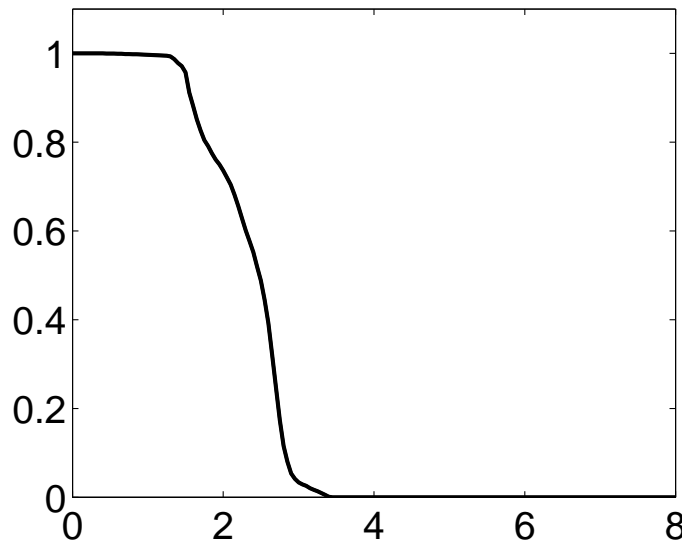
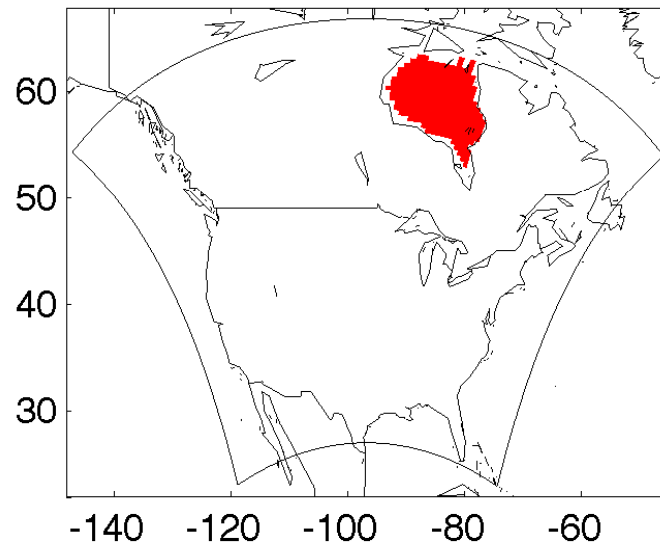
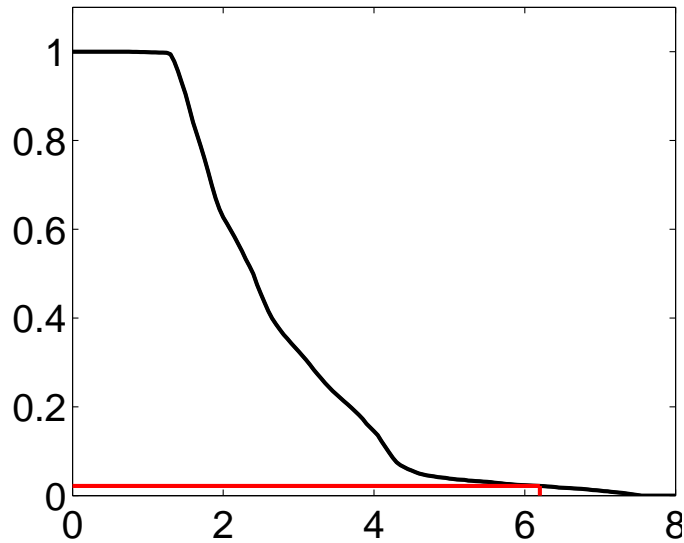
Linked SPOT-Function Plots, for $k = 5.8^\circ\text{C}$



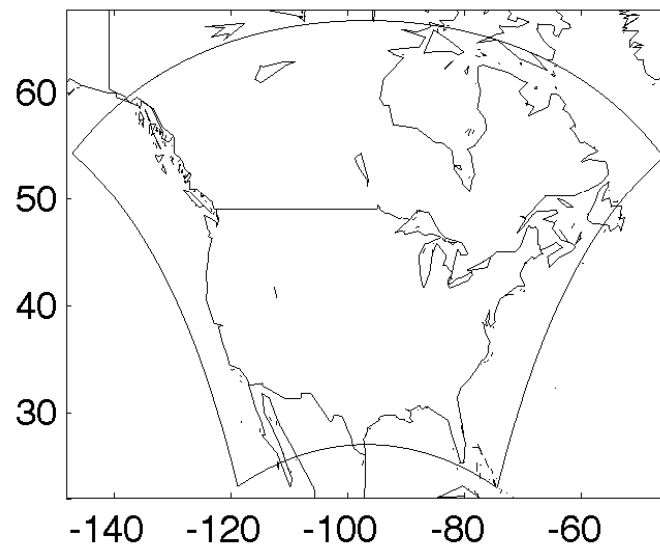
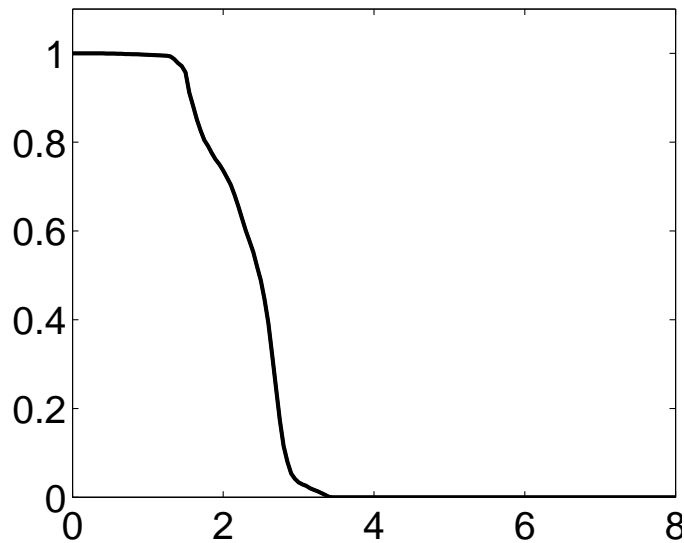
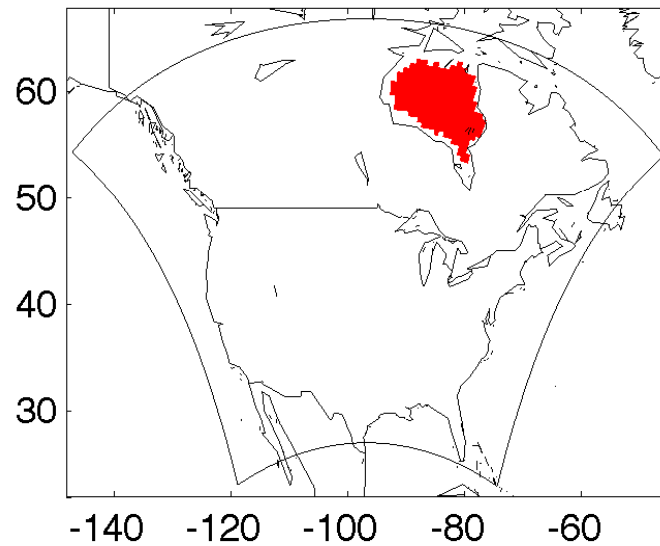
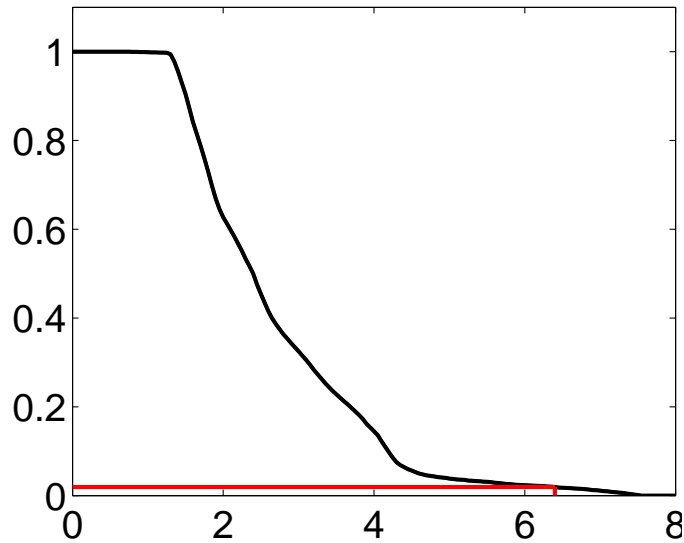
Linked SPOT-Function Plots, for $k = 6.0^\circ C$



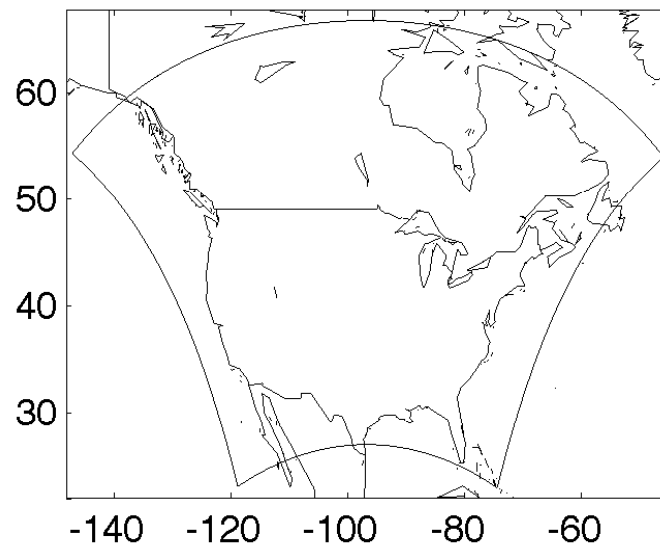
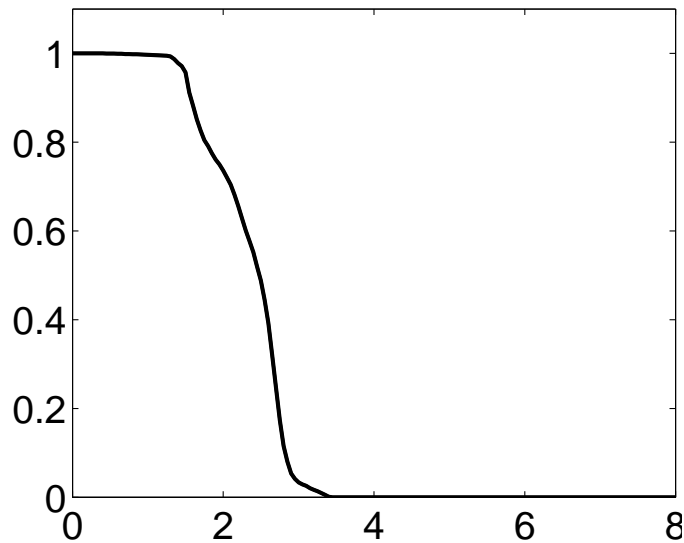
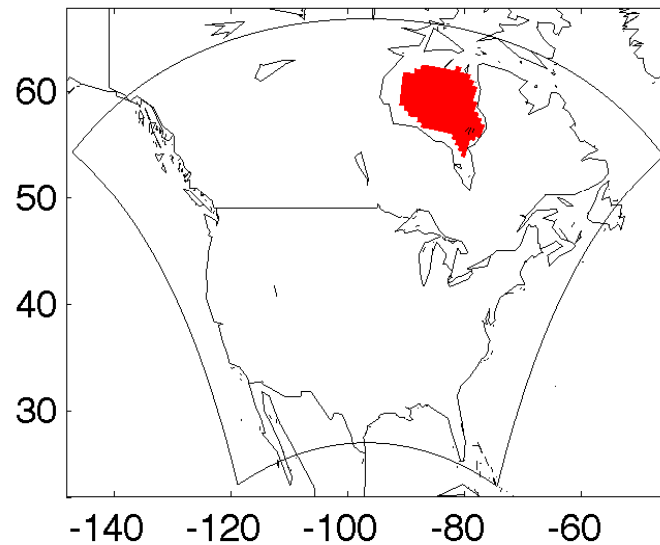
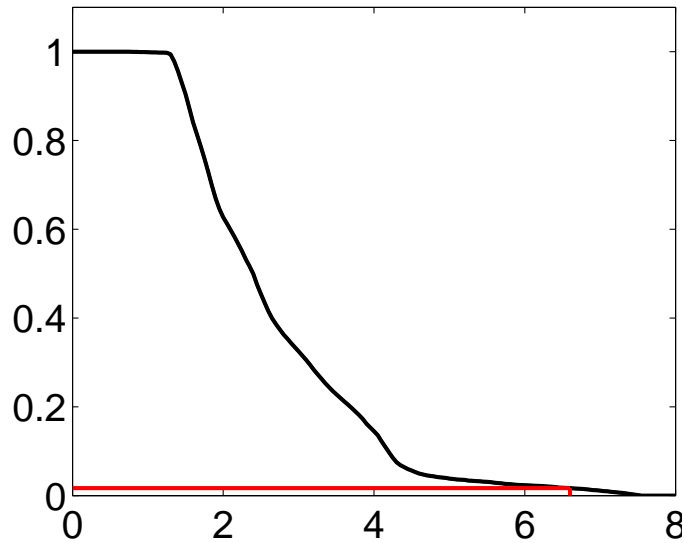
Linked SPOT-Function Plots, for $k = 6.2^\circ C$



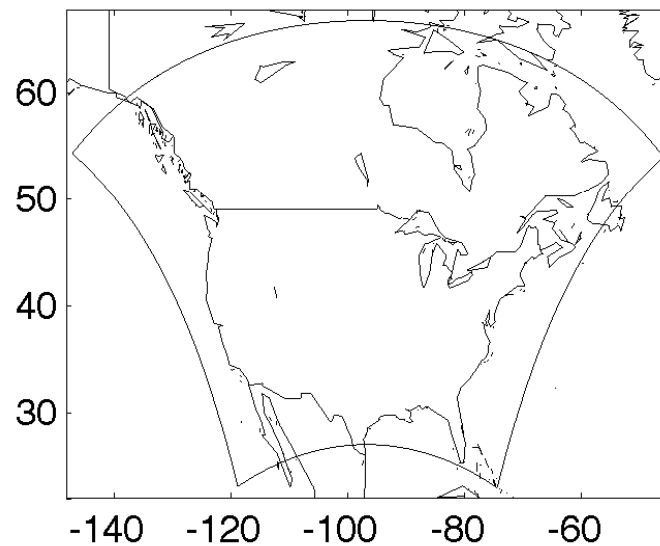
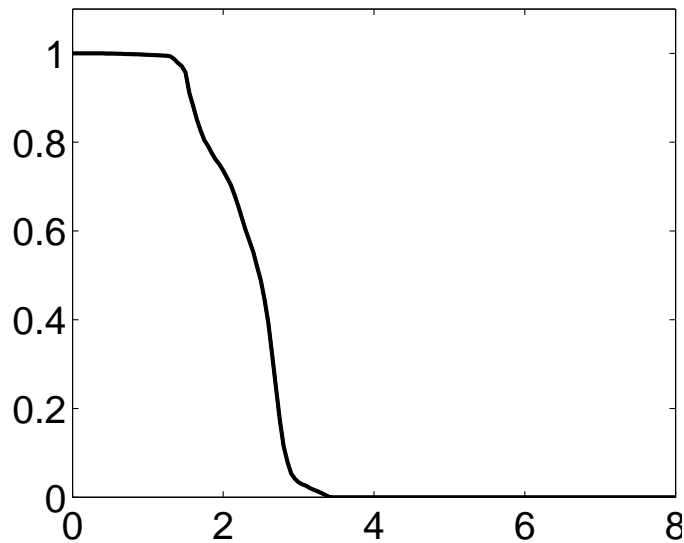
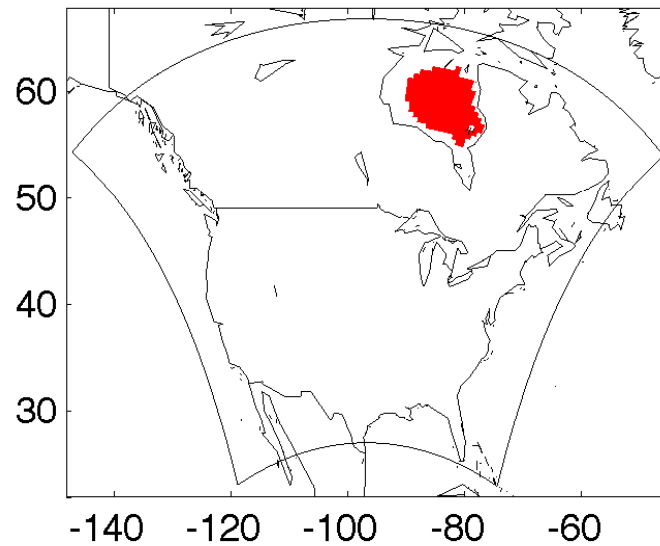
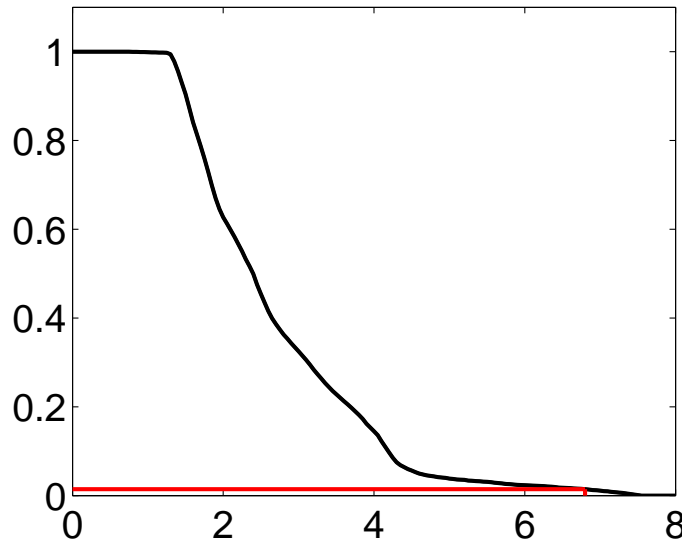
Linked SPOT-Function Plots, for $k = 6.4^\circ\text{C}$



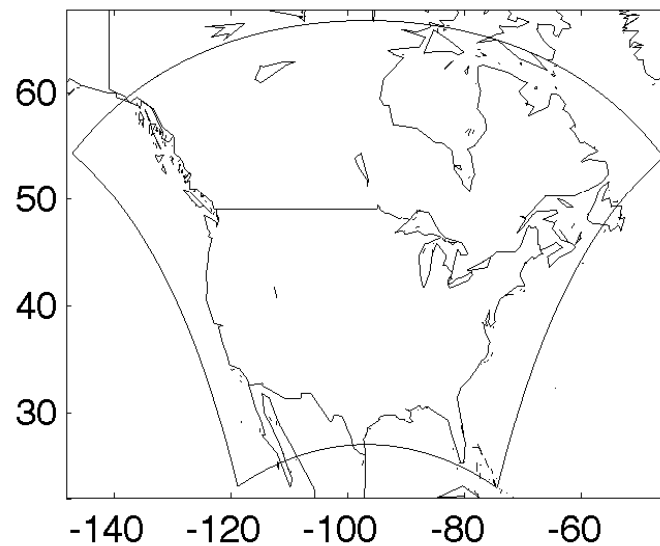
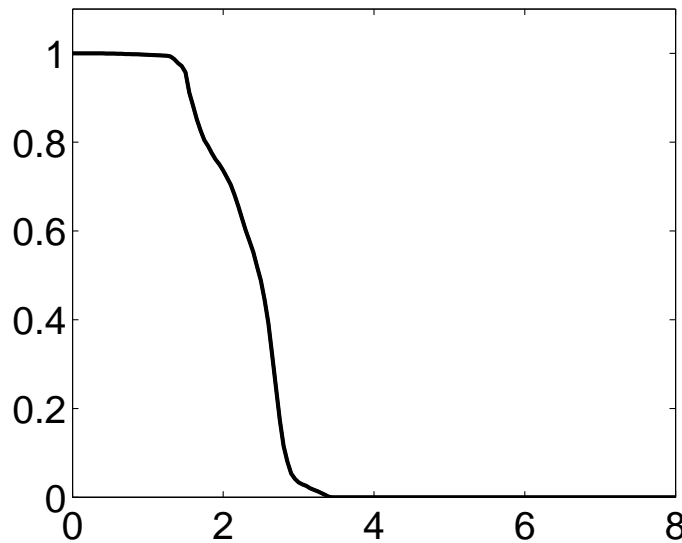
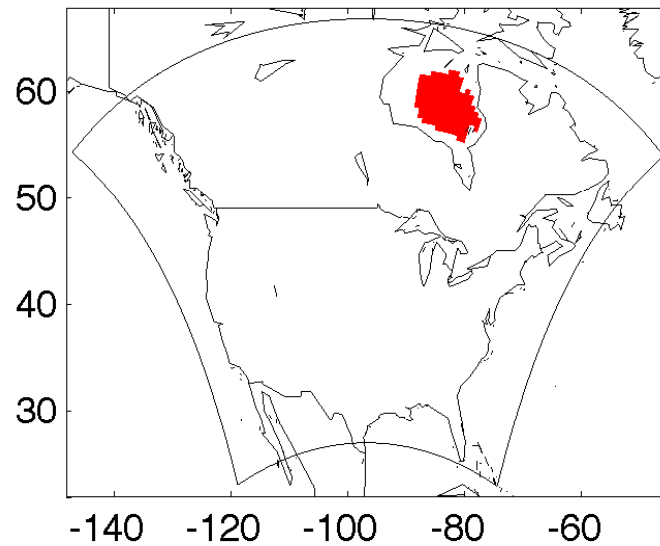
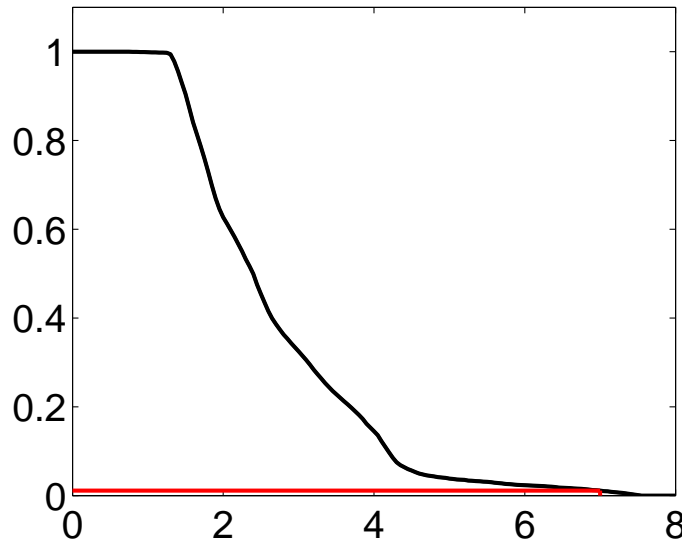
Linked SPOT-Function Plots, for $k = 6.6^\circ C$



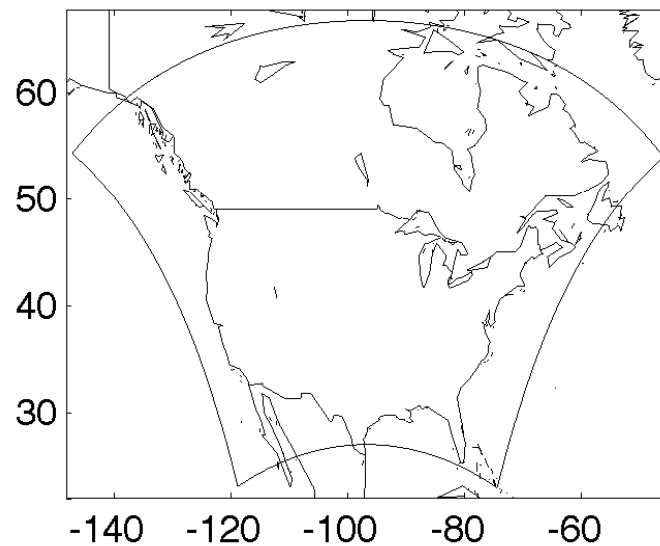
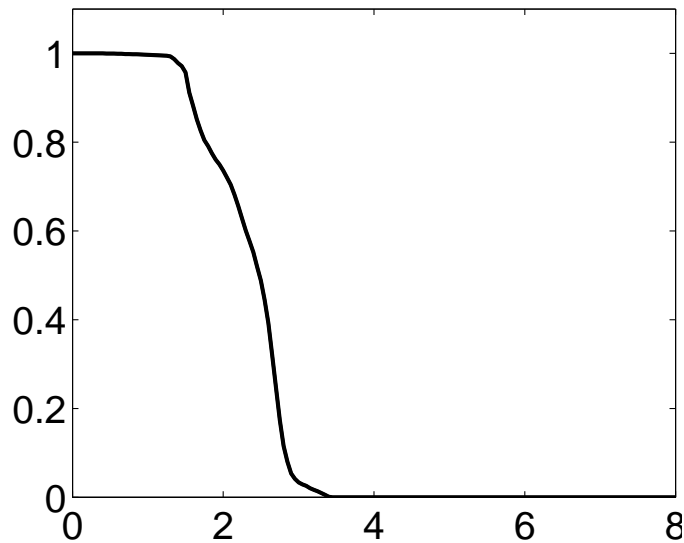
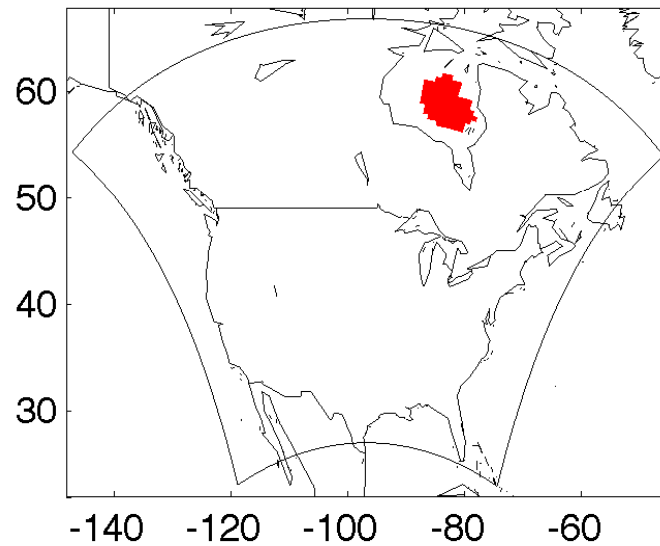
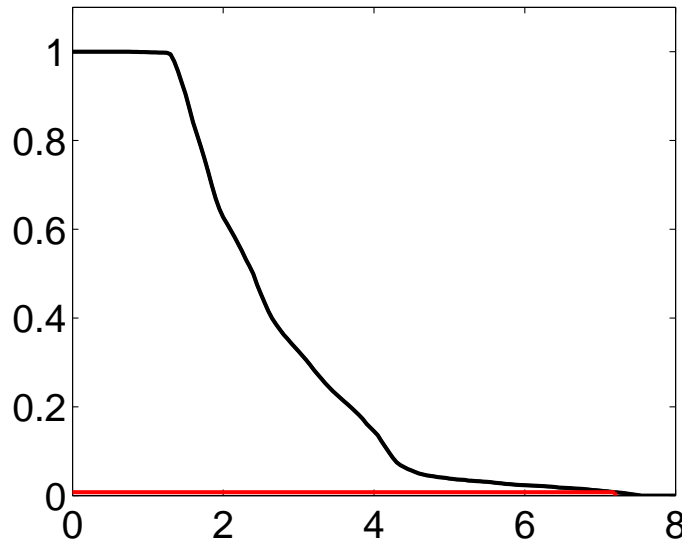
Linked SPOT-Function Plots, for $k = 6.8^\circ\text{C}$



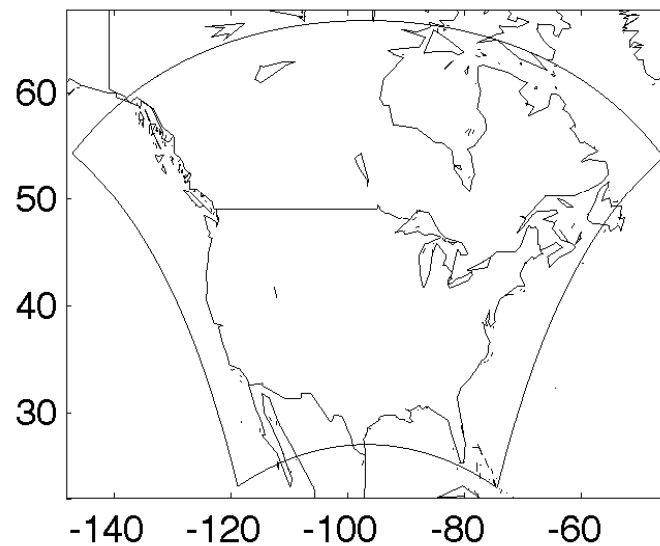
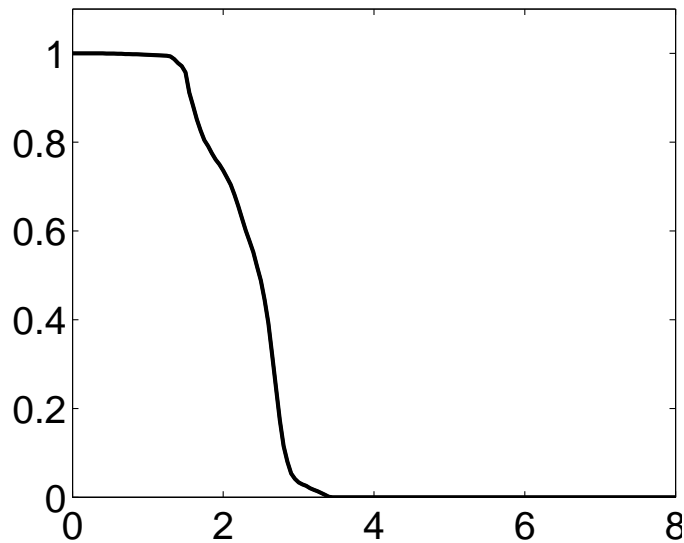
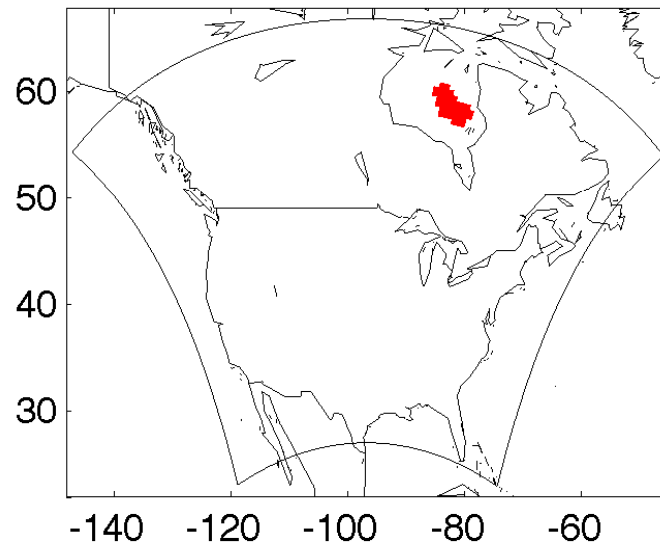
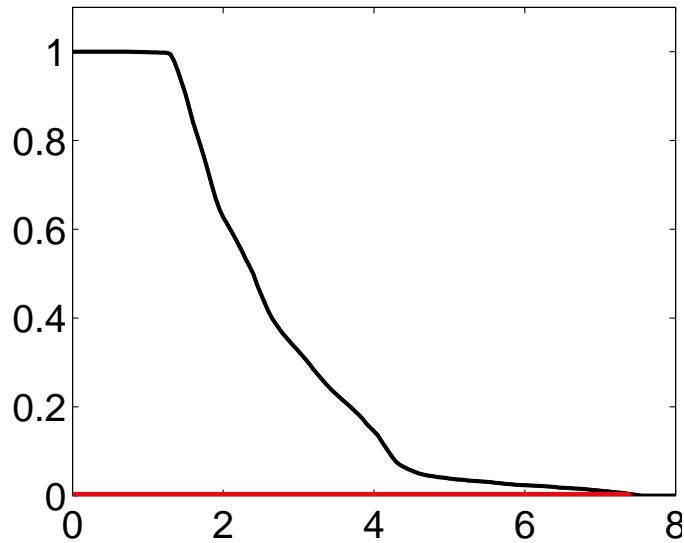
Linked SPOT-Function Plots, for $k = 7.0^\circ\text{C}$



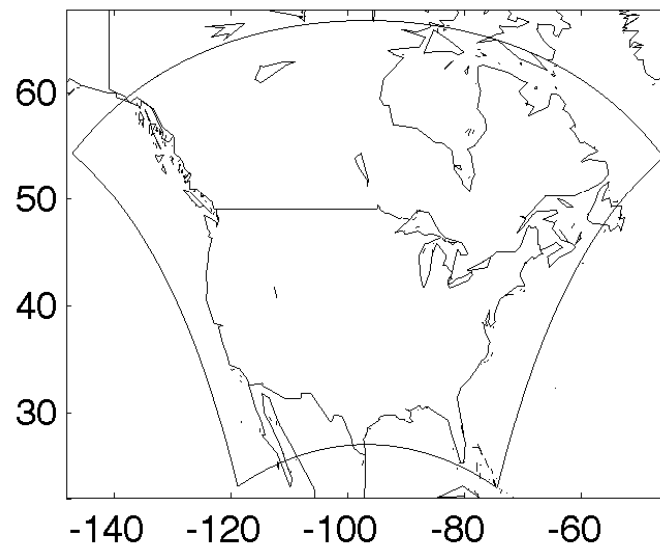
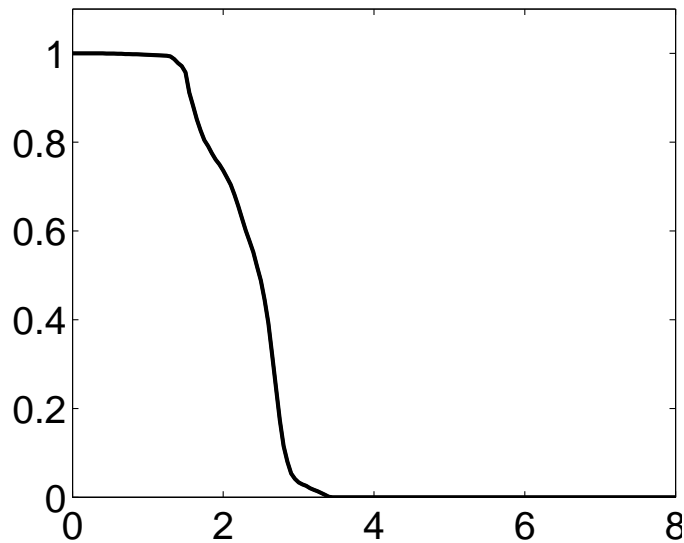
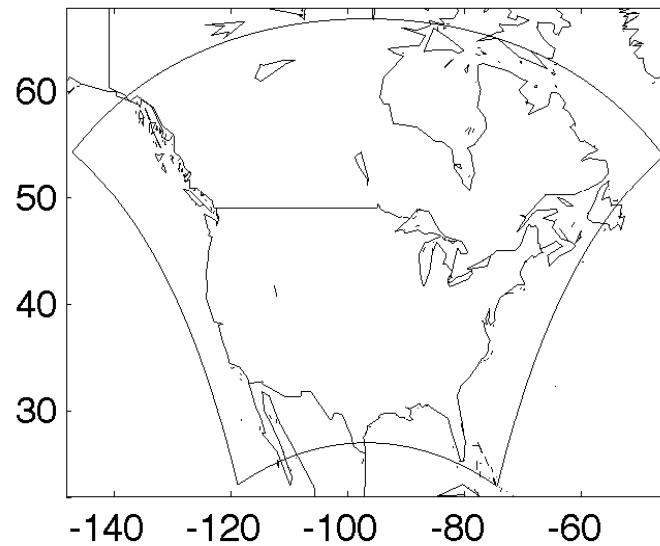
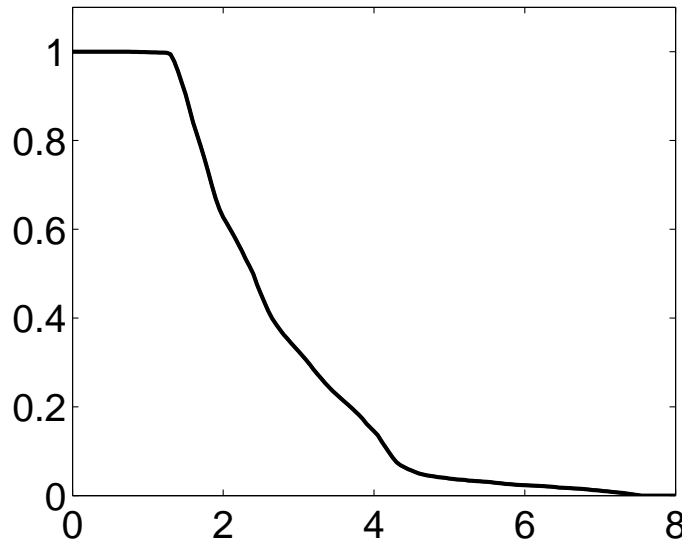
Linked SPOT-Function Plots, for $k = 7.2^\circ C$



Linked SPOT-Function Plots, for $k = 7.4^\circ\text{C}$



Linked SPOT-Function Plots, for $k = 7.6^\circ\text{C}$



Uncertainty Quantification (UQ) through Bayesian statistical inference

http://www.stat.osu.edu/~sses/collab_warming.html

Statistical Modeling of Climate Model Outputs

- Most previous articles focus on **GCM outputs** without considering spatial dependence (e.g., Tebaldi et al., 2005; Berliner and Kim, 2008; Smith et al., 2009; Tebaldi and Sansó, 2009)
- Recent **spatial statistical analyses** of RCM outputs include:
 - Kaufman and Sain (2010); relatively small datasets
 - Salazar et al. (2011); NARCCAP RCM outputs in the Southwest of the United States
 - Kang, Cressie, and Sain (2012); NARCCAP Phase I RCM outputs
 - Sain and Kaufman (2012); homogeneous Markov random fields
 - Kang and Cressie (2012); temperature change by season and region
- Results from Kang and Cressie (2012) are summarized and explained at:
http://www.stat.osu.edu/~sses/collab_warming.html
(Cressie, Mannshardt, and Kang)

Spatial Statistical Modeling of “Big Data”

- Approximation in computation: Covariance tapering (Furrer, Genton, and Nychka, 2006); predictive processes (e.g., Banerjee et al., 2008)
- Constructing Markov random fields for Gaussian processes (Lindgren, Rue, and Lindström, 2011)
- Spatial Random Effects (SRE) model (Cressie and Johannesson, 2006, 2008)

Bayesian Hierarchical Spatial Model

- Data model
- Process model: SRE model allows for spatial heterogeneity and dimension reduction
- Parameter (prior) model

Process model: A spatial ANOVA model (where $i = 1, 2$ RCMs and $j = 1, 2, 3, 4$ seasons) is assumed on the reduced-dimensional space upon which the spatial random effects (SREs) are defined

$$\mathbf{D}_{ij} = \mathbf{Y}_{ij} + \boldsymbol{\varepsilon}_{ij}; i = 1, 2, j = 1, \dots, 4$$

- The **spatial-only temperature-change** projection is \mathbf{Y}_{ij} , for the i -th RCM and for the j -th season, and $\boldsymbol{\varepsilon}_{ij}$ is independent of \mathbf{Y}_{ij}
- $\{\boldsymbol{\varepsilon}_{ij}\}$ are independently distributed as Gaussian random vectors with mean zero and $\text{var}(\boldsymbol{\varepsilon}_{ij}) = \sigma_{\varepsilon}^2 \mathbf{V}_{ij}$, where $\{\mathbf{V}_{ij}\}$ are known $n \times n$ diagonal matrices, and σ_{ε}^2 is an unknown parameter. (Temporal correlation between successive seasons will be very weak due to the short duration of weather systems and the considerable averaging.) For $\ell = 1, \dots, n$,

$$V_{ij}(\mathbf{s}_{\ell}) \equiv \frac{1}{30} \sum_{t=2041}^{2070} \frac{(Z_{ij}(\mathbf{s}_{\ell}; t) - Z_{ij}(\mathbf{s}_{\ell}; t - 70) - D_{ij}(\mathbf{s}_{\ell}))^2}{29}$$

- Equivalent data-model prescription: For $i = 1, 2$, and $j = 1, \dots, 4$,

$$\mathbf{D}_{ij} | \{\mathbf{Y}_{ij}\}, \sigma_{\varepsilon}^2 \sim \text{ind. Gau}(\mathbf{Y}_{ij}, \sigma_{\varepsilon}^2 \mathbf{V}_{ij})$$

Process Model

- We first model the temperature-change projection for the i -th RCM and for the j -th season, $Y_{ij}(s)$, as a **spatial Analysis of Variance (ANOVA)**:

$$Y_{ij}(s) = \mu(s) + a_i(s) + b_j(s) + (ab)_{ij}(s); i = 1, 2, j = 1, \dots, 4, s \in D,$$

where

- $\{\mu(\cdot)\}$ represents the **baseline**
 - $\{a_i(\cdot)\}$ are the main-effect contrasts between **RCMs**
 - $\{b_j(\cdot)\}$ are the main-effect contrasts between **seasons** (sp, su, au, wi)
 - $\{(ab)_{ij}(\cdot)\}$ are the **interaction** contrasts **between RCMs and seasons**
- Consequently,

$$Y_{.j}(s) = \mu(s) + b_j(s); j = 1, \dots, 4, s \in \mathbb{D}$$

captures the seasonal spatial variability, and $Y_{..}(s) = \mu(s); s \in \mathbb{D}$, captures the overall spatial variability

Spatial Models for Large-to-Massive Spatial Datasets

- As pointed out by Banerjee et al. (2008) and Cressie and Johannesson (2008), **large or even massive n** will cause computational difficulties for traditional spatial statistical methods (e.g., kriging)
- Cressie and Johannesson (2006, 2008) proposed an **exact** model for large-to-massive spatial datasets, namely the **Spatial Random Effects (SRE) model**
 - Scalable computation
 - Nonstationary, flexible spatial model
 - Change-of-support is straightforward
- Kang and Cressie (2011) extended the SRE model to a fully Bayesian hierarchical framework
- Kang, Cressie, and Sain (2012) used it in a fully Bayesian analysis of high-resolution RCM outputs in NARCCAP Phase I
- Kang and Cressie (2012) did the same for NARCCAP Phase II

We choose to model main and interaction effects with the **SRE model**:

$$a_i(\mathbf{s}) = \mathbf{S}(\mathbf{s})' \boldsymbol{\delta}_i, \quad b_j(\mathbf{s}) = \mathbf{S}(\mathbf{s})' \boldsymbol{\gamma}_j, \quad \text{and} \quad (ab)_{ij}(\mathbf{s}) = \mathbf{S}(\mathbf{s})' \boldsymbol{\zeta}_{ij},$$

where

- $\mathbf{S}(\cdot) \equiv (S_1(\cdot), \dots, S_r(\cdot))'$ is a vector of r ($r \ll n$) deterministic, known, multi-resolutional, not-necessarily-orthogonal **spatial basis functions**
- The r -dimensional vectors,

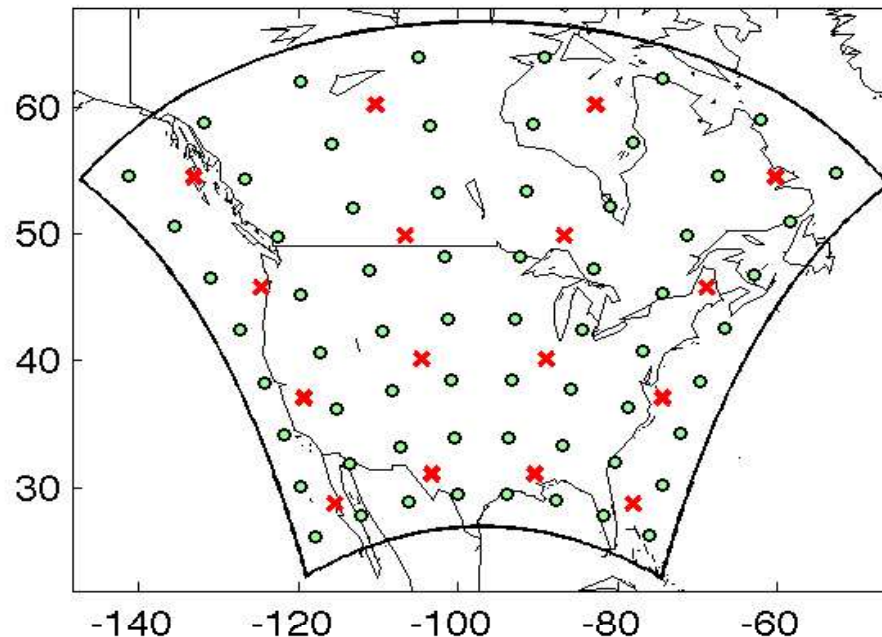
$$\boldsymbol{\delta}_i \equiv (\delta_{1,i}, \dots, \delta_{r,i})', \quad \boldsymbol{\gamma}_j \equiv (\gamma_{1,j}, \dots, \gamma_{r,j})', \quad \boldsymbol{\zeta}_{ij} \equiv (\zeta_{1,ij}, \dots, \zeta_{r,ij})',$$

are Gaussian *random vectors* that capture main effects and interactions on a **reduced-dimensional space**

- We do our modeling and inference on **r -dimensional spaces**. Then our Bayesian approach allows **inference on any summary of $\{Y_{ij}(\cdot) : i = 1, 2, j = 1, \dots, 4\}$**

Spatial Basis Functions

- We use the same set of $r = 85$ spatial basis functions as in Kang, Cressie, and Sain (2012). The map shows the centers of two resolutions of local bisquare (i.e., locally quartic, bell-shaped) functions
- Elevation and indicator functions for land, the Great Lakes, Hudson Bay, and the coastlines, respectively, are part of the set of 85 basis functions



For the r -dimensional random vectors, we assume:

$$\delta_i \sim \text{Gau}(\mathbf{0}, K_1); i = 1, 2,$$

$$\gamma_j \sim \text{Gau}(\mathbf{0}, K_2); j = 1, 3,$$

$$\gamma_j \sim \text{Gau}(\mathbf{0}, K_3); j = 2, 4,$$

$$\zeta_{ij} \sim \text{Gau}(\mathbf{0}, K_4); i = 1, 2, j = 1, 3,$$

$$\zeta_{ij} \sim \text{Gau}(\mathbf{0}, K_5); i = 1, 2, j = 2, 4.$$

Notice that **we allow the covariance matrices to differ** between the mild (spring and fall)

seasons and the extreme (summer and winter) seasons

Sherman-Morrison-Woodbury Identity

- We do our modeling and inference on **reduced-dimensional spaces**
- Consider the $n \times n$ diagonal matrix D and the $r \times r$ matrix K . In all our inferences, we avoid computational bottlenecks because the SRE model allows us to use the **Sherman-Morrison-Woodbury Identity**:

$$(D + PKP')^{-1} = D^{-1} - D^{-1}P\{K^{-1} + P'D^{-1}P\}^{-1}P'D^{-1},$$

for any $n \times r$ matrix P

- The inverse of the $n \times n$ matrix, $(D + PKP')$, only involves **inversion of fixed-rank $r \times r$ matrices** and **of $n \times n$ diagonal matrices**
- **Computing is really fast.** All of the approx. 100,000 data were processed in a fully Bayesian hierarchical setting

Parameter (Prior) Model

- Parameters are $\{\boldsymbol{\mu}, \sigma_\varepsilon^2, K_1, \dots, K_5\}$
- We assume prior independence:

$$[\boldsymbol{\mu}, K_1, \dots, K_5, \sigma_\varepsilon^2] = [\boldsymbol{\mu}] \cdot [K_1] \cdots [K_5] \cdot [\sigma_\varepsilon^2].$$

- Prior on $\boldsymbol{\mu}$:

$$\boldsymbol{\mu} \sim \text{Gau}(\boldsymbol{\mu}_0, \sigma_0^2 I)$$

- Prior on σ_ε^2 :

$$\sigma_\varepsilon^2 \sim \text{IG}(a, b)$$

- For the $r \times r$, positive-definite covariance matrices $\{K_m : m = 1, \dots, 5\}$, we consider the multi-resolution **Givens-angle prior** (Kang and Cressie, 2011)

Givens-Angle Representation of K_m

- Consider the spectral decomposition of K_m ,

$$K_m = P_m \Lambda_m P_m',$$

where

- $\Lambda_m = \text{diag}(\lambda_{1,m}, \dots, \lambda_{r,m})$, with $\lambda_{1,m} \geq \lambda_{2,m} \geq \dots \geq \lambda_{r,m} > 0$
- P_m is the corresponding orthogonal matrix of eigenvectors
- Parameterize P_m in terms of the $r(r-1)/2$ Givens angles, denoted by $\theta_{ij,m}$, for $i = 1, \dots, r-1$ and $j = i+1, \dots, r$:

$$P_m = (G_{12,m} G_{13,m} \cdots G_{1r,m}) \cdot (G_{23,m} \cdots G_{2r,m}) \cdots G_{(r-1)r,m}$$

- $G_{ij,m}$ is a modification of the $r \times r$ identity matrix whose i -th and j -th diagonal elements of 1 are replaced by $\cos(\theta_{ij,m})$ and whose (i,j) and (j,i) elements of 0 are replaced by $-\sin(\theta_{ij,m})$ and $\sin(\theta_{ij,m})$, respectively

- We define

$$\boldsymbol{\lambda}_m \equiv (\lambda_{1,m}, \dots, \lambda_{r,m})'$$

$$\boldsymbol{\theta}_m \equiv (\theta_{12,m}, \dots, \theta_{1r,m}, \theta_{23,m}, \dots, \theta_{2r,m}, \dots, \theta_{(r-1)r,m})'$$

- We assume

$$[\boldsymbol{\lambda}_m, \boldsymbol{\theta}_m] = [\boldsymbol{\lambda}_m] \cdot [\boldsymbol{\theta}_m]$$

- We assign priors on $\boldsymbol{\lambda}_m$ and $\boldsymbol{\theta}_m$ as suggested by Kang and Cressie (2011), so that the prior on K_m has a *multi-resolutional structure* brought about by the choice of multi-resolutional spatial basis functions in the SRE model

Statistical Computing based on MCMC

- Gibbs sampling with Metropolis-Hastings updates is used to obtain the posterior distributions of the unknowns given data $\{\mathbf{D}_{ij}\}$
- Computation was carried out in Matlab on a dual-core 2.88GHz Intel Xeon processor with 96GB of memory running Linux
 - Two parallel chains were run for 12,500 iterations each and the first 2,500 were discarded as burn-in
 - Because of the large number of parameters and process values involved, we checked convergence of the MCMC on selected quantities that respected the multi-resolutional structure
 - Bayesian inference took approx. 40 CPU hours

Results: Posterior Inferences

- The first thing we computed was the **posterior mean and posterior distribution** of the average temperature-change projections, averaged over RCMs and seasons. This spatial field of **overall** temperature differences is:

$$Y_{..}(\mathbf{s}) = \sum_{i=1}^2 \sum_{j=1}^4 Y_{ij}(\mathbf{s})/8; \mathbf{s} \in D$$

- We then did the same for the **seasonal** temperature differences:

$$Y_{.j}(\mathbf{s}) = \sum_{i=1}^2 Y_{ij}(\mathbf{s})/2; \mathbf{s} \in D,$$

where $j = 1$ (spring), $j = 2$ (summer), $j = 3$ (autumn), and $j = 4$ (winter)

Posterior Inferences for $Y_{..}(\cdot)$

- Our Bayesian analysis enables us to consider any summaries of the full posterior distribution of $Y_{..}(\cdot)$
 - Pixelwise posterior mean: $\hat{Y}_{..}(\cdot) \equiv E(Y_{..}(\cdot) | \text{data})$
 - pixelwise posterior standard deviation: $\hat{\sigma}_{Y_{..}}(\cdot) \equiv \{\text{var}(Y_{..}(\cdot) | \text{data})\}^{1/2}$
 - Pixelwise **posterior 2.5th and 97.5th percentiles**:

$$\hat{Y}_{..}^{(2.5)}(\cdot) \text{ and } \hat{Y}_{..}^{(97.5)}(\cdot),$$

where posterior percentile computations provide us with a pixelwise posterior probability interval (or **prediction interval**):

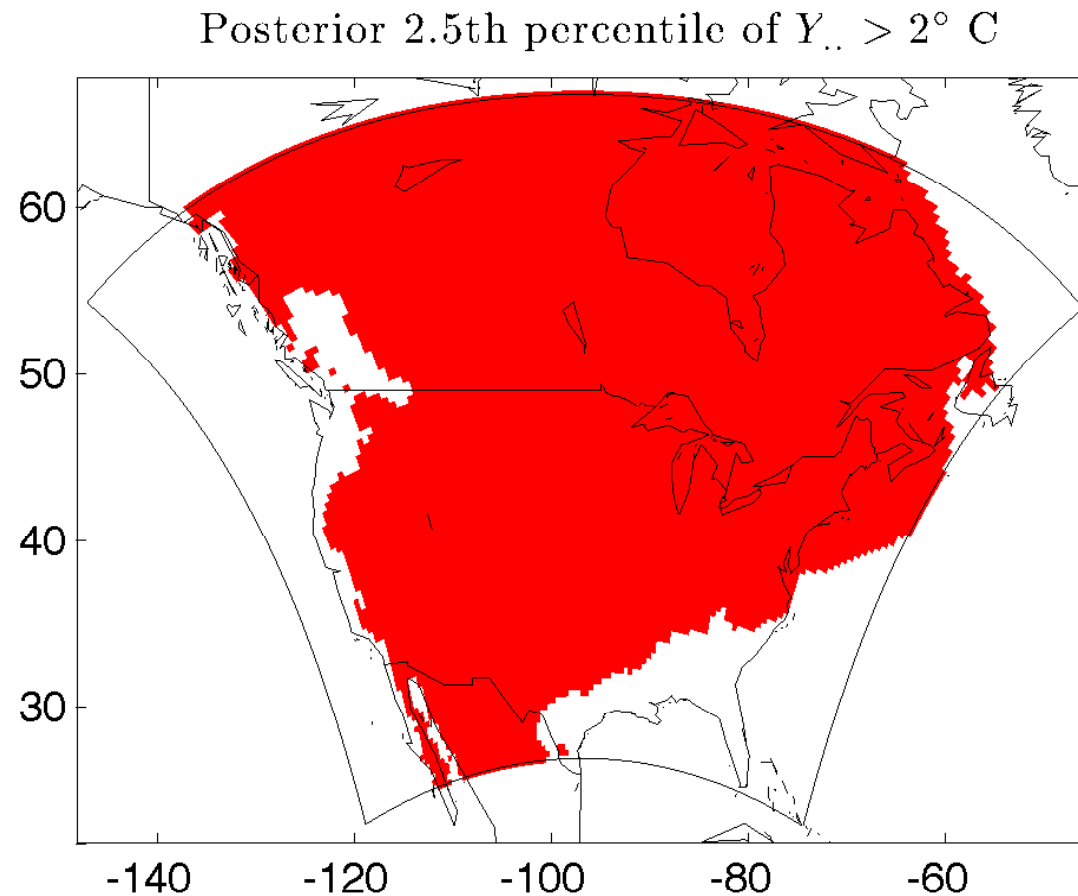
$$Pr(\hat{Y}_{..}^{(2.5)}(\mathbf{s}) \leq Y_{..}(\mathbf{s}) \leq \hat{Y}_{..}^{(97.5)}(\mathbf{s}) | \{\mathbf{D}_{ij}\}) = 0.95$$

The Consequences of a Much Warmer World

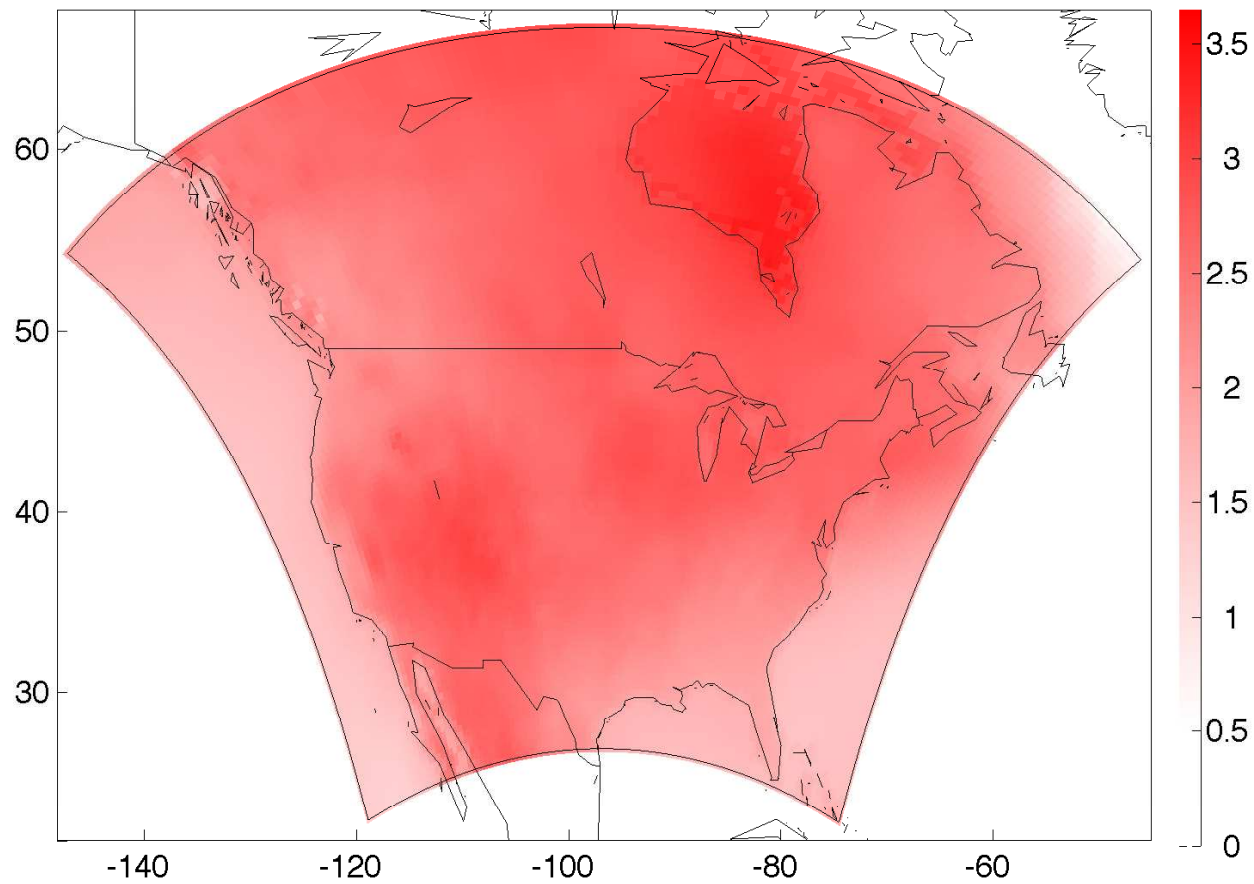
- 2°C tolerable threshold (defined by the European Union)
 - This is defined as the difference between temperatures of the future and the pre-industrial period (1861–1890)
 - The average global temperature of the pre-industrial period is about 0.8°C cooler than the current period
(http://ec.europa.eu/clima/policies/brief/eu/index_en.htm)
- Therefore, the following summaries from our analysis are even more alarming:
 - About two thirds of the pixels have posterior 2.5th percentiles greater than 2°C
 - More than three fourths of the pixels have posterior 97.5th percentiles greater than 2°C
 - Pixels over water are generally cooler; that is, almost all the land pixels are indicating warming above 2°C

Uncertainty Quantification: Regions of Unsustainable Warming

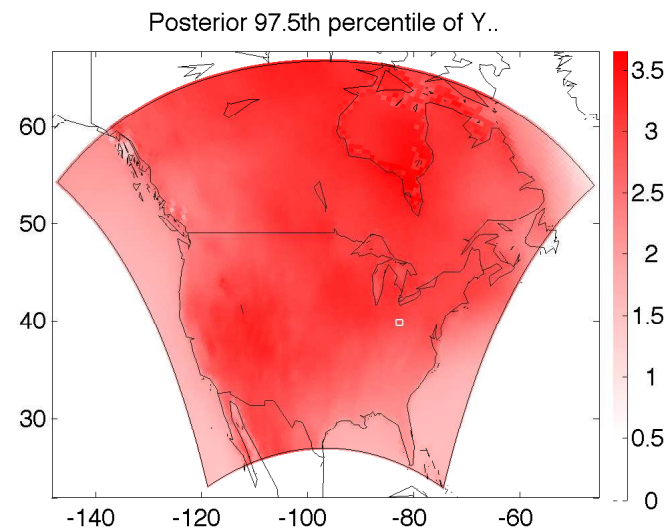
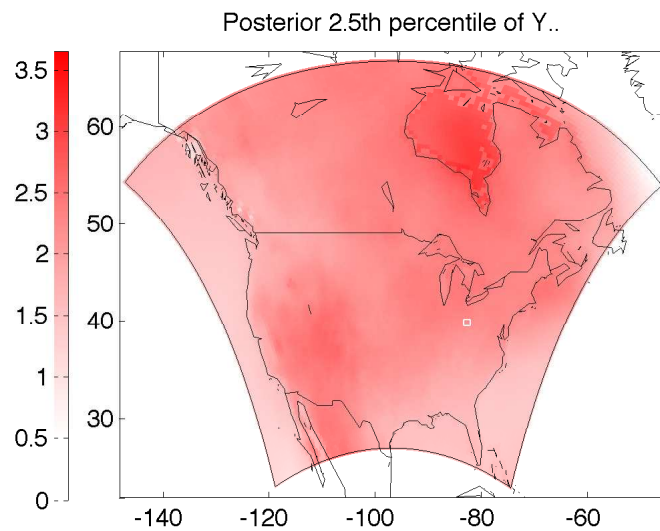
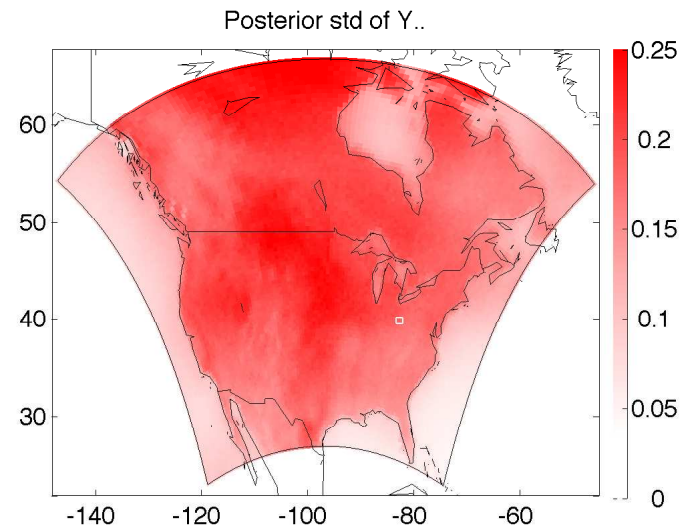
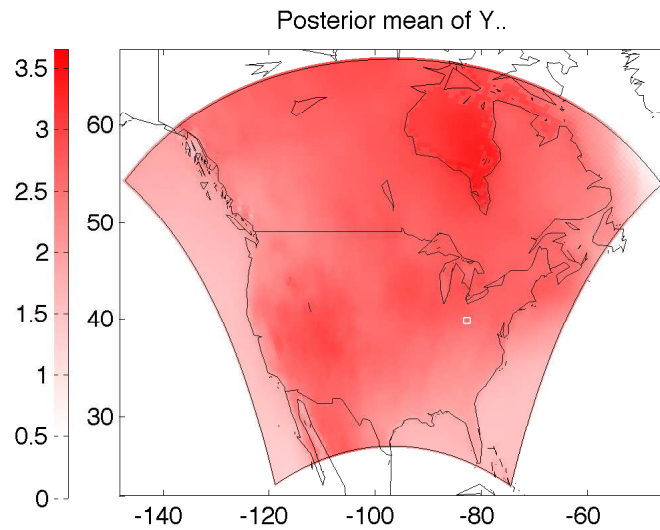
- Large regions of North America (shown in red) have pixelwise posterior 2.5th percentiles **above the sustainability limit** of 2°C



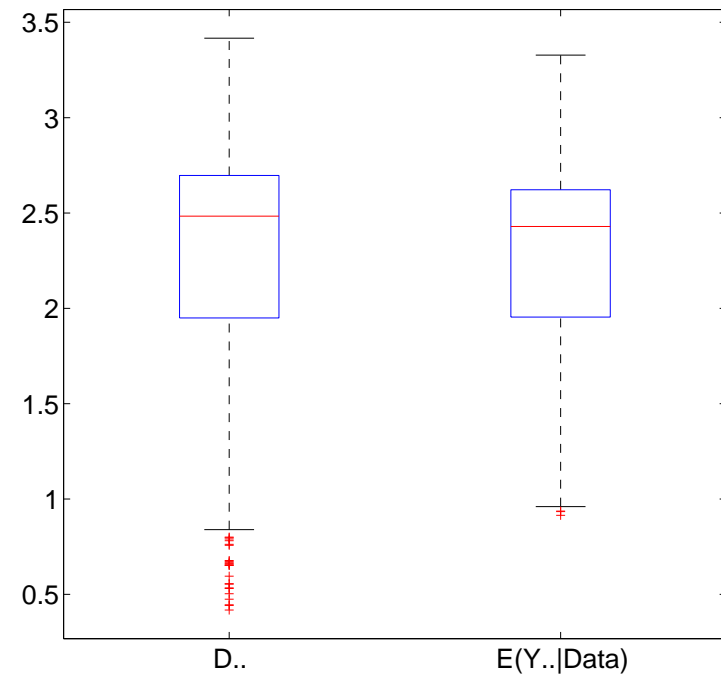
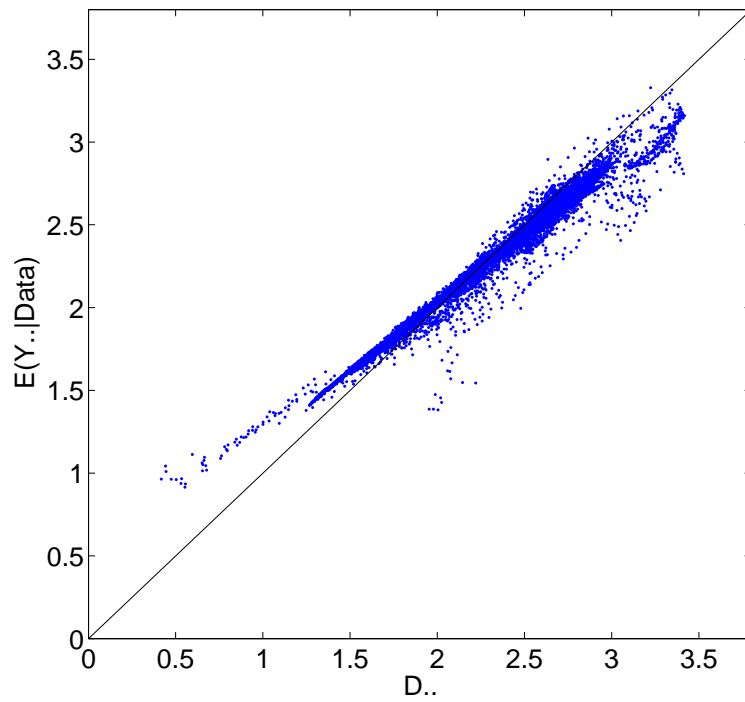
Map of $\hat{Y}_{..}(\cdot) = E[Y_{..}(\cdot)|data]$



Uncertainty Quantification: $\hat{Y}_{..}(\cdot)$, $\hat{\sigma}_{Y_{..}}(\cdot)$, $\hat{Y}_{..}^{(2.5)}(\cdot)$, $\hat{Y}_{..}^{(97.5)}(\cdot)$



$\hat{Y}_{..}(\cdot)$ vs. $D_{..}(\cdot)$



The plot shows shrinkage

Uncertainty Quantification: Individual Pixel

- Our Bayesian statistical analysis yields an approx. 100,000-dimensional joint posterior distribution:

$$[\{Y_{ij}(\mathbf{s}_\ell) : i = 1, 2, j = 1, \dots, 4, \ell = 1, \dots, 11760\}]$$

- Fix a pixel \mathbf{s}_0 (e.g., the **pixel containing Columbus**)

- We can produce the posterior distributions:

$$[Y_{..}(\mathbf{s}_0) | \text{data}], [Y_{.1}(\mathbf{s}_0) | \text{data}], \dots, [Y_{.4}(\mathbf{s}_0) | \text{data}];$$

in particular for each distribution we can produce its mean, 2.5-th percentile, and 97.5-th percentile

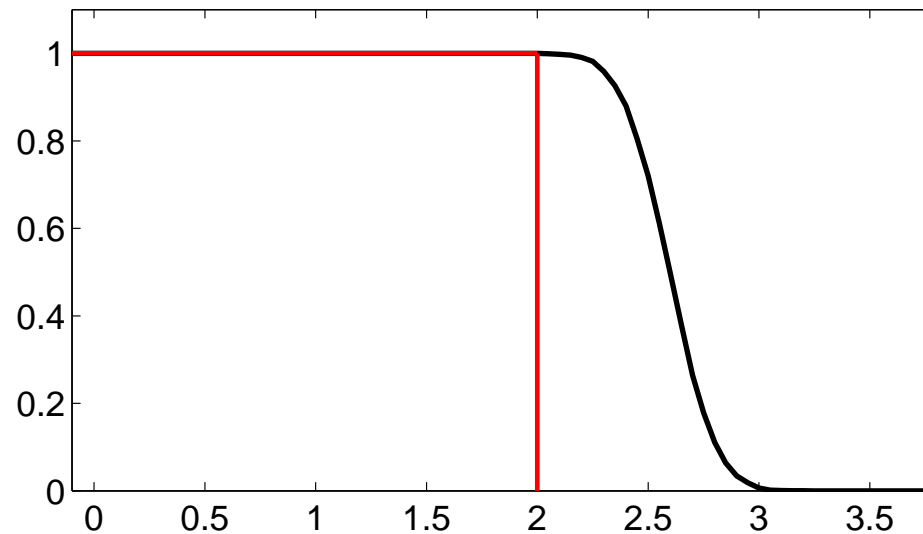
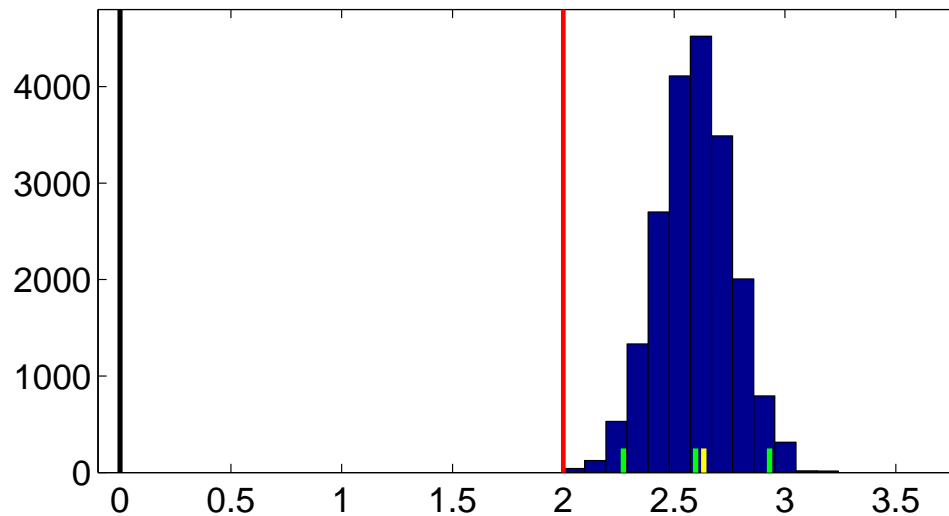
- From these posterior distributions, we can compute:

$$Pr(Y_{..}(\mathbf{s}_0) > k | \text{data})$$

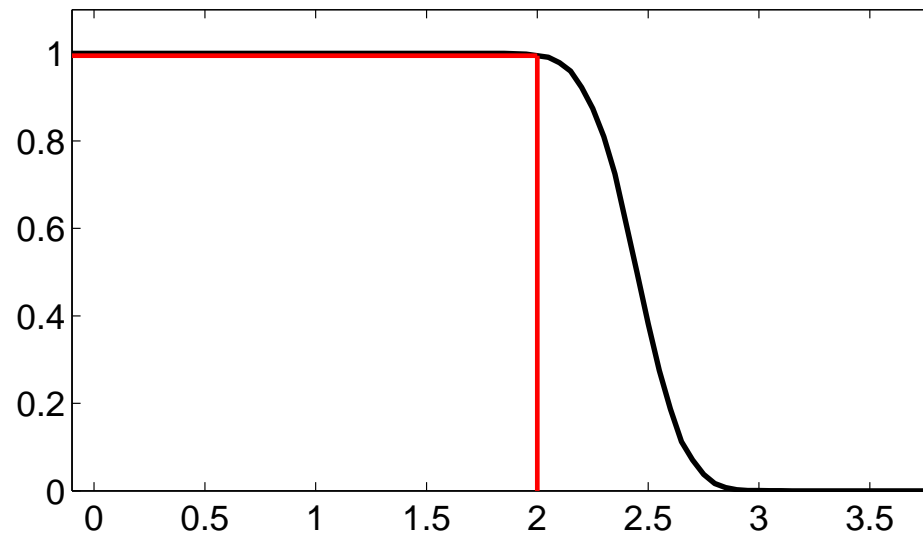
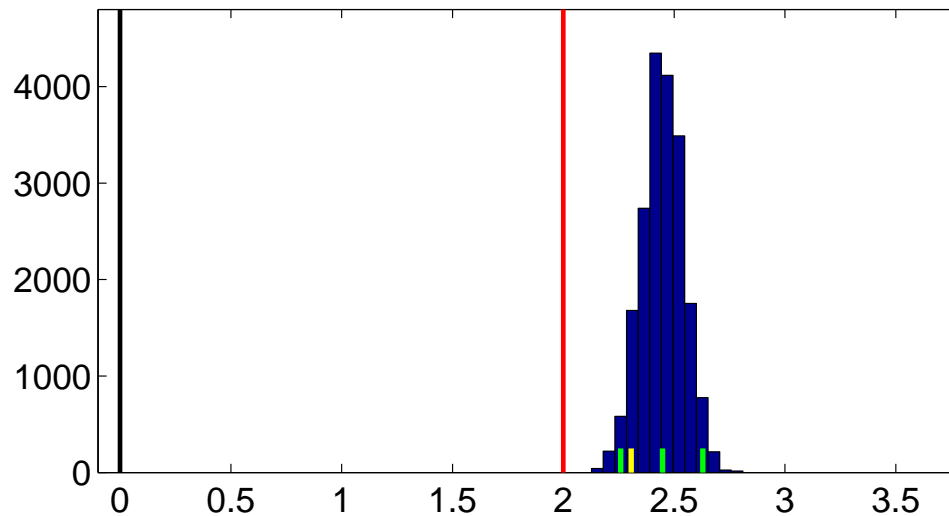
$$Pr(Y_{.1}(\mathbf{s}_0) > k | \text{data}), \dots, Pr(Y_{.4}(\mathbf{s}_0) > k | \text{data})$$

- Choose \mathbf{s}_0 to be the **“Columbus” pixel** and $k = 2^\circ C$ (upper limit of sustainability)

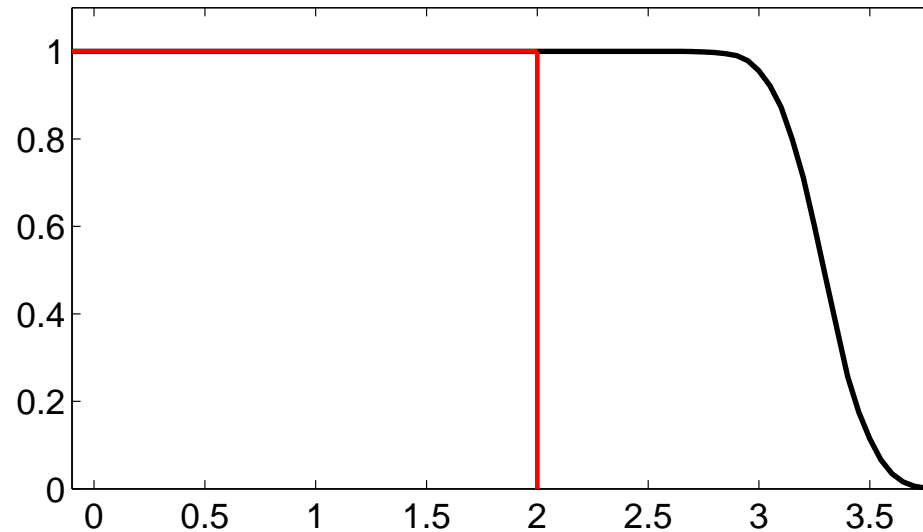
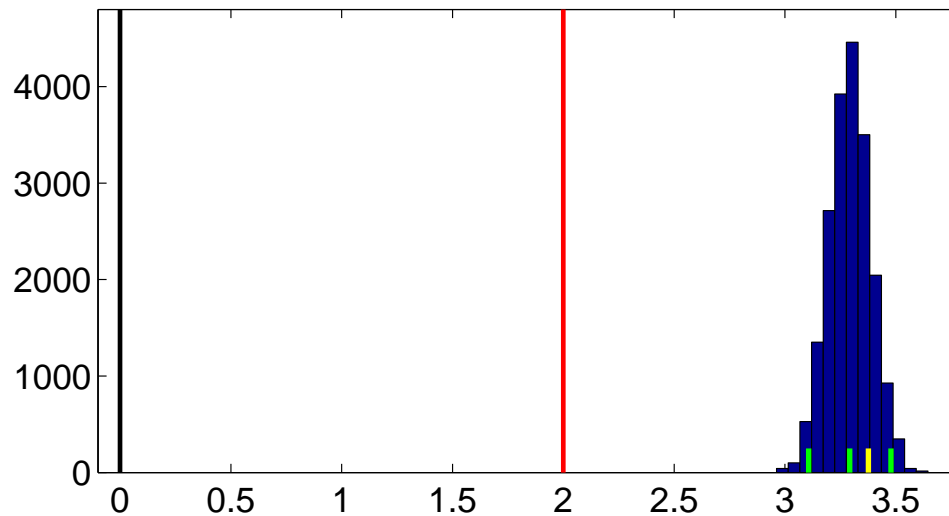
Uncertainty Quantification: “Columbus” Pixel; Overall



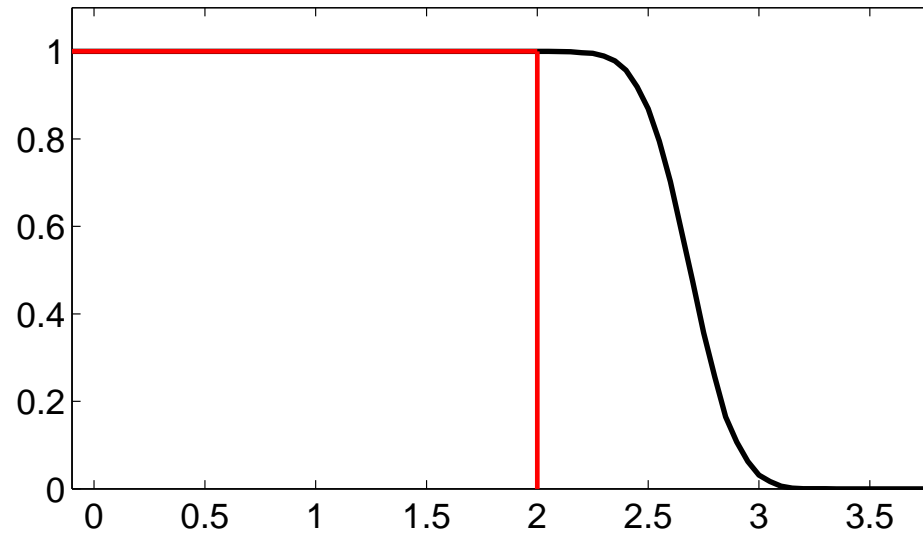
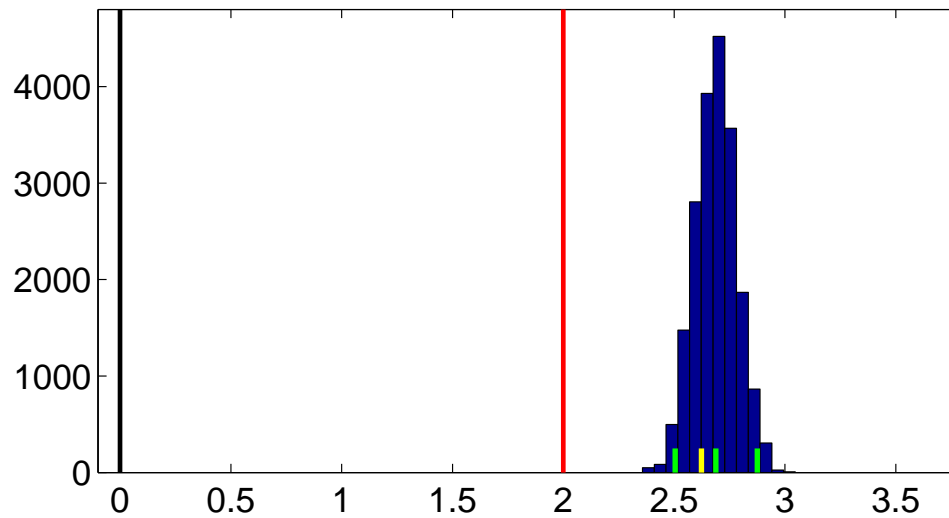
Uncertainty Quantification: “Columbus” Pixel; Spring



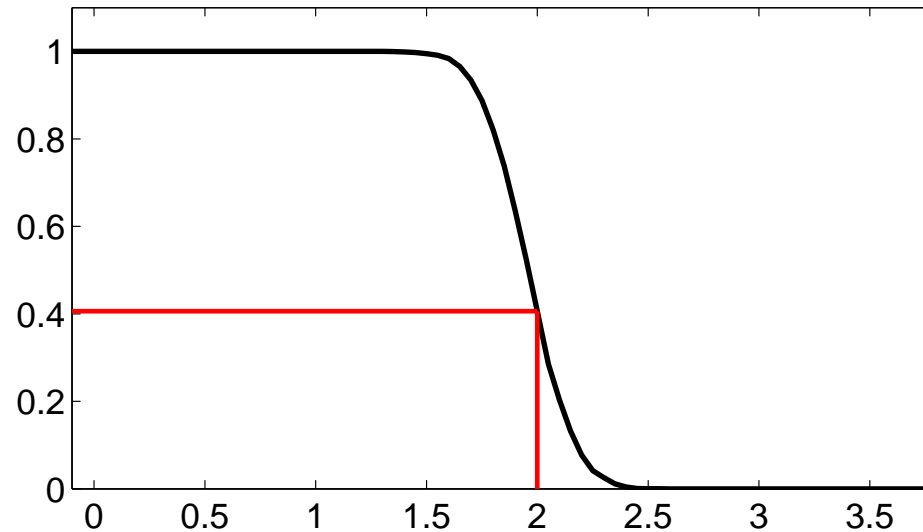
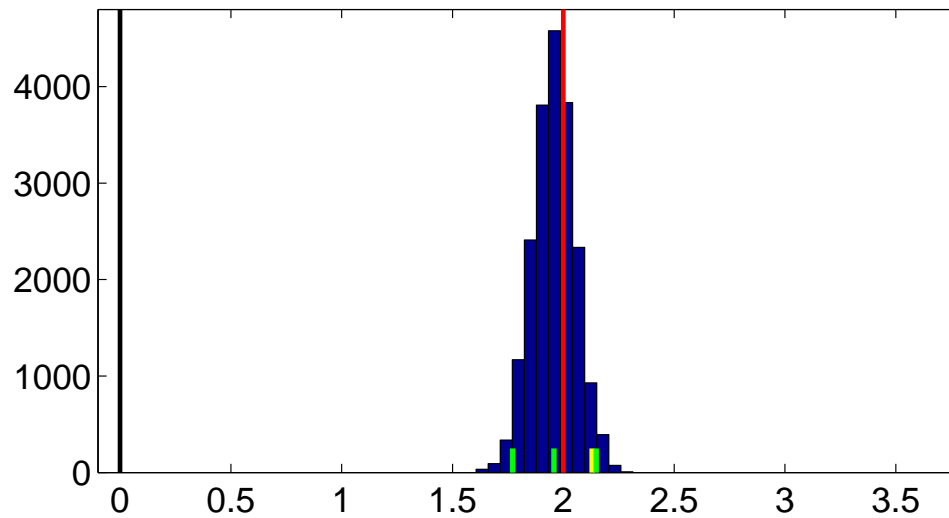
Uncertainty Quantification: “Columbus” Pixel; Summer



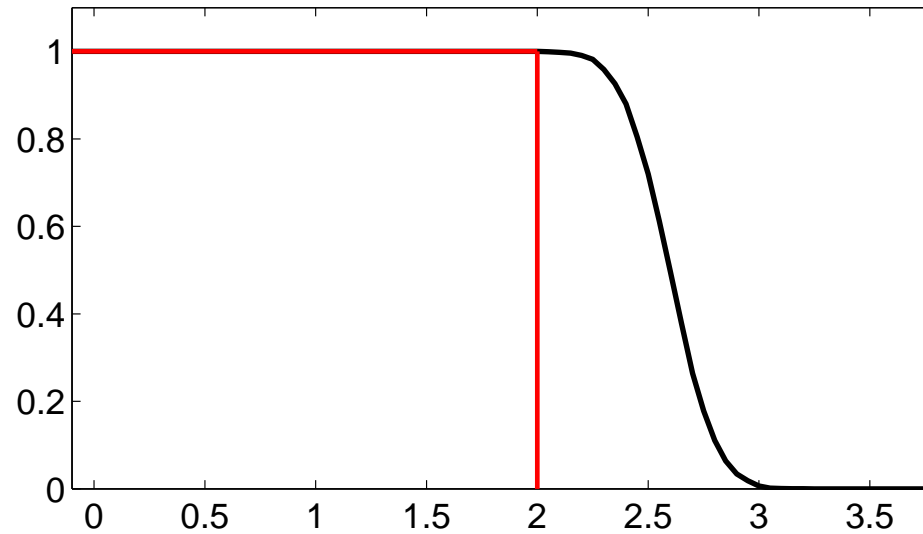
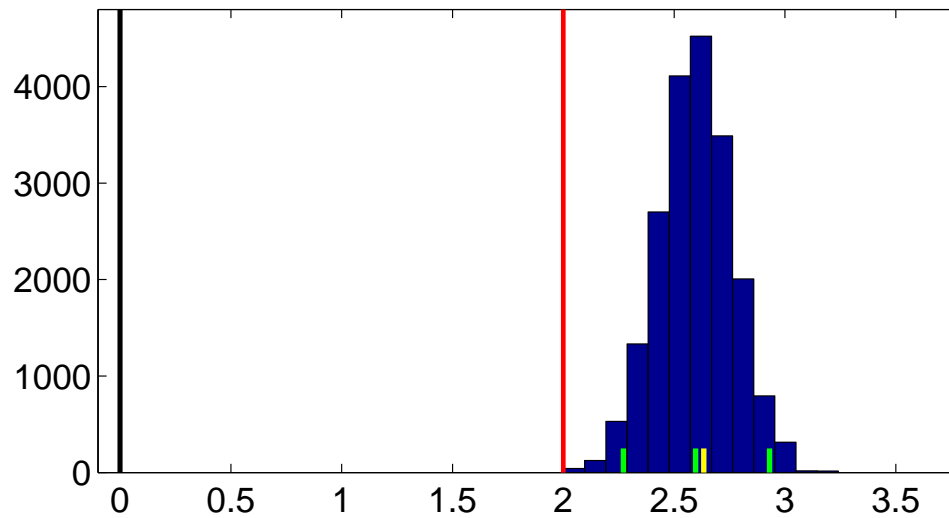
Uncertainty Quantification: “Columbus” Pixel; Autumn



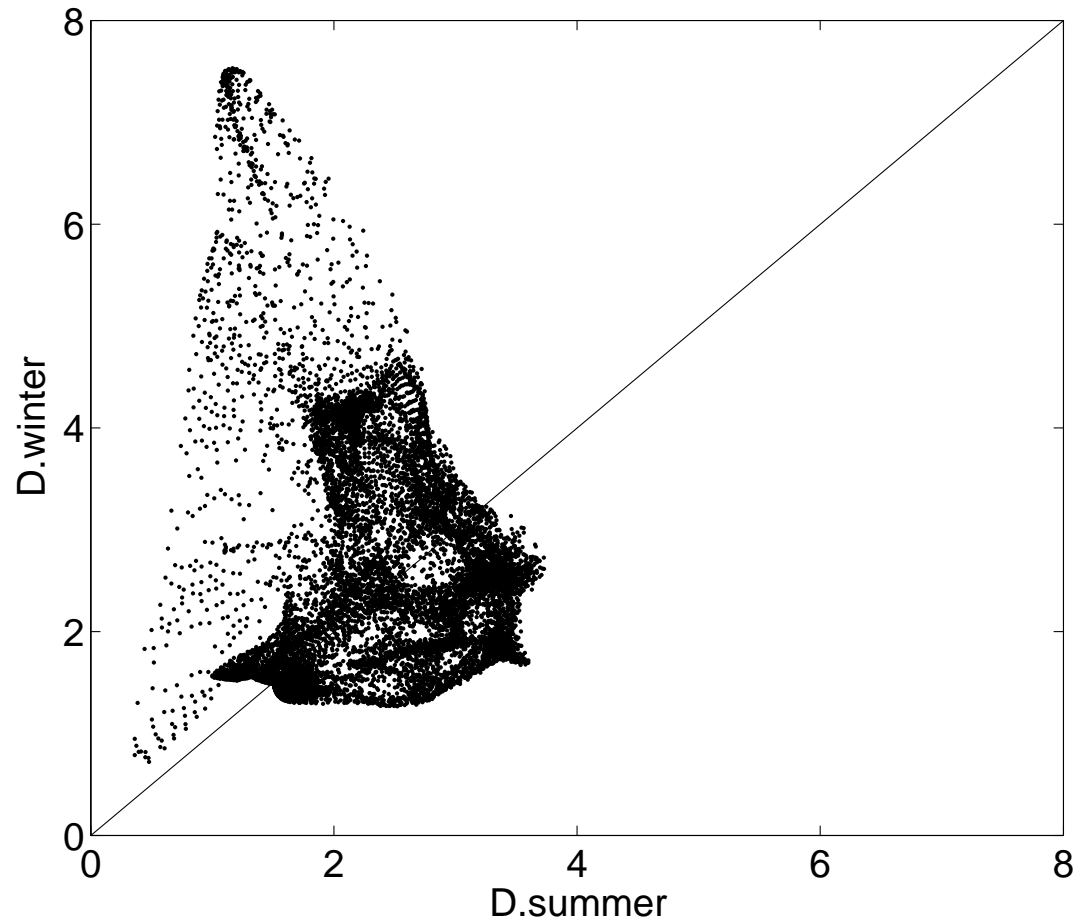
Uncertainty Quantification: “Columbus” Pixel; Winter



Uncertainty Quantification: “Columbus” Pixel; Overall



Temperature Change in Winter vs. Summer



Uncertainty Quantification: All of North America

- Our Bayesian statistical analysis yields an approx. 100,000-dimensional posterior distribution:

$$[\{Y_{ij}(\mathbf{s}_\ell) : i = 1, 2, j = 1, \dots, 4, \ell = 1, \dots, 11760\}],$$

but so far we considered only the marginal distributions associated with the pixel containing Columbus

- From our exploratory spatial data analysis, summer ($j = 2$) and winter ($j = 4$) show the strongest patterns: In summer, there is more warming in the south. In winter, there is more warming in the north
- Maps of pixelwise posterior probabilities of being greater than the threshold k can be computed. For all $\mathbf{s} \in D$, we compute and map

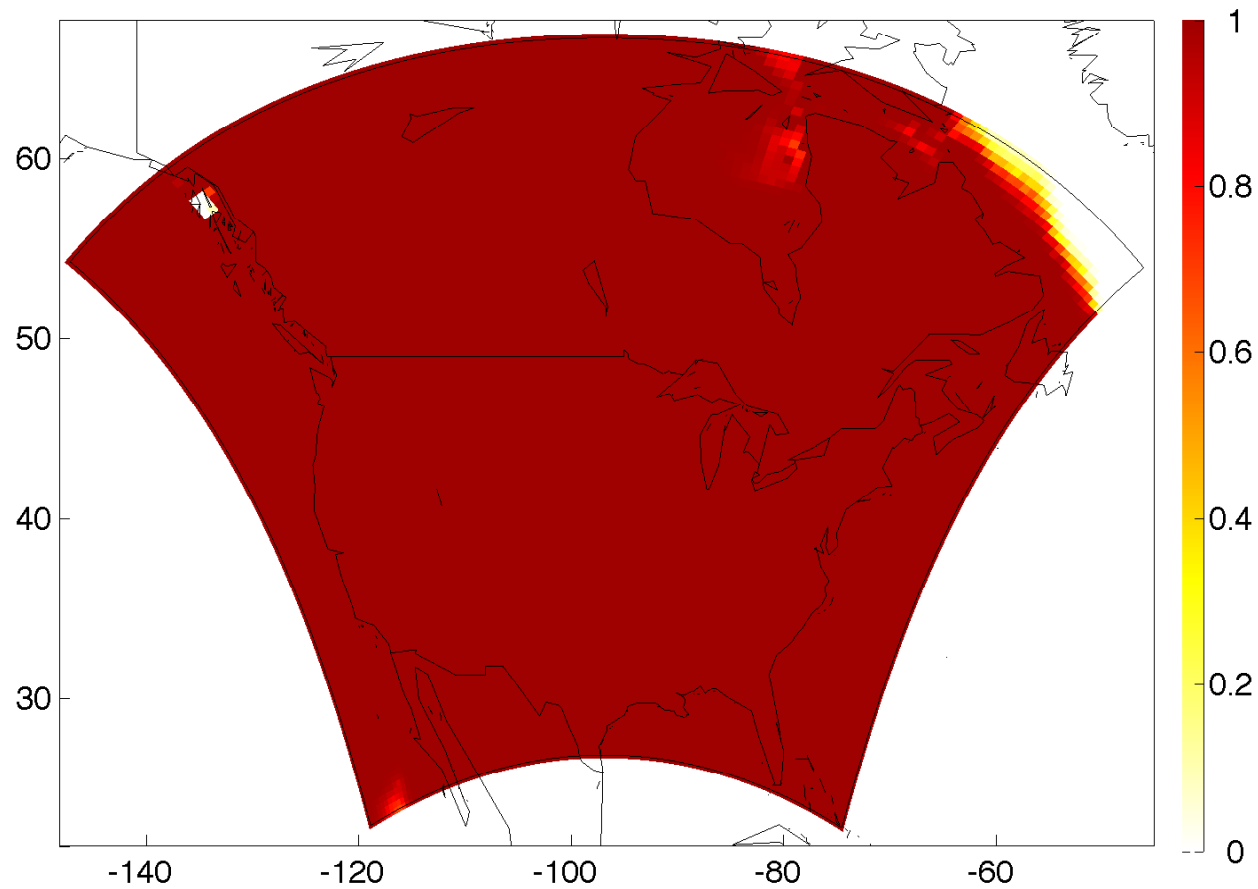
$$Pr(Y_{\cdot j}(\mathbf{s}) > k \mid \text{data}), \text{ for } j = 2 \text{ (summer), and } j = 4 \text{ (winter)}$$

The maps are inferential versions of the SPOT functions

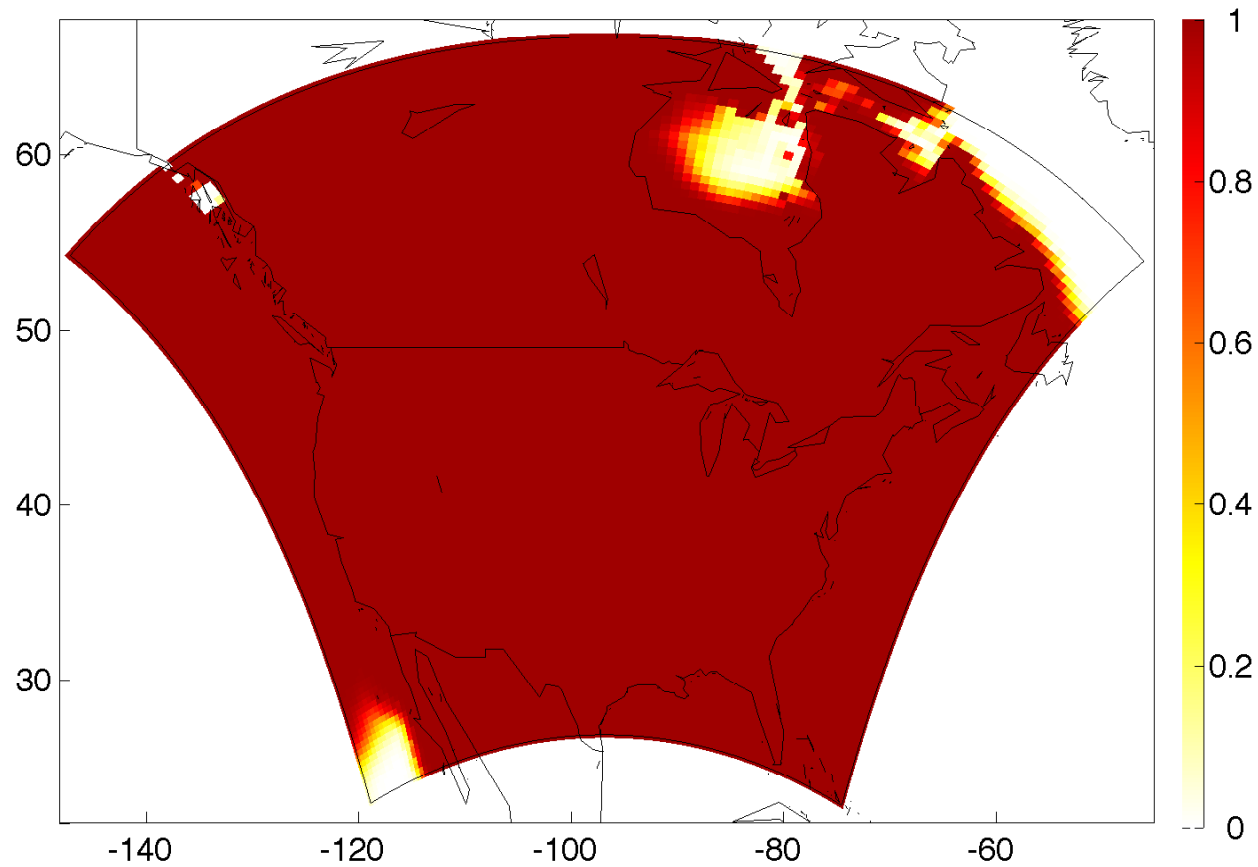
Summer

Summer

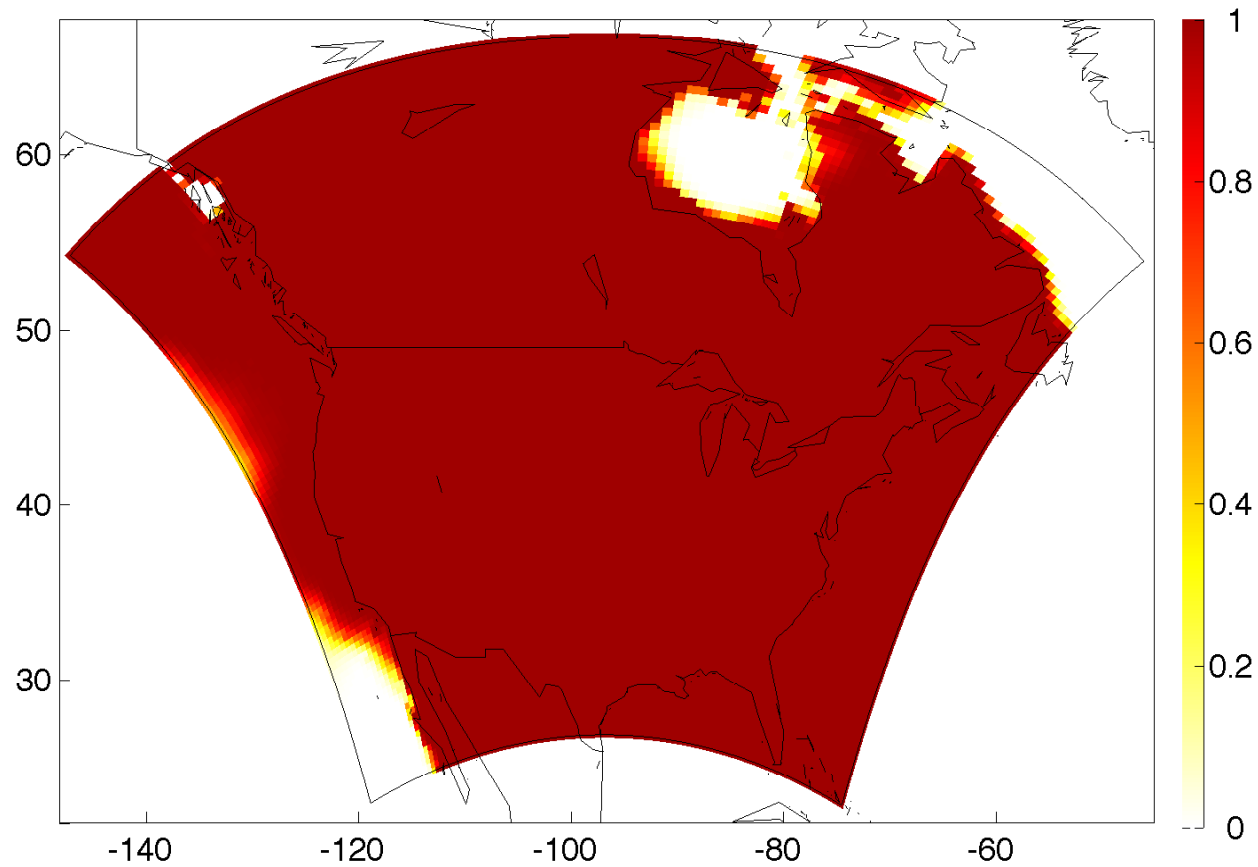
Summer: $Pr(Y_2(\cdot) > k | \text{data})$, for $k = 1.0^\circ\text{C}$



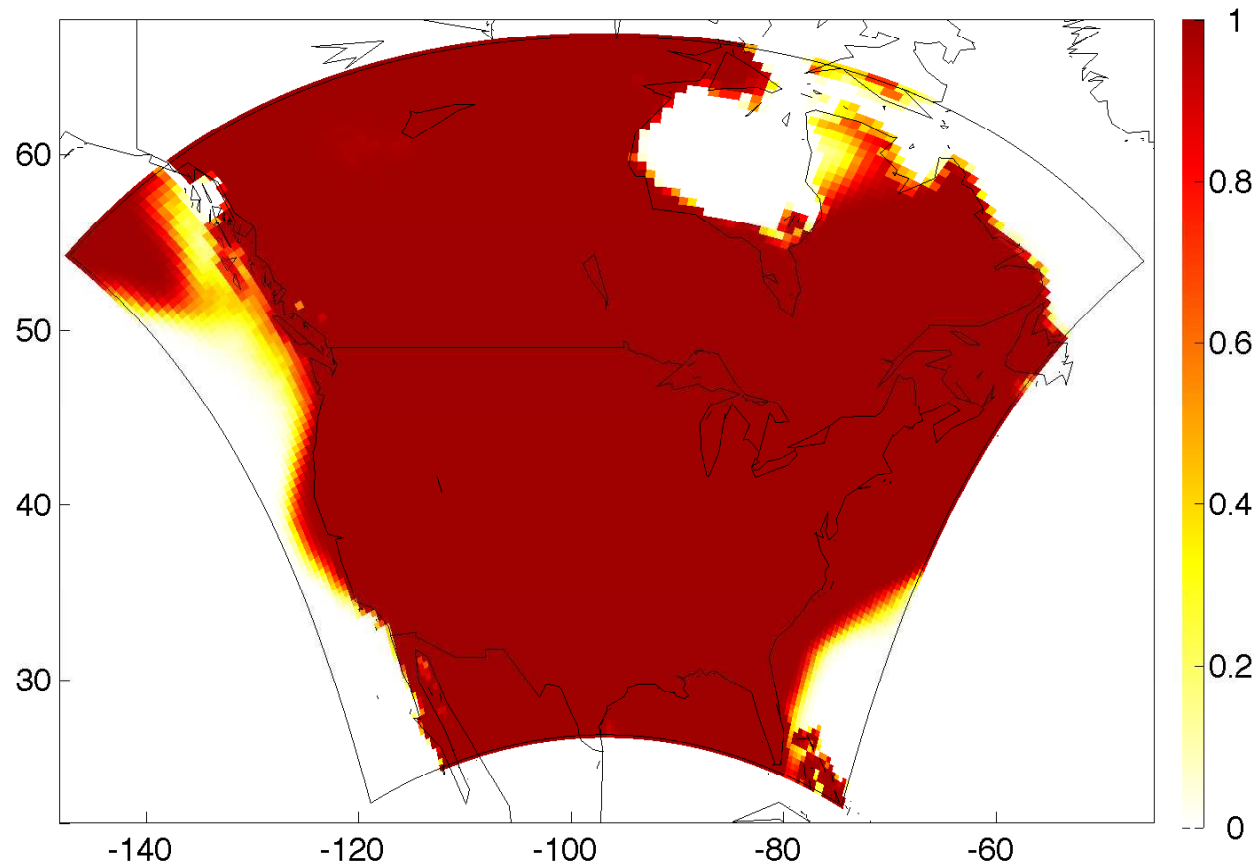
Summer: $Pr(Y_2(\cdot) > k | \text{data})$, for $k = 1.2^\circ\text{C}$



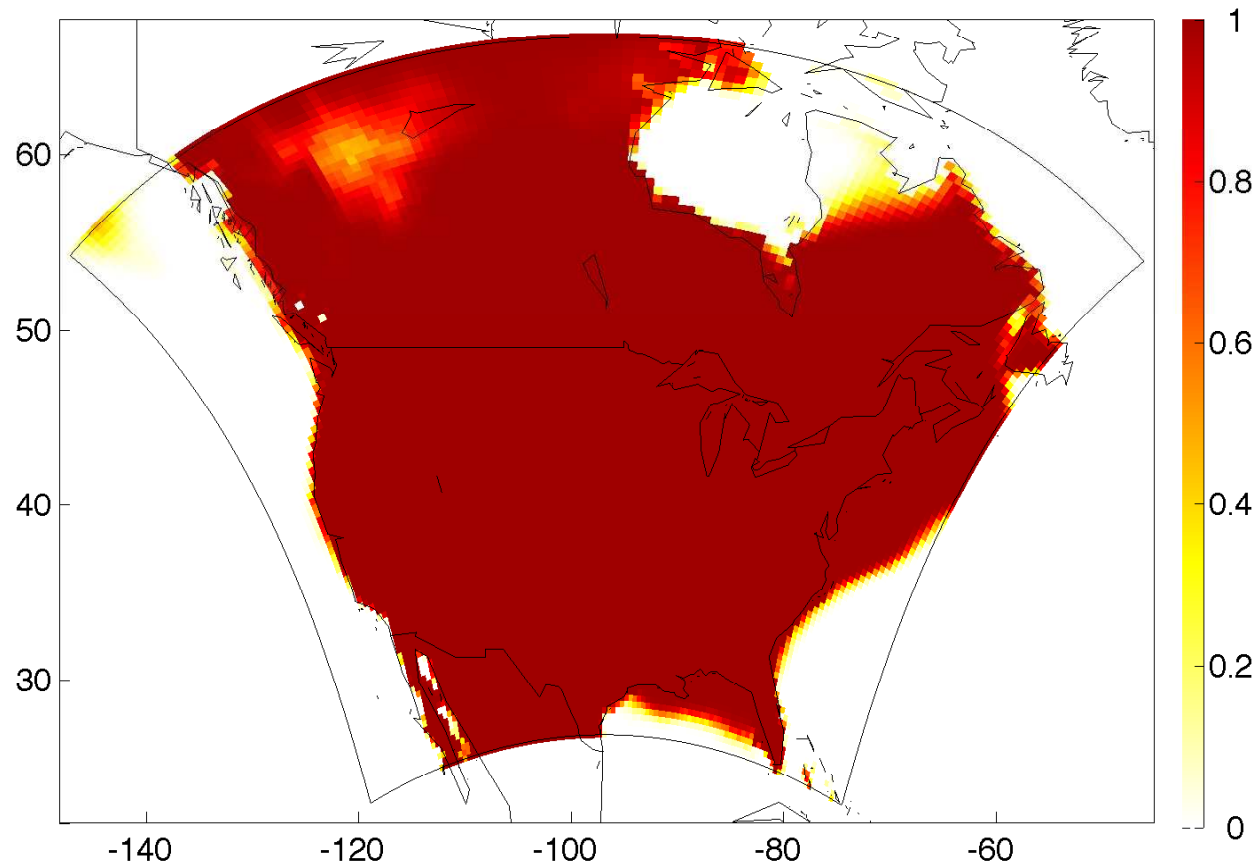
Summer: $Pr(Y_2(\cdot) > k | \text{data})$, for $k = 1.4^\circ\text{C}$



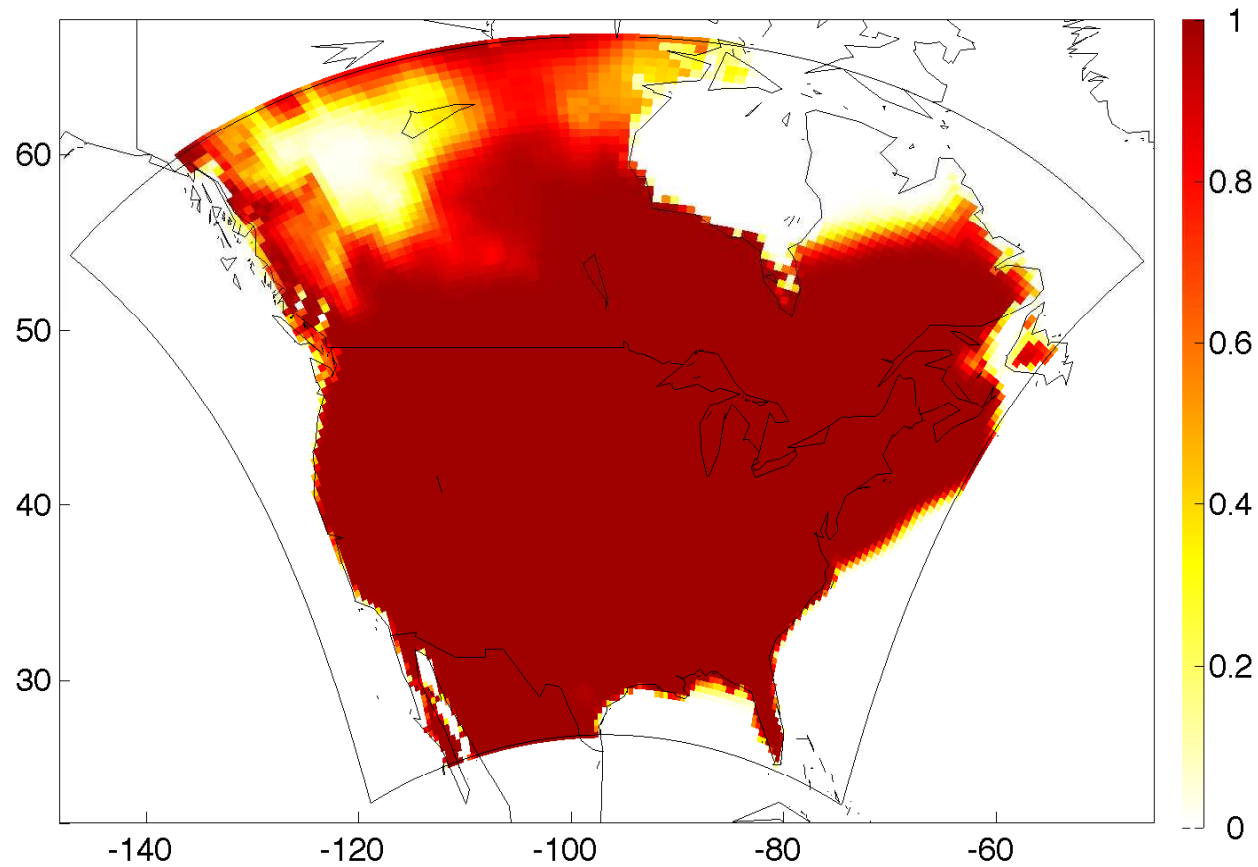
Summer: $Pr(Y_2(\cdot) > k | \text{data})$, for $k = 1.6^\circ\text{C}$



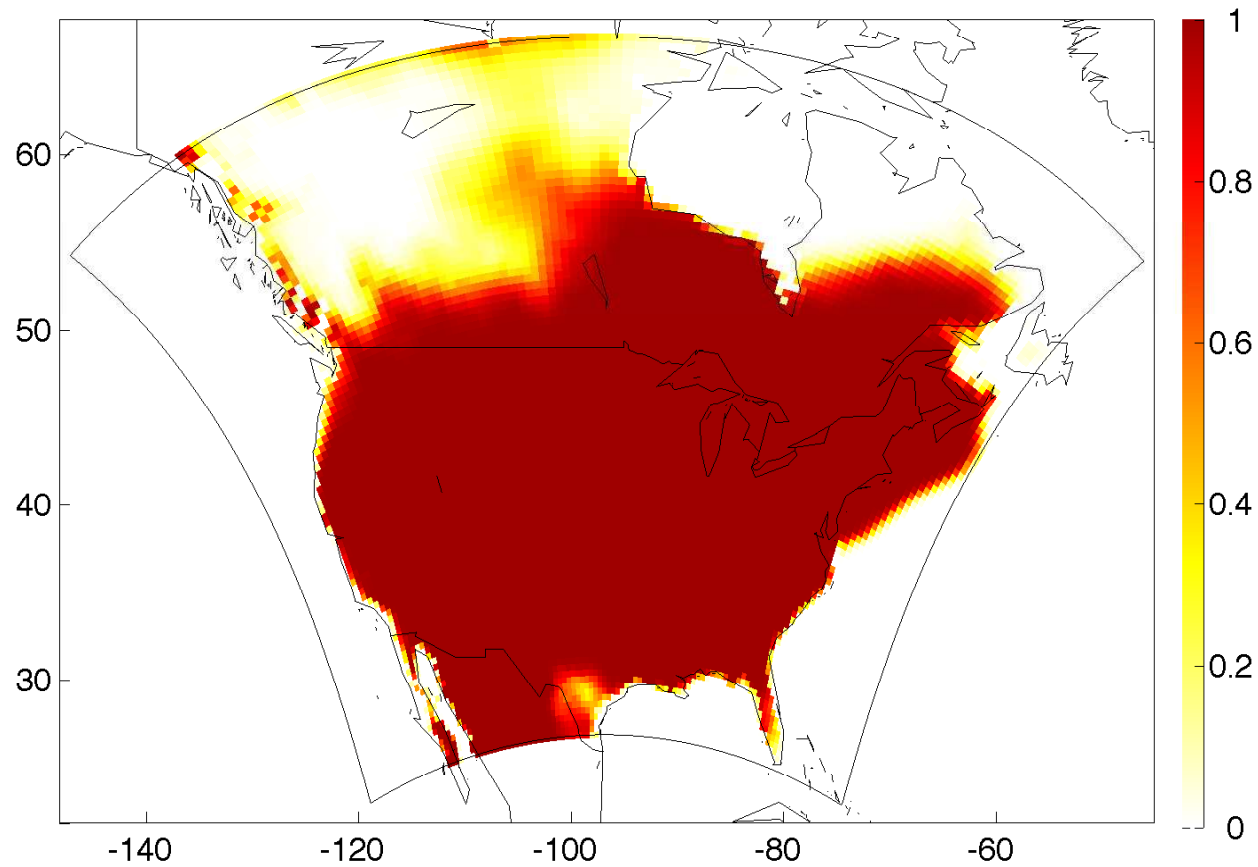
Summer: $Pr(Y_2(\cdot) > k | \text{data})$, for $k = 1.8^\circ\text{C}$



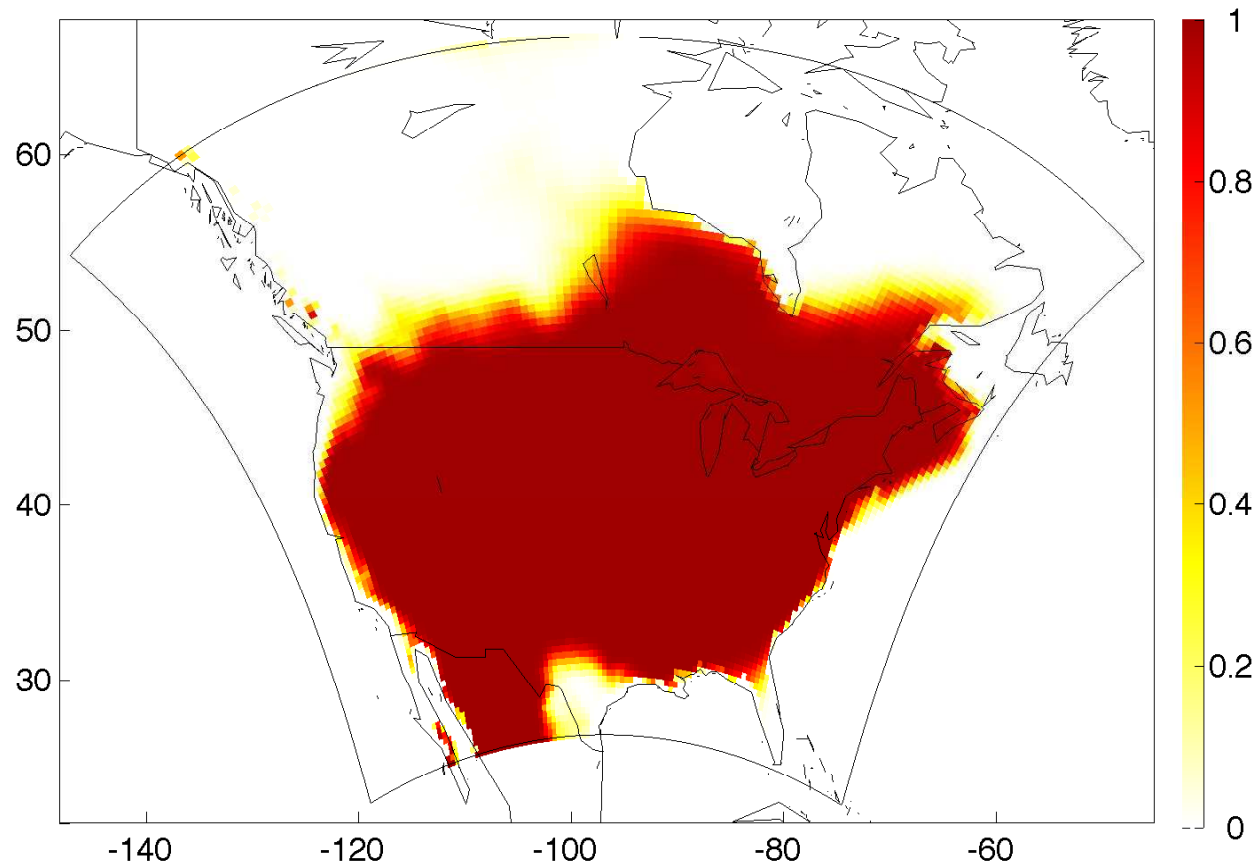
Summer: $Pr(Y_2(\cdot) > k | \text{data})$, for $k = 2.0^\circ\text{C}$



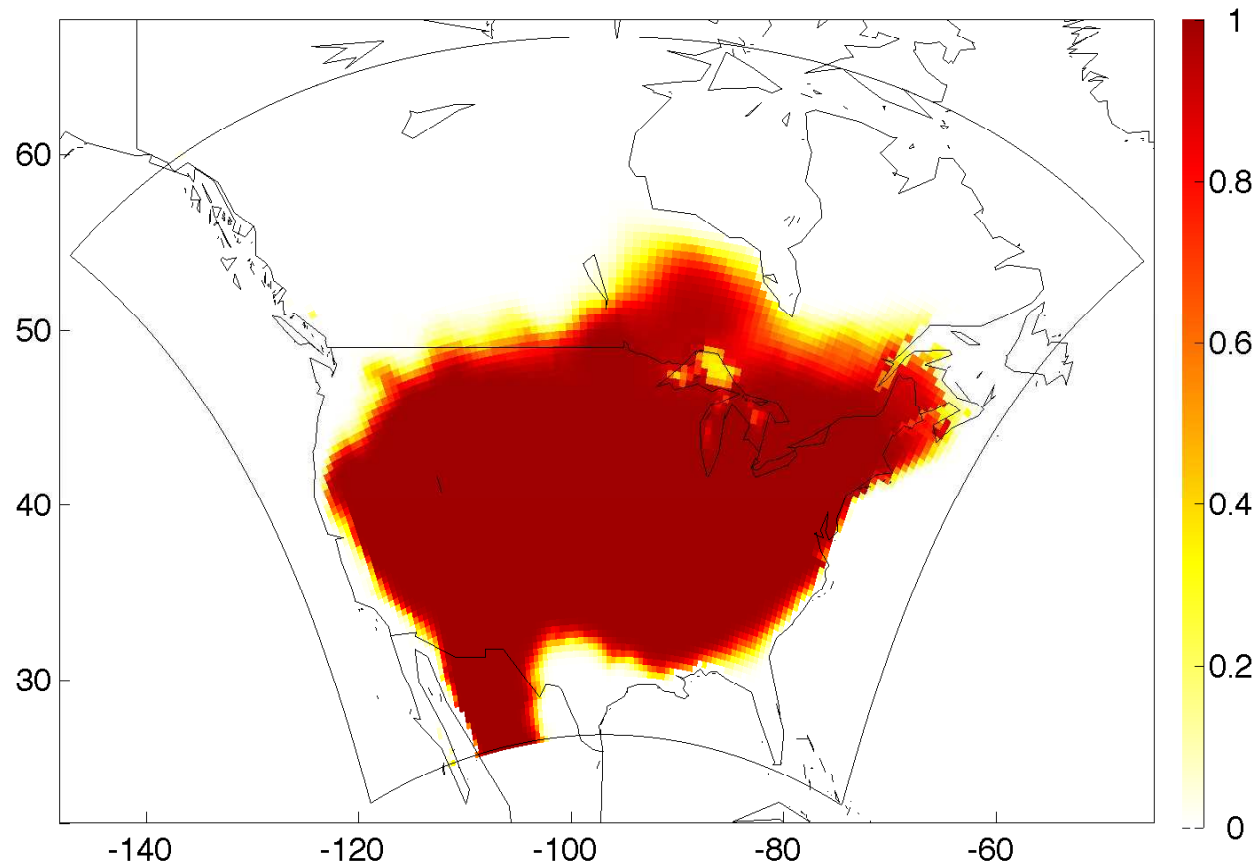
Summer: $Pr(Y_2(\cdot) > k | \text{data})$, for $k = 2.2^\circ\text{C}$



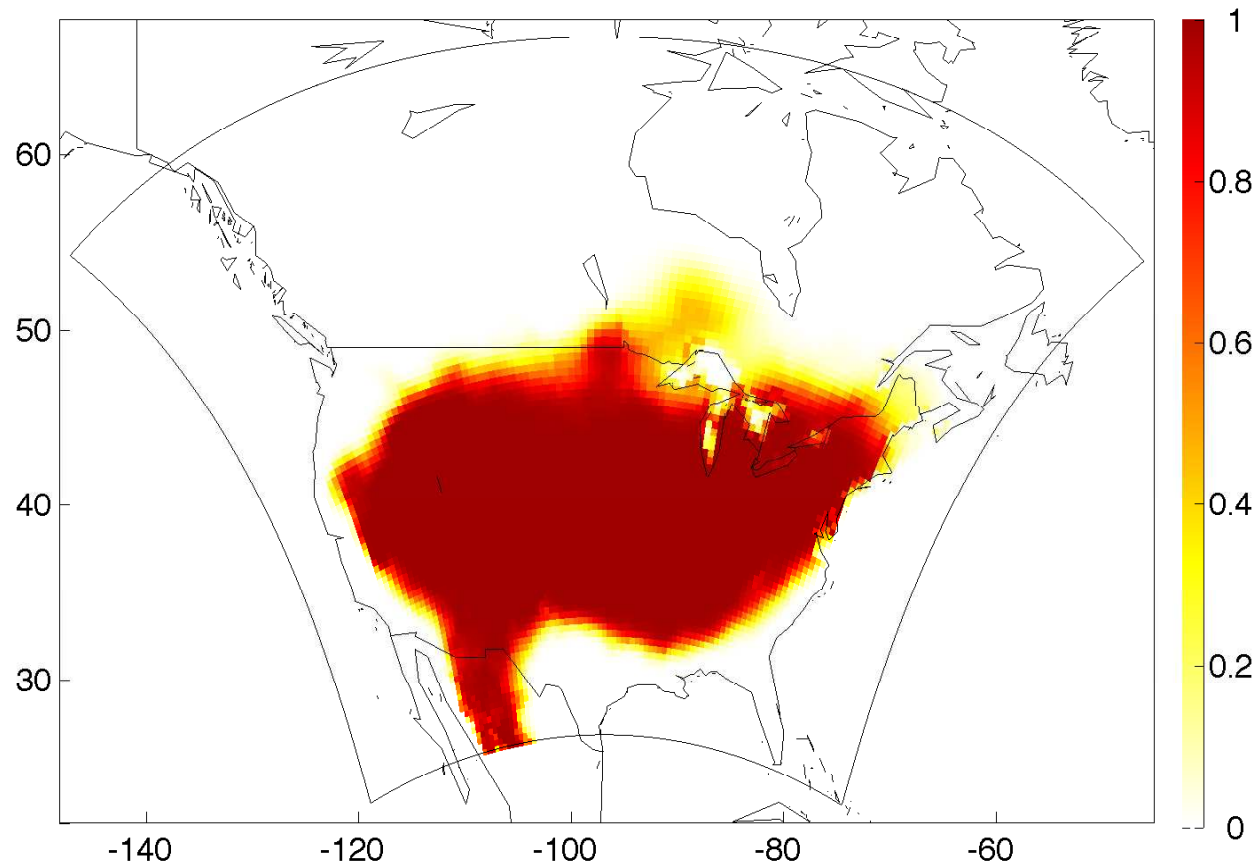
Summer: $Pr(Y_2(\cdot) > k | \text{data})$, for $k = 2.4^\circ\text{C}$



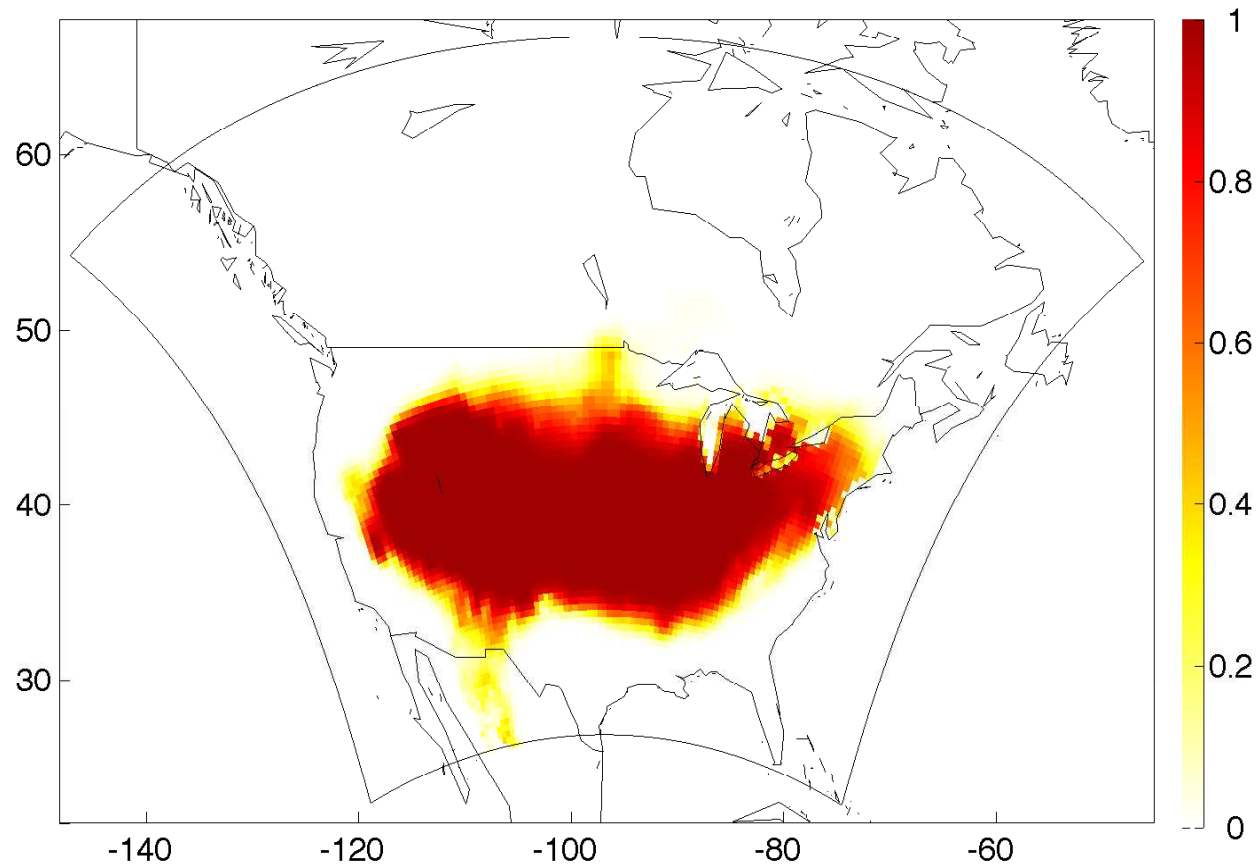
Summer: $Pr(Y_2(\cdot) > k | \text{data})$, for $k = 2.6^\circ\text{C}$



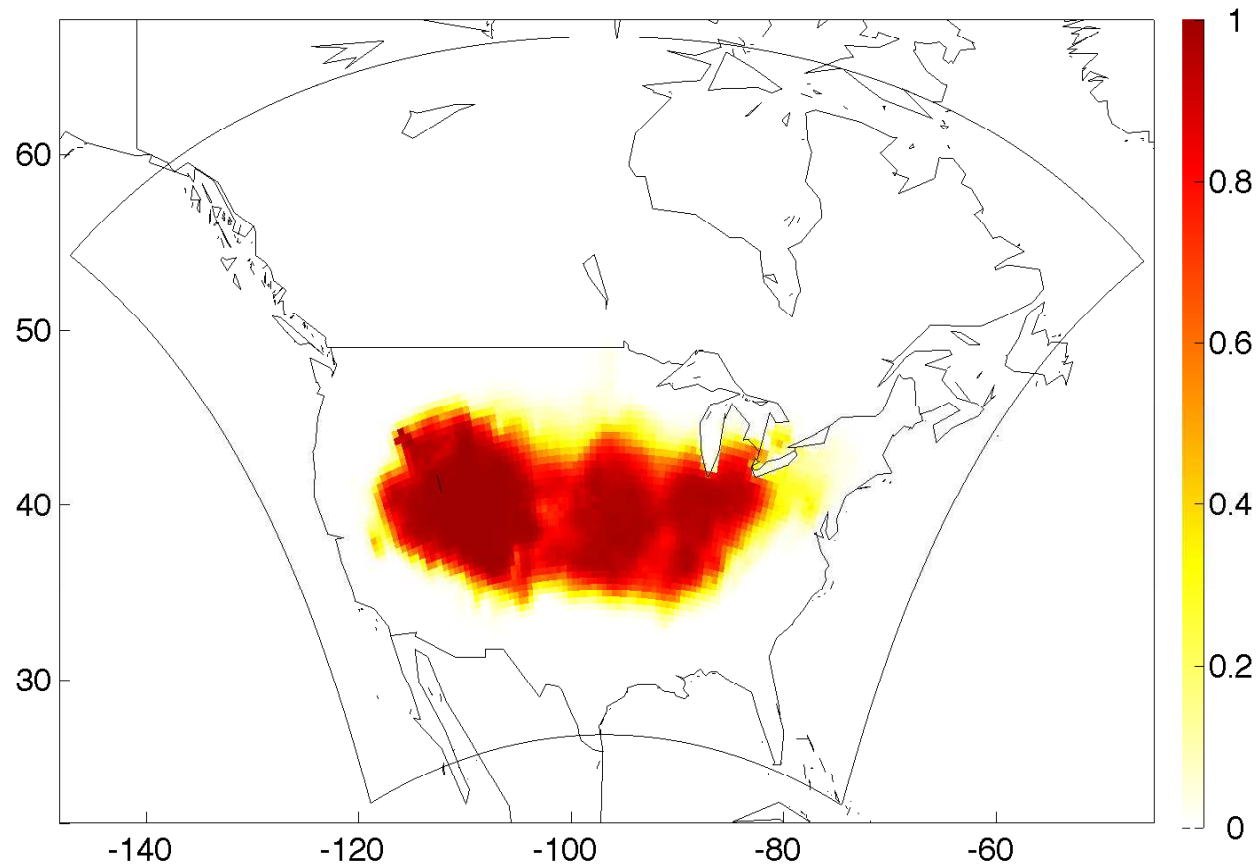
Summer: $Pr(Y_2(\cdot) > k | \text{data})$, for $k = 2.8^\circ\text{C}$



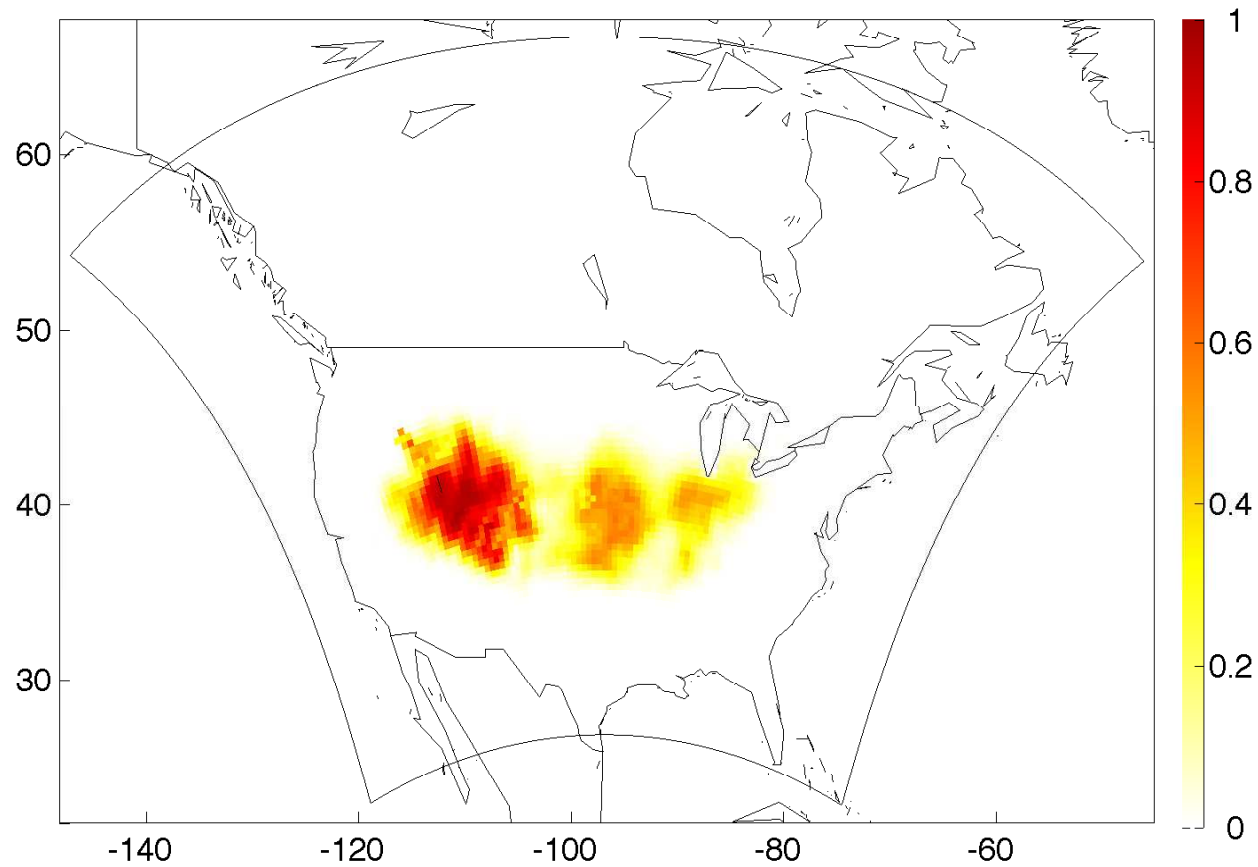
Summer: $Pr(Y_2(\cdot) > k | \text{data})$, for $k = 3.0^\circ\text{C}$



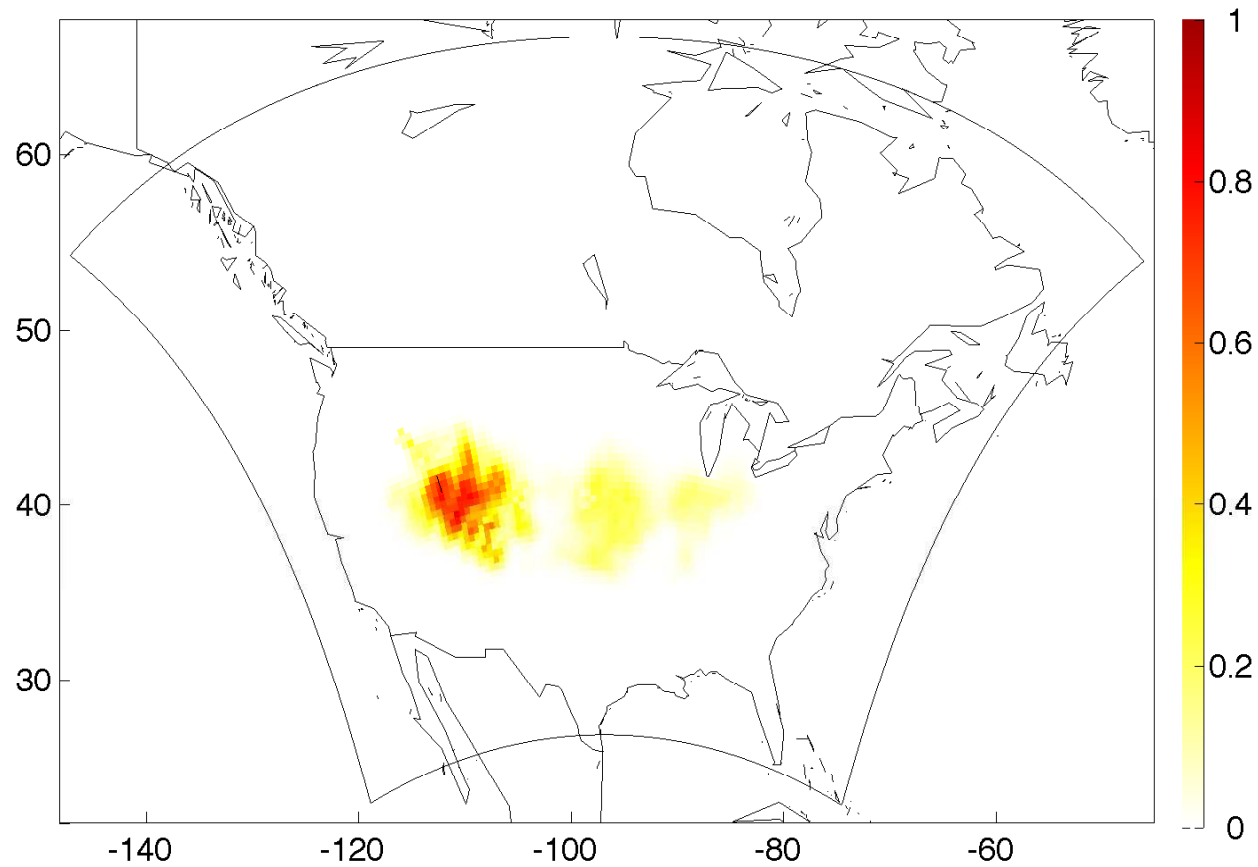
Summer: $Pr(Y_2(\cdot) > k | \text{data})$, for $k = 3.2^\circ\text{C}$



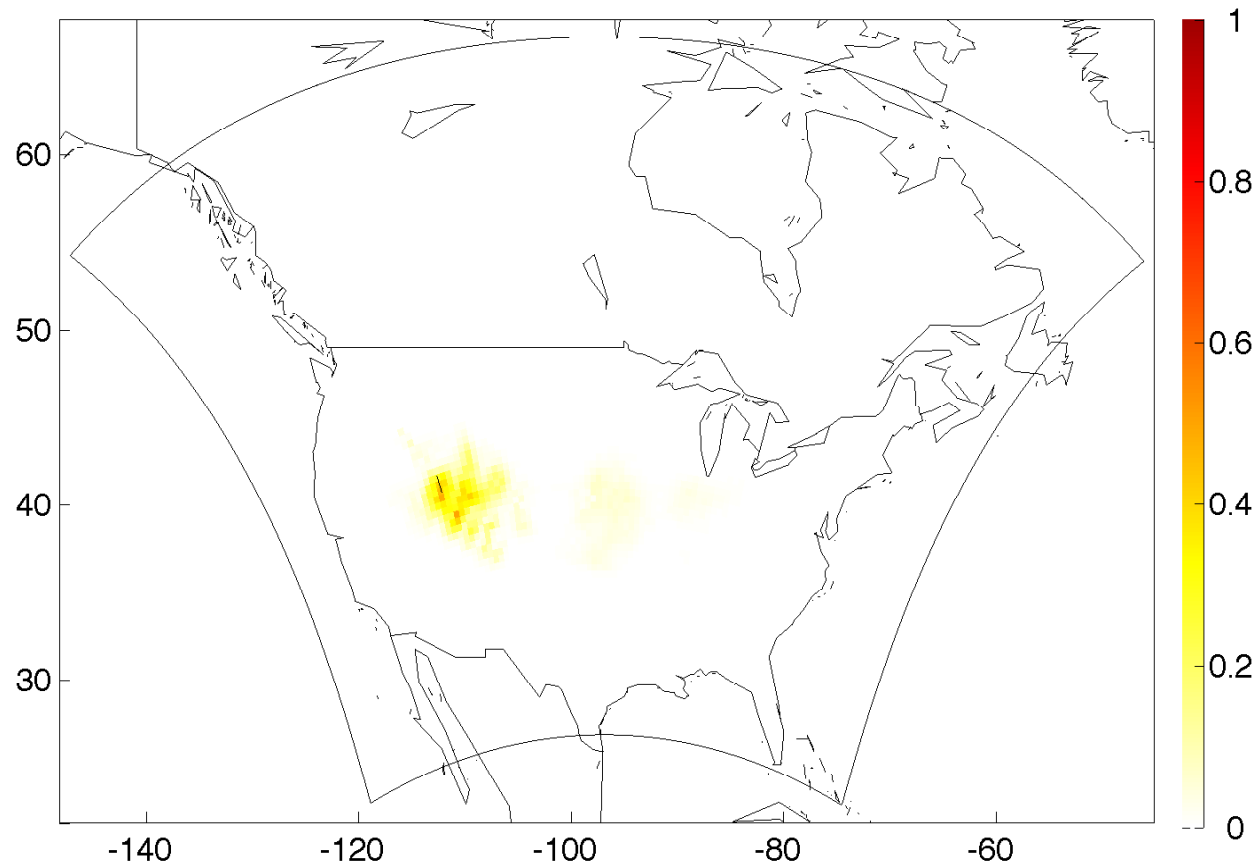
Summer: $Pr(Y_2(\cdot) > k | \text{data})$, for $k = 3.4^\circ\text{C}$



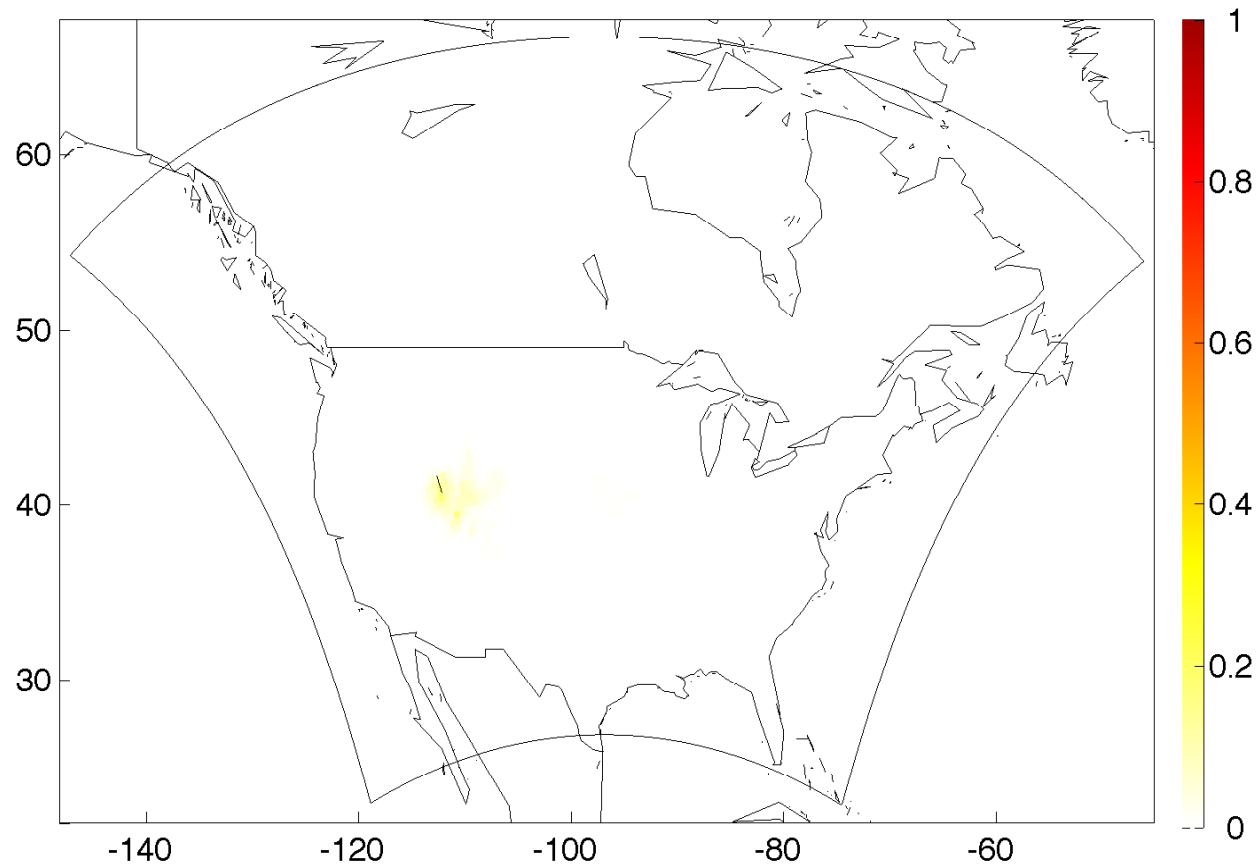
Summer: $Pr(Y_2(\cdot) > k | \text{data})$, for $k = 3.5^\circ\text{C}$



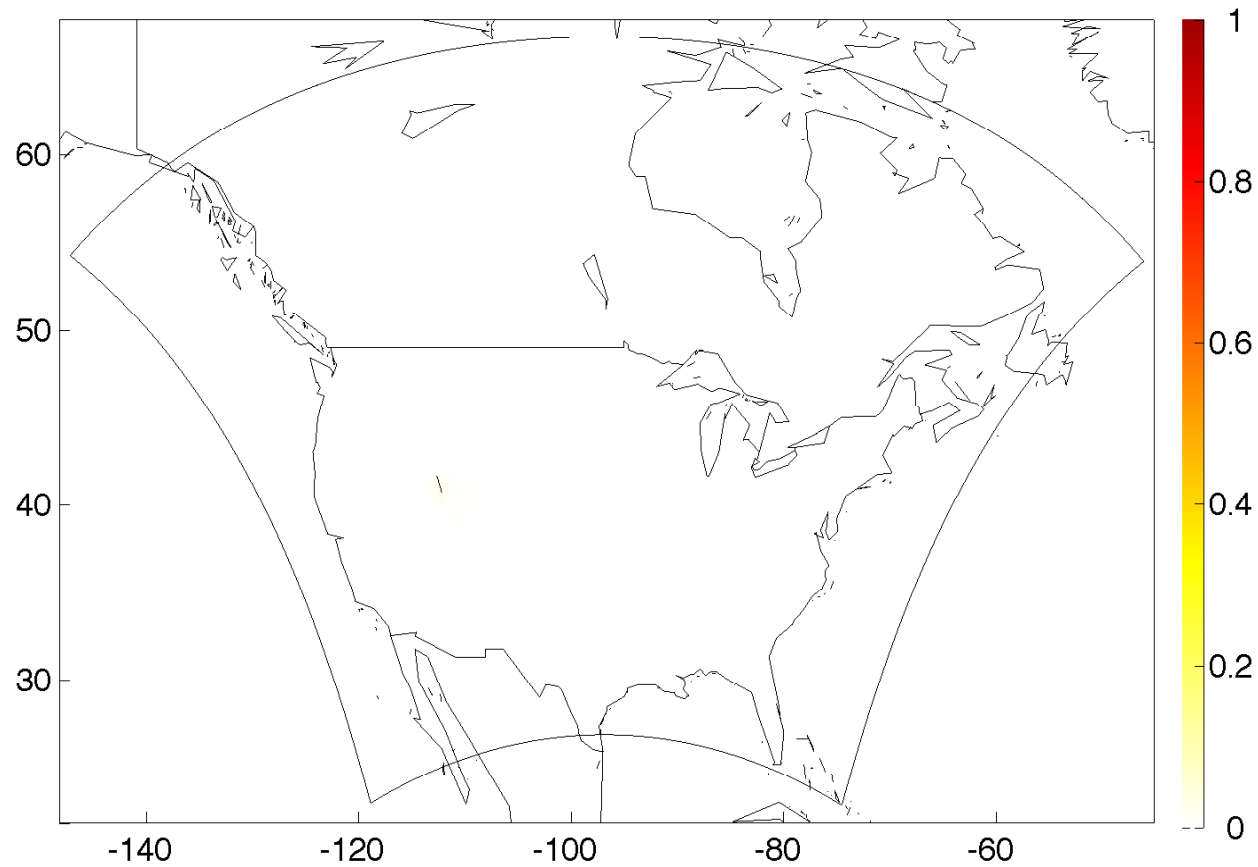
Summer: $Pr(Y_2(\cdot) > k | \text{data})$, for $k = 3.6^\circ\text{C}$



Summer: $Pr(Y_2(\cdot) > k | \text{data})$, for $k = 3.7^\circ C$



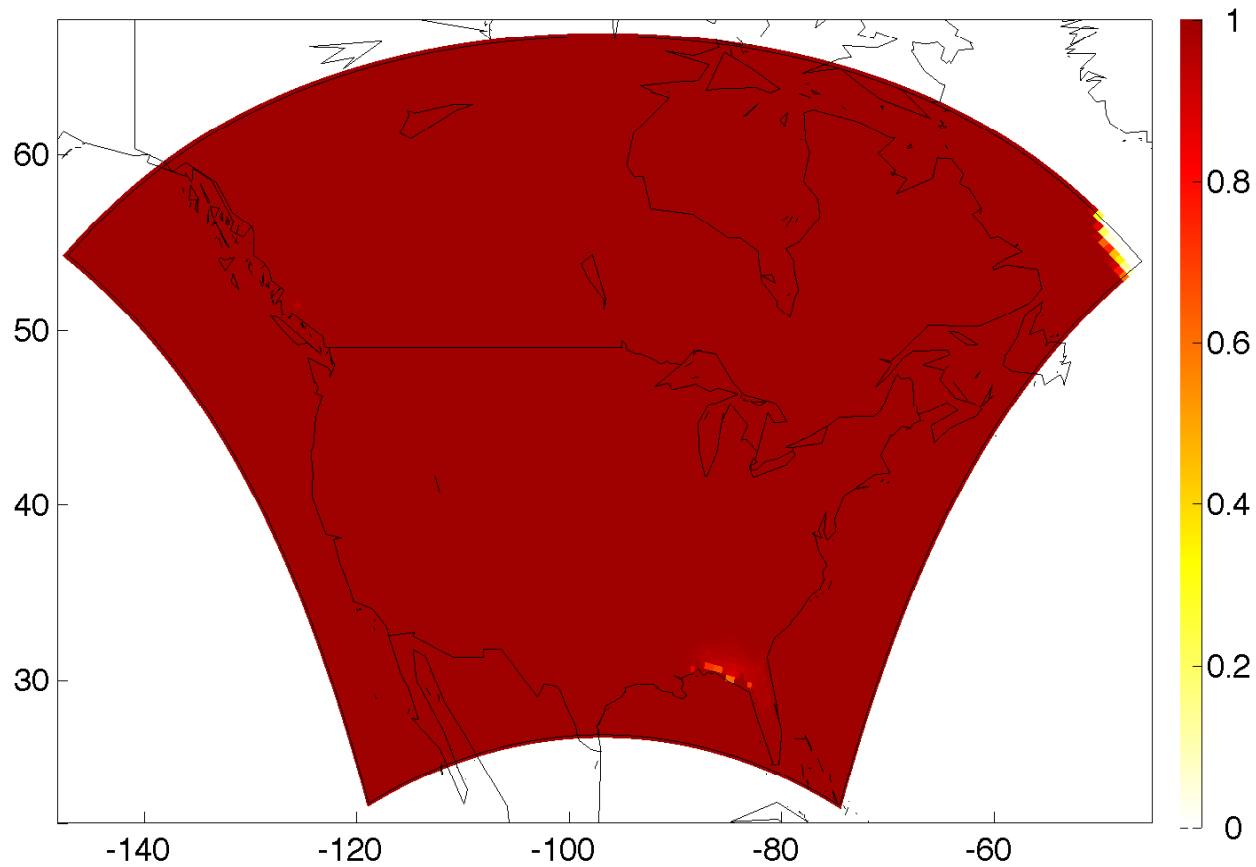
Summer: $Pr(Y_2(\cdot) > k | \text{data})$, for $k = 3.8^\circ\text{C}$



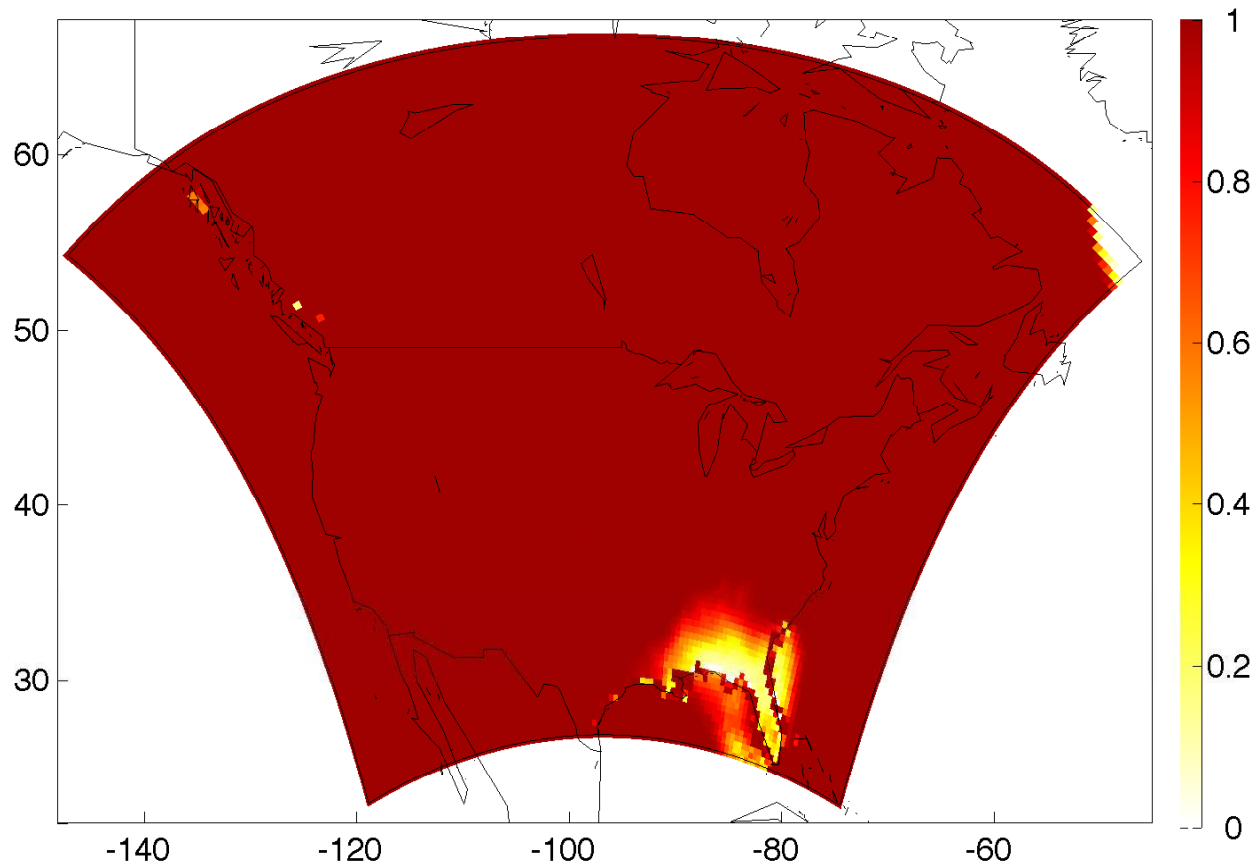
Winter

Winter

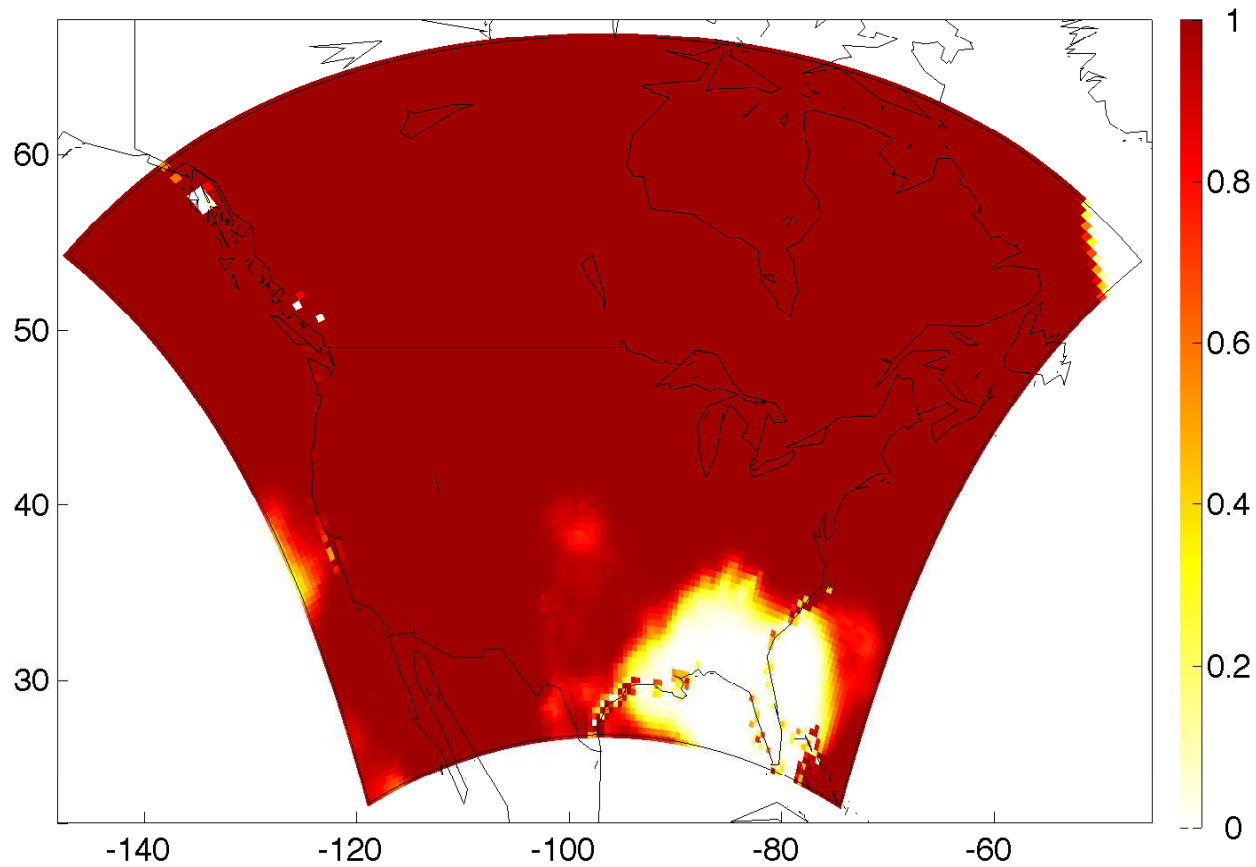
Winter: $Pr(Y_{.4}(\cdot) > k | \mathbf{data})$, for $k = 1.0^\circ C$



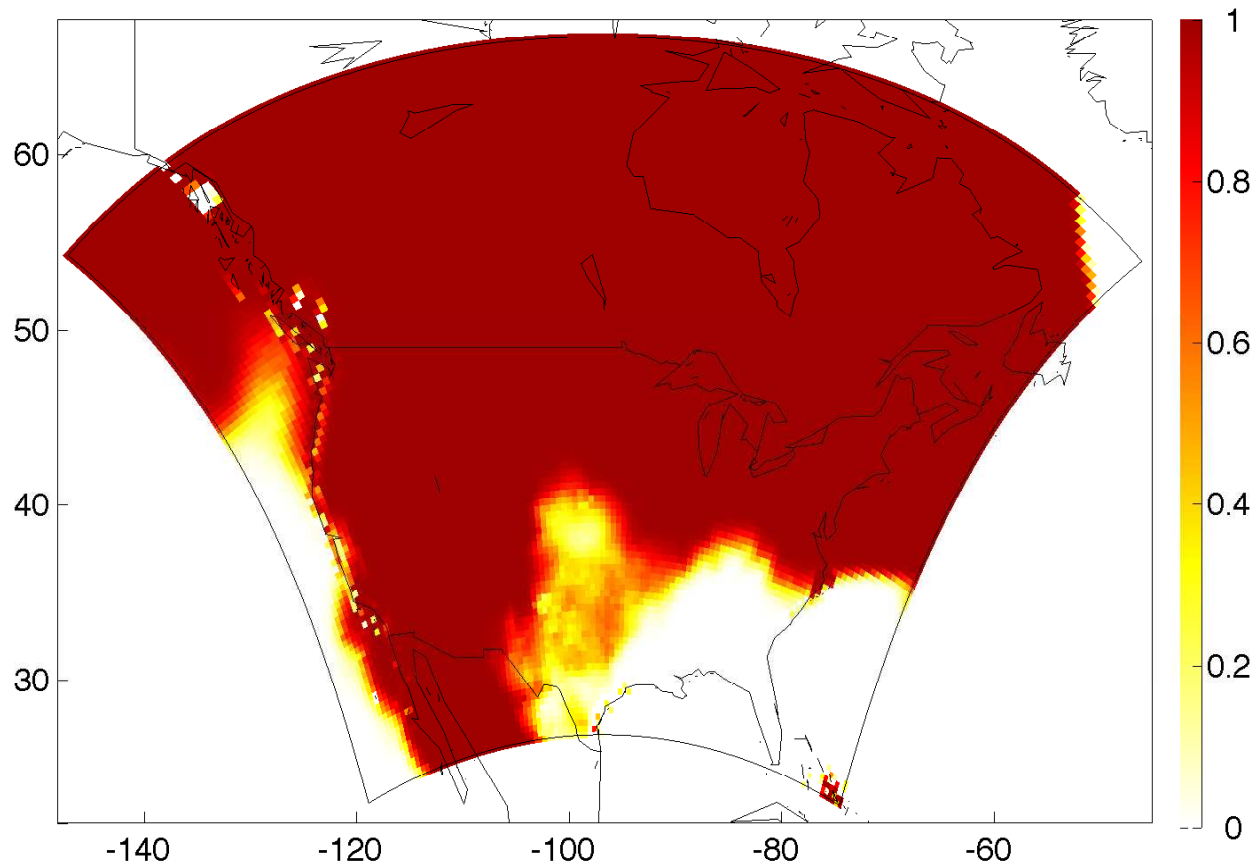
Winter: $Pr(Y_4(\cdot) > k | \mathbf{data})$, for $k = 1.2^\circ C$



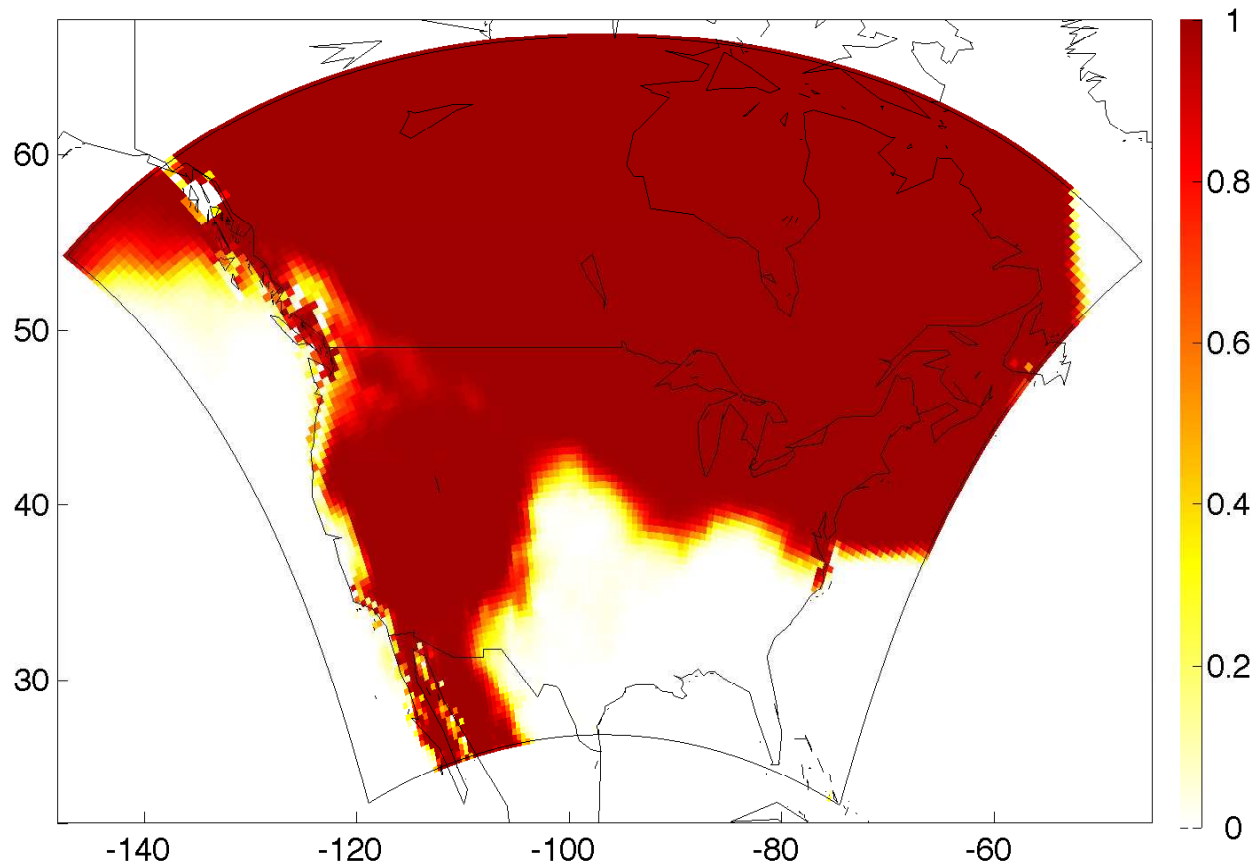
Winter: $Pr(Y_4(\cdot) > k | \mathbf{data})$, for $k = 1.4^\circ C$



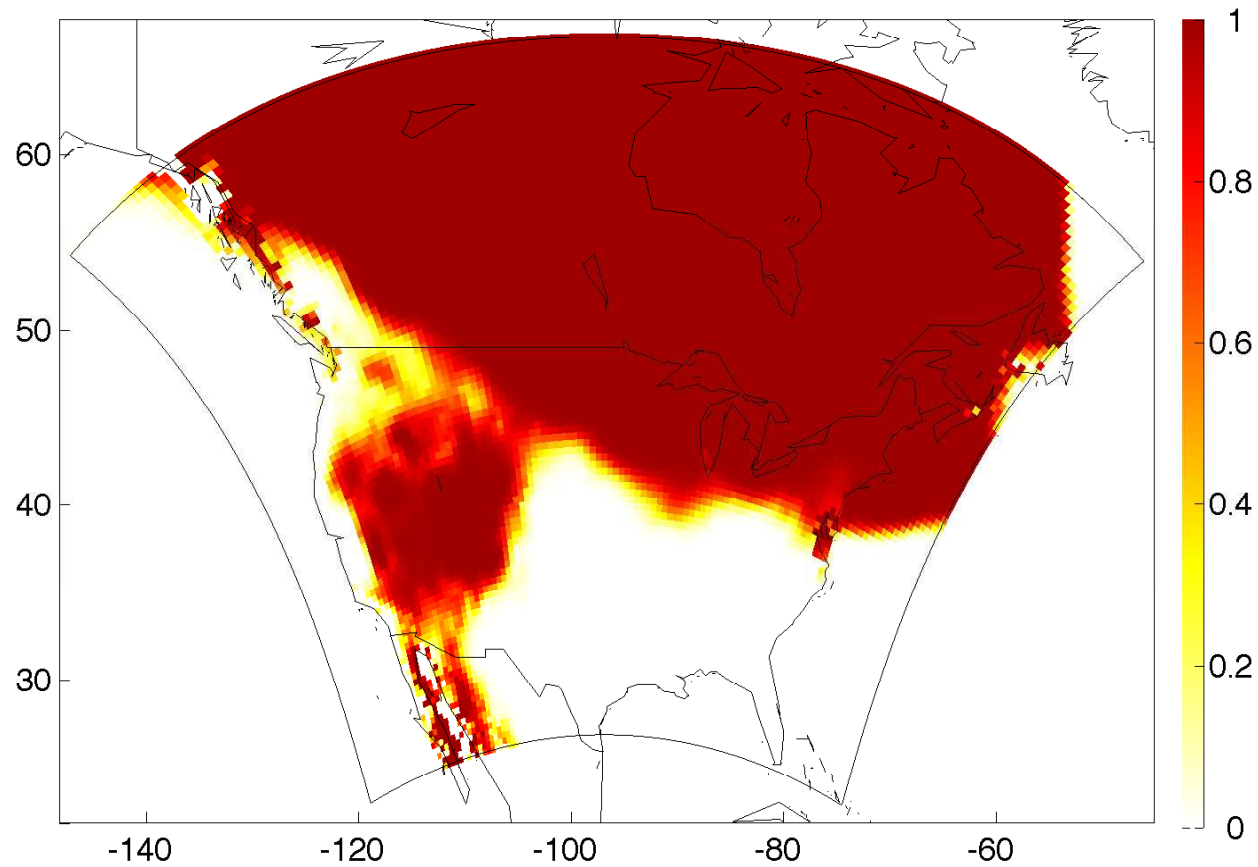
Winter: $Pr(Y_{.4}(\cdot) > k | \mathbf{data})$, for $k = 1.6^\circ C$



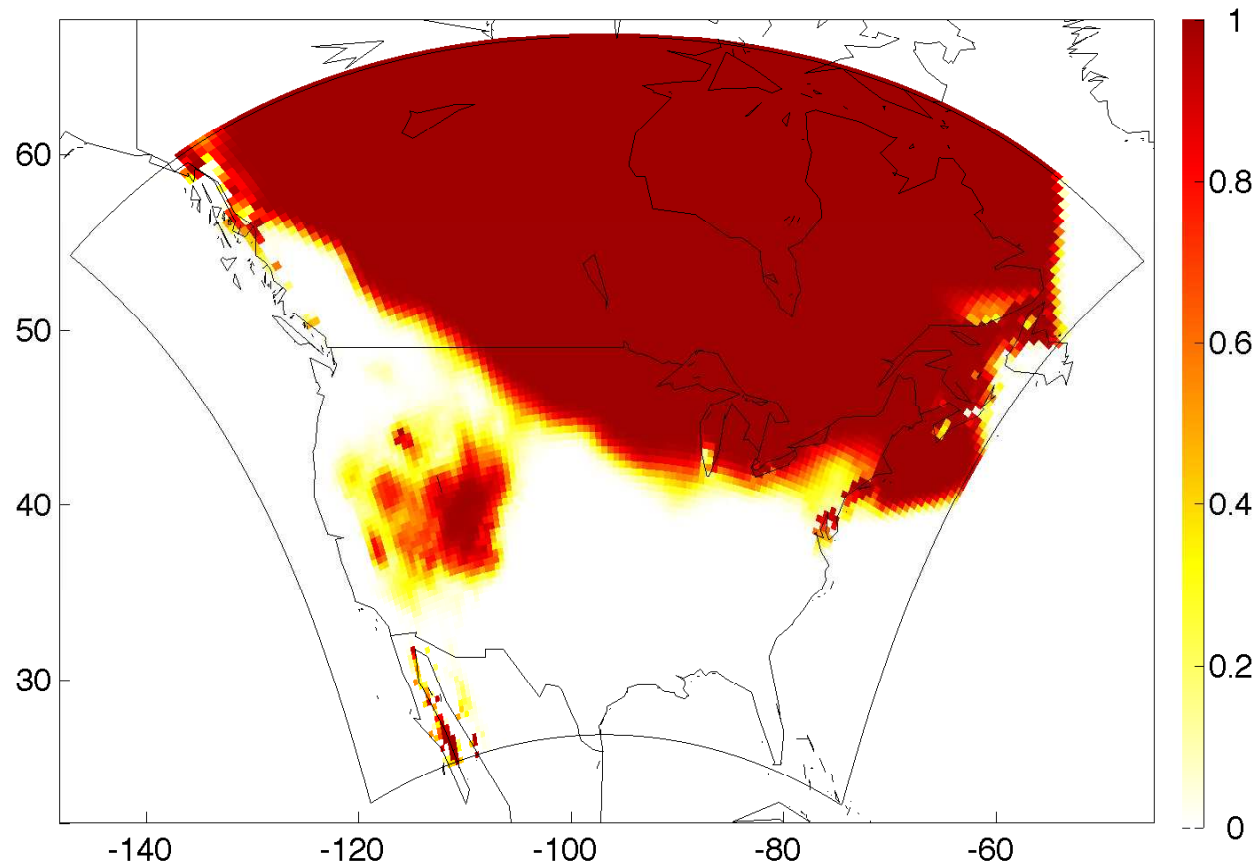
Winter: $Pr(Y_{.4}(\cdot) > k | \mathbf{data})$, for $k = 1.8^\circ C$



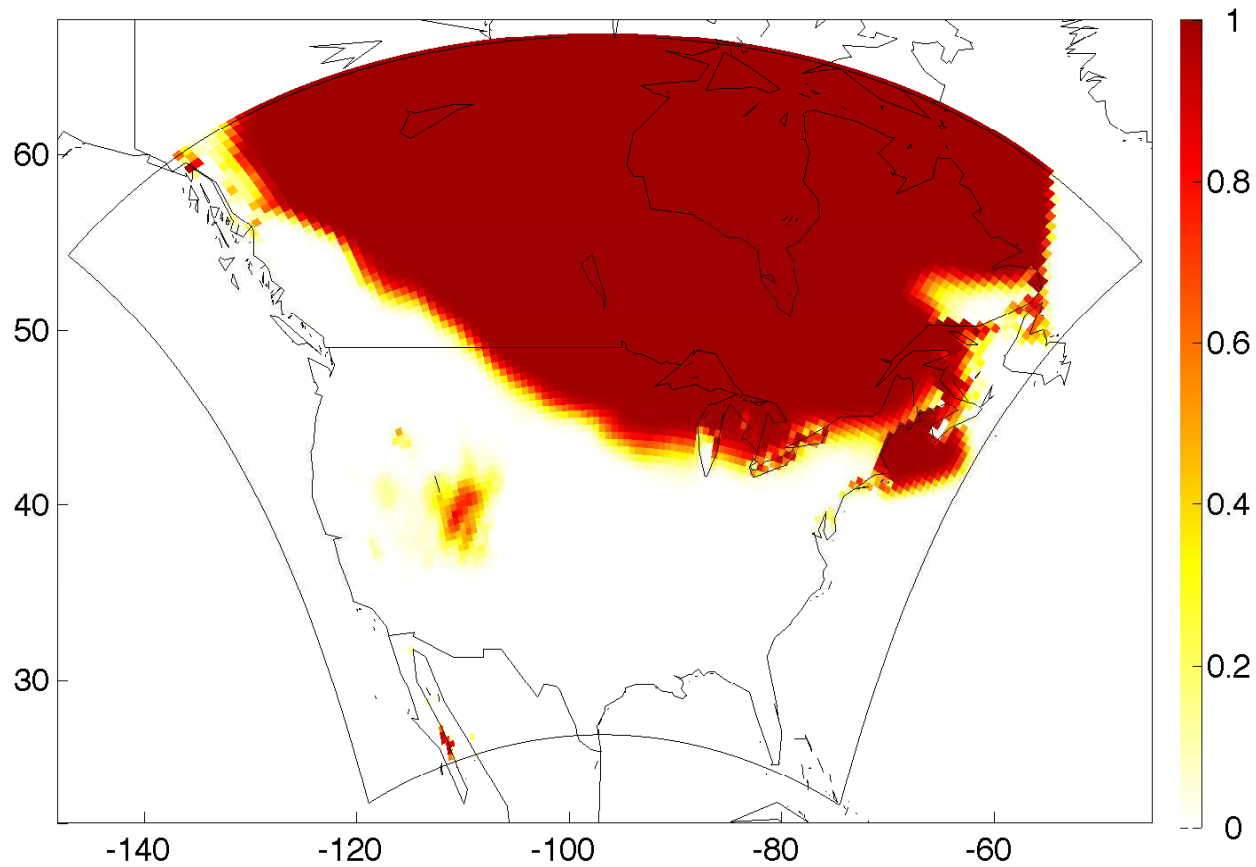
Winter: $Pr(Y_4(\cdot) > k | \mathbf{data})$, for $k = 2.0^\circ C$



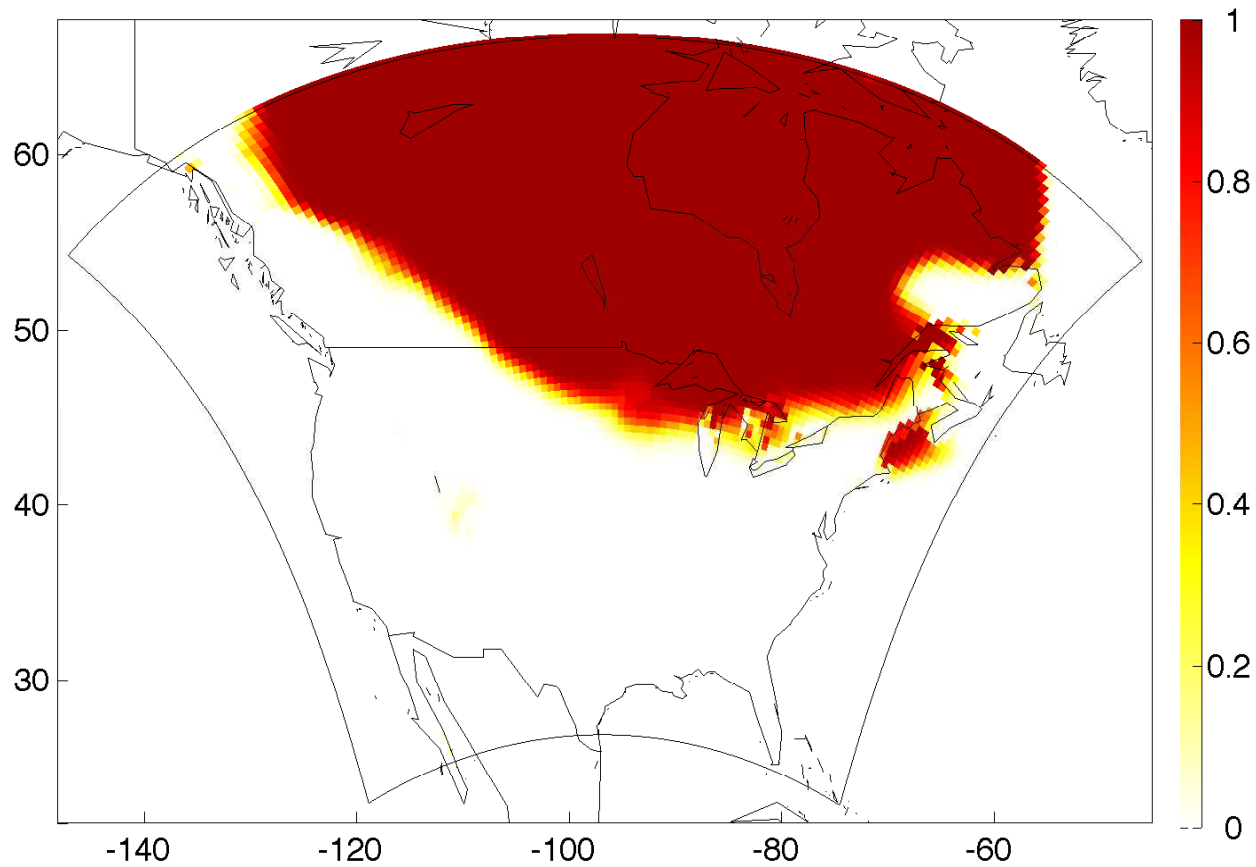
Winter: $Pr(Y_{.4}(\cdot) > k | \mathbf{data})$, for $k = 2.2^\circ C$



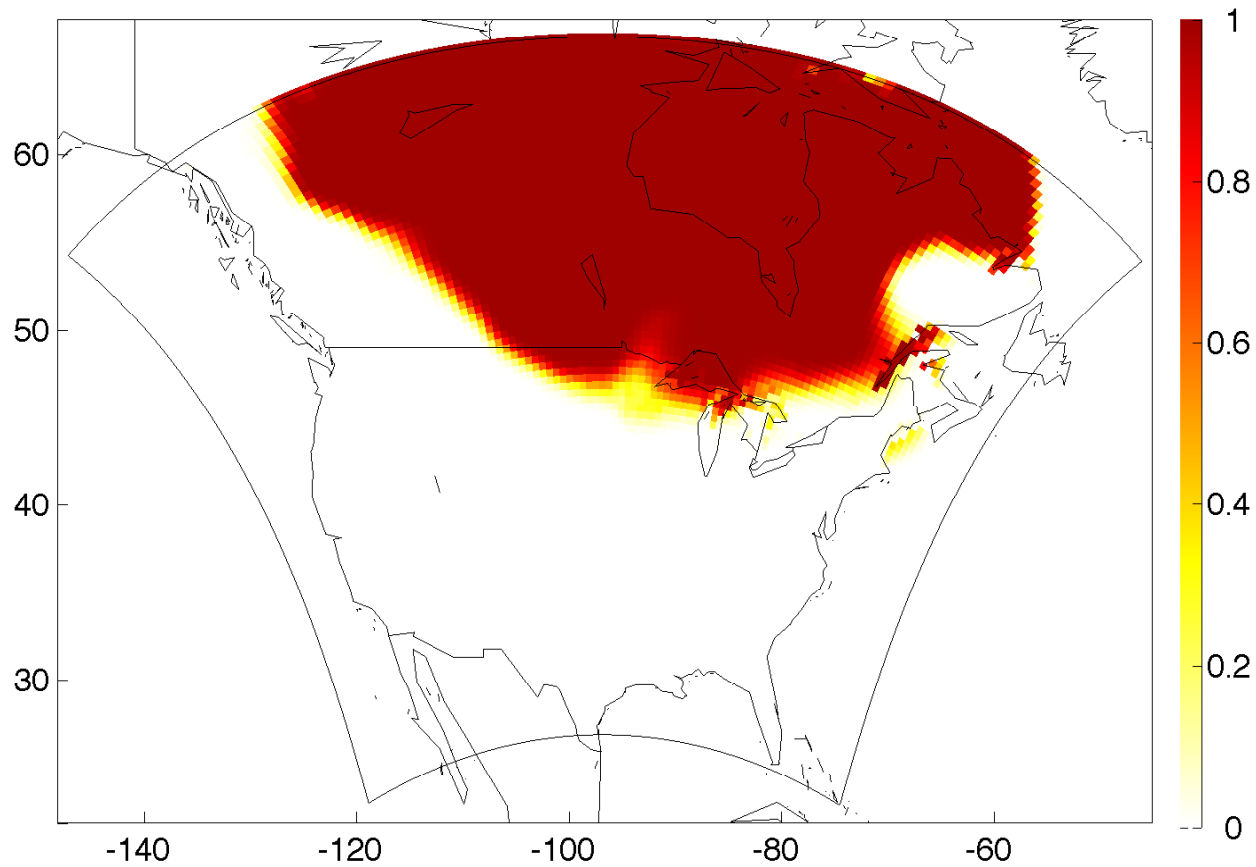
Winter: $Pr(Y_{.4}(\cdot) > k | \mathbf{data})$, for $k = 2.4^\circ C$



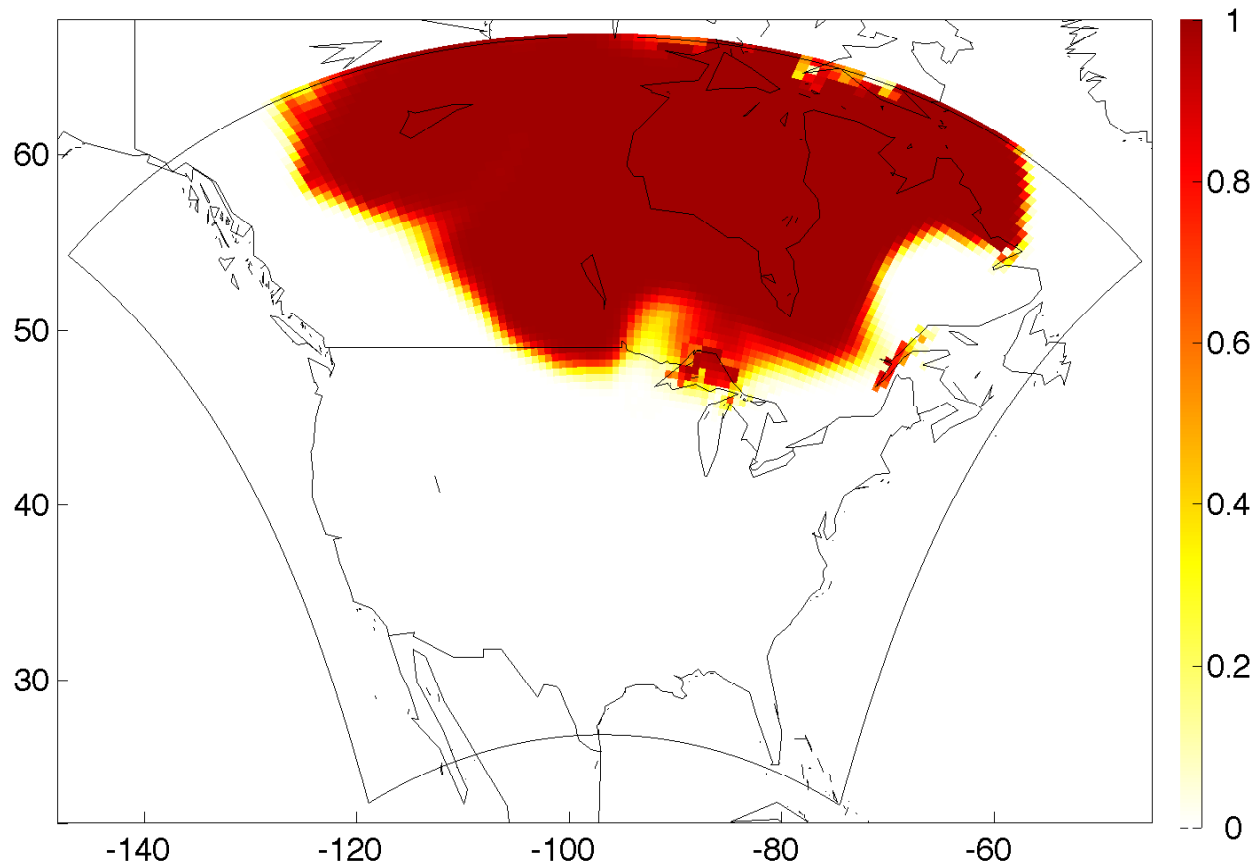
Winter: $Pr(Y_4(\cdot) > k | \mathbf{data})$, for $k = 2.6^\circ C$



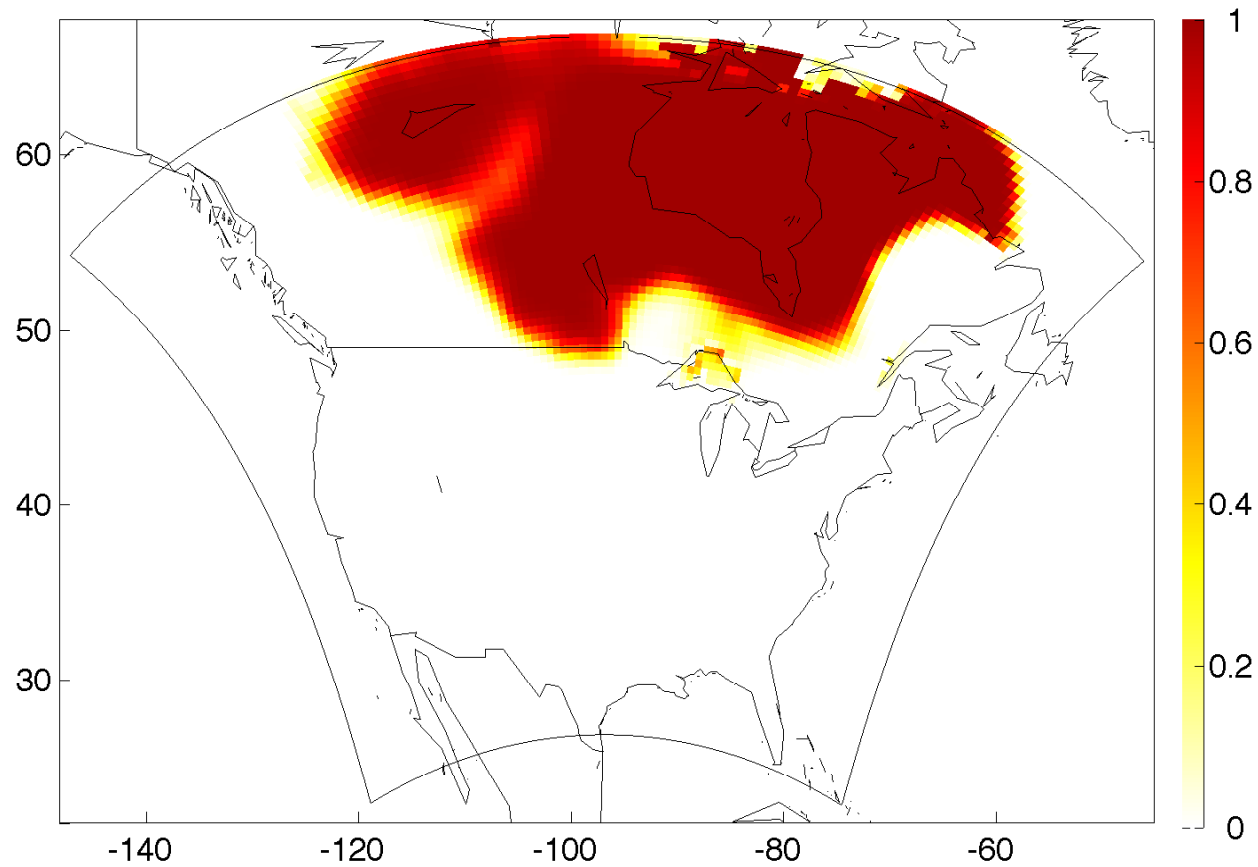
Winter: $Pr(Y_{.4}(\cdot) > k | \mathbf{data})$, for $k = 2.8^\circ C$



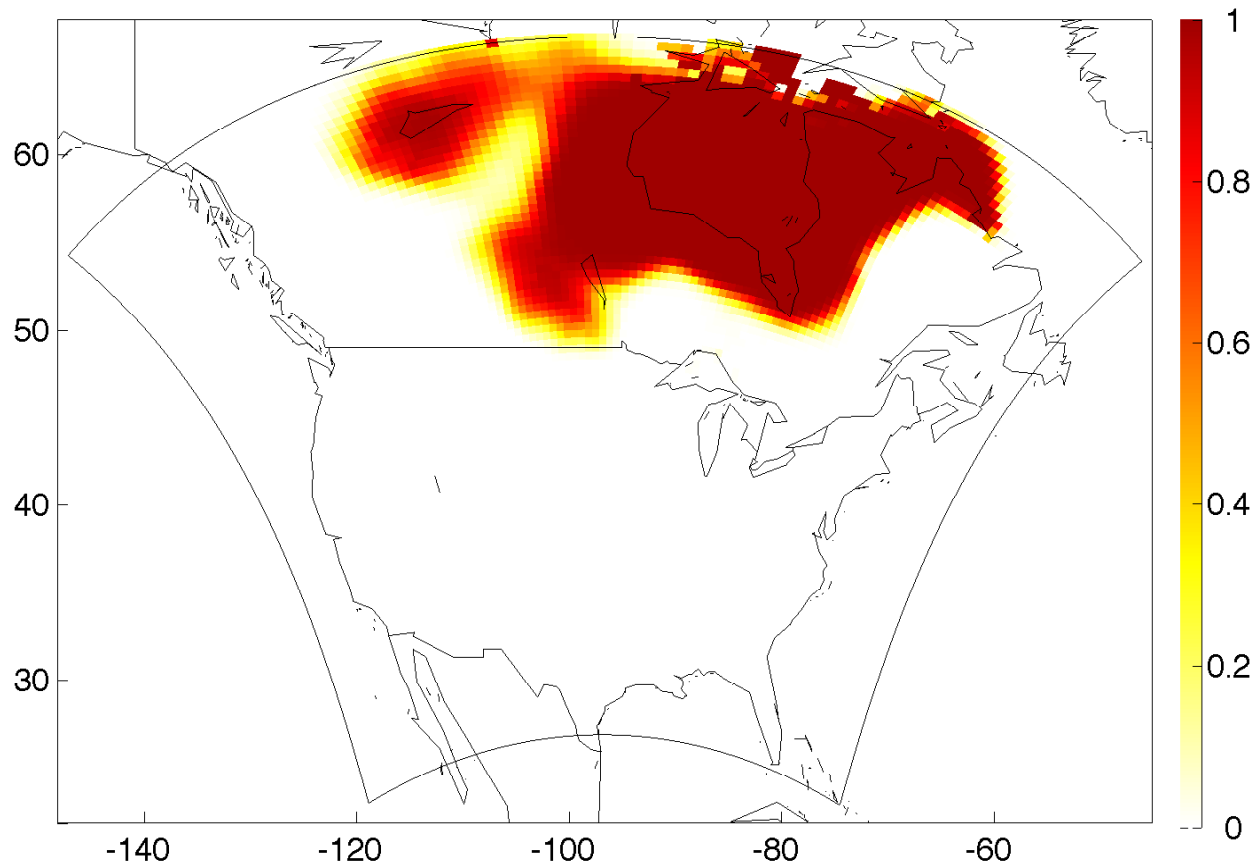
Winter: $Pr(Y_{.4}(\cdot) > k | \mathbf{data})$, for $k = 3.0^\circ C$



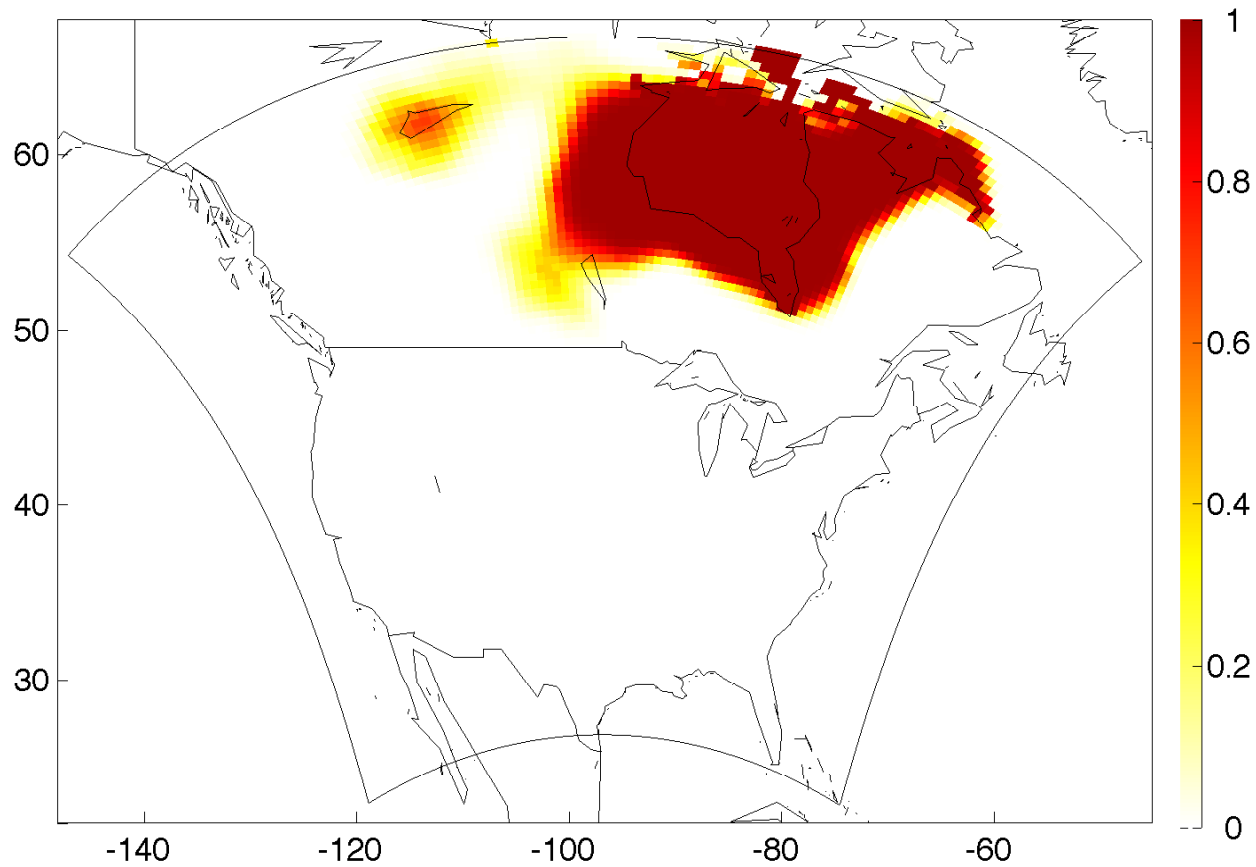
Winter: $Pr(Y_4(\cdot) > k | \text{data})$, for $k = 3.2^\circ C$



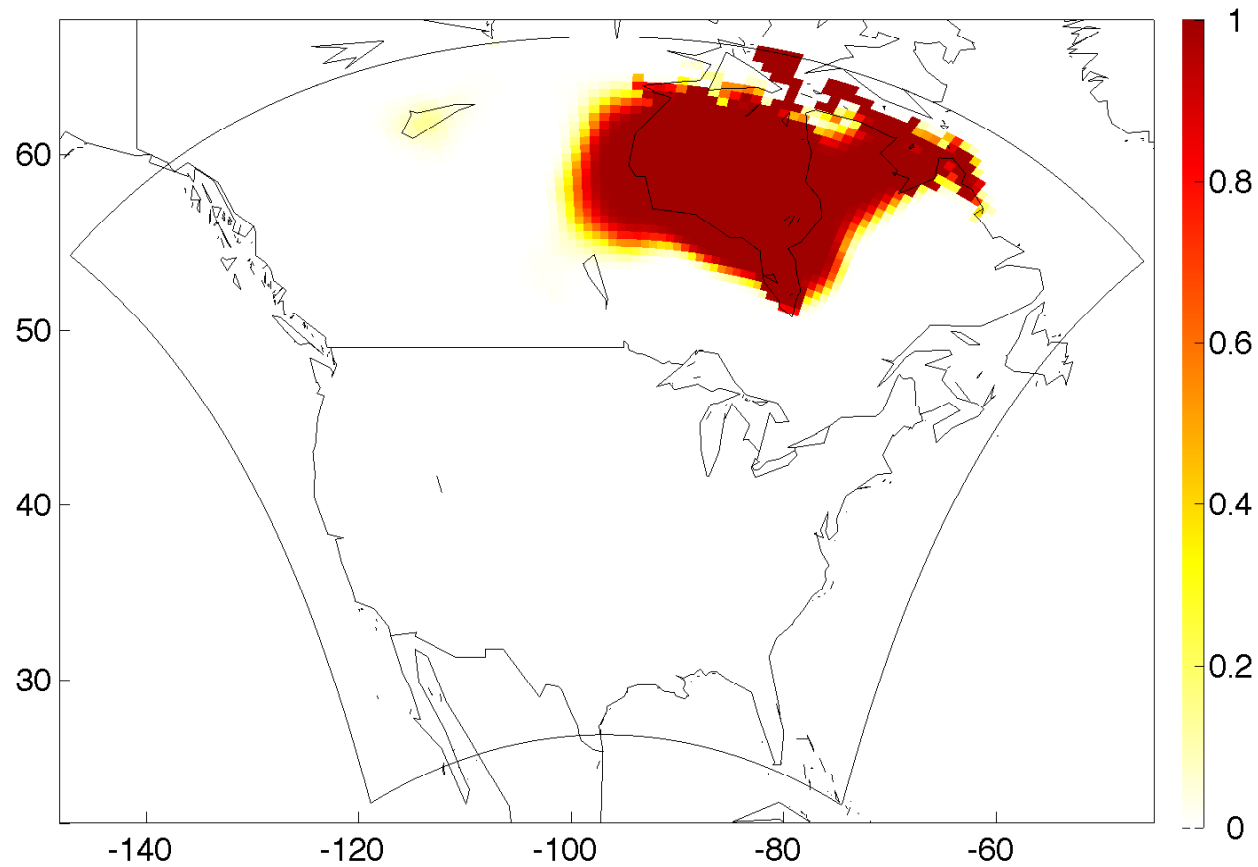
Winter: $Pr(Y_{.4}(\cdot) > k | \mathbf{data})$, for $k = 3.4^\circ C$



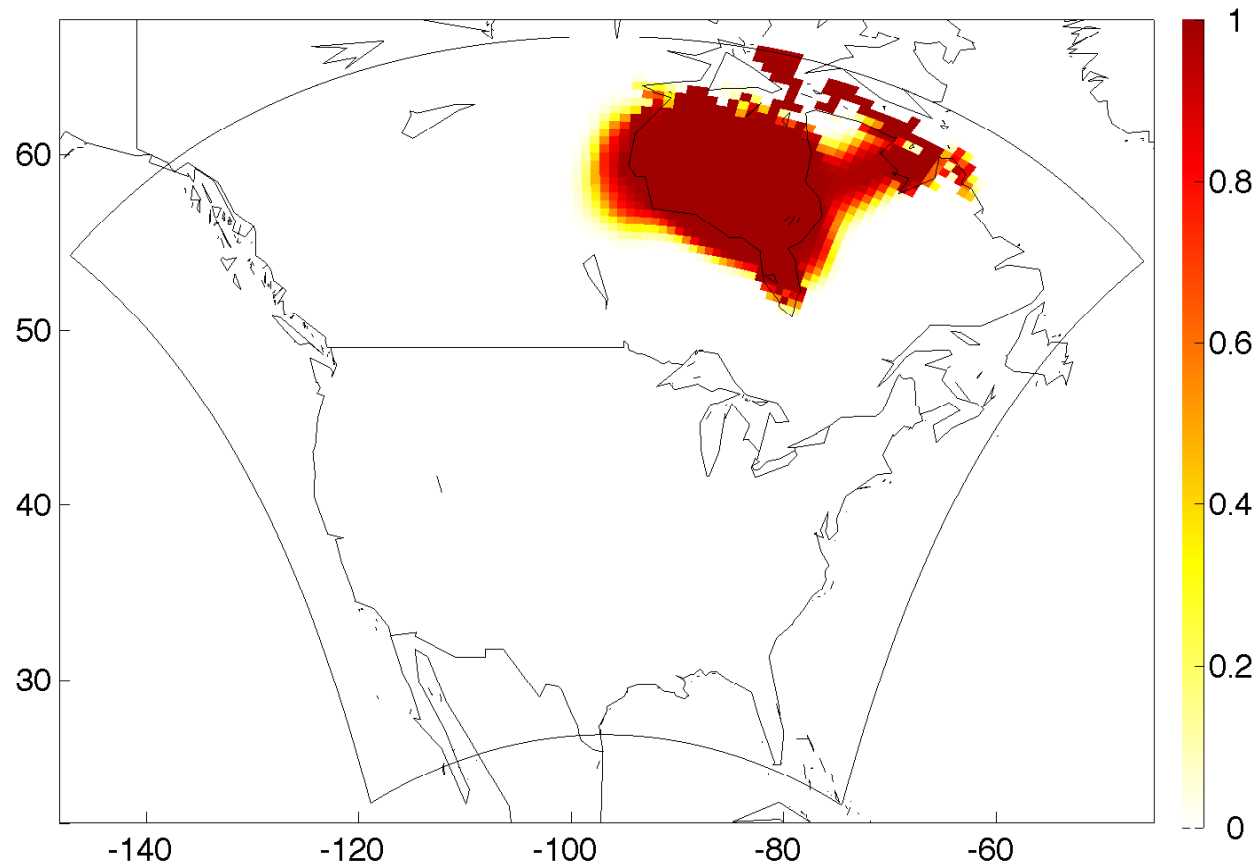
Winter: $Pr(Y_{.4}(\cdot) > k | \mathbf{data})$, for $k = 3.6^\circ C$



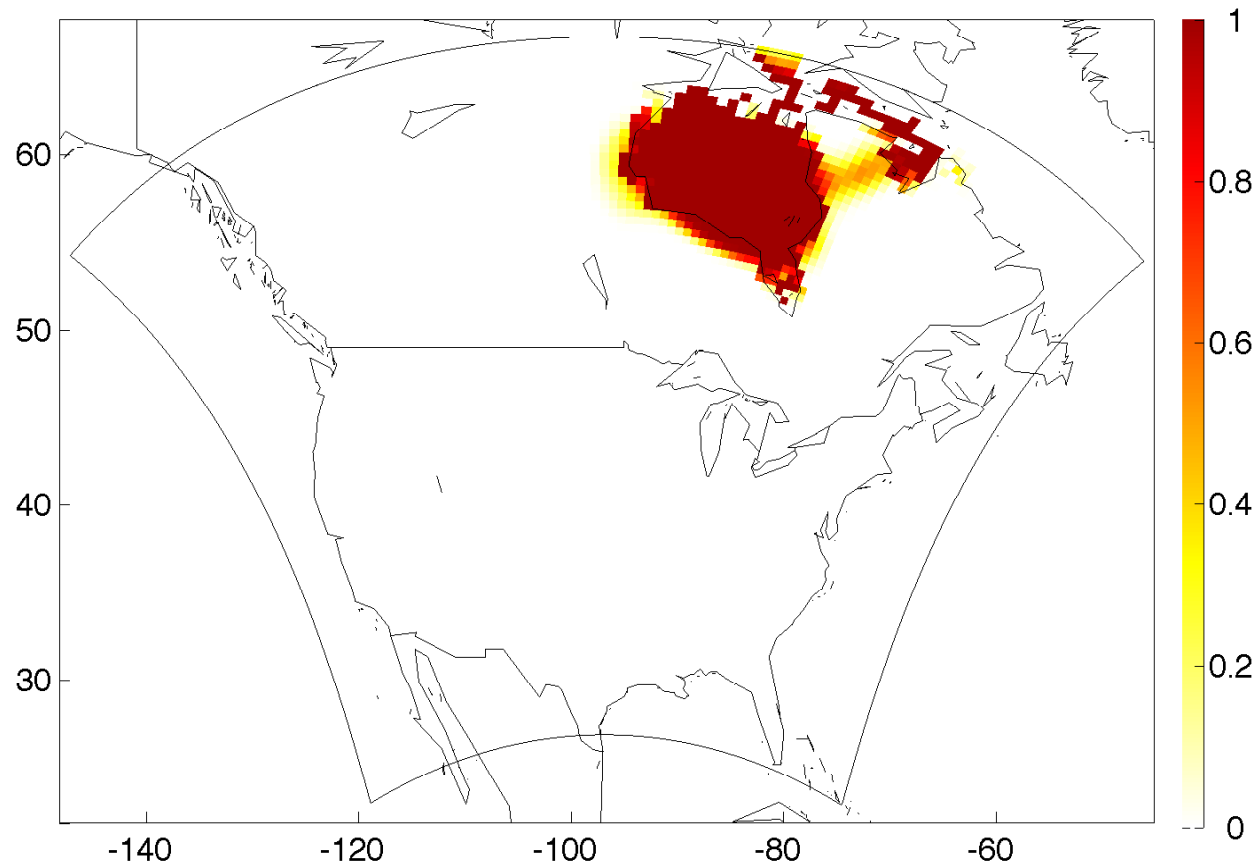
Winter: $Pr(Y_{.4}(\cdot) > k | \mathbf{data})$, for $k = 3.8^\circ C$



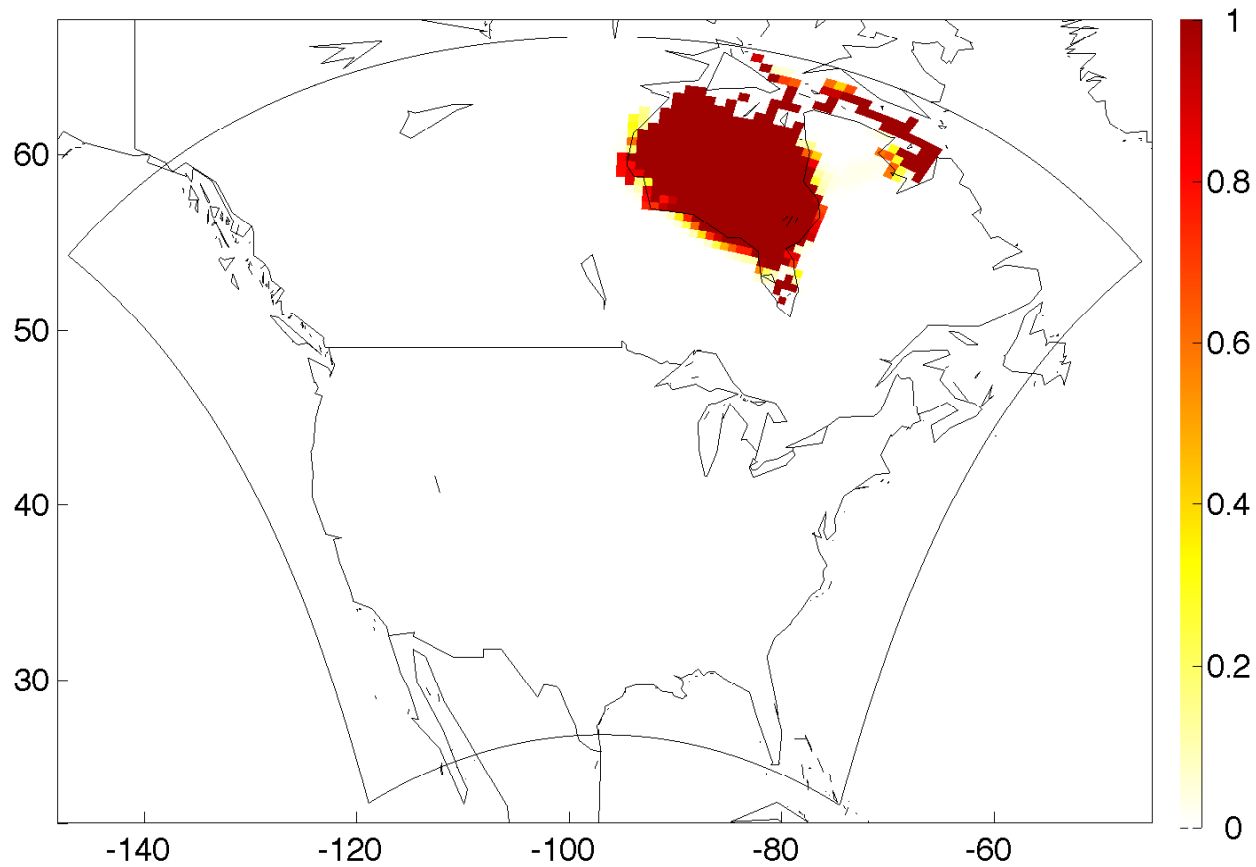
Winter: $Pr(Y_{.4}(\cdot) > k | \mathbf{data})$, for $k = 4.0^\circ C$



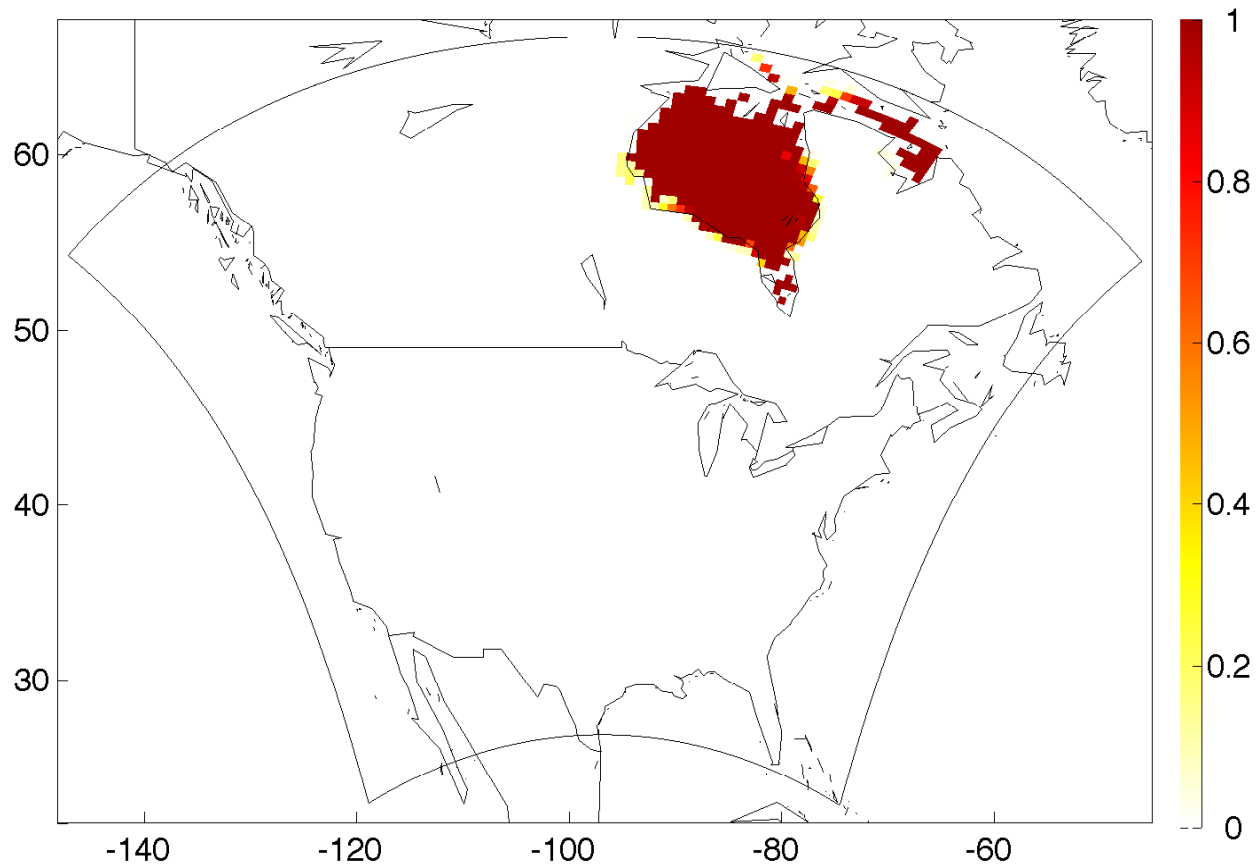
Winter: $Pr(Y_{.4}(\cdot) > k | \mathbf{data})$, for $k = 4.2^\circ C$



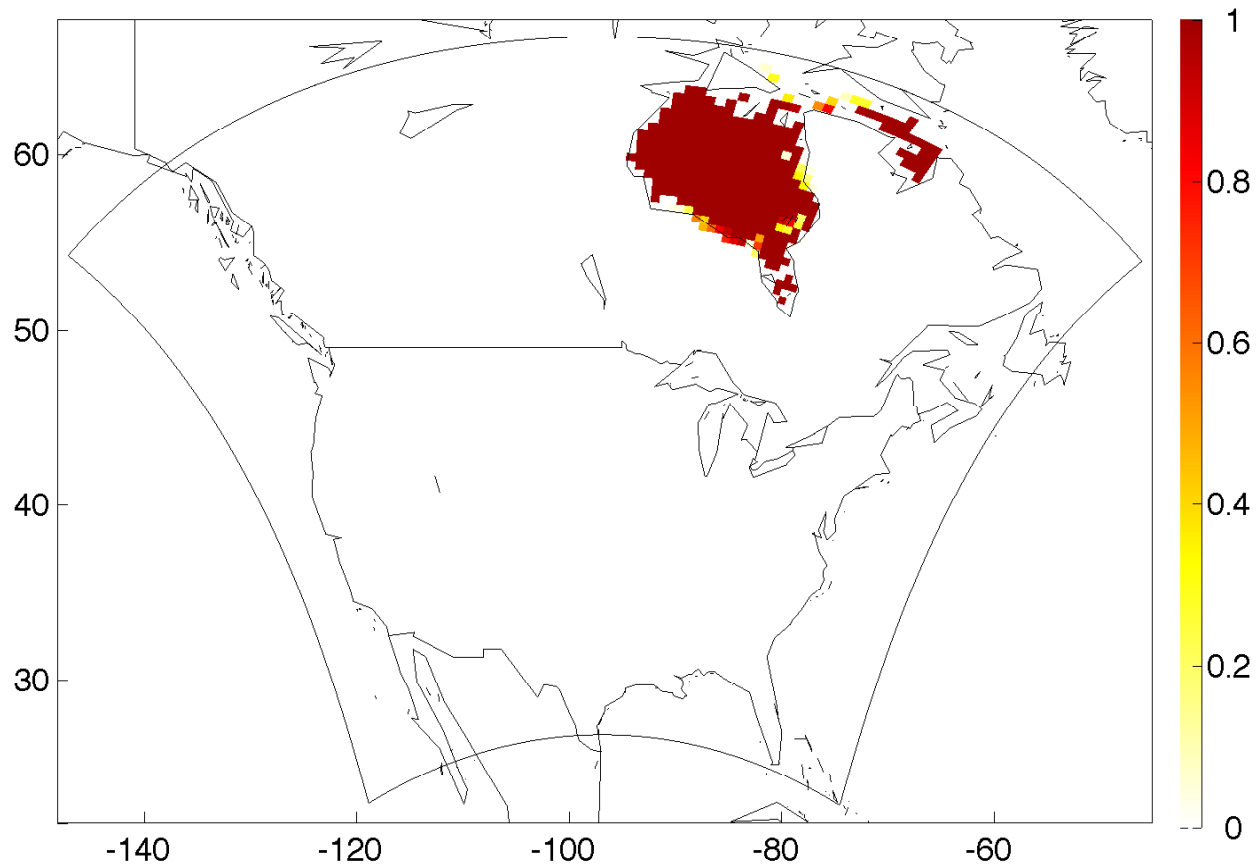
Winter: $Pr(Y_{.4}(\cdot) > k | \mathbf{data})$, for $k = 4.4^\circ C$



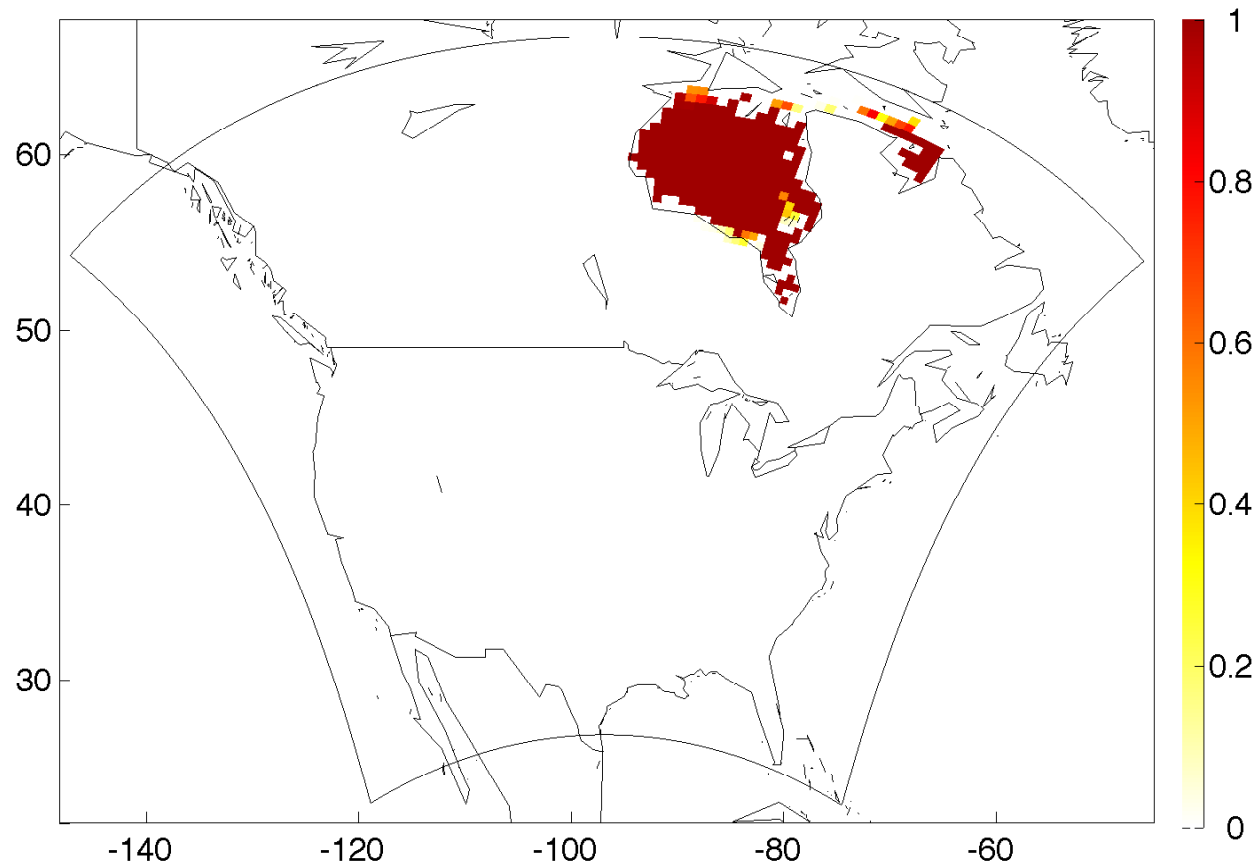
Winter: $Pr(Y_4(\cdot) > k | \mathbf{data})$, for $k = 4.6^\circ C$



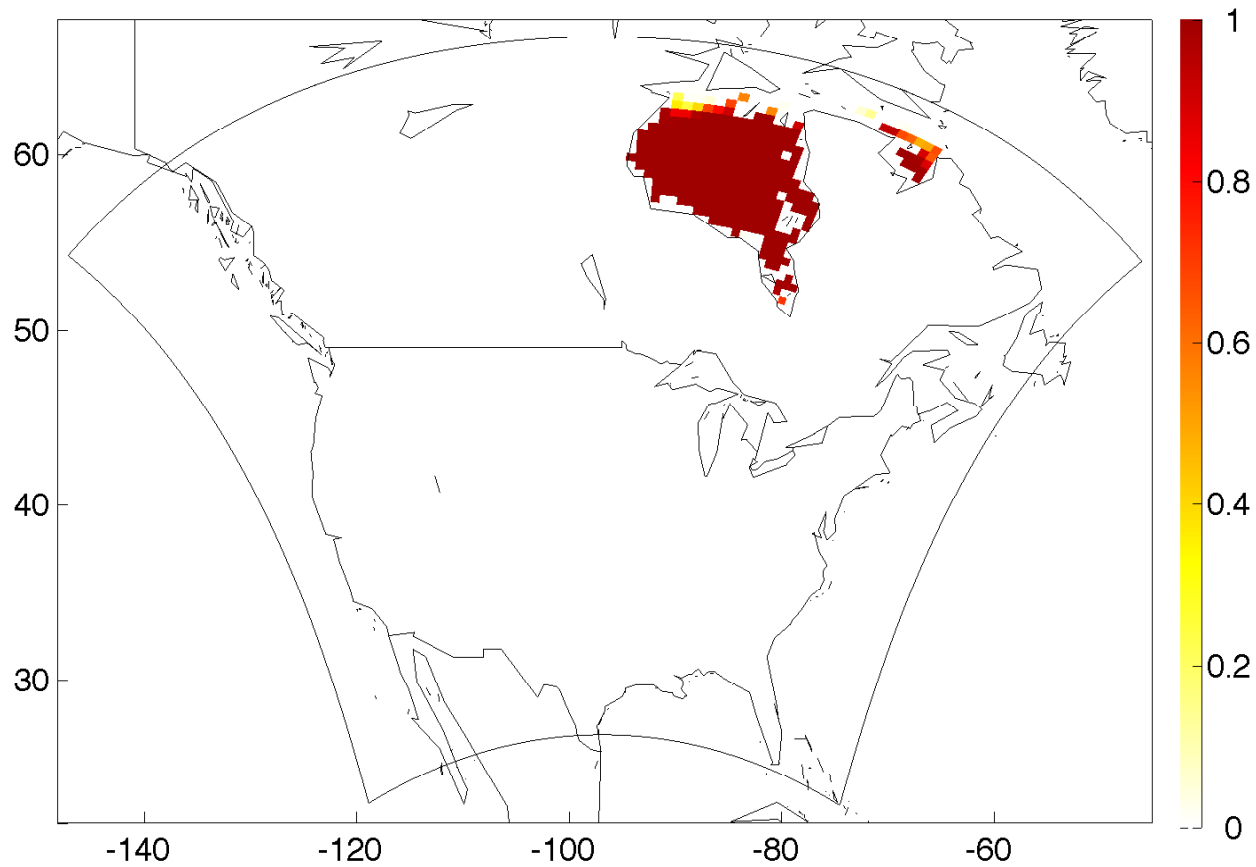
Winter: $Pr(Y_{.4}(\cdot) > k | \mathbf{data})$, for $k = 4.8^\circ C$



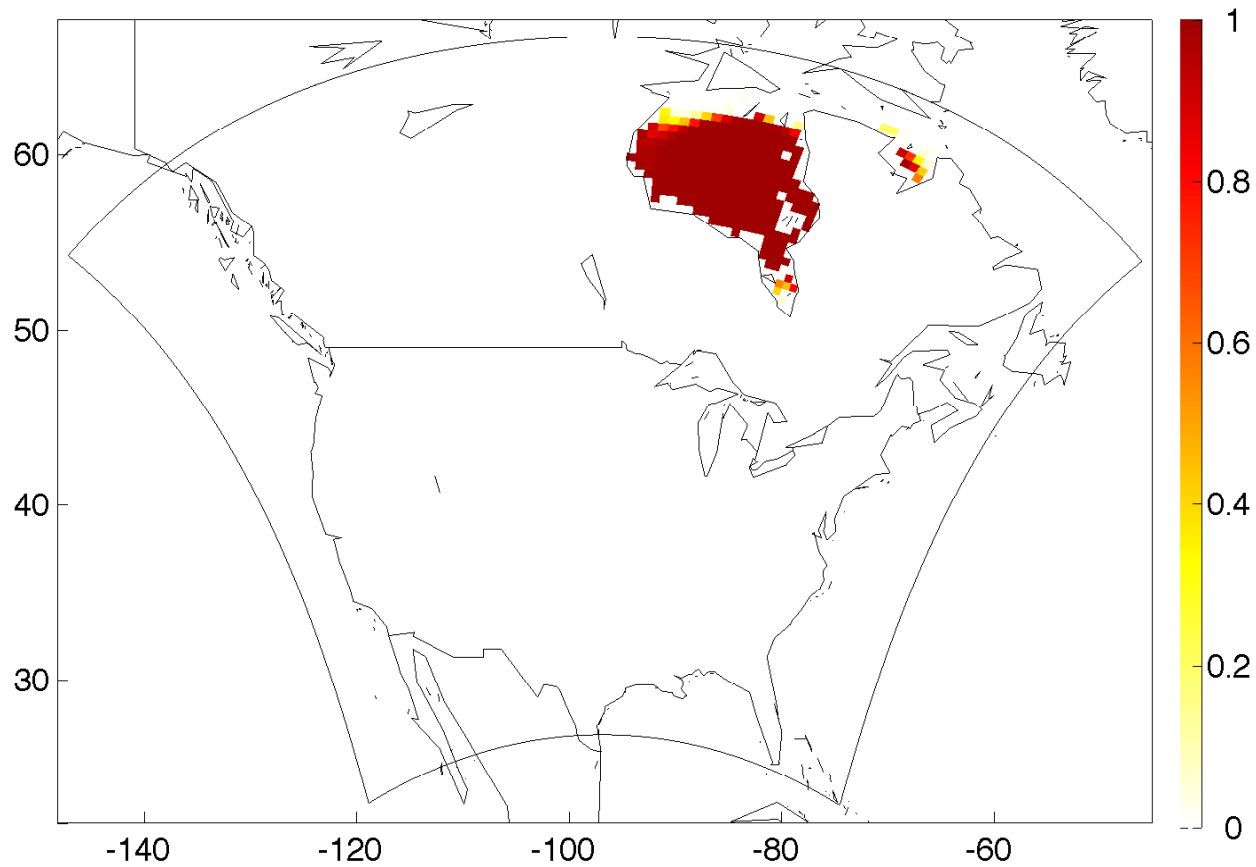
Winter: $Pr(Y_{.4}(\cdot) > k | \mathbf{data})$, for $k = 5.0^\circ C$



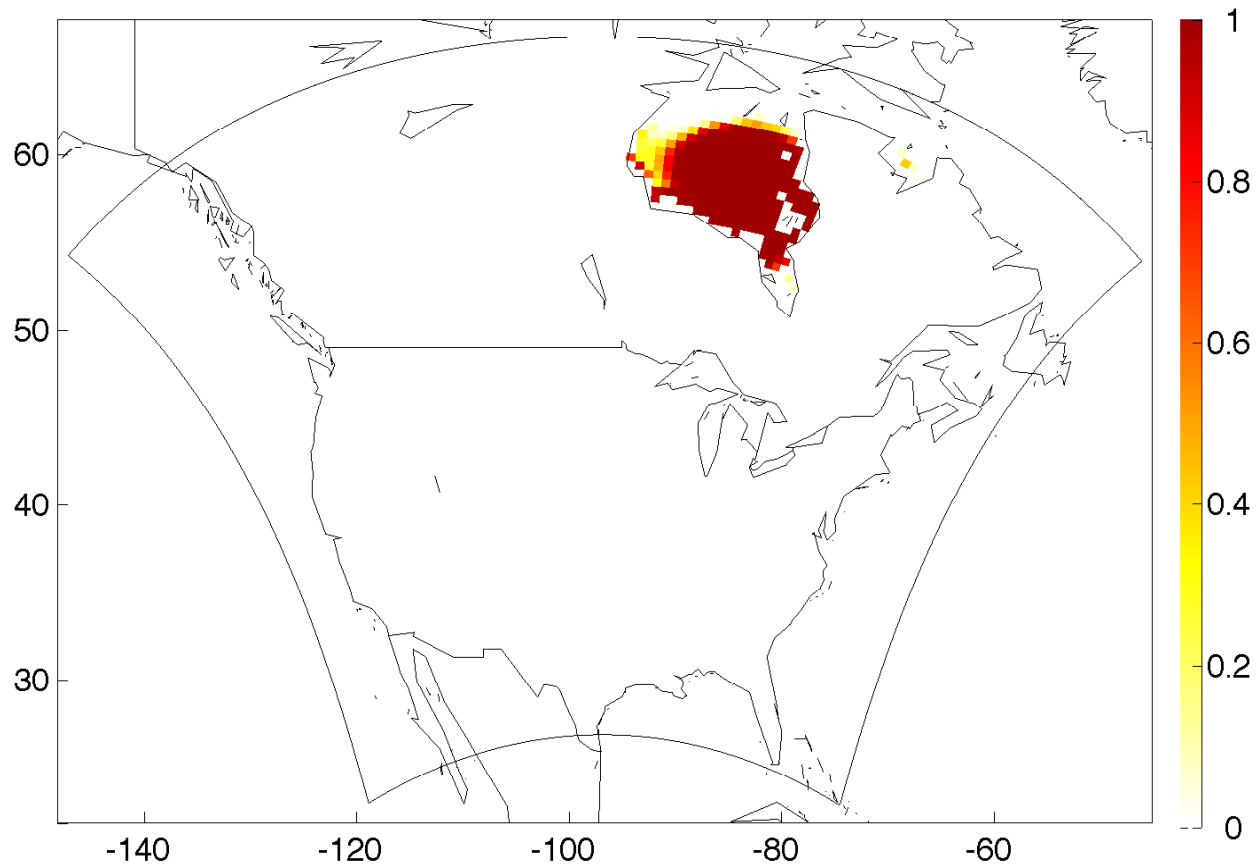
Winter: $Pr(Y_{.4}(\cdot) > k | \mathbf{data})$, for $k = 5.2^\circ C$



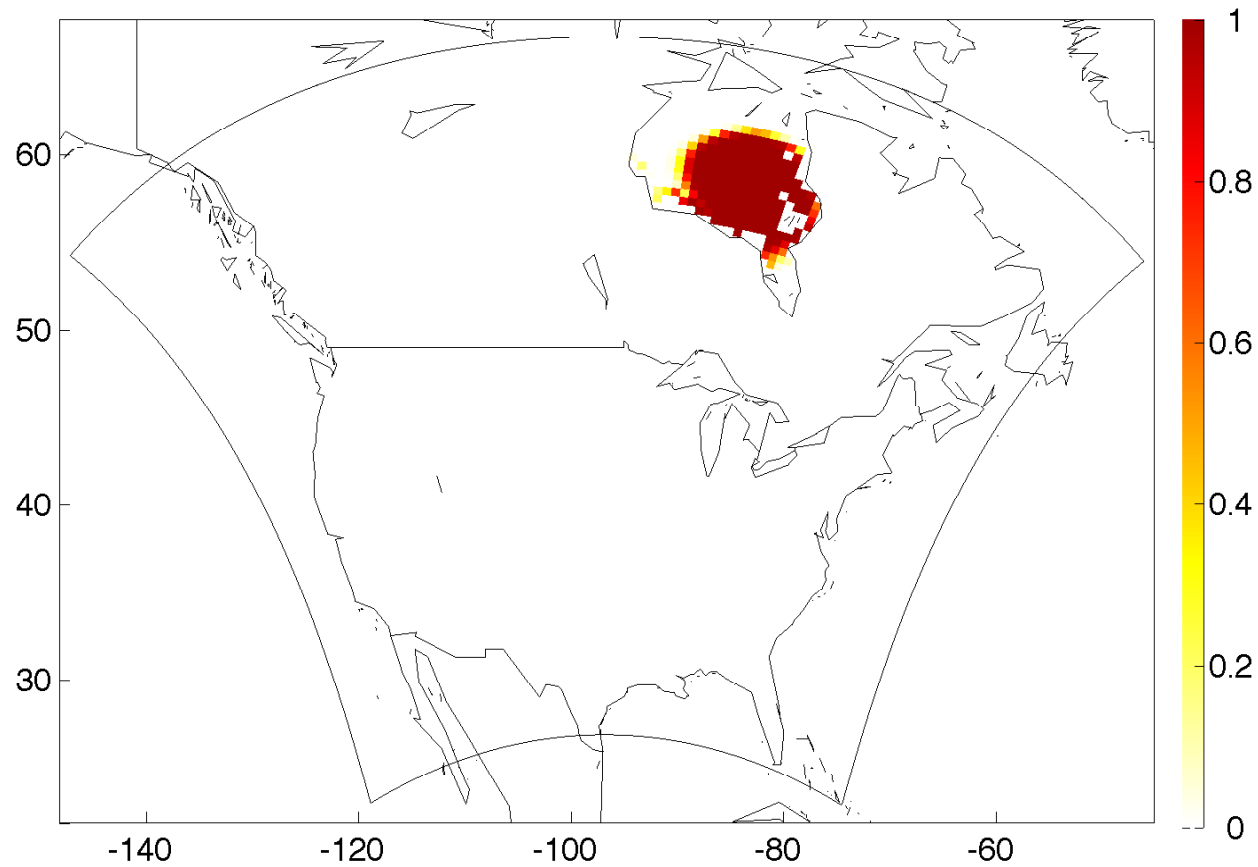
Winter: $Pr(Y_{.4}(\cdot) > k | \mathbf{data})$, for $k = 5.4^\circ C$



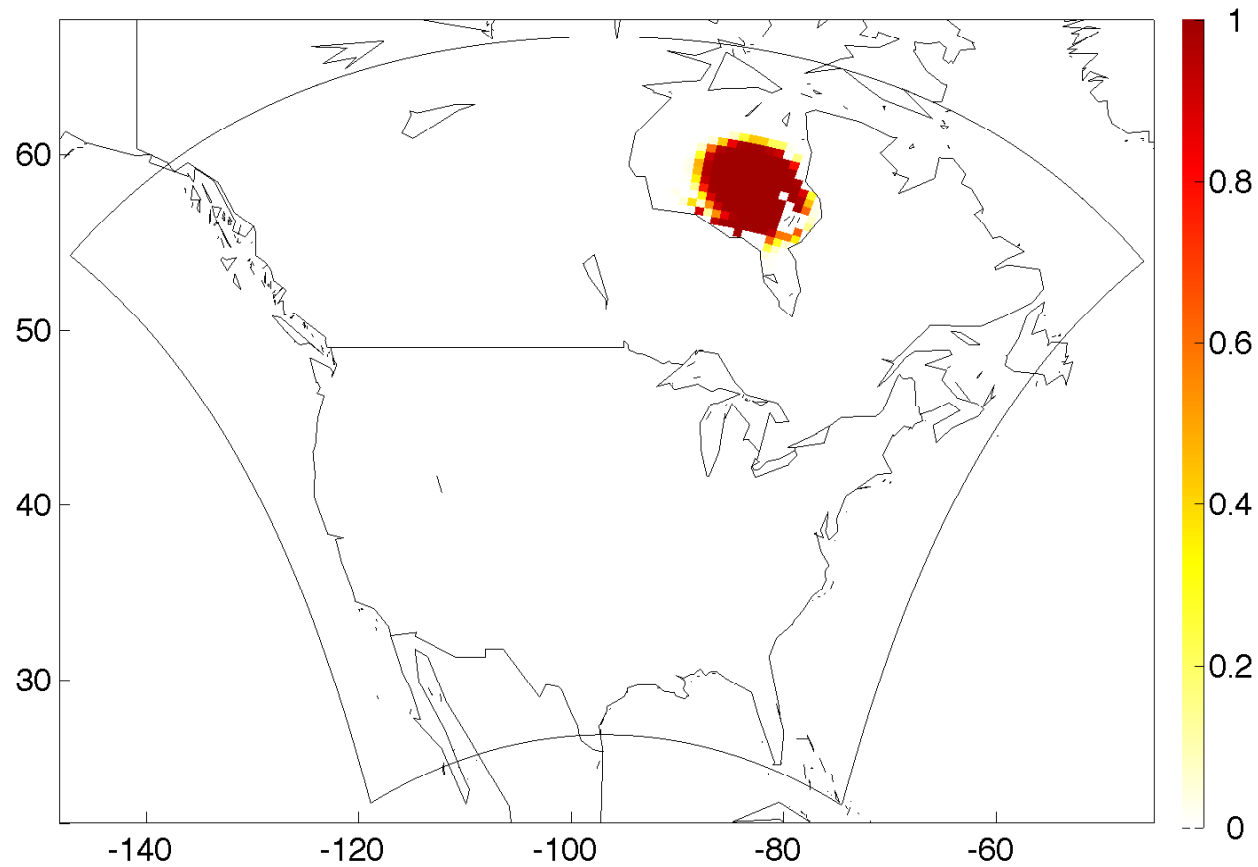
Winter: $Pr(Y_{.4}(\cdot) > k | \mathbf{data})$, for $k = 5.6^\circ C$



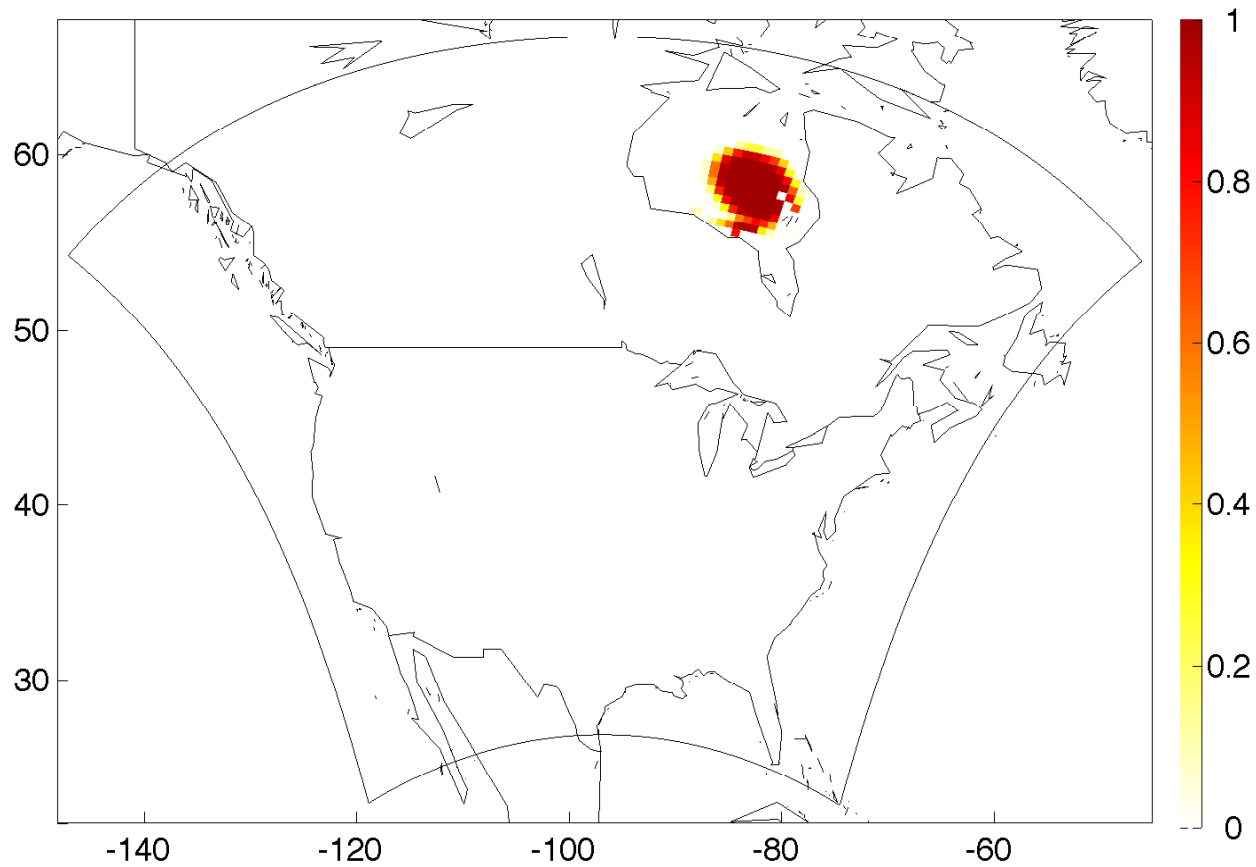
Winter: $Pr(Y_{.4}(\cdot) > k | \mathbf{data})$, for $k = 5.8^\circ C$



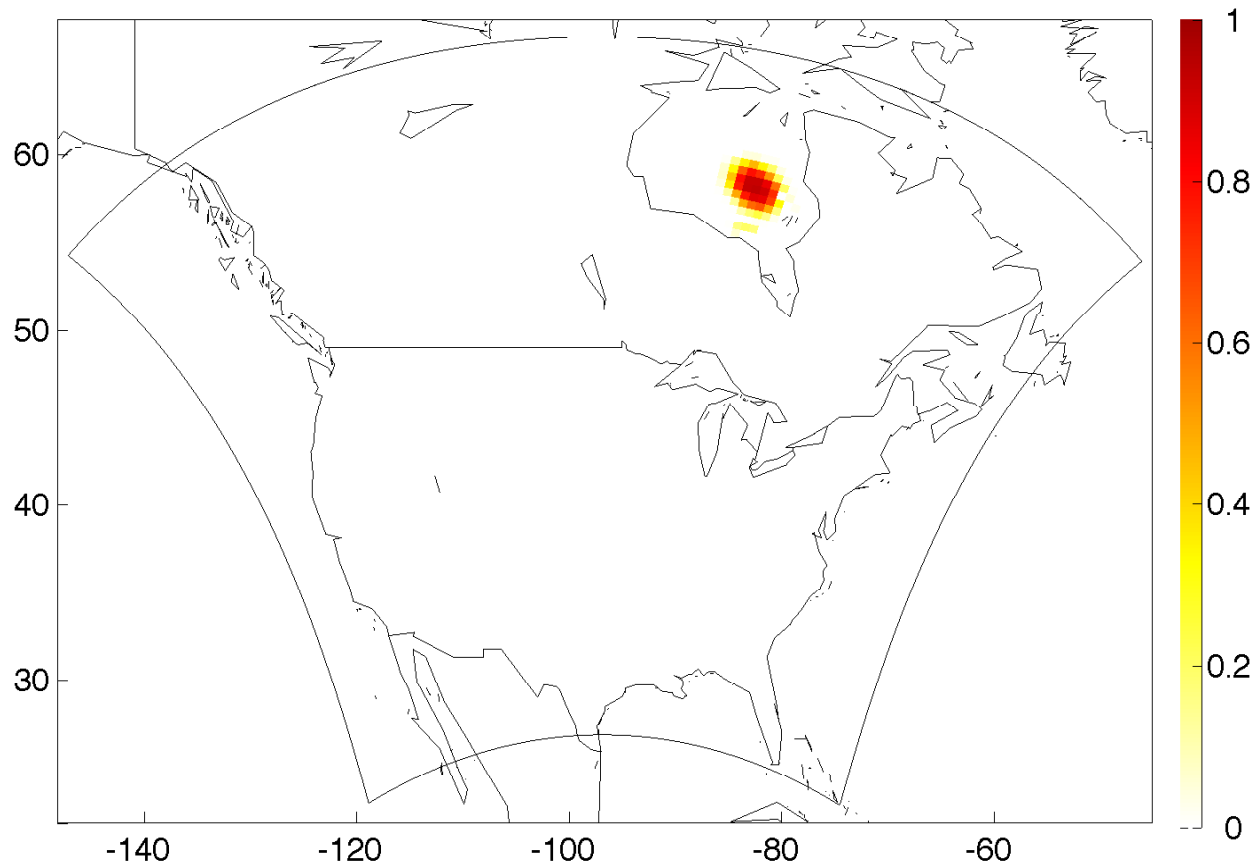
Winter: $Pr(Y_{.4}(\cdot) > k | \mathbf{data})$, for $k = 6.0^\circ C$



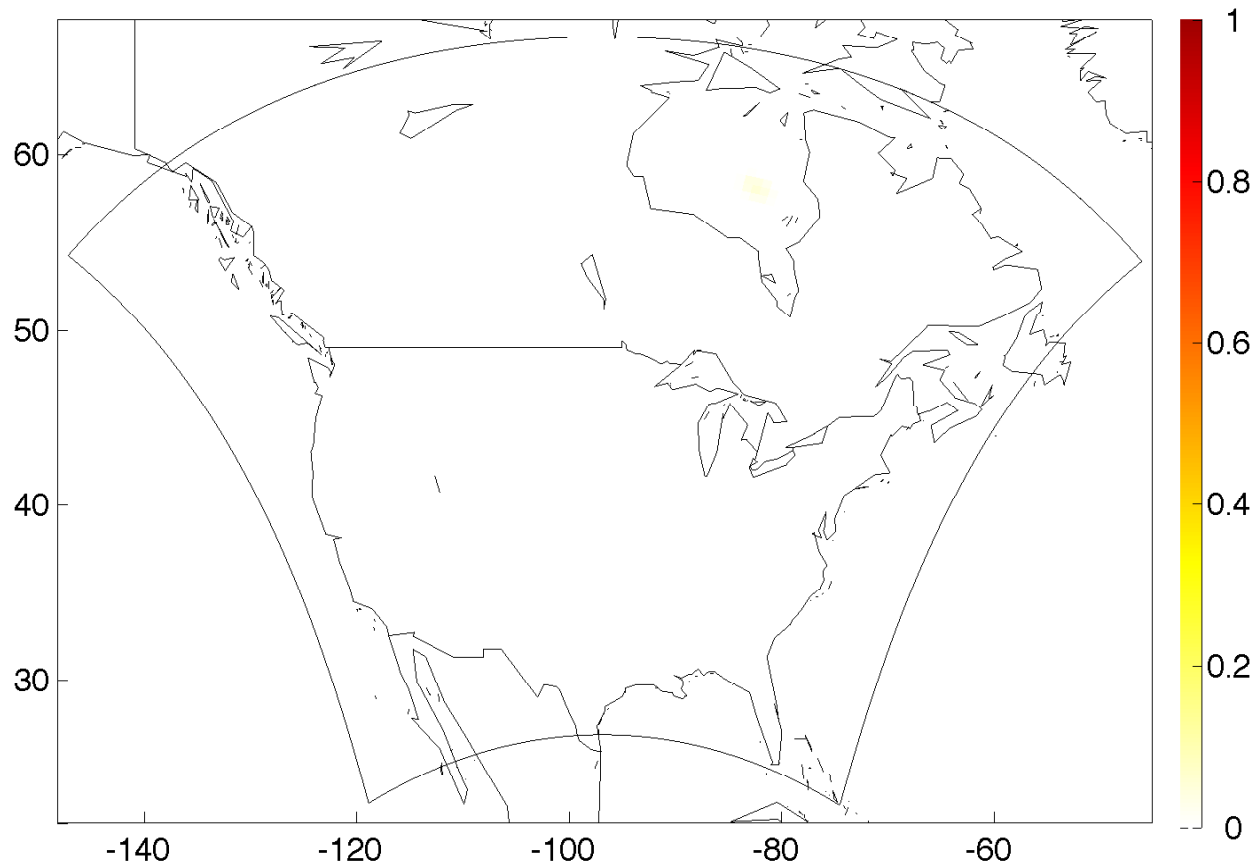
Winter: $Pr(Y_4(\cdot) > k | \mathbf{data})$, for $k = 6.2^\circ C$



Winter: $Pr(Y_{.4}(\cdot) > k | \mathbf{data})$, for $k = 6.4^\circ C$

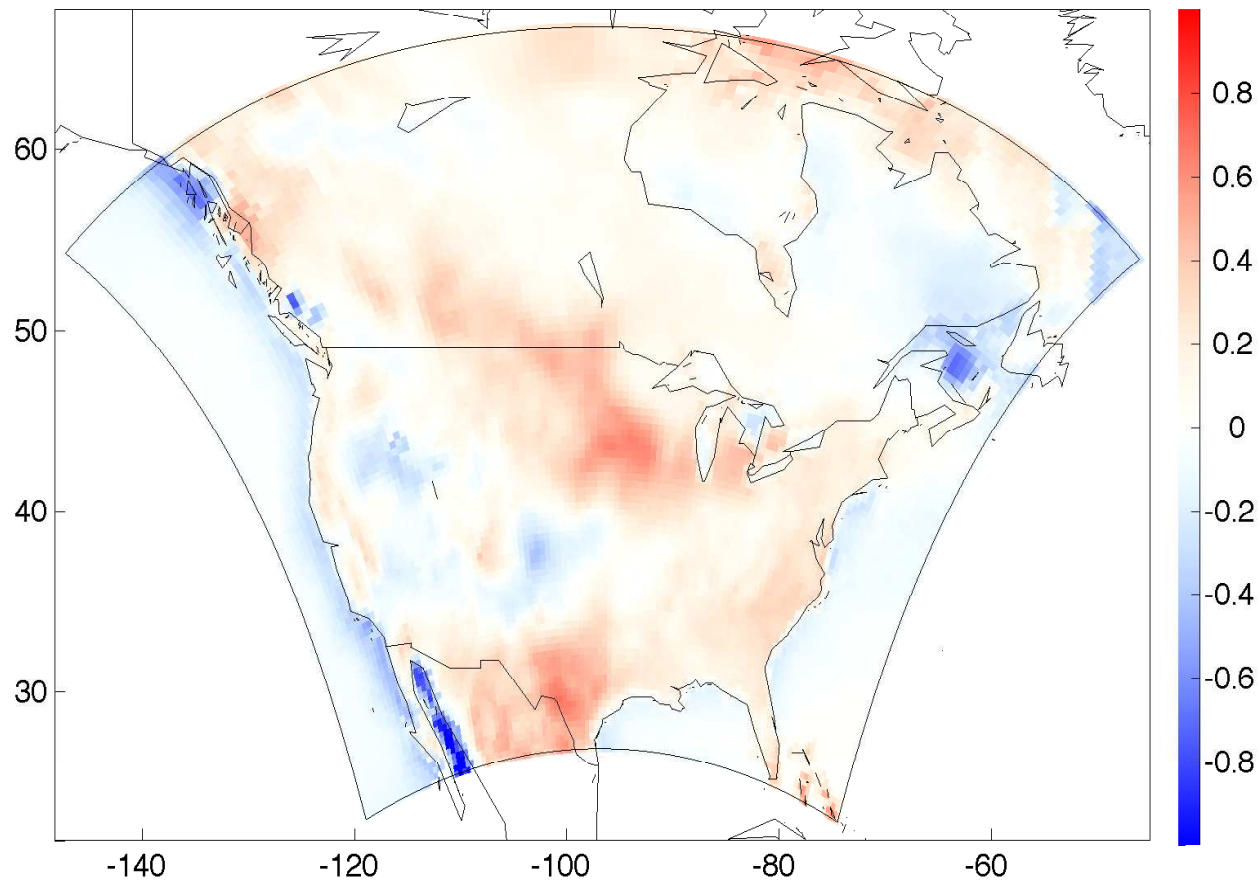


Winter: $Pr(Y_4(\cdot) > k | \mathbf{data})$, for $k = 6.6^\circ C$



Difference Between the Two RCMs' Output

● RCM differences: $D_1 - D_2$ (in $^{\circ}\text{C}$)



Uncertainty Quantification: Variability Due to RCMs

We investigate how large the variability due to “RCM” is, compared to the projected temperature change. Consider the measure:

$$R_0 \equiv \frac{\sqrt{\sum_{s \in S_0} (Y_{1.}(s) - Y_{2.}(s))^2 / (2|S_0|)}}{\sum_{s \in S_0} Y_{..}(s) / |S_0|}$$

- S_0 : The entire domain \mathbb{D} , the land, Great Lakes, Hudson Bay, the coastline, or the ocean
- The numerator: A measure of the variability between the two RCMs in the region S_0
- The denominator: The projected climate change averaged over the same region
- R_0 : The relative magnitude of variability between RCMs, compared to the averaged projected climate change

Uncertainty Quantification: Variability Due to RCMs, ctd

Table: Posterior mean of R_0 and 95% prediction interval $(\hat{R}_0^{(2.5)}, \hat{R}_0^{(97.5)})$, for various choices of S_0 .

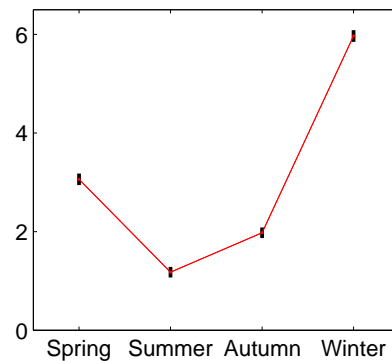
Region S_0	Post. Mean of R_0	$(\hat{R}_0^{(2.5)}, \hat{R}_0^{(97.5)})$
\mathbb{D}	0.0455	(0.0443, 0.0467)
Land	0.0424	(0.0410, 0.0438)
Great Lakes	0.0322	(0.0224, 0.0428)
Hudson Bay	0.0246	(0.0200, 0.0296)
Coastline	0.0494	(0.0470, 0.0518)
Ocean	0.0583	(0.0564, 0.08602)

- For all regions S_0 considered, R_0 is estimated to be very small, on the order of 5%
- The variability due to RCMs is much smaller than the projected temperature change

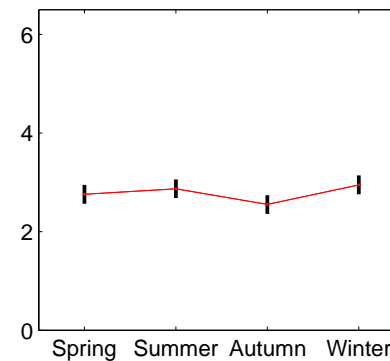
Uncertainty Quantification: Seasonal Effects and Credible Intervals

Seasonal temperature-change projections for 50km × 50km pixels in (clockwise) the Hudson Bay, the Great Lakes, the Midwest, and the Rocky Mountains. Vertical bars are 95% credible intervals based on the posterior distribution

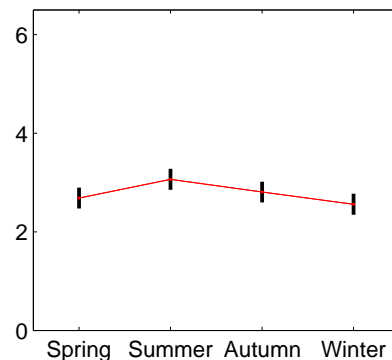
Hudson
Bay



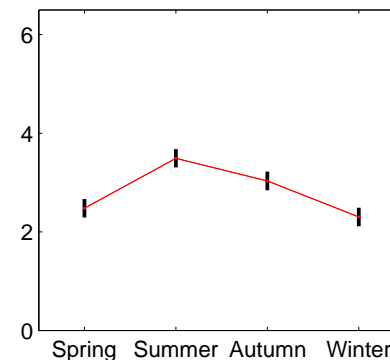
Great
Lakes



Midwest



Rocky
Mountains



Conclusions

- Visualization of spatial summaries is a powerful way to explore sources of variability (ESDA)
- Observed and conjectured patterns can be confirmed by fitting spatial statistical models. Uncertainties are quantified, and statistical inference takes the uncertainties into account
- We carried out a Bayesian statistical analysis of RCM temperature-change projections from NARCCAP Phase II
 - Over much of North America, temperature change by 2070 is projected to be above a 2°C sustainability threshold
 - The projected warming differs substantially over areas and seasons
 - The variability between RCMs is very small, when compared to the projected warming

Discussion

- The SRE-modeling approach can be easily applied to other large/massive environmental datasets
- Similar ANOVA-type models could be applied to investigate a geophysical quantity (e.g., atmospheric CO_2) using datasets from various sensing instruments
- The model can be extended to the full NARCCAP Phase II runs: We could build a spatial three-way ANOVA model by adding a factor for GCM
- A spatial four-way ANOVA could handle several greenhouse-gas-emission scenarios; however, NARCCAP uses only the SRES A2 scenario
- Validation with observations can be done on the current climate but obviously not on the climate projections

References

- Banerjee, S., Gelfand, A. E., Finley, A. O. and Sang, H. (2008), *J. R. Statist. Soc. B*, **70**, 825–848.
- Berliner, L. M. and Kim, Y. (2008), *J. Climate*, **21**, 1891–1910.
- Cressie, N. and Johannesson, G. (2006), *Mastering the Data Explosion in the Earth and Environmental Sciences: Proceedings of the Australian Academy of Science Elizabeth and Frederick White Conference*, Canberra: Australian Academy of Science, pp. 1–11.
- Cressie, N. and Johannesson, G. (2008), *J. R. Statist. Soc. B*, **70**, 1–18.
- Furrer, R., Genton, M. G. and Nychka, D. (2006), *J. Comput. Graph. Statist.*, **90**, 1189–1199.
- Kang, E. L. and Cressie, N. (2011), *J. Amer. Statist. Assoc.*, **106**, 972–983.
- Kang, E. L. and Cressie, N. (2012), *Int. J. Appl. Earth Obs. and Geoinf.*, on-line.
- Kang, E. L., Cressie, N. and Sain, S. R. (2012), *J. R. Statist. Soc. C*, **61**, 291–313.
- Kaufman, C. G. and Sain, S. R. (2010), *Bayesian Analysis*, **5**, 123–150.
- Lindgren, F., Rue, H. and Lindström, J. (2011), *J. R. Statist. Soc. B*, **73**, 423–498.
- Lahiri, S.N., Kaiser, M.S., Cressie, N., and Hsu, N.J. (1999). *J. Amer. Statist. Assoc.*, **94**, 86–110.

References, ctd.

- Mearns, L. O., Gutowski, W. J., Jones, R., Leung, L. Y., McGinnis, S., Nunes, A. M. B., Qian, Y. (2009), *Eos*, **90**, 311–312.
- Nakicenovic, N., Alcamo, J., Davis, G., de Vries, B., Fenhann, J., et al. (2000), Technical Report, Environmental Molecular Sciences Laboratory, Pacific Northwest National Laboratory, Richland, WA, USA.
- Sain, S. R. and Kaufman, C. (2012), under submission.
- Salazar, E., Sansó, B., Finley, A., Hammerling, D., Steinsland, I., Wang, X. and Delamater, P. (2011), *J. Agric. Biol. Envir. Statist.*, **16**, 586–605.
- Smith, R. L., Tebaldi, C., Nychka, D. and Mearns, L. O. (2009), *J. Amer. Statist. Assoc.*, **104**, 97–116.
- Tebaldi, C. and Sansó, B. (2009), *J. R. Statist. Soc. A*, **172**, 83–106.
- Tebaldi, C., Smith, R. L., Nychka, D., and Mearns, L. O. (2005), *J. Climate*, **18**, 1524–1540.